UC Berkeley
UC Berkeley Electronic Theses and Dissertations

Title
Designing Synthetic Culture Systems for Human Stem Cell Culture

Permalink
https://escholarship.org/uc/item/6hc5r7zr

Author
Kohen, Naomi

Publication Date
2012

Peer reviewed|Thesis/dissertation

eScholarship.org Powered by the California Digital Library
University of California

Designing Synthetic Culture Systems for Human Stem Cell Culture

By

Naomi Tehila Kohen

A dissertation submitted in partial satisfaction of the

requirements for the degree of

Doctor of Philosophy

in

Engineering - Materials Science and Engineering

in the

Graduate Division

of the

University of California, Berkeley

Committee in charge:

Professor Kevin E. Healy, Chair
Professor Ting Xu
Professor Song Li

Fall 2012

Abstract

Designing Synthetic Culture Systems for Human Stem Cell Culture

By

Naomi Tehila Kohen

Doctor of Philosophy in Materials Science and Engineering

University of California, Berkeley

Professor Kevin E. Healy, Chair

Human embryonic stem (hES) cells and human induced pluripotent stem (hips) cells can differentiate into all cell types of the body and therefore hold great therapeutic value. Applications ranging from *in situ* regenerative medicine, *ex vivo* tissue generation, and drug screening have consequently been proposed for these pluripotent cells. However, the current culturing techniques for both hES and hiPS cells hinder the clinical feasibility of their use. Pluripotent cell culture protocols have historically involved the use of animal products, which can introduce pathogens as well as limit the scalability and reproducibility of these platforms. While media formulations have been optimized to include only human or recombinant proteins, the current gold standard for human stem cell culture substrate is still Matrigel, an excretion from a mouse tumor that resembles the extra cellular matrix. It is therefore crucial to engineer materials that replace Matrigel in human pluripotent stem cell culture.

Despite the complexity of the native cell niche, key characteristics of the cell niche must be considered and chosen for emulation in constructing a synthetic system to replace Matrigel. Mechanical environment and paracrine signaling were deemed to be parameters that were both crucial for such an application and feasible to incorporate. Toward that end, a process to create tunable cell culture surfaces to replace Matrigel, and to conduct fundamental studies on the effects of mechanical environment and paracrine signaling was developed in this dissertation. A number of strategies for patterning hydrogels were considered for the creation of this synthetic human pluripotent substrate, as the hydrogel could provide mechanical cues to the cells and the patterning would control paracrine signaling by regulating cell colony size and spacing. Ultimately, a strategy involving concurrent UV illumination and microcontact printing of a UV activated crosslinker onto a low swelling hydrogel was selected, as it showed the highest pattern fidelity of the strategies explored, due to its minimization of ink diffusion. Hydrogels as compliant as 140 Pa could be patterned with this technique, and such hydrogels were shown to support hES cells in the short term.

To emphasize the limitations of Matrigel based cell culture platforms, the physical properties of Matrigel on variety of typical cell culture surfaces were studied, and it was found that the substrate beneath Matrigel was capable of influencing cell behavior such as proliferation and pluripotency, by altering the physical properties of Matrigel.

The need to create surfaces with defined cell colony sizes and spacing, thereby introducing standardization into the cell culture platform, was further emphasized by the results of our short term study conducted on the effects of mechanical environment on hES cells. While proliferation was influenced by substrate modulus, pluripotent gene expression was too variable to show any significant differences as a function of substrate modulus.

The patterning methodology developed in this dissertation for creating a modular synthetic culture surface for human pluripotent stem cells can be used not only for the maintenance of the pluripotency of the cells, but also for the directed differentiation of the cells. As a step toward using these platforms for directed differentiation protocols, the patterned surfaces were shown to support cardiomyocytes directly differentiated from iPS cells from a patient with long QT3 syndrome, with cells beating synchronously within a cell colony.

Designing Synthetic Culture Systems For Human Stem Cell Culture

Table of Contents

Table of Contents i

List of Figures iv

List of Tables ix

List of Abbreviations x

List of Symbols xii

List of Equations xiii

Acknowledgements xiv

Chapter 1: Hypothesis and Specific Aims 1
1.1 Introduction 2
1.2 Objective 3
1.3 Specific Aims 3

Chapter 2: Characterizing Matrigel Interfaces During Defined Human Embryonic Stem Cell Culture 4
2.1 Introduction 5
2.2 Methods and Materials 6
2.2.1 Reagents 6
2.2.2 Matrigel Adsorption Studies 7
2.2.2.1 Surface Modification 7
2.2.2.2 Quartz Crystal Microbalance 8
2.2.2.3 Ellipsometry 8
2.2.2.4 Scanning Electron Microscopy 9
2.2.2.5Environmental Scanning Electron Microscopy 9
2.2.2.6 Atomic Force Microscopy 9
2.2.3 Cell Culture 10
2.2.3.1 Human Embryonic Stem Cell Culture 10
2.2.3.2 Cell Attachment and Proliferation Studies 10
2.2.3.3 Immunoctyochemistry 10
2.2.3.4 Flow Cytometry 11
2.3 Results and Discussion 11

2.3.1 Cellular Response: Proliferation and Differentiation 11
2.3.2 Physio-chemical Characterization of Matrigel 14
2.4 Conclusions 22

Chapter 3: Developing Mechanically Tunable Chemically Patternable Substrates for Human Stem Cell Culture 23
3.1 Introduction 24
3.1.1 Need for Chemically Patterned Mechanically Tunable Substrates 24
3.1.1.1 Limits of Current Alternative hES cell Culture Platforms 24
3.1.1.2 Mechanical Environment 25
3.1.1.3 Colony Size 26
3.1.2 Existing Hydrogel Patterning Technologies and their Limitations 28
3.2 Overview of UV-activated hydrogel printing 31
3.2.1 Materials Selection 32
3.2.1.1 Polyacrylamide System 32
3.2.1.2. Sulfo-SANPAH 36
3.2.1.4 Adhesive Ligands 37
3.2.2 Methods 39
3.2.2.1 Polyacrylamide Gels 39
3.2.2.2 Photolithography 40
3.2.2.3 Fibronectin 40
3.2.2.4 Cell Culture 41
3.2.3 Results and Discussion 41
3.2.3.1 Quartz Substrate 41
3.2.3.2 Acrylamide Protein Resistance 42
3.2.3.3 Crosslinker and Buffer properties 43
3.2.3.4 Concentration of Fibronectin 46
3.2.3.5 Photolithography 48
3.2.3.6 Sterility 51
3.2.3.7 Summary of Patterning Protocol 52
3.2.3.8 Patterning with 3T3s 54
3.3 Modulating the Fouling Behavior of Acrylamide with PEG 55
3.3.1 Introduction 55
3.3.2 Methods and Materials 58
3.3.3. Results and discussion 59
3.4 Patterning Acrylamide with Adhesion Peptides 61
3.4.1 Introduction 61
3.4.2 Methods and Materials 64
3.4.3 Results and discussion 64
3.5 Alternative Patterning Methodologies Explored 69
3.5.1 Photomask 69
3.5.1.1 Methods and Materials 70
3.5.1.2 Results and Discussion 70
3.5.2 Stamping with Protein Ink 71
3.6 Conclusions and Future Work 74

Chapter 4: **The Influence of Modulus on Human Embryonic Stem Cells** **75**
4.1 Introduction 76
4.2 Methods and Materials 76
4.2.1 Human Embryonic Stem Cell Culture 76
4.2.2. Polyacrylamide Substrates 77
4.2.3 Proliferation 78
4.2.4 Quantitative RT-PCR 79
4.2.5 Immunocytochemistry 79
4.2.6 Statistical Analysis 80
4.3 Results and Discussion 80
4.3.1 Proliferation 80
4.3.2 Pluripotent Gene Expression 84
4.3.3 Patterning 88
4.4 Conclusions 91

Chapter 5: Induced Pluripotent Stem Cells Studies **92**
5.1 Introduction 93
5.2 Methods and Materials 96
5.2.1 Cell Culture 96
5.2.2 Patterned Surfaces Preparation 98
5.2.2 Immunocytochemistry 98
5.2.3 Electrophysiology 98
5.3 Results and Discussion 99
5.4 Conclusions 102
4.3.3
Chapter 6: Summary and Future Work **103**
6.1 Results Summary 104
6.1.1 Matrigel Characterization 104
6.1.2 Chemically Patterned Hydrogels 104
6.1.3 Effect of Substrate Modulus on Human Embryonic Stem Cells 106
6.1.4 Pluripotent Cells on Patterned Hydrogels 106
6.2 Future Work 106

Bibliography **107**
Chapter 1 107
Chapter 2 107
Chapter 3 110
Chapter 4 121
Chapter 5 124

Appendices **129**
Appendix A.1 Polyacrylamide Gels Protocol 129
Appendix A.2 SU-8 Master Protocol 133
Appendix A.3 UV-Activated Microcontact Printing Protocol 134
Appendix A.4 Limitations of cell counting methods for hES cells 140
Figure Appendix 142

List of Figures

Figure 2.1 Phase images and proliferation of hES cells grown on Matrigel-coated tissue culture polystyrene (TCPS), polystyrene (PS), and glass. (a) Phase images (b) Attachment of hES cells to TCPS, PS, and glass surfaces coated with Matrigel after 3 hours (c) Attachment of hES cells to TCPS, PS, and glass surfaces coated with Matrigel after 5 days 12

Figure 2.2 Expression of the embryonic stem cell markers Oct-4 and SSEA-4 of hES cells grown on Matrigel-coated TCPS, PS, and glass after 5 days. (a) Immunocytochemistry of Oct-4 and SSEA-4 on HSF-6 cells. (b) Quantification of SSEA-4 and Oct-4 via flow cytometry for cells cultured on Matrigel-coated surfaces, after 5 days of culture for H9 and HSF-6 cell lines 13

Figure 2.3 Immunocytochemistry for the embryonic stem cell markers Oct-4 and SSEA-4 on Matrigel coated tissue culture polystyrene (TCPS), polystyrene (PS), and glass with the H9 cell line. 14

Figure 2.4 SEM of bare substrates and substrates with Matrigel. A-C bare substrates. (A) polystyrene (B) oxygen treated polystyrene (C) is glass. D-F adsorbed Matrigel (D) Matrigel on polystyrene (E) Matrigel on oxygen plasma treated polystyrene (F) is Matrigel on glass. 16

Figure 2.5 QCM-D frequency and dissipation responses to Matrigel adsorption and subsequent rinses on the surfaces: polystyrene, oxygen plasma treated polystyrene, and glass 17

Figure 2.6 Differences in kinetics of adsorption and conformation of Matrigel on the three surfaces are manifest in the adsorption rates (A) and ΔF-ΔD plots for adsorption (B). 19

Figure 3.1 H1 hES cells grown on Matrigel with mTeSR media, using Accutase and ROCK inhibitor. Cell colonies display a variety of areas and perimeters when grown in this typical culture fashion. 27

Figure 3.2 From Wang et al. The authors used a PDMS stencil technique to pattern acrylamide, however there are cells missing from the pattern and there are non-patterned areas which show cellular adhesion. 29

Figure 3.3 From Engler et al. Acrylamide gel patterned via micropatterned glass reservoir. There is limited long range pattern fidelity as seen demonstrated by cellular adhesion. 29

Figure 3.4 From Hahn et al. micropatterning a polyethylene glycol based hydrogel with an acrylated RGD peptide. (A) Fluorescent peptide. and (B)cell images. Both peptide and cells are clearly visible outside of the patterned areas. 30

Figure 3.5 Overview of UV activated microcontact printing technique 32

Figure 3.6 Polyacrylamide gel polymerization scheme. (A) structure of monomers and polyacrylamide. (B) Free radical intiation via APS and TEMED 34

Figure 3.7 (A) structure of sulfo-SANPAH. (B) The possible reactions of the azide from sulfo-SANPAH upon UV activation 37

Figure 3.8 Polymerizing polyacrylamide hydrogels directly in tissue culture polystyrene plates. Gels have delaminated from the bottom of the well in the course of swelling. 42

Figure 3.9 Delamination of a 3T3 cell sheet from a fibronectin conjugated 10 kPa polyacrylamide gel, which occurs once the cell sheet has become confluent. 47

Figure 3.10 On sufficiently compliant fibronectin conjugated gels (< 0.1 kPa), 3T3 cells cannot spread or proliferate 47

Figure 3.11 Inking PDMS stamps with a standard inkpad and testing pattern transfer onto a stiff, less diffusive surface than acrylamide, namely paper. Stamp posts were 400 μm in diameter. Glass backing is required to prevent roof collapse 49

Figure 3.12 Determining an acrylamide gel drying time that can sufficiently prevent gross ink diffusion. Polyacrylamide gel drying times prior to stamping: (A) 1 minute (B) 5 minutes (C) 10 Minutes (D) 1 hour 50

Figure 3.13 Comparing polyacrylamide gel drying as a function of acrylamide gel storage solution: (A) Deionized water and (B) PBS. 51

Figure 3.14 3T3 cells patterned on fibronectin (.5 mg/mL) conjugated polyacrylamide gels (1 kPa). PDMS stamps with post diameters: (A) 400 μm, (B) 600 μm, and (C) 800 μm were used to generate these patterns. 54

Figure 3.15 3T3 cellular islands can contract on fibronectin patterned polyacrylamide gels. 1 kPa gels. Scale bar = 500 μm. (A) day 1 after seeding (B) 5 days after seeding. The red circle is a visual guide to show cell island contraction, and it represents the area of a cell island at day 1 55

Figure 3.16 The ability of polyacrylamide gels to support rat mesenchymal stem cell adhesion 1 day after seeding at 20,000 cells/cm^2 in the presence of serum. (A) 10 kPa acrylamide; (B) 10 kPa acrylamide conjugated to sulfo-SANPAH; (C) 10 kPa acrylamide conjugated to fibronectin via sulfo-SANPAH. 56

Figure 3.17 Two small molecules investigated as backfillers to minimize adsorption of proteins and cells onto residual unconjugated sulfo-SANPAH. (A) Aminoethoxyethanol (AEOE) (B) tris(hydroxymethyl)aminomethane (TRIS) 57

Figure 3.18 Exploring the use of backfillers to decrease the fouling of suflo-SANPAH conjugated acrylamide gels, by observing cell attachment onto: (A) TRIS conjugated to acrylamide via sulfo-SANPAH; (B) AEOE conjugated to acrylamide via sulfo-SANPAH; (C) sulfo-SANPAH conjugated polyacrylamide; (D) fibronectin conjugated to polyacrylamide via sulfo-SANPAH. 60

Figure 3.19 Diamino-PEG chains of varying length affect the ability of cells to attach to 10 kPa polyacrylamide gels. (A) PEG chain MW= 2,000 (B) PEG chain MW=3,400 (C) PEG chain MW= 5,000 (D) control without PEG chain: 10 kPa polyacrylamide gel. 61

Figure 3.20 PEAS structure 62

Figure 3.21 Using fibronectin to determine sufficient concentrations of PEAS crosslinker, and to validate reducing protocol for PEAS 65

Figure 3.22 3T3 cells on surfaces created by conjugating adhesive ligands to 10 kPa polyacrylamide via 200 uM PEAS. (A) adhesive ligand = fibronectin (B) adhesive ligand = serum (C) adhesive ligand = 100 uM RGD (input concentration) (D) adhesive ligand = 400 uM RGD (input concentration) 66

Figure 3.23 3T3 cells on surfaces created by conjugating adhesive ligands to 10 kPa polyacrylamide via 200 μM PEAS. (A) no adhesive ligand; (B) adhesive ligand = 0.5 mg/mL fibronectin; (C) adhesive ligand = 100 μM RGD; (D) adhesive ligand = 400 μM RGD; (E) adhesive ligand = DMEM media with 15% FBS 68

Figure 3.24 Microcontact printing the crosslinker sulfo-SANPAH and then exposing to UV, yields messy patterns that are not well defined, and show a significant amount of background fouling. 69

Figure 3.25 Schematic of using a photomask to selectively illuminate sulfo-SANPAH, as a patterning methodology.. 70

Figure 3.26 3T3 cells stuck to the entire polyacrylamide gel surface, when the gel was patterned with fibronectin via a photomask, illustrating the failure of this technique ,which allows for sufficient mobility of the ink (sulfo-SANPAH crosslinker) to cover the entire surface. 71

Figure 3.27 The difficulty in preparing uniformly coated protein stamps. At high protein (0.1 mg/mL) and buffer concentrations (200mM HEPES), protein does not dry uniformly onto PDMS stamp (A) and the film can be seen leaving rings around the PDMS posts. Protein films never fully dry when (A) left to air dry for

1 hour or (B) & (C) dried with a nitrogen gun for 5 minutes, as salt in buffer can be acting as kosmotrope. (D) Cells patterned using protein stamps, can show an inverse pattern to the stamp with cells only binding where the PDMS posts did not contact the polyacrylamide gel. 72

Figure 4.1 H1 hES cell proliferation on Matrigel conjugated surfaces. (A) Cell attachment on day 1 and (B) proliferation normalized to Matrigel on TCPS at day 1 82

Figure 4.2 H1 hES cell proliferation on fibronectin conjugated surfaces. (A) Cell attachment on day 1 and (B) proliferation normalized to fibronectin on TCPS at day 1 83

Figure 4.3 Expression of pluripotency genes at day 4 for H1 hES cells grown on substrates of varying stiffness. Values presented are mean and standard deviation. None of the genes showed statistically significant differences between the substrates examined. 84

Figure 4.4 H1 hES cells on (A) Matrigel on TCPS and (B) Matrigel conjugated to 10 kPa polyacrylamide. (C) and (D) are magnifications of (A) and (B). Cells on Matrigel on TCPS are more spread and less dense than cells on Matrigel on 10 kPa polyacrylamide. Additionally, colonies on 10 kPa polyacrylamide are more phase bright at their edges, with cells less likely to spread to the same extent on colony edges as they do on Matrigel on TCPS. 87

Figure 4.5 Colony area and perimeter distribution for H1 hES cells grown on Matrigel on TCPS at day 4 (from 3 wells). Area = 52,243 ± 60,790 and perimeter = 1303 ± 1004 μm (mean ± standard deviation) 87

Figure 4.6 H1 hES cells attach and display typical morphology on a 140 Pa polyacrylamide gel patterned with Matrigel 89

Figure 4.7 H1 hES cells co-stained for pluripotency markers OCT4 and Nanog on fibronectin patterned 140 Pa polyacrylamide gels on day 4 after passaging, demonstrating the ability of H1 hES cells to remain pluripotent on the patterned surface. 90

Figure 4.8 H1 hES cells on 1 kPa polyacrylamide gels uniformly conjugated with fibronectin, vitronectin, or Matrigel, 1 day and 2 days after passaging with Accutase and ROCK inhibitor. When used at the same concentration, vitronectin supports more hES cells than fibronectin 91

Figure 5.1 Schematic electrocardiogram of (A) normal heart and (B) long QT syndrome heart. 94

Figure 5.2 1 kPa fibronectin patterned acrylamide gels can support cardiac cells directly differentiated from long QT patient iPS cells, as indicated by protein expression (green) of cardiac lineage (A) smooth muscle myosin (B) cardiac troponin T..... 100

Figure 5.3 Stills from videos of beating hiPS cardiac cells. The phase bright cells in the islands were the beating cells, while the cells that looked more fibroblast-like did not beat. Islands had mixed populations of beating and non-beating cells, with cells in the same island beating synchronously. Contracting cells in the colony could ultimately deform the colony from its original shape. 101

Figure AF.1 Environmental Scanning Electron Microscopy (ESEM) images of air-dried Matrigel on Tissue Culture Polystyrene (TCPS), Polystyrene (PS), and SiO_2 (glass). On all three surfaces, salt dendrites from air-drying are visible..... 142

Figure AF.2 Atomic Force Microscopy of Matrigel on (A) polystyrene; (B) SiO_2; (C) TCPS. Height images and phase images. All surfaces show characteristic salt dendrites from air-drying..... 143

Figure AF.3 On non-fouling or poorly adhesive surfaces, hES cells form aggregates that float in solution, similar to embryoid bodies..... 144

Figure AF.4 H1 hES cell and colony shape and density change as a function of time when they are passaged with Accutase and ROCK inhibitor (ROCK inhibitor is removed at day 1 by media exchange). (A) cells on Matrigel on TCPS and (B) cells on Matrigel conjugated to 10 kPa polyacrylamide 145

List of Tables

Table 2.1 Matrigel™ (Growth Factor Reduced) Composition[15] 5

Table 2.2 Sessile Water-in-Air Contact Angles of Test Surfaces 15

Table 2.3 Adsorption Properties of Matrigel™ 15

Table 2.4 Kinetics of Matrigel™ adsorption and effect of rinsing on network stability 20

Table 3.1 Conditions found in literature for conjugating an adhesive ligand to a polyacrylamide gel 44

Table 3.2 Radius of Gyration and Critical Concentration C* as a function of PEG chain molecular weight 59

Table 4.1 ANOVA p-values for pluripotency genes of H1 hES cells cultured on surfaces with variable moduli 85

List of Nomenclature and Abbreviations

AEOE	2-(2-aminoethoxy)ethanol
AAm	acrylamide
AAc	acrylic acid
AC	alternating current
AFM	atomic force microscope
APS	ammonium persulfate
ANOVA	analysis of variance
ASIB	1-(p-azidosalicylamido)-4-(iodoacetamido) butane
ASTM	American society for testing and materials
bFGF	basic fibroblast growth factor
BMP	bone morphogenic protein
BPM	beats per minute
BSA	bovine serum albumin
DAPI	4',6-diamidino-2-phenylindole
DMEM	Dulbecco's modified Eagle media
ECM	extra-cellular matrix
EDTA	ethylenediaminetetraacetic acid: 2-({2-[Bis(carboxymethyl)amino]ethyl} (carboxymethyl)amino)acetic acid
EGF	epidermal growth factor
ESEM	environmental scanning electron microscope
EHS	Engelbreth–Holm–Swarm (sarcoma from which Matrigel is derived
FBS	fetal bovine serum
HEPES	4-(2-hydroxyethyl)-1-piperazineethanesulfonic acid
H1	human embryonic stem cell line derived at WiCell Research Institute (also referred to as WA09)
HSF-6	human embryonic stem cell line derived at UCSF
H9	human embryonic stem cell line derived at WiCell Research Institute (also referred to as WA09)
hES	human embryonic stem (cell)
hPS	human pluripotent stem (cell)
IGF-1	insulin-like growth factor 1
iPS	induced pluripotent stem (cell)
IPA	isopropyl alcohol
IPN	interpenetrating polymer network
LIF	leukemia inhibitory factor
KO-DMEM	knock-out Dulbecco's modified Eagle media
mES	mouse embryonic stem (cell)
MEF	mouse embryonic fibroblast
MTMS	methacryoxypropyltrimethoxysilane
NC-SF	non-conditioned serum free (media)
NHS	*N*-hydroxysuccinimide
NGF	nerve growth factor

OCT4	octamer4. A transcription factor in the POU family. Nessecary for maintenance of pluripotency in embryonic stem cells
PBS	phosphate buffered saline
PDGF	platelet derived growth factor
PDMS	polydimethylsiloxane
PEAS	N-((2-Pyridyldithio)ethyl)-4-Azidosalicylamide Heterobifunctional crosslinker with UV activated azide end, and thiol-reactive end
PEG	polyethylene glycol
PEGDA	polyethylene glycol diacrylate
PMEDSAH	poly[poly(ethylene glycol) methyl ether methacrylate]
PS	polystyrene
pSMAD1	phosphorylated SMAD1 protein. Part of the TGFβ pathway
RGD	peptide sequence Arginine-Glycine-Aspartic acid integrin engaging cell adhesive peptide sequence
ROCK	Rho associated kinase
SEM	scanning electron microscope
SPBS	Phosphate buffered saline with bovine serum albumin. Used for immunocytochemistry
SSEA-4	stage specific embryonic antigen 4. Protein on cell membrane that indicates pluripotency in embryonic stem cells
SU-8	a negative photoresist from Microchem
Sulfo-SANPAH	*N*-Sulfosuccinimidyl-6-(4'-azido-2'-nitrophenylamino) hexanoate Heterobifunctional crosslinker with UV activated azide end, and thiol-reactive end
TEMED	tetramethylethylenediamine
TCPS	tissue culture polystyrene
TGFβ	transforming growth factor beta
TRIS	tris(hydroxymethyl)aminomethane
UV	ultra-violet
QCM-D	quartz microbalance with dissipation monitoring
XPS	x-ray photoelectron spectroscopy

List of Symbols

Ellipsometry:

λ	wavelength
ϕ	angle of incidence (ellipsometry)
n	index of refraction

Quartz crystal microbalance with dissipation:

n	overtone number
Δ	change relative to starting value
m	mass
f	frequency
D	dissipation
G	complex shear modulus
G'	storage modulus
G''	loss modulus
μ	elastic shear modulus
η	shear viscosity
τ	relaxation time

Polymers

C*	critical overlap concentration
MW	molecular weight
Rg	radius of gyration
N_A	Avogadro's number

Other:

θ_{H_20}	sessile water-in-air contact angle
ν	Poisson's ratio
E	Young's modulus

List of Equations

Equation 2.1 Sauerbrey Relation 16

Equation 2.2 Voigt model for QCM-D 18

Equation 3.1 Relationship between shear modulus and Young's modulus 39

Equation 3.2 Critical overlap concentration of polymers 58

Equation 3.3 Radius of gyration as a function of molecular weight, for PEG 59

Acknowledgements

I would like to thank my advisor Kevin Healy for his support, advice, and inspiration during my time at UC Berkeley. In addition, I would like to thank all of the Healy Lab members during my many years in the group. Ray Schmidt, Beth Irwin, Jacob Pollock, and Lauren Little were invaluable friends in my first few years in the lab. I am also very grateful for all of the new members of the Healy Lab who have made my experience that much more enjoyable, particularly Mariana Garcia, Felicia Svedlund, Eda Altiok, Natalie Marks, Or Gadish, Zhen Ma, and Wes Jackson. I would especially like to thank Lauren, Or and Zhen who worked closely with me on parts of this dissertation, and Wes Jackson for knowing everything, and always being available.

I would like to thank Professor Ting Xu for access to much of her lab's equipment and her wonderful support in general. I would also like to thank Professor Clay Radke and his graduate student Sam Maurer for technical support and use of their ellipsometry equipment; Professor Gabor Somorjai and his graduate student George Holinga for use of their QCM-D, and Guangwei Min for technical support and use of the scanning electron microscope at the Electron Microscopy Lab at UC Berkeley.

I thank my family and especially my parents for their never-ending support. Practically family, I would also like to thank Jeff Doker and Ben Cannon, my roommates and best friends since the beginning of graduate school. This work was generously funded by a Berkeley Futures Grant, an Applied Biology and Bioprocess Engineering NIH Training Grant, and an NIH Enabling Technologies grant. Lastly, a portion of this work was previously published in *Biointerphases*, and I accordingly thank my co-authors and the editorial staff for their help.

Chapter 1
Hypotheses and Specific Aims

1.1 Introduction
1.2 Objective
1.3 Specific Aims

1.1 Introduction

Embryonic stem cells, which are derived from the inner cell mass (ICM), are capable both of self-renewal and differentiation into all cell types in the body. Embryonic stem cells were first isolated from mice in 1981 by two separate groups,[1] and it was not until 15 years later that they were isolated in humans.[2] More recently, a new type of stem cell has been created, known as the induced pluripotent stem cell, which is a terminally differentiated cell that has been reprogrammed into a pluripotent state.[3, 4] Both human embryonic stem (hES) cells and human induced pluripotent stem (hiPS) cells have been touted in the field of regenerative medicine for their potential use in *ex vivo* tissue regeneration applications or for drug testing on organ-like equivalents.

In order for either hES or for hiPS cells to be used in such applications, they must be expanded *ex vivo* to large numbers, while maintaining their pluripotency and normal karyotype. As with all cell culture techniques, the techniques developed for hES cell culture strive to mimic the native environment that cells would be exposed to in the body. In the body, the decision for a stem cell to self-renew or differentiate is regulated by its niche, which is comprised of a myriad of chemical and mechanical signals, neither of which, alone or in concert, are fully understood or defined. In the absence of a full understanding of the native requirements for maintaining the self-renewal of hES cells, the development of an appropriate biomimetic cell culturing system for hES cells has remained elusive.

Tissue culture, and later cell culture, began only a century ago with Ross Harrison, who used frog lymph to secure a frog brain explant between two glass slides, in an attempt to study the origin of nerve growth.[5] It was only in the 1950s that monolayer cell culture as we know it today began to take shape, with the use of aseptic techniques, antibiotics, the standardization of media formulations, and most importantly the use of Trypsin to allow for subculture.[6] In fact, human cells were not successfully cultured until George Gey, a researcher at John's Hopkins, had been able to culture cells from a patient's cervical cancer in 1951, thus developing the first immortal human cell line. Even during Gey's time, cell culture medium was prepared by each individual lab, and involved the purchase of a variety of animal bloods from the local butcher, and the manual homogenizing of animal embryos to obtain "embryo extract", a key undefined component in cell culture media.[6, 7] Since then, cell culture protocols and media formulations have been standardized for many established cells lines, even in the absence of a full understanding of the native *in vivo* environment of the cells.

Likewise, hES cell culture techniques have come a long way since the first hES cells were derived by James Thomson. However, current hES cell culture techniques are still limited because of their use of animal products, which can introduce pathogens as well as limit the scalability and reproducibility of these platforms. While media formulations have been optimized to include only human or recombinant proteins, the current gold standard for hES cell culture substrate is

Matrigel, an excretion from a mouse tumor that resembles the extra cellular matrix. It is therefore necessary to design synthetic alternatives to Matrigel, if either hES or iPS cells are to be used clinically. It is the goal of this dissertation to create a Matrigel replacement that recapitulates salient features of the stem cell niche, in a modular fashion, with specific emphasis on controlling the mechanical environment of the cells, and paracrine signaling by controlling cell colony size and spacing. With such an approach, these surfaces can also be used, not only to maintain the pluripotency of human pluripotent cells, but also to direct their differentiation.

1.2 Objectives and Outline

In this dissertation, I wanted to study the physiochemical properties of Matrigel, the currently used substrate for hES cell culture, and then I sought to develop a substrate that could replace Matrigel. In the following chapters, I present my work toward those objectives. In chapter 2, I use characterization methods such as quartz crystal microbalance with dissipation, scanning electron microscopy, and ellipsometry to show that Matrigel structures differently depend on the underlying substrate, and that this difference leads to varied cell behavior in terms of proliferation and maintenance of pluripotency. In chapter 3, I develop a platform that allows for the chemical patterning of hydrogels for use with human pluripotent stem cells. The patterned hydrogels allow for the simultaneous control of the mechanical environment (*via* gel modulus) and the size and spacing of cell colonies. A number of patterning methodologies are explored, and ultimately, a method based on microcontact printing a UV-activated crosslinker onto a low swelling hydrogel is selected and presented in chapter 3. In chapter 4, I test the hypothesis that substrate modulus affects embryonic stem cell behavior by looking at the short term proliferation and pluripotency expression of human embryonic stem cells grown on variable moduli surfaces. Additionally, I demonstrate the ability to pattern human embryonic stem cells on the surfaces developed in chapter 3. In chapter 5, I demonstrate the ability of the patterned surfaces to support cardiac cells derived from human induced pluripotent stem cells. Lastly, in chapter 6, I present a summary of the results obtained in this dissertation, and I propose future work based on the findings of my dissertation.

1.3 Specific Aims

- To characterize Matrigel on various substrata used for human embryonic stem cell culture
- To develop a method to chemically pattern mechanically tunable hydrogels
- To determine the effect of substrate modulus on human embryonic stem cells
- To investigate the behavior of human pluripotent stem cells on chemically patterned hydrogels

Chapter 2
Characterizing Matrigel Interfaces During Defined Human Embryonic Stem Cell Culture

2.1 Introduction
2.2 Methods and Materials
    2.2.1 Reagents
    2.2.2 Matrigel Adsorption Studies
        2.2.2.1 Surface Modification
        2.2.2.2 Quartz Crystal Microbalance
        2.2.2.3 Ellipsometry
        2.2.2.4 Scanning Electron Microscopy
        2.2.2.5 Environmental Scanning Electron Microscopy
        2.2.2.6 Atomic Force Microscopy
    2.2.3 Cell Culture
        2.2.3.1 Human Embryonic Stem Cell Culture
        2.2.3.2 Cell Attachment and Proliferation Studies
        2.2.3.3 Immunoctyochemistry
        2.2.3.4 Flow Cytometry
2.3 Results and Discussion
    2.3.1 Cellular Response: Proliferation and Differentiation
    2.3.2 Physio-chemical Characterization of Matrigel
2.4 Conclusions

2.1 Introduction

Human embryonic stem (hES) cells have the potential to differentiate into all cell types in the adult body and hold great promise for regenerative medicine[1, 2]; however, large-scale expansion of undifferentiated hES cells remains a major challenge.[3] Self-renewal, i.e. undifferentiated proliferation, of hES cells requires co-culturing these cells with either mouse or human fibroblast cells (i.e. a feeder layer of cells).[4-6] Culturing with mouse fibroblast cells increases the risk of zoonoses and the expression of foreign oligosaccharide residues acquired from the murine feeder cells and culture medium.[7] Culturing with feeder layer cells, either human or murine, also poses significant disadvantages in reproducibility and scalability that greatly limit their clinical potential. More recently, several groups have described methods to culture hES cells under chemically-defined conditions (reviewed in [8]).[9-13] These systems use either animal or human-derived extracellular matrix (ECM) proteins adsorbed to the culture substrata and non-conditioned serum-free (NC-SF) media to support the undifferentiated state. Compared to the cell-based feeder systems, ECM proteins offer several advantages, including reduced risk of pathogen transmission and relative ease of scale-up. The most exploited of these ECM analogues is Matrigel™, an extraction from Engelbreth–Holm–Swarm (EHS) mouse sarcomas that contains not only basement membrane components (laminin, collagen IV, heparin sulfate proteoglycans and entactin), but also matrix degrading enzymes, their inhibitors, and numerous growth factors (*see*, **Table 2.1** for composition used in hES cell culture).[14]

Table 2.1 Matrigel™ (Growth Factor Reduced) Composition[15]

Protein	Percentage (%)	Growth Factor	Concentration (ng/ml)
Laminin	61	bFGF	0-0.0001
Collagen IV	30	EGF	<0.5
Enactin	7	IGF-1	5
Heperan Sulfate Proteoglycan (mainly perlecan)	Not Available	PDGF	<0.005
		NGF	<0.2
		TGFβ	1.7

However, the ECM proteins used in these cultures systems are expensive, hard to produce in large enough quantities for widespread clinical use, exhibit lot to lot variability, introduce unwanted contaminants, and do not support self-renewal of some hES cell lines.[4 5]

The derivation, self-renewal, and differentiation of hES cells within a completely synthetic environment would offer significant advantages and progress towards a source of clinically usable hES cells. However, replacing the complex ECM components that hES cells require with a synthetic matrix has proven challenging, and Matrigel adsorbed to the cell culture surface in NC-SF media is still the best

currently available method to culture hES cells, in spite of the aforementioned limitations. In this work, we sought to characterize the physical properties of adsorbed Matrigel to aid in understanding the mechanisms by which hES cells interact with this complex mixture of ECM proteins. Ultimately, we envisage using this knowledge to engineer precise synthetic culture environments to control human stem cell behavior.

Accordingly, we have observed that hES cells behave differently when they are grown on Matrigel adsorbed onto different surfaces, suggesting that the adsorption of Matrigel and its resulting physical chemical properties may influence cell function. Three substrates have typically been used for mammalian cell culture platforms: borosilicate glass, polystyrene, and polystyrene treated with an oxygen plasma for tissue culture, i.e. tissue culture polystyrene (TCPS). Borosilicate glasses were the first platform used for cell culture, but with the advent of easily and cheaply manufactured clear, high strength plastics, such as polystyrene, glass was replaced as the cell culture platform. Initially, one of the leading manufacturers of plastics for cell culture, coated glass onto plastic, as it was empirically recognized that a hydrophilic surface was necessary for optimal cell growth.[16] Gas plasma treatments were subsequently developed to render polystyrene surfaces hydrophilic.[17] As such, tissue culture polystyrene and glass are both hydrophilic and have similar wetting properties, (water-in-air contact angle of TCPS ≤ 29°C and of glass ≤ 29°C).[18, 19] Despite those similarities, hES cells behave differently when they are grown on Matrigel adsorbed onto each surface. In this work, the room temperature gelling of Matrigel was replicated inside a quartz crystal microbalance. Quartz crystals with functionalized surfaces (i.e., SiO_2, polystyrene, and oxygen plasma treated polystyrene) were used to monitor the adsorption dynamics and viscoelastic properties of Matrigel. Scanning electron microscopy and ellipsometry were used to observe the topography and thickness of the adsorbed Matrigel, respectively. We correlated measured properties with observed hES cell behavior and determined that ECM proteins in Matrigel adsorb as viscoelastic multilayer networks, they have distinct morphology and density based on the underlying substrate, and they either promote self-renewal or differentiation depending on the network structure.

2.2 Methods and Materials

2.2.1 Reagents

All water used in this study was ultrapure ASTM type I reagent grade water (18.2 MΩ-cm. All glassware was cleaned by immersion in 2% CONTRAD 70 (Decon Labs Inc. King of Prussia, PA) in water for at least 2 hours. Following thorough rinsing, the glassware was baked dry at 120° C. Growth factor reduced Matrigel™ was obtained from BD Biosciences (Bedford, MA) (Table I). Matrigel at 2mg/mL was diluted into Knockout Dulbecco's Modified Eagle Medium (KO-DMEM) (Life Technologies) in two steps. In the first step the Matrigel was diluted into 5 mL of KO-DMEM and mixed thoroughly with a pipette, with caution to avoid bubbles. In

the second step, the diluted Matrigel was further diluted with 20 mL of KO-DMEM and thoroughly mixed with a pipette. Phosphate buffered saline (PBS) (Life Technologies) used was at pH 7.4 and it did not contain calcium chloride or magnesium chloride. Hellmanex (Hellma GmbH & Co. KG) was used at 2% concentration. Polystyrene, Mw ~ 197,000 with 1.05 polydispersity (Sigma-Aldrich) was diluted into HPLC grade toluene (Fisher Scientific) to form a 2 wt % solution for spin casting onto the substrates.

2.2.2 Matrigel Adsorption Studies

In this study, we replicated standard procedures for coating hES cell culture substrata with Matrigel. Matrigel was stored at -20°C until ready for use and was then diluted with Knockout Dulbecco's modified Eagle's minimal essential medium (KO-DMEM), for stem cell culture.[9] The diluted Matrigel (~0.067 mg/mL) was stored at 4°C in a liquid state. For cell culture, diluted Matrigel was pipetted onto the tissue culture surfaces and allowed to gel at room temperature for at least 30 minutes. Prior to cell seeding, the remaining liquid was removed with a pipette. Cells were then seeded and placed in an incubator at 37°C and 5% CO_2.

2.2.2.1 Surface Modification

Gold coated and Si/SiO_2 coated AT-cut quartz crystals (Qsense Inc., Glen Burnie, MD) and Si and SiO_2 wafers (International Wafer Service, Inc, Colfax, CA) were sonicated in the following solvents for 15 minutes: water, acetone, hexane, acetone, water. Crystals and wafers were then dried with nitrogen and exposed to an oxygen plasma at 0.5 Torr O_2 partial pressure and 75 W power for 5 minutes. The SiO_2 coated quartz crystals and SiO_2 wafers were not subjected to any further treatment prior to an adsorption experiment. To prepare the polystyrene surfaces, 2mL of 2 wt% polystyrene in toluene was spun cast onto the topside of a quartz crystal (for QCM-D) or a Si wafer (for ellipsometry and scanning electron microscopy) with a Headway Research Spincaster (model PWM32). Toluene was dropped onto the gold crystals/Si wafers, which were then spun at 2000 rpm for 1 minute to evaporate the toluene. Subsequently, 2 mL of 2 wt% polystyrene solution was dropped onto the center of the topside of the gold crystals/Si wafers, which were then spun at 2000 rpm for 1 minute. The backside of the gold crystals were cleaned with a toluene soaked q-tip (to ensure the backside electrode was not coated in polystyrene). The gold crystals/Si wafers were annealed at 110°C for at least 24 hours. A spectroscopic reflectivity based thin film thickness measuring system (Filmetrics F120, San Diego, CA) was used to collect a reflectance spectrum for the polystyrene film and determine its thickness as ~ 100 nm. After annealing, untreated polystyrene coated crystals were immediately introduced into the QCM-D chamber, and untreated polystyrene coated Si wafers for were immediately coated with KO-DMEM diluted Matrigel for ellipsometry and SEM studies. Some of the polystyrene coated samples were treated to mimic tissue culture polystyrene by

exposure to an oxygen plasma at 0.5 Torr O_2 partial pressure and 75 W power for 30 seconds (Plasmod, Tegal Inc, Richmond CA). From the reflectance spectrum, it was determined that less than 15 nm of polystyrene was etched off of the crystal during this step. After treatment with oxygen plasma, the polystyrene coated crystals were immediately introduced into the QCM-D chamber and the oxygen plasma treated polystyrene coated Si wafers were immediately coated with KO-DMEM diluted Matrigel for ellipsometry and SEM studies.

2.2.2.2 Quartz Crystal Microbalance

A quartz crystal microbalance with dissipation monitoring QCM-D E4 (Q-Sense, Sweden) was used in this study and is described in detail elsewhere.[20] Briefly, an AC voltage is applied to the piezoelectric quartz crystal so that it oscillates in a shear mode at its resonant frequency. Only negative overtones can be excited electrically, and in the Qsense system, the first, third, fifth, seventh, ninth, eleventh, and thirteen overtones (designated as F1, F3, F5, F7, F9, F11, F13) are excited by sequentially by applying the associated voltage. The dampening factor, or the dissipation, which is defined as the inverse of the Q-factor, is the energy dissipated per oscillation divided by the total energy stored in the system. When the driving power is turned off, the decay from each overtone is recorded yielding the absolute values of the frequency (F1, F5, F7, F9, F11, F13) and dissipation of each overtone (D1, D3, D5, D7, D9, D11, D13). In this experiment F1 and D1 were ignored as they were not reliable.[20, 21]

Frequency and dissipation values were recorded in air for all crystals. All liquids were allowed to reach room temperature before introduction into the QCM-D chamber, which was set to 25°C. To obtain a baseline, PBS was introduced into the chamber at a rate of 200 μL/min and allowed to thermally equilibrate with the chamber. After ensuring a steady signal (drift less than 1 Hz/10 min on any normalized overtone), KO-DMEM diluted Matrigel was flowed through the chamber and allowed to adsorb onto the functionalized quartz crystal (i.e. SiO_2, polystyrene, or oxygen plasma treated polystyrene). After the adsorption was complete, PBS was flowed through the chamber at 200 μL/min until the signal was steady. Finally, the detergent Hellmanex was flowed through the chamber at 200 μL/min. Three crystals were prepared and measured for each substrate type.

2.2.2.3 Ellipsometry

Matrigel film thickness on each substrate (i.e., SiO_2, polystyrene, and oxygen plasma treated polystyrene) was determined by ellipsometry (Sentech SE400, HeNe laser λ = 632.8 nm, angle of incidence ϕ = 70°). A drop of KO-DMEM diluted Matrigel sufficient to cover the entire surface was deposited on appropriately treated wafers (i.e., SiO_2 no treatment, polystyrene coating, polystyrene coating and subsequent oxygen plasma treatment). The Matrigel was left to gel for at least 30 minutes prior to ellipsometry measurements. Measurements employed the following refractive indices for each surface: $n_{silicon} = 3.874–0.016i$ [22]; for the silicon

support; $n_{silicon\ oxide} = 1.457$ [22]; $n_{polystyrene} = 1.59$[23]; $n_{Matrigel} = 1.46$ [24] and, $n_{PBS} = 1.33$ [25]. The thicknesses of individual layers in the film were measured prior to deposition of subsequent layers. Hence, the thicknesses of the silicon oxide and polystyrene layers were accounted for independently from thickness values measured for the Matrigel. When the thickness of Matrigel was measured, PBS was continuously flowed at 8mL/min over the substrate, so as to keep the system hydrated, and details of the flow chamber used are described elsewhere.[25] It was necessary to keep the Matrigel hydrated during ellipsometry, as it had been observed that upon exposure to air Matrigel thin films dried out and contracted within minutes. Three surfaces were prepared and measured for each substrate type (i.e., SiO_2, polystyrene, oxygen plasma treated polystyrene).

2.2.2.4 Scanning Electron Microscope

Samples were imaged with a Hitachi S-5000 Scanning Electron Microscope with an acceleration voltage of 10 kV. A drop of KO-DMEM diluted Matrigel sufficient to cover the entire surface was deposited on appropriately treated wafers (i.e., SiO_2 no treatment, polystyrene coating, polystyrene coating and subsequent oxygen plasma treatment). Samples were left to gel for 30 minutes and then tilted to allow excess fluid above the Matrigel layer to slide off. The fluid was wicked off by a kimwipe. The Matrigel samples were then fixed in 2% glutaraldehyde in 0.1M Sodium cacodylate buffer, pH 7.2 for 2 hours. They were rinsed three times in 0.1M sodium cacodylate buffer, pH 7.2 for 15 minutes each rinse. Samples were then dehydrated in graded ethanol to 100%. Samples were critical point dried, mounted onto stubs, dried overnight, then sputter coated with gold prior to imaging.

2.2.2.5 Environmental Scanning Electron Microscopy

Samples were imaged with a Hitachi TM-1000 Scanning Electron Microscope with an acceleration voltage of 15 kV. A drop of KO-DMEM diluted Matrigel sufficient to cover the entire surface was deposited on appropriately treated wafers (i.e., SiO_2 no treatment, polystyrene coating, polystyrene coating and subsequent oxygen plasma treatment). Samples were left to gel for 30 minutes and then tilted to allow excess fluid above the Matrigel layer to slide off. The fluid was wicked off by a kimwipe, and samples were allowed to air dry.

2.2.2.6 Atomic Force Microscopy

Tapping mode Atomic Force Microscopy (AFM) images were recorded with a NanoForce IIIa AFM (Veeco) with high aspect ratio tips (Nanosensors, AR5-NCHR,aspect ratio > 5:1). A drop of KO-DMEM diluted Matrigel sufficient to cover the entire surface was deposited on appropriately treated wafers (i.e., SiO_2 no treatment, polystyrene coating, polystyrene coating and subsequent oxygen plasma treatment). Samples were left to gel for 30 minutes and then tilted to allow excess

fluid above the Matrigel layer to slide off. The fluid was wicked off by a kimwipe, and samples were imaged immediately or they were allowed to air dry.

2.2.3 Cell Culture

2.2.3.1 Human Embryonic Stem Cell Culture

Human embryonic stem cells (HSF-6, University of California at San Francisco, and H9 lines, Wicell, Madison, WI) were maintained on hES cell qualified Matrigel™ coated tissue culture treated polystyrene (TCPS) dishes in X-Vivo 10 medium (Lonza, Switzerland) supplemented with 80 ng/mL basic fibroblast growth factor (FGF-2, R&D Systems, Minneapolis MN) and 0.5 ng/mL transforming growth factor-beta1 (TGF-β1, R&D Systems). This medium has previously been found to support hES cell self-renewal over extended periods of time.[9, 26] Cells were passaged with 200 U/mL Collagenase IV (Invitrogen) and seeded at 100,000 cells/cm^2 on Matrigel-coated TCPS, polystyrene, and glass. The medium was exchanged every day on the samples.

2.2.3.2 Cell Attachment and Proliferation Studies

For attachment and proliferation studies, cells were seeded at 100,000 cells/cm^2 and grown on Matrigel-coated tissue culture polystyrene (TCPS), glass, or polystyrene (PS) for either 3 hours to assess attachment or 5 days for proliferation. Attachment studies were also performed at the same initial cell seeding densities on uncoated TCPS, glass, and PS surfaces. All coated and uncoated surfaces were washed once with phosphate-buffered saline (PBS) after the 3 hour incubation to remove unattached cells. Cell numbers for both studies were quantified with the Cyquant Cell Proliferation Kit (Invitrogen). Statistical significant differences were determined using ANOVA between samples with a Tukey-Kramer *post hoc* test with $p < 0.05$. Statistics were only computed for samples of the same cell line.

2.2.3.3 Immunocytochemistry

On the fifth day after seeding, immunocytochemistry was performed on the samples for the POU family transcription factor OCT-4 and for the cell surface marker SSEA-4, which are both highly specific and necessary markers for undifferentiated hES cells. Cells were fixed in 4% paraformaldehyde and then permeabilized with 0.1% Triton X-100. The cells were incubated with 0.5% SDS, blocked with 2% BSA, and first incubated with the Rabbit Oct-4 antibody (Abcam, Cambridge, MA) or SSEA-4 antibody (Millipore, Billerica, MA) overnight and then incubated with anti-Rabbit Alexa 546 or anti-Mouse Alexa 488 secondary antibodies (Invitrogen). DAPI (4',6-diamidino-2-phenylindole), a nuclear stain (Invitrogen) was added to the cells and then the cells were imaged.

2.2.3.4 Flow Cytometry

Oct-4 and SSEA-4 Expression were quantified with flow cytometry (Cytomics FC 500, Beckmann Coulter). For flow cytometry, cells were seeded and grown on Matrigel-coated TCPS, glass, or PS surfaces for 5 days. Cells were incubated with 2 mM EDTA in PBS for 10-15 minutes to dissociate cells into single cells.
Cells to be examined for Oct-4 expression were first fixed in 2% Formaldehyde in PBS for 20 minutes and washed with 2% Fetal Bovine Serum (FBS) (Invitrogen) in PBS twice. Cells were then permeabilized with 1 mg/mL Saponin (Fluka, St. Louis, MO) in 10% Bovine Serum Albumin dissolved in PBS (SPB) for 15 minutes, and then incubated with Oct-4 Antibody (Abcam) for 1 hour. Cells were washed with SPB then incubated with anti-Rabbit Alexa 488 antibody (Invitrogen) for 1 hour. Cells were then washed with SPB and then resuspended in 2% Fetal Bovine Serum (FBS) in PBS for analysis in a flow cytometer.

Cells to be examined for SSEA-4 were incubated with SSEA-4 Antibody (Millipore) for 30 minutes, immediately after the EDTA cell dissociation described above. Cells were washed in 2% FBS in PBS twice and then incubated with Anti-Mouse Alexa 488 (Invitrogen) for 30 minutes. Cells were then washed twice in 2% FBS in PBS and then resuspended in 2% FBS in PBS for analysis in a flow cytometer. Statistical significant differences for Oct-4 and SSEA-4 expression were determined using ANOVA between samples with a Tukey-Kramer *post hoc* test with $p < 0.05$. Statistics were only computed for samples of the same cell line.

2.3 Results and Discussion

2.3.1 Cellular Response: Proliferation and Differentiation

The initial attachment and growth of hES cells on Matrigel was influenced by the underlying substrate (**Figure 2.1**). In comparison to tissue culture polystyrene (TCPS) surfaces coated with Matrigel, glass and polystyrene (PS) surfaces coated with Matrigel exhibited less initial cell attachment (**Figure 2.1B**). For the HSF-6 cell line, we found that ~ 30% of the cells attached to the Matrigel-coated TCPS surface, while glass and PS surfaces had 15% and 20% of the cells attached after 3 hours, respectively. There was no detectable cell attachment on any substrate when Matrigel was absent from the surface. Since our culture medium was serum-free, and did not contain serum-derived products, there were no proteins in the media that could adsorb and promote cell attachment. The phase images of the two cell lines (HSF-6 and H9) grown on Matrigel adsorbed onto PS, glass, and TCPS **(Figure 2a**) and cell growth data (comparison of **Figures 2.1B** and **2.1C**) indicate that cells proliferated on Matrigel adsorbed onto hydrophilic surfaces (glass and TCPS), with the highest proliferation rates observed on TCPS. Matrigel adsorbed onto the hydrophobic surface, polystyrene, showed the greatest level of cell detachment during media exchange (comparison of **Figure 2.1B** and **2.1C**), rendering polystyrene a poor substrate for hES cell culturing. Additionally, Matrigel adsorbed onto PS and glass had a higher percentage of differentiated cells, than Matrigel

adsorbed onto TCPS, as can be seen by the increased presence of non-spherical cells in the phase images and in the low percentage of cells expressing the pluripotency markers Oct-4, a nuclear marker, and SSEA-4, a cell surface marker (**Figure 2.2** and **Figure 2.3**).

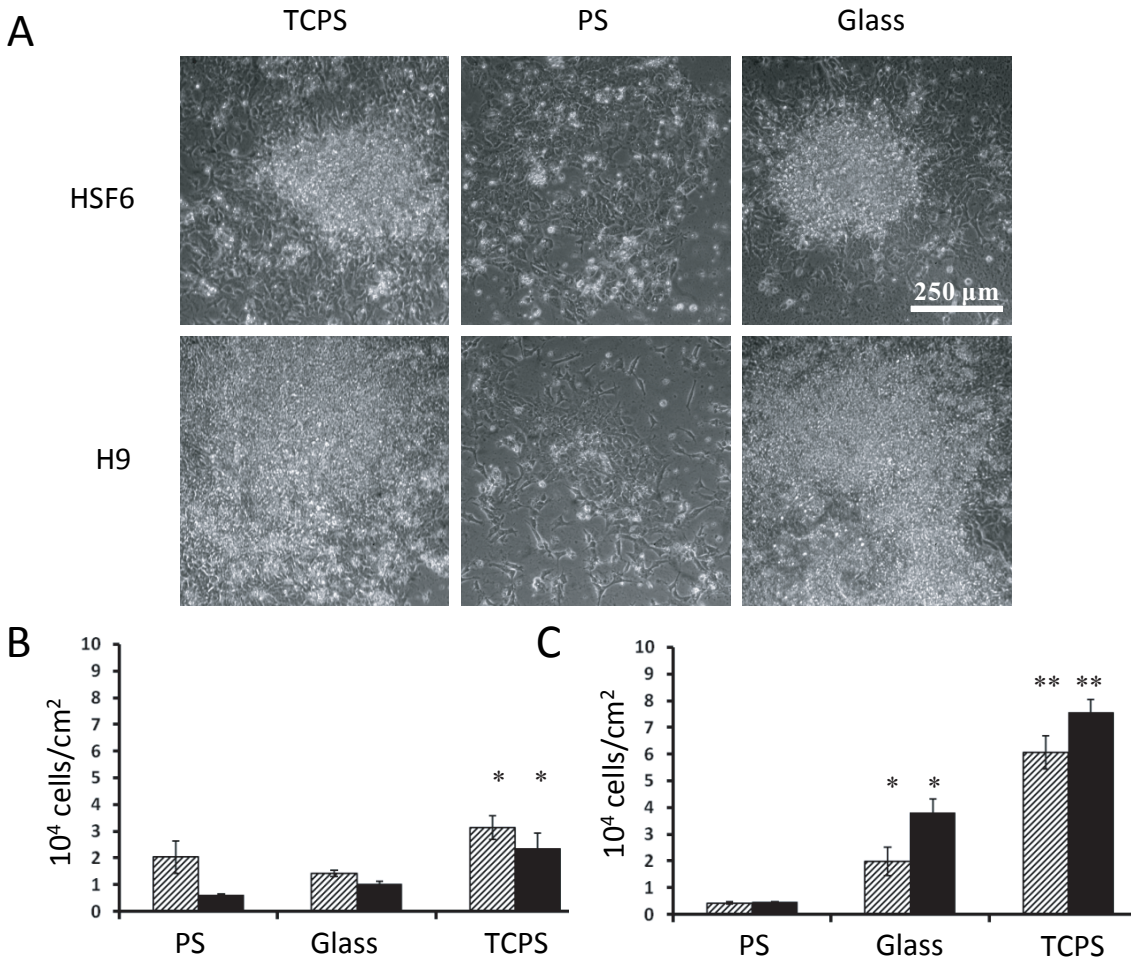

Figure 2.1 Phase images and proliferation of hES cells grown on Matrigel-coated tissue culture polystyrene (TCPS), polystyrene (PS), and glass. (a) After 5 days, both HSF-6 and H9 cells have colonies on TCPS indicated by closely packed cells. On PS, both cell lines differentiate to a larger extent as indicated by spread cells. On glass, both hES cell lines appear to have some colonies with morphology similar TCPS. Although these colonies do not have the typical hESC colony morphology seen with feeders, the exhibited morphology without colony borders is typical of some hESC lines on Matrigel.[6, 26] (b) Attachment of hESCs to TCPS, PS, and glass surfaces coated with Matrigel. After 3 hours, HSF-6 (◪) cells attached on Matrigel-coated TCPS at higher levels than on Matrigel-coated PS or glass. On surfaces without Matrigel, the amount of attached cells was below the detection level of the assay. Data represent mean ± standard deviation. Values not in the same group (*) were statistically different from one another ($p < 0.05$ using ANOVA between groups with Tukey-Kramer significant difference post hoc test). (c) After 5 days, both hES cell lines HSF-6 (◪) and H9 (■) had significantly higher cell proliferation on Matrigel-coated TCPS as compared to Matrigel-coated glass or Matrigel-coated PS. Values not in the same group (* or **) were statistically different from one another ($p < 0.05$ using ANOVA between groups with Tukey-Kramer significant difference post hoc test)

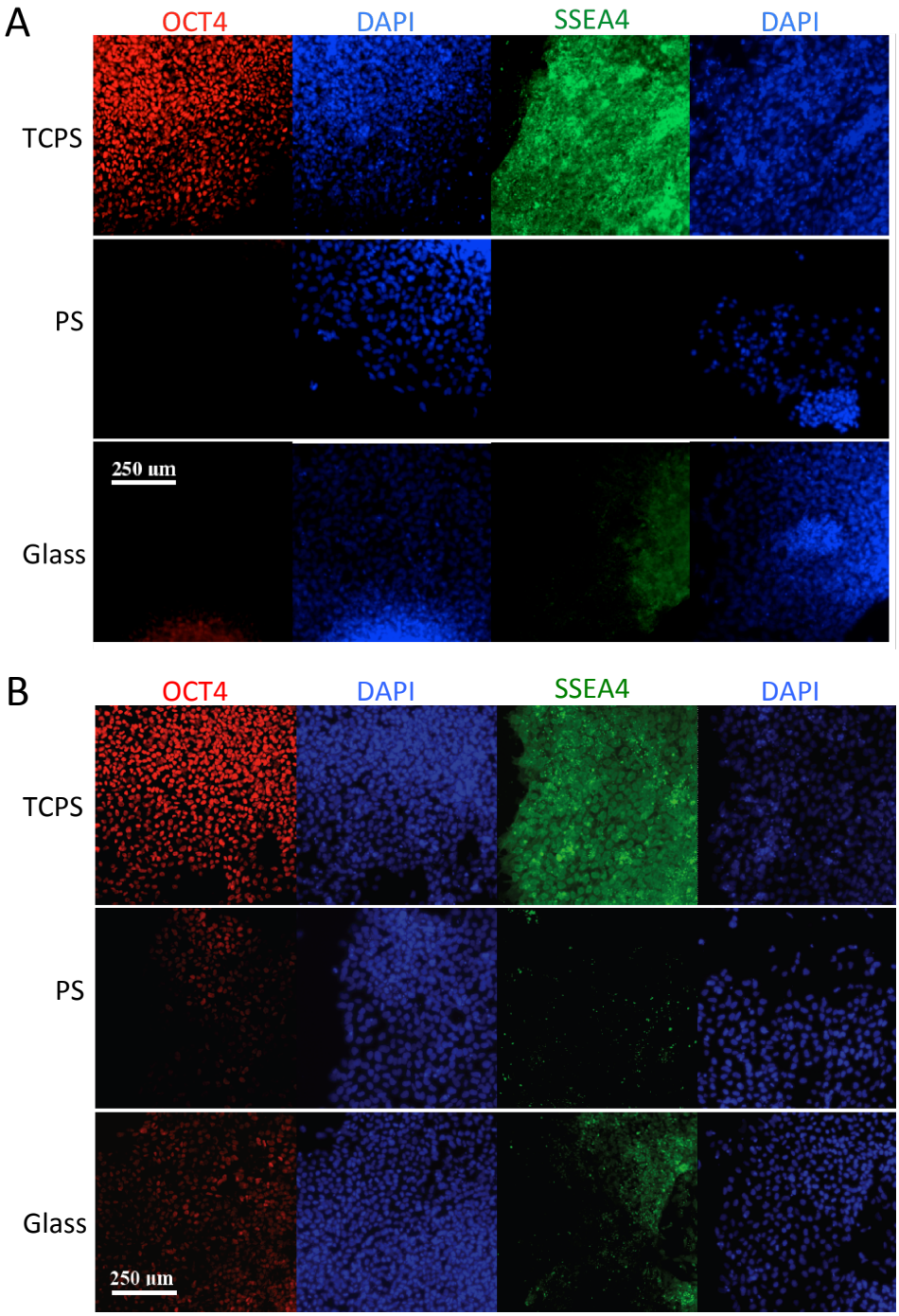

Figure 2.2 Immunocytochemistry for the embryonic stem cell markers Oct-4 and SSEA-4 on Matrigel coated tissue culture polystyrene (TCPS), polystyrene (PS), and glass with the (A) HSF6 cell line and the (B) H9 cell line.

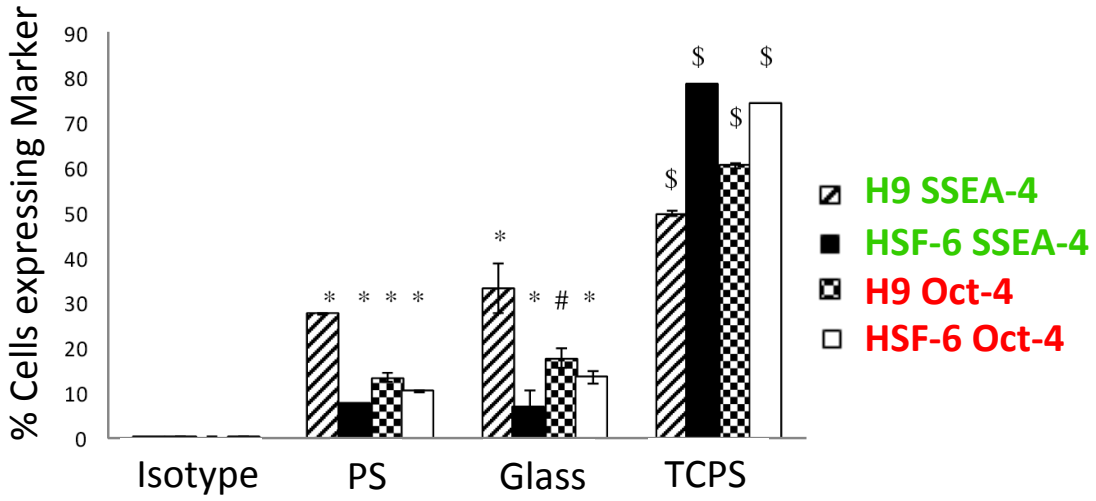

Figure 2.3 Quantification of SSEA-4 and Oct-4 via flow cytometry for cells cultured on Matrigel-coated surfaces, after 5 days of culture for H9 and HSF-6 cell lines. Matrigel-coated TCPS showed the largest percentage of cells expressing SSEA-4 for both hES cell lines H9 ( ) and HSF-6 ( ), as compared to Matrigel-coated PS and Matrigel-coated glass which showed a lower, statistically similar amount of cells expressing SSEA-4. Matrigel-coated TCPS also showed the largest percentage of cells expressing Oct-4 for both hES cell lines: H9 ( ) and HSF-6 ( ). The H9 cell line showed significantly more Oct-4 expression on Matrigel-coated glass than on Matrigel-coated PS, but HSF-6 showed similar levels of expression on those two surfaces. Values not in the same group (*, #, or $) were statistically different from one another ($p < 0.05$ using ANOVA between groups with Tukey-Kramer significant difference post hoc test). Only samples within the same cell line and for the same marker were compared statistically.

2.3.2 Physio-chemical Characterization of Matrigel

To better understand the cell proliferation and differentiation observations, the adsorption and film properties of Matrigel on the varying substrates were characterized by ellipsometry, QCM-D, SEM, environmental SEM, and atomic force microscopy (AFM). Sessile drop contact angle measurements of the prepared surfaces were performed with water in air and results, demonstrating the similar hydrophilicity of oxygen plasma treated polystyrene and glass are reported in **Table 2.2**.

Table 2.2 Sessile Water-in-Air Contact Angles of Test Surfaces

Substrate	θ_{H_2O}
Untreated Glass slide, SiO_2	28
SiO_2 coated quartz crystal rinsed in water after toluene exposure	78
SiO_2 coated quartz crystal immersed in water bath for 30 minutes after toluene exposure	26
SiO_2 coated quartz crystal immersed in water bath over 24 hours	14
SiO_2 coated quartz crystal treated with O_2 plasma	<10
Polystyrene coated quartz crystal	91
Oxygen plasma treated polystyrene coated quartz crystal	<10

Adsorbed Matrigel displayed similar thicknesses on all three surfaces, with polystyrene showing the thickest Matrigel layer, and oxygen plasma treated polystyrene surfaces showing the greatest variability in Matrigel film thickness (**Table 2.3**).

Table 2.3 Adsorption Properties of Matrigel™

	Polystyrene (n=3)	**SiO_2 (n=3)**	**Oxygen Plasma treated SiO2 (n=3)**
Thickness (nm) †	453.6 ± 2.6	430.4 ± 1.6	432.9 ± 31.0
Maximum ΔF7/7 *	-51.7 ± 3.3	-171 ± 1.0	-211.5 ± 0.8
Maximum ΔD7 *	10.7 ± 0.4	44.1 ± 0.8	45.6 ± 0.7
Maximum (ΔF7/7) / (ΔD7) *	4.82 ± 0.2	3.88 ± 0.1	4.64 ± 0.1

† From ellipsometry; * after PBS wash

The assumption, when modeling ellipsometry data, is that of flat homogenous interfaces, and from SEM images (**Figure 2.4A-C**), it is evident that oxygen plasma treated polystyrene has a rougher surface than polystyrene or SiO_2, thus leading to the higher expected variability in Matrigel film thickness on that surface. The ellipsometry results also indicate that the ECM proteins in Matrigel form an adsorbed layer approximately two orders of magnitude greater in thickness than a typical protein monolayer[27], implying that the proteins form a multilayer, most likely an associative network or gel.

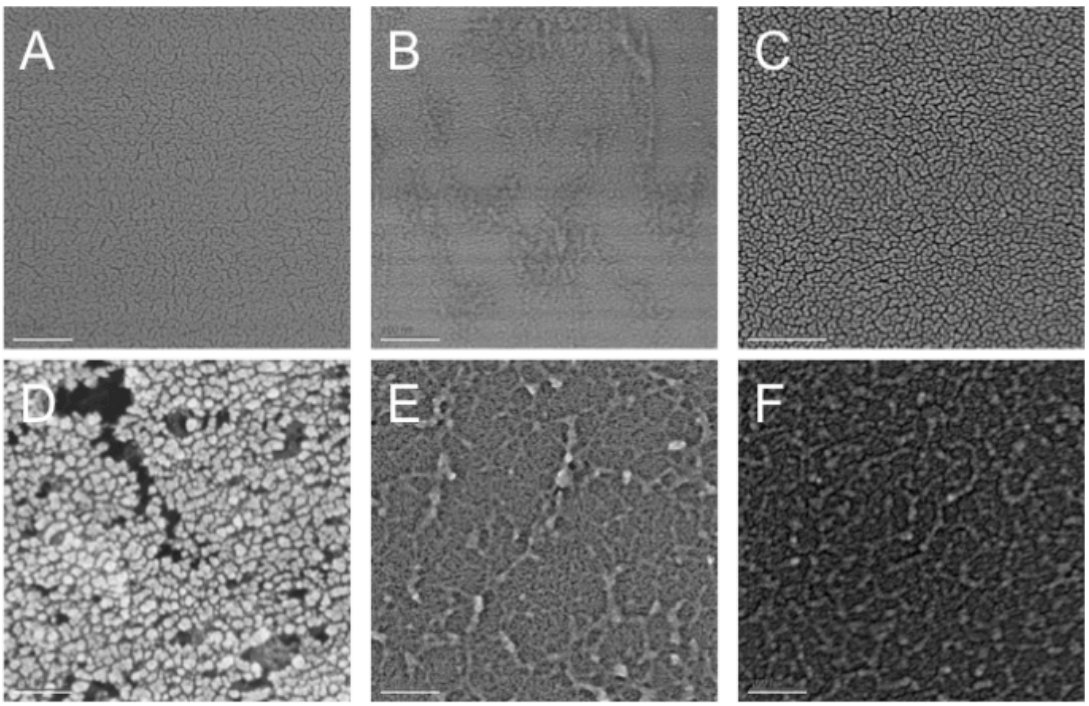

Figure 2.4 SEM of bare substrates and substrates with Matrigel. Scale bar = 100 nm. A-C bare substrates. (A) polystyrene (B) oxygen treated polystyrene (C) is glass. D-F adsorbed Matrigel (D) Matrigel on polystyrene (E) Matrigel on oxygen plasma treated polystyrene (F) Matrigel on glass.

We sought to confirm the gel nature of the Matrigel films with QCM-D. If Matrigel behaved as a rigid thin elastic film (such as an idealized protein monolayer), the change in resonant frequency (Δf) of the quartz crystal upon Matrigel adsorption would be directly proportional to the change in mass, and the change in mass could be calculated from the Sauerbrey equation:

$$\Delta m = C\Delta f/n \qquad \textbf{Eq. 2.1}$$

where m is the mass, f/n is the normalized resonant frequency overtone and C is a constant which depends on the density, shear modulus, and transverse wave velocity in the crystal. [28] **Figure 2.5** displays the frequency and dissipation responses of the functionalized (i.e. SiO_2, polystyrene, and oxygen plasma treated polystyrene) quartz crystals during the Matrigel adsorption experiment. Two features in those response curves indicate that Matrigel must be forming a gel on all three substrates. The first notable feature indicating that Matrigel is viscoelastic is the high dissipation (ΔD) of the film on all three surfaces. For monolayer protein films, which can be considered elastic, typical ΔD values are on the order of 1E-6.[29] In contrast, ΔD was greater than 1.5E-5 for Matrigel films on all surfaces (relative to the baseline of PBS on the crystal), and Matrigel on glass and oxygen plasma treated polystyrene surfaces showed ΔD values as high as 5E-5. Additionally, when a film is rigid and elastic, the normalized overtones will overlap; however, the normalized

overtones do not overlap for any of the surfaces (**Figure 2.5**). Therefore, on all of the surfaces tested, Matrigel forms an associative network or gel, and not a monolayer of mixed proteins.

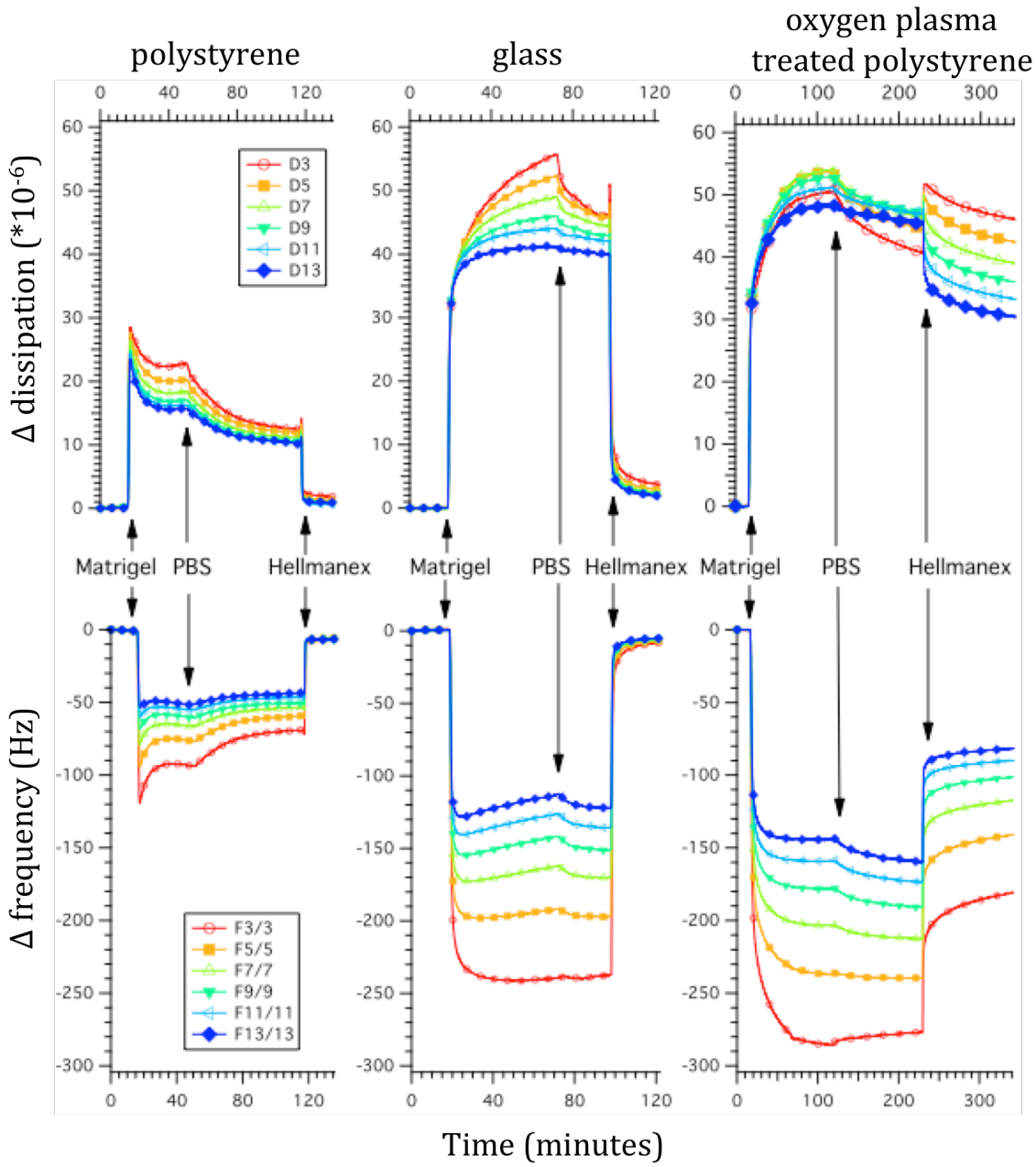

Figure 2.5 Frequency and dissipation responses to the experimental procedure on all three surfaces probed. Baseline frequency and dissipation were established with PBS flowing on the QCM-D crystal. Matrigel was then flowed over the quartz crystal until it saturated the surface. After maximum adsorption had been achieved, the crystal was rinsed with PBS. For the last step, the crystal was rinsed with the detergent Hellmanex. The arrows and letters indicate when each step occurred (M = Matrigel; P = PBS; H = Hellmanex).

For a viscoelastic film, such as Matrigel, the Voigt model can be used to describe the complex shear modulus such that

$$G^* = G' + iG'' = \mu_f + i2\pi f\eta_f = \mu_f(1 + i2\pi f\tau) \quad \textbf{Eq. 2.2}$$

where G' is the storage modulus and G" is the loss modulus, μ_f is the elastic shear modulus (storage modulus) of the film, η_f is the shear viscosity, f is the oscillation frequency and τ is the characteristic relaxation time of the film (which is proportional to the frequency and inversely proportional to the dissipation). Voinova *et al.* have shown that when a viscoelastic film, under a semi-infinite bulk Newtonian liquid, has a shear acoustic wave applied to it (via elastic quartz below it), the change in resonant frequency and dissipation can be related to the film properties (thickness, density, elastic modulus, and viscosity) and to the bulk fluid properties (density, viscosity).[30] However, since the viscosity and density of our Matrigel films are unknown, it was not possible to reliably deduce thickness or modulus from the frequency and dissipation data from the QCM-D experiments. In fact, our SEM images demonstrate that the density of Matrigel is not identical on the three surfaces (**Figures 2.4D-F**). Nevertheless, comparing information on the trends in frequency and dissipation changes during the Matrigel adsorption experiment can still provide useful information.

One useful metric for comparing structural information from QCM-D data is the relationship $\Delta F/\Delta D$. We used the 7th overtone to show representative data and trends. Matrigel adsorbed onto glass and onto oxygen plasma treated polystyrene had similar thicknesses as determined by ellipsometry, and similar dissipation values at maximum adsorption (**Table 2.3**). However, $\Delta F/\Delta D$ at maximum adsorption was different for the two surfaces, with the ratio $\Delta F/\Delta D$ larger for oxygen plasma treated polystyrene than for glass (**Table 2.3**). Since thickness and dissipation were similar for the two surfaces, this indicates that either the elastic modulus, the viscosity, and/or the density differs for the two surfaces, supporting the notion that Matrigel has a different structure on glass than it does on oxygen plasma treated polystyrene, potentially leading to the varied cell behavior observed on those surfaces.

Examining the change in frequency and dissipation for the adsorption of Matrigel films on the varying substrates, it was seen that the kinetics of adsorption depended on the substrate (**Figure 2.6A** and **Table 2.4**). The kinetics of Matrigel adsorption were characterized by the time required to reach 75% of the maximum adsorption in the frequency curves (prior to any wash step). Matrigel adsorption was 4 times faster on glass than on oxygen plasma treated polystyrene surfaces. On polystyrene, a rapid initial adsorption was followed by an immediate desorption (prior to any rinse step) (**Figure 2.5**) indicative of the weak and somewhat reversible bonds between Matrigel and the hydrophobic surface. Since the concentration of Matrigel flowed over each surface was identical, we assumed that the effective diffusivity of proteins in Matrigel was the same for each experiment and that differences in time to maximum adsorption could therefore only reflect differences in either an initial affinity to the surface, surface restructuring based on

conformation changes in the adsorbed proteins, or exchange reactions (i.e., the Vroman effect, in which proteins with a lower bulk concentration and a higher affinity for the surface will replace proteins with higher bulk concentration and lower surface affinity that reached the surface first).[31] If the initial affinity had been dominant in contributing to the differences in adsorption times, then we would expect the surface with the fastest adsorption time to have the strongest bonds with Matrigel. In fact, we saw the opposite phenomenon: the oxygen plasma treated polystyrene, which demonstrated the slowest adsorption kinetics, displayed the highest resistance to the Hellmanex (surfactant) rinse.

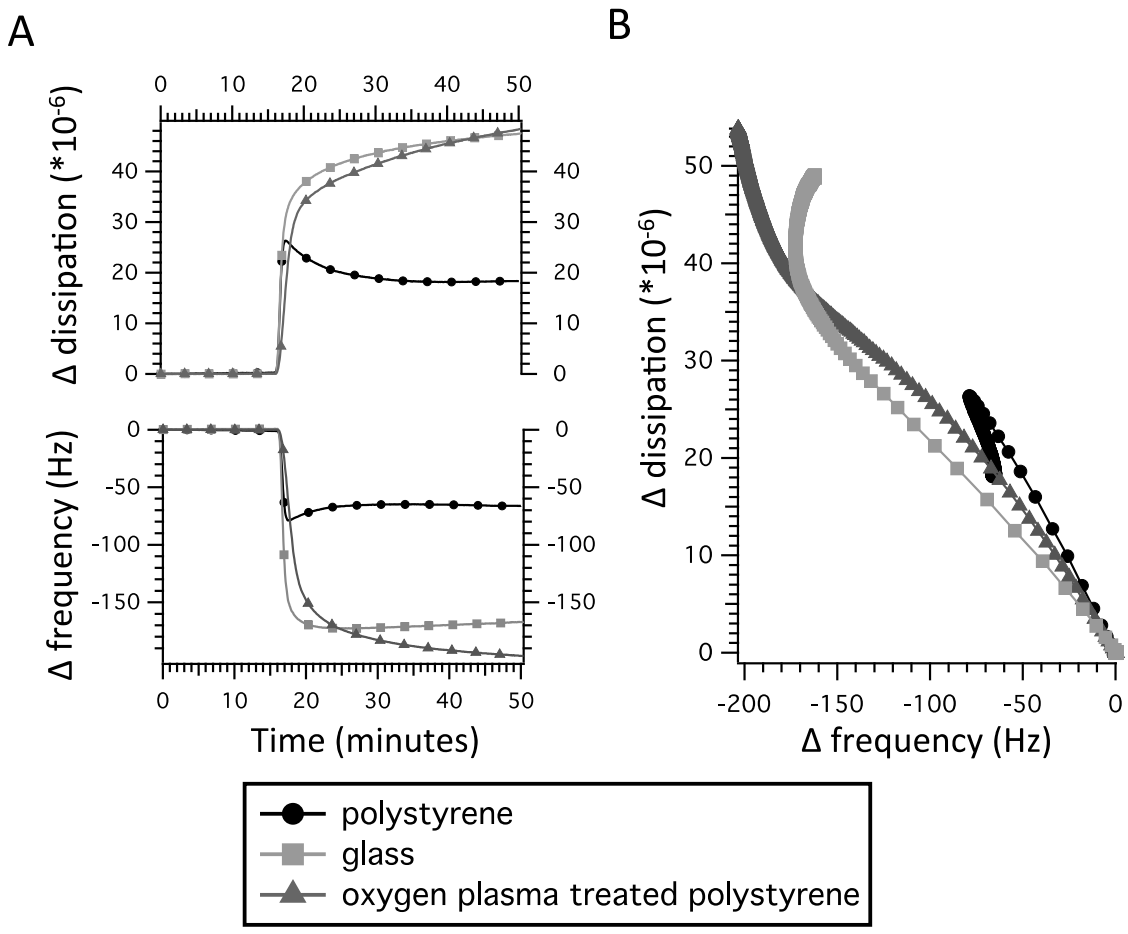

Figure 2.6 Differences in kinetics of adsorption and conformation of Matrigel on the three surfaces are manifest in the adsorption rates (A) and ΔF-ΔD plots for adsorption (B)

Table 2.4 Kinetics of Matrigel™ adsorption and effect of rinsing on network stability

	Polystyrene (n=3)	**SiO_2 (n=3)**	**Oxygen Plasma treated SiO2 (n=3)**
Time to 75% adsorption (sec)	**	62.0 ± 0.1	255.7 ± 8.3
Hellmanex rinse final ΔF7/7	-4.2 ± 1.8 (8.1%)	-4.1 ± 4.4 (2.4%)	-118.6 ± 2.4 (55.4%)
Hellmanex rinse final ΔD7	0.3 ± 0.5 (3.4%)	3.7 ± 1.9 (8.4%)	39.1 ± 0.6 (83.3%)

** The adsorption curve showed a rapid initial adsorption followed by an immediate desorption prior to any wash steps (see **Figure 2.5**) rendering the time to 75% adsorption unclear for the polystyrene surface

To assess whether the adsorption event contained structural changes in the protein network, ΔF-ΔD plots were constructed, where a change in slope would indicate a change in structuring, or potentially a Vroman effect behavior.[29] The simplest ΔF-ΔD plot for protein monolayer adsorption exhibits a linear relationship. None of the surfaces examined showed a linear relationship for the entire adsorption range (**figure 2.6B**). Both polystyrene and glass exhibited an initial linear region (at low frequency and low dissipation) followed by a non-monotonic region. For polystyrene this feature may indicate either an initial desorption (both frequency and dissipation decrease right after adsorption) or a conformational change in the ECM proteins, where the proteins unfold to expose hydrophobic regions to dehydrate the interface and minimize interfacial free energy. Oxygen plasma treated polystyrene, exhibits linearity only at very low frequency/dissipation values and then at high frequency/high dissipation. Even though glass and oxygen treated polystyrene are hydrophilic surfaces, the differences in adsorption rate and ΔF-ΔD plots indicate that they structure Matrigel in a different manner.

We also observed that the surfaces had different responses to elution buffers. On the polystyrene surface, the PBS wash decreased both the magnitude of the frequency and dissipation responses (ΔF and ΔD), while on the hydrophilic surfaces (glass and oxygen plasma treated polystyrene) the magnitude of the frequency increased while the magnitude of the dissipation decreased (**Figure 2.5**). It is likely that the PBS removed loosely adhered proteins on the polystyrene, hence a decrease in both parameters. It is less clear how the PBS rinse affected the hydrophilic Matrigel-coated surfaces, however we believe that PBS controls the swelling of Matrigel on those surfaces. This interpretation of the data is supported by the SEM images (**Figure 2.4**), which show that Matrigel on polystyrene forms a structure composed of globules, while Matrigel on hydrophilic surfaces forms a fibrillar network. When the Matrigel proteins deposit on polystyrene they presumably change conformation to expose hydrophobic pockets and expel water. Ultimately, the associative gel composed of those proteins will have exposed hydrophobic areas and resist water uptake, yielding a more compressed and rigid structure in PBS

(which can be seen in the low dissipation values). The hydrophilic surfaces (glass and oxygen plasma treated polystyrene) both have fibrillar structures reminiscent of protein hydrogels, and large dissipation values implying that they are soft, which can be a consequence of associated water.[32] If adsorbed Matrigel acts a hydrogel, it is likely that PBS controls its swelling behavior.

The most pronounced difference between the hydrophilic surfaces was the response of Matrigel to the Hellmanex wash (**Figure 2.5**). Hellmanex is composed of wetting agents, emulsifiers, ampholytic surfactants, complexing agents and potassium phosphate. The ease with which Hellmanex can remove Matrigel from a surface can be indicative of the strength of the gel structure of Matrigel and/or the bonding strength between Matrigel and the underlying substrate. Hellmanex was able to remove nearly all the Matrigel on the polystyrene and glass surfaces (**Figure 2.5 and Table 2.4**), as indicated by the frequency and dissipation reaching near baseline values on those surfaces after the Hellmanex wash. In contrast, the oxygen plasma treated polystyrene showed a markedly smaller response to the Hellmanex wash, with 55.4% of the adsorption frequency and 83.3% of the adsorption dissipation remaining after the wash. The inability of the surfactant to remove most of the protein network on the oxygen plasma treated polystyrene surface leads us to believe that the interface and part of the gel structure involve strong nearly irreversible bonds. Considering that the Matrigel-substrate interfacial bond varies drastically with substrate type, we suggest that ECM proteins in Matrigel orient differently at the interface with each substrate, exposing different proteins and/or chemical moieties, depending on the topography and chemistry of the substrate, and that the initial protein deposition affects gel formation, ultimately leading to the varied cell behaviors observed. Ideally it would be informative to measure the composition of Matrigel adsorbed to each surface. However, this is an impossible task as Matrigel contains over a 1,000 different proteins[33], and therefore techniques do not exist to give a quantitative measurement of composition of the adsorbed proteins.

To determine how the underlying substrate affects the Matrigel-liquid interface (i.e., the surface which cells interrogate), scanning electron microscopy and atomic force microscopy was performed on all three surfaces with Matrigel. Environmental Scanning Electron Microscopy (ESEM) and Atomic Force Microscopy(AFM). The later two modes relied on air drying of Matrigel, which introduced artifacts into the images. Drying lead to salt dendrites, which were visible in both the AFM images **(Appendix Figure AF.1)** and the ESEM images **(Appendix Figure AF.2).**

In order to avoid the artifacts introduced by drying, samples were fixed, dehydrated, critical point dried, and sputter coated to maintain their secondary structure for high vacuum SEM imaging and without Matrigel **(Figure 2.4).** Polystyrene and glass surfaces were both smoother than oxygen treated polystyrene surfaces **(Figure 2.4A-C).** It is possible that the differences in topography between oxygen plasma treated polystyrene and glass, in addition to the differences in chemistry, affect Matrigel adsorption. On the polystyrene surface, Matrigel forms a porous structure made up of globular units. On both the glass surface and the oxygen plasma treated polystyrene, Matrigel is characterized by a fibrillar and less

globular structure. Adsorbed ECM proteins may need to form a fibrillar network in order to support hES cell attachment, as cells attach readily on Matrigel that has been adsorbed onto either oxygen treated polystyrene or glass, but not onto Matrigel adsorbed onto untreated polystyrene. Even though both hydrophilic surfaces caused Matrigel to form a fibrillar structure, the Matrigel network that formed on SiO_2 was a morphologically distinct, denser network than the network that formed on oxygen treated polystyrene. We therefore conclude that the differences observed for cell proliferation and differentiation on Matrigel adsorbed onto the hydrophilic surfaces were due to differences in Matrigel structuring on each surface. As we have shown with QCM-D and SEM, the density and the mechanical properties of Matrigel were not identical on the two surfaces. The density of the structure affects cell fate by dictating the distance between chemical moieties and ligands, ultimately controlling internal cell signaling.[34-38] Many studies have also demonstrated the link between the mechanical environment surrounding the cell (i.e., the extracellular matrix) and internal cell signaling,[39-42] specifically linking the mechanical properties of the ECM with cell proliferation[43, 44] and differentiation[45-47]. It is therefore, not surprising that differing structures of Matrigel on the examined substrates lead to differing cell fates.

2.4 Conclusions

We found that human embryonic stem cells respond differently to Matrigel treated surfaces depending on the underlying substrate, and our findings may be exploited as design parameters for the development of artificial ECM systems for human embryonic stem cell culture. Hydrophobic substrates did not support the attachment and proliferation of human embryonic stem cells, and we correlated this observation with Matrigel adsorption behavior. Additionally, we have shown that despite the similar wetting properties of glass and oxygen plasma treated polystyrene, Matrigel exhibits differing mechanical properties, film stability, and structure on those surfaces, ultimately leading to enhanced cell proliferation and maintenance of the pluripotent state on Matrigel-coated oxygen plasma treated polystyrene relative to Matrigel-coated glass.

Chapter 3
Developing Mechanically Tunable Chemically Patternable Substrates for cell culture

3.1 Introduction
- 3.1.1 Need for Chemically Patterned Mechanically Tunable Substrates
  - 3.1.1.1 Limits of Current Alternative hES cell Culture Platforms
  - 3.1.1.2 Mechanical Environment
  - 3.1.1.3 Colony Size
- 3.1.2 Existing Hydrogel Patterning Technologies and their Limitations

3.2 Overview of UV-activated hydrogel printing
- 3.2.1 Materials Selection
  - 3.2.1.1 Polyacrylamide System
  - 3.2.1.2. Sulfo-SANPAH
  - 3.2.1.4 Adhesive Ligands
- 3.2.2 Methods
  - 3.2.2.1 Polyacrylamide Gels
  - 3.2.2.2 Photolithography
  - 3.2.2.3 Fibronectin
  - 3.2.2.4 Cell Culture
- 3.2.3 Results and Discussion
  - 3.2.3.1 Quartz Substrate
  - 3.2.3.2 Acrylamide Protein Resistance
  - 3.2.3.3 Crosslinker and Buffer properties
  - 3.2.3.4 Concentration of Fibronectin
  - 3.2.3.5 Photolithography
  - 3.2.3.6 Sterility
  - 3.2.3.7 Summary of Patterning Protocol
  - 3.2.3.8 Patterning with 3T3s

3.3 Modulating the Fouling Behavior of Acrylamide with PEG
- 3.3.1 Introduction
- 3.3.2 Methods and Materials
- 3.3.3. Results and discussion

3.4 Patterning Acrylamide with Adhesion Peptides
- 3.4.1 Introduction
- 3.4.2 Methods and Materials
- 3.4.3 Results and discussion

3.5 Alternative Patterning Methodologies Explored
- 3.5.1 Photomask
  - 3.5.1 Methods and Materials
  - 3.5.2 Results and Discussion
- 3.5.2 Stamping with Protein Ink

3.6 Conclusions and Future Work

3.1 Introduction

As discussed in chapter 2, the heavy reliance on animal products in the current human embryonic stem cell and induced pluripotent stem cell culture methodologies, severely hinders the clinical feasibility of using these cells for regenerative medicine. The hindrance is due to the lot-to-lot variability of biological products, the difficulty in scale up, and the introduction of non-human proteins and sugars, which may become present on or within the cells, and illicit immune responses in the recipients of the cells. Towards that end, we are looking to both standardize the culture system and eliminate non-human products.

3.1.1 Need for Chemically Patterned Mechanically Tunable Substrates for Human Stem Cell Culture

In order to overcome the shortcomings of the feeder layer and Matrigel hES cell culture systems discussed in chapter 2, we sought to create a synthetic surface upon which to culture and maintain the pluripotency of hES cells.

3.1.1.1 Limits of Current Alternative hES Cell Culture Platforms

A number of groups have been working towards synthetic or standardized surfaces upon which to grow hES cells, but all current available surfaces have some substantial shortcomings, which the mechanically tunable, chemically patternable system described herein can improve upon.

To avoid using Matrigel, attempts at creating synthetic substrates have been explored by several groups. The first synthetic surfaces created could support hES cell attachment for a few days, but not for many passages.[1-3] More recently, a number of groups have sought to create surfaces, which could support stem cell expansion for multiple passages.[4-6] However, there is room for improvement in these reported systems. For example, the synthetic surface constructed by Villa-Diaz et al.,[6] poly[poly(ethylene glycol) methyl ether methacrylate] (PMEDSAH) was only successful in MEF (mouse embryonic fibroblast) conditioned media for 25 passages of one cell line. When the authors attempted to replace the MEF-conditioned media with human conditioned media, which is still not a defined product, the two hES cell lines evaluated could be passaged 15 times, but the number of cells adhering to each surface was dramatically different for each cell line. When the authors lastly used their surface in non-conditioned media, they found that neither cell line could be passaged with the defined media mTeSR, while only one line could be passaged for 10 passages in ProStem media. These results are not surprising given that the PMEDSAH surface has no biological functionality, requiring the media to mediate the cellular response to the surface. In order to avoid that pitfall, some groups have tried tethering peptides to synthetic surfaces, but there was significant variability in results such as doubling time (30-90 hours) and oct-4 expressions (ranging from 65-95%) regardless of media and cell line examined.[4]

There are two parameters, which we believe can be engineered into these synthetic stem cell culture systems to improve the currently available synthetic technologies. We believe that creating a synthetic surface that mimics the modulus the cells may experience in vivo may increase the percentage of cells expressing oct-4, as this effect has been demonstrated in mES cell culture.[7] Additionally, we believe that controlling colony size may decrease the variability in hES cell performance in terms of doubling rate and stem marker expression. Using the micropatterning system described in the qualifying exam proposal, these two parameters (modulus and colony size) can be controlled independently.

3.1.1.2 Mechanical Environment

Cells have been historically cultured and studied on stiff surfaces such as glass and tissue culture polystyrene, whose elastic moduli are in the GPa range - at least an order of magnitude stiffer than the stiffest tissue in the body (bone), and eight orders of magnitude stiffer than the most compliant tissues in the body (brain and fat) [8, 9]. In the last few decades, scientists have appreciated the role of the mechanical environment on cellular behavior and they have sought techniques to make softer and specifically tunable stiffness surfaces upon which to culture and study cells. Recent studies have demonstrated the link between the mechanical environment surrounding the cell (i.e., the extracellular matrix (ECM)) and internal cell signaling,[10-13] specifically linking the mechanical properties of the ECM with cell proliferation[14, 15] and differentiation.[16-18] In fact, quiet a number of thorough review papers exist summarizing all the research to date on the impact of the mechanical environment on cell behavior.[8, 9] Two notable reports demonstrated that adult stem cells could be directed down specifically cell lineages, while keeping the cell culture media constant, merely by changing the stiffness of the polyacrylamide gel substrate upon which the cells were grown.[19, 20]

Independent of species, there is a paucity of data on the effect of mechanical environment on embryonic stem cells. Currently, there is one paper regarding the effect of mechanical environment on mouse embryonic stem cells, and there are no reports for human embryonic stem cells.[7] In that report, mouse embryonic stem cells were cultured on collagen conjugated polyacrylamide gels of varying stiffness and the authors noticed that on 1 kPa polyacrylamide gels the cells maintained pluripotency markers in the absence of Leukemia Inhibitory Factor (LIF) (a factor believed to be required for the maintenance of mouse embryonic stem cells),[21, 22] while cells on stiffer surfaces differentiated. This exact experiment has not been performed with human embryonic stem cells, as LIF, in contrast to mouse cells ,is not required to maintain pluripotency in human cells.[21, 22] However it is possible that growing hES cells on softer surfaces can change which transcriptional factors are required to maintain pluripotency in hES cells.

For either maintaining pluripotency or for directed differentiation of human pluripotent stem (hPS) cell applications, one hypothesis is to match the stiffness of the underlying substrate to that of the tissue it is meant to mimic. In the human body the relevant range of moduli spans 10Pa (fat) to 100MPa (bone).[8]

For the application of maintaining the pluripotency of hES cells, one would want to create gels that mimic the stiffness of the inner cell mass (ICM) of the embryo. It does not appear as though there is any work to date characterizing the modulus of a human embryo, or any other mammalian embryo, however some work has been done to characterize the stiffness of amphibian embryos, specifically frogs.[23-25] The authors of these works used micropipetting techniques to measure the stiffness of the frog embryos in the gastrulation stages and found moduli ranging from 10-100 Pa, which is significantly lower than stiffness of tissue culture polystyrene (~GPa).

Additionally, one can attempt to construct gels with moduli mirroring those of the ECM or Matrigel. A number of groups have attempted to measure the elastic and shear moduli of Matrigel with AFM and rheometry respectively. There is a variation in values determined, with shear moduli reported at about 50 Pa[26, 27] and elastic moduli reported at 120-650 Pa.[28-30] Soofi et al.[30] reported elastic moduli of ~ 450 Pa but the standard deviations were approximately 200 Pa, with one lot having some spots with elastic moduli in the kPa region. The variation may be due to differences in sample preparation, Matrigel concentration used, temperature of testing, the localness of testing methodology, and Matrigel lot-lot variability. This range, which coincides with that of the frog embryos however, does provide a good starting point for moduli to employ in the printed hydrogel stem cell culture systems described herein.

3.1.1.3 Colony Size

In addition to mechanical cues, paracrine and juxtacrine signaling between cells is known to regulate cell fate. Paracrine and juxtacrine signaling are particularly important in controlling morphogenesis and development, so they are parameters which should be considered when designing embryonic cell culture systems. Peter Zandstra's group has tried to control these signals by controlling hES cell colony size, by patterning Matrigel onto TCPS via microcontact printing.[31-33] They generated islands varying in size from 200-800 μm separated by 500 or 1000 μm. After growing hES cells in X-vivo media for 48 hours without the addition of any exogenous growth factors, such as TGFβ and FGF which are required in order to maintain pluripotency, they observed that a larger percentage of cells in smaller colonies underwent differentiation as indicated by increased expression of psmad1.[31] Additionally, they demonstrated that colony size affected hES cell differentiation into mesoderm or endoderm lineage when grown on microcontact printed Matrigel islands in the presence of Activin A and BMP.[32, 33] Larger colonies showed higher expression of mesoderm markers than smaller colonies, and smaller colonies showed a higher expression of endoderm markers relative to larger colonies.

There is however an upper bounds for tailoring that the size of a human embryonic stem cell colony, as it has been demonstrated by Saha et. al[34] that extremely large colonies have a propensity to differentiate in the center of the colony. In Saha's work, UV/ozone was used to functionalize polystyrene through a

mask, rendering the un-functionalized areas non-cell adhesive (in the presence of BSA and the medium mTeSR. They found that colonies below ~2mm in diameter exhibited lower expression of the pluripotency marker 0CT4 and longer doubling rates as compared to colonies smaller than ~2mm in diameter. It is therefore clear that there is an optimal range of sizes that hES cell colonies should be grown at, for either pluripotency maintenance or directed differentiation.

Controlling the colony size also minimizes the heterogeneity seen in typical hES culture, in which a variety of colony sizes, as defined by area and perimeter, are present. **Figure 3.1** shows the typical variability in cell colony size and shape for H1 hES culture on Matrigel.

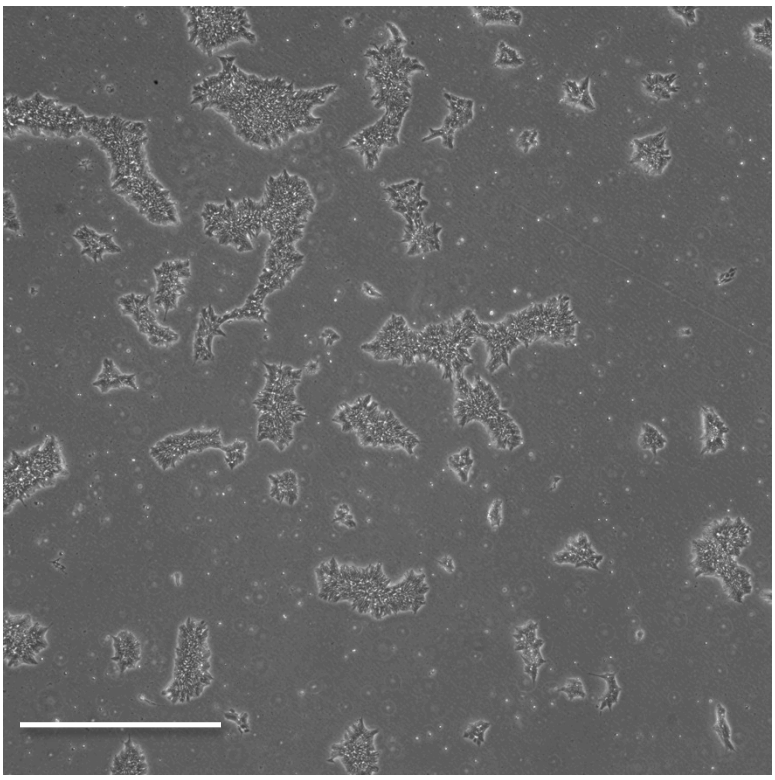

Figure 3.1 H1 hES cells at day 4 after passaging, grown on Matrigel with mTeSR media, using Accutase and ROCK inhibitor for passaging. Scale bar = 1 mm. Cell colonies display a variety of areas and perimeters when grown in this typical culture fashion.

Furthermore, it is desirable to regulate the geometry of the colonies, as it has been shown to be a parameter that affects cell fate. Work from Ruiz et al.[35] demonstrated that the differentiation trajectory of human mesenchymal stem cells grown on microcontact printed fibronectin in mixed media (1:1 osteogenic inducing to adipocytic inducing) was dependant on cell position within the pattern, where cells on the edges adopted an osteogenic lineage and cells on the inside of the pattern became adipocytes. They further deduced that the convexity of the pattern was also influencing cell fate. Finally, they demonstrated that in the presence of growth medium, cells on the convex part of the pattern exerted tractional forces on the substrate that were much higher than tractional forces exerted on the substrate by cells in concave areas. Often, hES cells in culture are subject to non-homogenous

curvature conditions, underscoring the importance of controlling curvature or pattern shape in micropatterning schemes, which could increase consistency and reproducibility of cell behavior.

3.1.2 Existing Technologies and their Limitations

Patterning of hydrogels emerged in the early 2000s as a means to monitor cell traction forces on surfaces with tunable moduli; however the existing technologies are not suitable for hES cell or induced pluripotent stem iPS cell culture purposes.[36] Due to the solvated and deformable nature of hydrogels it is not as easy to pattern them with high fidelity as it is to pattern a thin stiff dehydrated surfaces. In the original work, patterning hydrogels to monitor cell traction forces, long range pattern fidelity was not necessary as these surfaces were constructed for single cell mechanistic studies. In contrast, for hES cell culture, it is more critical to have long range order and a non-fouling background to adequately account for paracrine effects in the cell culture system. In most of the existing technologies for patterning hydrogels, there is either insufficient long range order, insufficient pattern fidelity, an insufficiently non-fouling background, or a combination of all or some of the aforementioned insufficiencies.

In the pioneering work to pattern hydrogels, Wang et al.[36] wanted to observe cell tractions, so it was sufficient to have only a few patterned cells, and observe the deformation of the underlying hydrogel beneath them. The authors created a stencil out of polydimethylsiloxane (PDMS), and applied that stencil onto a polyacrylamide gel. Applying vacuum, they coated the surface with sulfo-SANPAH, UV activated the sulfo-SANPAH, rinsed, and then incubated with collagen over night while the PDMS stencil was on the hydrogel. After the stencil was removed, the newly exposed acrylamide was filled with BSA and cells were then seeded. **Figure 3.2** shows cells seeded on the surfaces created by Wang et al.[36] and it is apparent cells are also adhering in the non-fouling areas. Techniques relying on a stencil are problematic as they require precise conformal contact with substrate to prevent the crosslinker or protein from getting into non-patterned areas. Even if conformal contact is ensured, if using small molecules such as peptides, the molecules can get trapped within the gel and diffuse out over time, acting as competitive binding agents towards the cells. While this innovative method allowed for measuring of tractional forces imposed by the cells on the underlying substrate, the amount of background cell adhesion is not desired for the application of a standardized, synthetic stem cell culture system with reproducible results. Additionally, while Wang's work used human airway smooth muscle cells and they were able to use BSA as a cell blocking agent, work by Irwin et al indicates that when deposited on certain surfaces, embryonic stem cells actually used BSA for attachment.[37]

Another attempt to pattern hydrogels comes from Engler et al.,[38] in an important study correlating the stiffness to which a myoblast is exposed, with proper striated myotube formation. In their technique, ECM proteins were chemically bound to sulfo-SANPAH activated acrylamide gel via a micropatterned glass reservoir. The glass reservoir was created by microetching glass and then filling in the etched grooves with the ECM protein of interest.

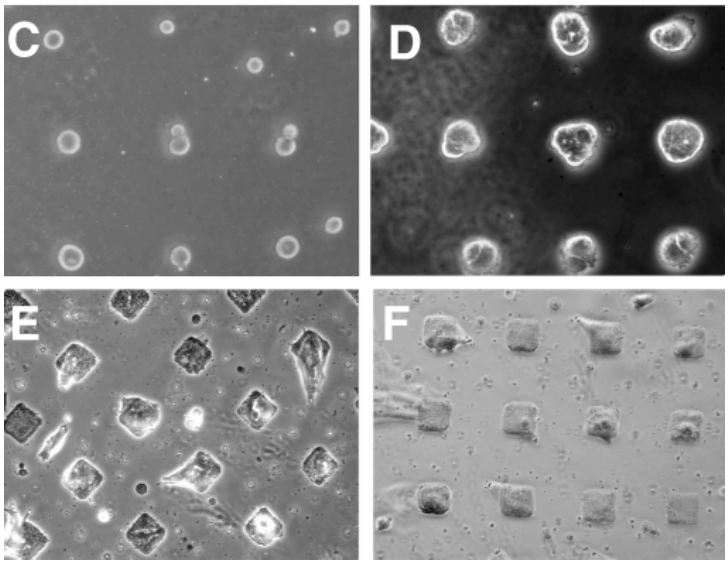

Figure 3.2 From Wang et al[36]. The authors used a PDMS stencil technique to pattern acrylamide, however there are cells missing from the pattern and there are non-patterned areas which show cellular adhesion.

As sulfo-SANPAH was bound to the entire surface, any protein that diffused away from the grooves or into the gel during the time of contact between the gel and the microreservoir could bind to regions that were not intended to be patterned. More problematic was how few cells actually stuck to the patterned regions, indicating that there may have been incomplete protein transfer from the wells to the acrylamide as can be seen in **Figure 3.3.**

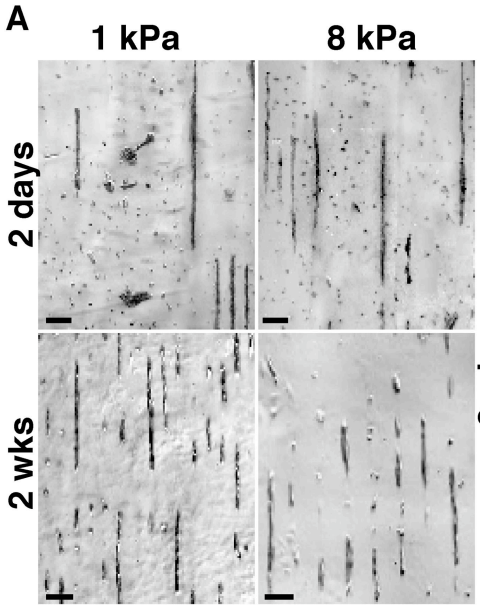

Figure 3.3 From Engler et al[38] Acrylamide gel patterned via micropatterned glass reservoir. There is limited long range pattern fidelity as seen demonstrated by cellular adhesion. Scale bar = 100μm

Hahn et al.[39] also attempted to micropattern hydrogels; however, using a polyethylene glycol diacrylate (PEGDA) and acrylated-RGD peptide based system. The acrylated peptide was deposited on top of the PEGDA hydrogel and a photomask was then placed a top of the hydrogel which was then illuminated with UV in the presence of photoinitiator. Since the peptide solution coated the entire hydrogel, there was significant opportunity for diffusion into the hydrogel. Additionally, since the photomask was a transparency, and the thickness of the PEGDA hydrogel was 0.5 mm, there was an increased likelihood of UV light diffracting. The diffracted UV light coupled with the peptide which was found throughout the whole gel leads to poor pattern fidelity as can be seen in **Figure 3.4.** Consequently, cells do not form neat patterns on these surfaces.

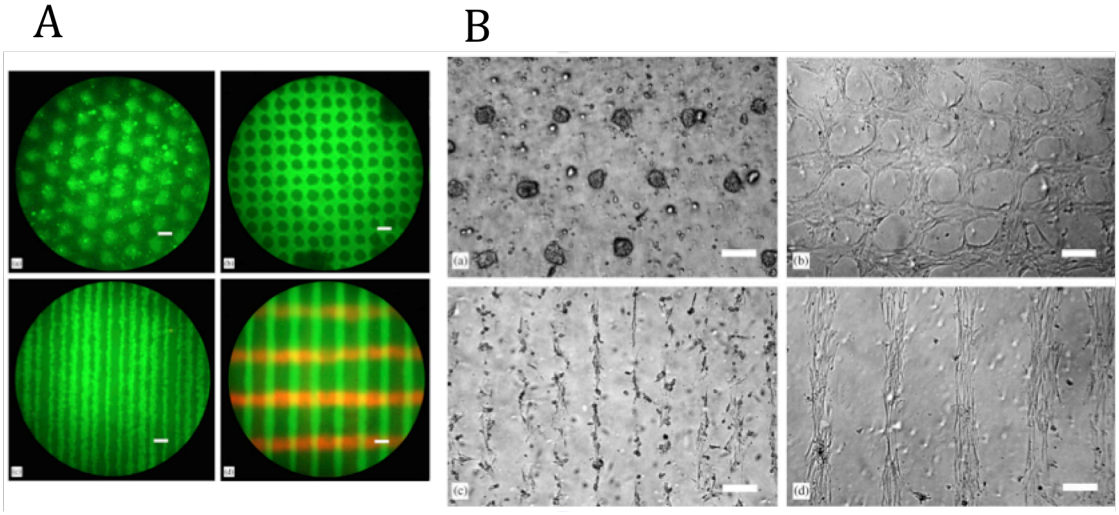

Figure 3.4 From Hahn et al.[39] micropatterning a polyethylene glycol based hydrogel with an acrylated RGD peptide. (A) Fluorescent peptide. Scale bar = 250 μm and (B) cell images scale bar = 200 μm. Both peptide and cells are clearly visible outside of the patterned areas.

More recently Lutolf et al.[40] have devised an interesting way to make patterned wells for cell culture. They created 3D microwells within a PEG hydrogel system. Their methodology however relies on precursors, which required 3 days to fabricate, and involve harsh chemical. The precursors then need to be stored under argon at -20°C, and degree conversion is not necessarily consistent between batches. The process of making the wells from gel precursor involves adding protein A, to copolymerize with the hydrogel, as part of the process, which involves microcontact printing and sandwiching, and then transferring and adhering to a TCPS well. Protein A binds very strongly to the Fc portion of antibodies, so Lutolf's scheme requires that whichever adhesive ligand is used for patterning has the ability to be modified to have an Fc unit attached to it. This caveat may ultimately limit the types of proteins/peptides that can be used in their application. Furthermore, we believe that the logistics of cell culture make it preferable to use a 2D rather than 3D microwell system. 3D microwell systems can have complicated fluid flow, and therefore non-uniform diffusion, which will affect paracrine signaling. Additionally, media exchanging and passaging is not as consistent in 3D microwell systems, due the complicated fluid flow.

While researchers have begun to address the need for patterned, solvated, deformable surfaces, the current solutions are lacking and can be improved upon. The UV-activated microcontact printing technique described herein allows for high fidelity functional pattern transfer because the ink, a crosslinker and not the peptide/protein itself, is only in contact with the desired pattern area for a few seconds, minimizing diffusion. Furthermore the ink is not applied to the whole surface, minimizing the chance of activated ink being in a non-patterned region. The protein/peptide is then applied to the hydrogel in the liquid state preventing the denaturing that can happen if it were to be applied to a stamp and then dehydrated. Additionally, this technique employs a polyacrylamide hydrogel system (described in **Section 3.2.1.1**), which can be dehydrated and rehydrated without the top surface experiencing buckling, due to the optimization of swelling ratio of the gel. The ability of the gel to resist buckling upon dehydration and rehydration allows one to pattern in the dry state and maintain pattern dimension in the solvated state, which is the state of the gel during stem cell culture.

3.2 Overview of UV-activated hydrogel printing

The UV-activated hydrogel printing technology developed in this thesis is described in this section, and a schematic is presented in **Figure 3.5**. First, a hydrogel with an easily tunable mechanical modulus is constructed. Polyacrylamide which is detailed in **Section 3.2.1.1** is used as the hydrogel for this technique, though any hydrogel with a tunable modulus and limited swelling ratio can be used. The swelling ratio has to be minimized in order to avoid buckling at the top surface of the hydrogel as it is created, as the gel will experience biaxial confinement when in a tissue culture vessel which will allow for swelling in only one direction. Once the gel is fabricated, the gel is dehydrated so that it can be put into conformal contact with a Polydimethylsiloxane (PDMS) stamp. Meanwhile the stamp is inked with a hetero-bifunctional crosslinker that can attach to the hydrogel via a UV activated reaction and to the adhesive protein of interest. The ink is then dried and the stamp is put into contact with the hydrogel. Concurrently, UV is illuminated through he stamp, activating one end of the hetero-bifunctional crosslinker and allowing it to bind to the hydrogel. The gel is then washed and the adhesive protein or peptide of interest is then deposited on top of the gel and allowed to adhere. Please see **Appendices A.1-A.3** for detailed methodology.

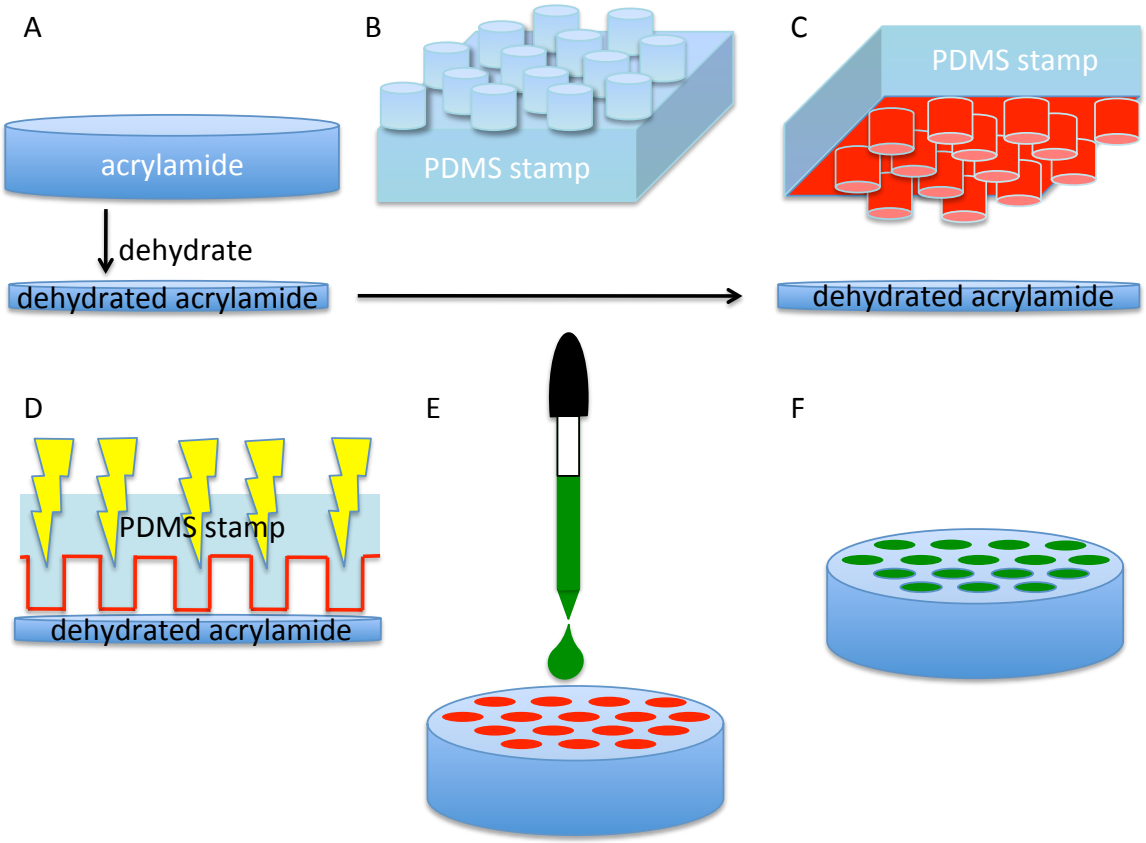

Figure 3.5 Hydrogel Micropatterning Technique. (A) dehydrate acrylamide gels (B) fabricate PDMS stamp with feature diameters equal to desired cell colony size (C) ink stamp with crosslinker (red), and bring into contact with dehydrated acrylamide (D)activate crosslinker with UV, while PDMS stamp is in conformal contact with acrylamide (remove stamp, wash acrylamide) (E) incubate acrylamide with cell adherent protein (green) (F) protein only binds where ink was activated, generating the micropattern.

3.2.1 Materials Selection

This section details the material choices made for the patterning project.

3.2.1.1 Polyacrylamide System

For this project, it was necessary to use a hydrogel with easily tunable mechanical properties in the biologically relevant range. Historically PDMS, polyacrylamide gels, and polyethylene glycol (PEG) gels have been used as flexible biomimetic substrates for cell culture and tissue engineering applications. In this section, the limitations of PDMS and PEG hydrogels will be described, and then justification for the use of polyacrylamide gels for cell patterning will be presented.

In the 1980s Harris et. al[41] pioneered the use of flexible silicone surfaces to observe and monitor cellular traction forces, which were too small to observe on stiff surfaces. They used the wrinkling of the silicone in response to cellular traction

and the known properties of the silicone substrate to study the magnitude of the cell tractions. The silicone used, PDMS is typically made by combining base monomer and curing agent in a 10:1 ratio, commercially available as "Sylgard" and then baking to cure. The base, is composed of a vinyl terminated dimethylsiloxane oligomers, a platinum catalyst, and silica filler.[42] The base undergoes a hydrosilation reaction with curing agent, dimethyl methylhydrogen siloxane.[42] Additionally, the curing agent contains the inhibitor tetremethyltetravinyl cyclotetrasiloxane. Due to its ease of manufacture, optical clarity, high thermal stability and "biocompatibility" PDMS has since been used extensively in the medical device community. [43-49] PDMS was therefore a natural selection for the early studies of cell contact guidance and mechanotaxis.[50-54] Theoretically, one can generate a variety of elastic moduli of PDMS by modulating the ratio of base to curing agent. However, the surface chemistry does not remain constant when the ratio of base to curing agent is changed, since the reactive groups on the base and the curing agent are not the same. More compliant compositions (those with less curing agent) will have more unreacted vinyl groups from the base, more platinum catalyst and more silica. Stiffer compositions (those with more curing agent) will have more unreacted methyl methylhdrogen siloxane groups, and excess inhibitor. The amount of remaining uncrosslinked groups will be a function of curing time and curing temperature, ultimately affecting the final mechanical properties. A significant drawback, of using PDMS for cellular studies is that low molecular weight uncrosslinked species can easily bloom to the surface and therefore change the surface properties, and stiffness of the PDMS between the time of fabrication and cell experiments.[42] Often, the surface of PDMS is treated with oxygen plasma to render it more hydrophilic, however the plasma treatment is not permanent as low molecular weight moieties can continue to bloom to the surface, after the plasma treatment.[42, 55-58]

Even if one could account for the differing surface chemistries caused by changing the ratio of base to curing agent, another significant problem with the PDMS system is the inability to generate elastomers as compliant as some tissues in the body. Using too little curing agent renders a particularly tacky, highly viscous material. In fact, the minimum PDMS stiffness achievable reported in literature is on the order of 50-500KPa, which is orders of magnitude higher than what would be desired for biomimetic embryonic stem cell culture, which requires surfaces with moduli that are in the range 100-1000Pa as discussed in **Section 3.1.1.2** .[42, 59]

In order to more accurately measure cell tractional forces, compared to the initial study by Harris et al.[41] in 1980, and to avoid the aforementioned limitations with the PDMS system, Pelham and Wang[12] borrowed the polyacrylamide system used by biologists for protein separation. The polyacrylamide system has since become one of the, if not the, most commonly used materials for studying the effect of the mechanical properties of the environment on cells. I have chosen acrylamide as a model hydrogel due to its extensive characterization in the field of biomaterials, in which a number of researchers have demonstrated relationships between monomer concentrations (acrylamide and bisacrylamide) and mechanical propteries.[12, 19, 60-63]

The polyacrylamide hydrogels are generated by combining the two monomers acrylamide and bisacrylamide in water and are polymerized via a free

radical polymerization (**Figure 3. 6**). The reaction can be initiated via any radical, as is typically initiated by a light sensitive radical such as those in the Irgacure family or a chemically generated radical such as riboflavin, or the radicals generated from the redox reaction between ammonium persulfate (APS) and tetramethylethylenediamine (TEMED).[64] The desired thickness (~ 70 μm) of the acrylamide gel for cell culture and cell studies precludes the use of light activated radicals, as the polymerized acrylamide attenuates UV, and can therefore greatly decrease radical generation deeper in the gel.

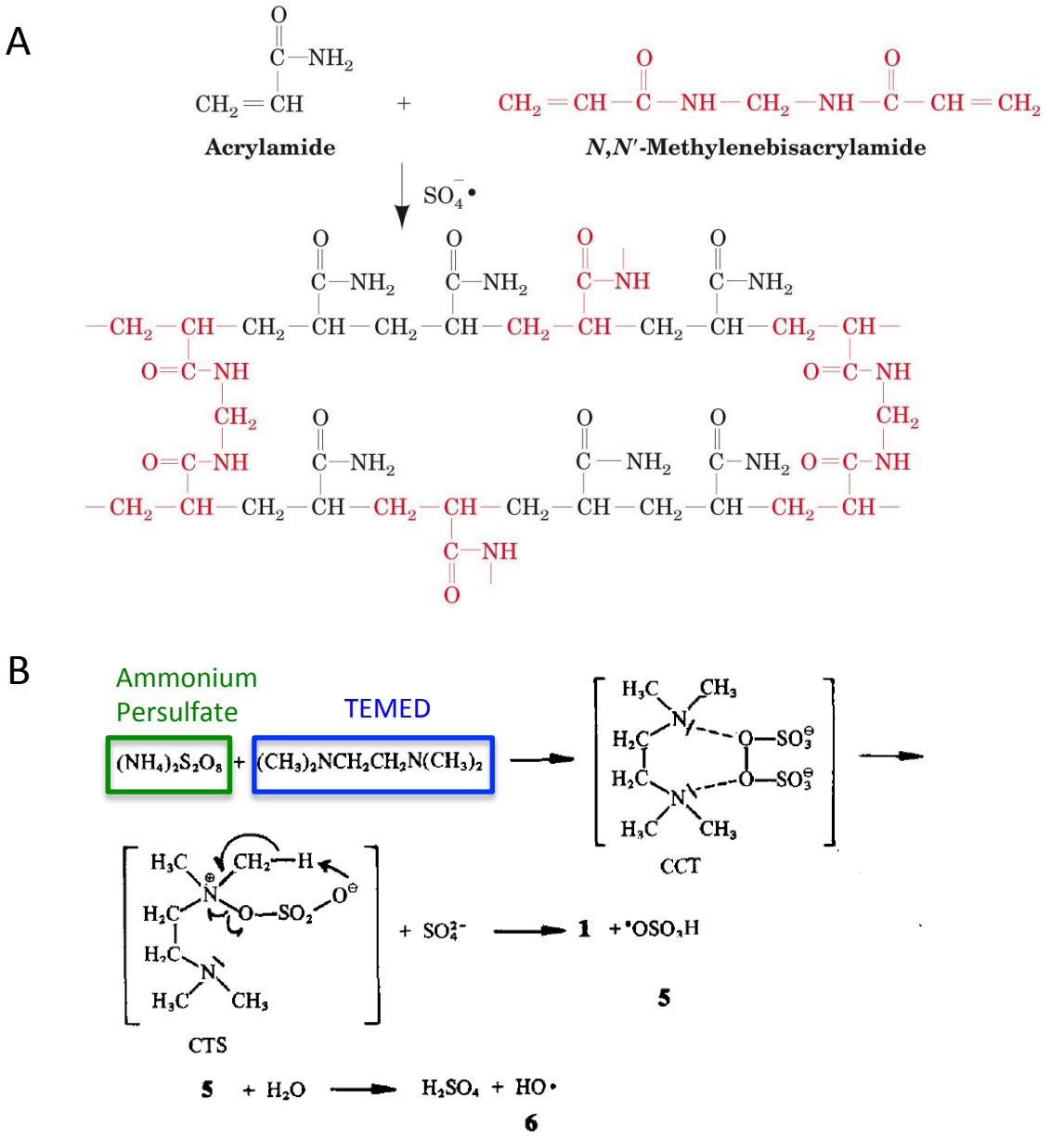

Figure 3.6 Polyacrylamide gel polymerization scheme. (A) The polyacrylamide hydrogel is created by co-polymerizing acrylamide with bisacrylamide and it is initiated via a free radical. Figure adapted from[65]. (B) The free radical can come from radicals generated from the redox reaction between ammonium persulfate with TEMED (or from UV activated initiator such as those from the Irgacure family (not shown)). Figure adapted from [64]

For cell culture applications, it is generally accepted that the acrylamide gel should be at least 70 μm thick so that the cell will not "sense" the underlying substrate (a maximum thickness may also be limited by the working distance of the objective lenses available for microscopy).[20] Maloney et al.[66] undertook the task of developing a model to calculate the minimum acrylamide coating thickness that could be considered semi-infinite from the perspective of a cell, employing elasticity theory. They discussed various definitions of critical cell-sensing depth (i.e. depth at which a certain strain exists, gel thickness that attenuates cell traction by a certain percentage, gel thickness that attenuates adhesion site displacement by a certain percentage, gel thickness that attenuates adhesion site distortion by a certain percentage, and coating thickness that maintains a certain traction-induced surface displacement or distortion). Their model's predication, and experimental results correlate well with the observations from Engler et al.[20] that fibroblast cell spreading was no longer a function of acrylamide gel thickness for gels > 70 μm.

Researchers have shown that the polyacrylamide system behaves as an ideal elastomer over an experimentally relevant range of monomer and crosslinker concentrations, with a Poisson's ratio very close to 0.5 (ν=0.48), and that for a given acrylamide concentration (in the range 3% and 10%), Young's modulus varies linearly with bisacrylamide concentration.[63, 67] Recent work in our lab in collaboration with Ryan Hayward at UMass Amherst has shown that when polyacrylamide gels are constructed on a rigid support, their swelling is constrained to the normal direction, and swelling ratios have been determined that avoid creasing at the top surface from the equibiaxial confinement induced by the unidirectional swelling.[63] With this knowledge, one can select monomer concentrations that will yield a desired elastic modulus, at the lowest possible swelling ratio, which will avoid introducing the effects of topography into the cell culture system. The ease with which the mechanical properties of the polyacrylamide gel can be tuned, render it particularly desirable for our application. Additionally, polyacrylamide resists protein attachment and therefore cell adhesion, a necessary requirement for any patterning application.[68-71]

Another hydrogel system that has also been used to study the effects of mechanical properties on cells is one based on crosslinked PEG,[18, 72, 73] due to its ubiquitous use as an anti-fouling material. [74-78] While the mechanisms responsible for polyethylene glycol's efficacy at protein adsorption resistance have not been fully elucidated, the success is usually attributed to the solvation and structuring of water around PEG.[79-81] Polyethylene glycol is, however, susceptible to oxidative degradation, and can eventually loose its antifouling behavior in the presence of serum even when grafted at densities high enough to theoretically occlude proteins, therefore limiting its anti-fouling behavior.[78, 82, 83] PEG hydrogels can be made with polyethylene glycol diacrylate as a the crosslinker and PEG chains of any length as the monomer. Since the monomer has to have a minimum number of repeat units to be antifouling, based on Harder et al.'s[80] work with ethylene glycol self-assembled monolayers, hydrogels composed of PEG moieties tend to have very high swelling ratios compared to those obtainable for polyacrylamide hydrogels. [39, 63, 80] The high

swelling ratio limits their use for a 2D cell patterning application, due to the surface creasing that can occur in typical cell culture wells which confine the gel to only swell along one direction.

While PEG based hydrogels, or any hydrogels for that case, can be used for the patterning technology described herein, the polyacrylamide gel system was chosen as a proof of principle hydrogel due to the standardization and availability of high quality monomers, demonstrated low swelling ratios, acceptable non-fouling behavior, and extensive characterization performed both by the biological community for protein separation applications and by the cell mechanotransduction community.

3.2.1.2. Sulfo-SANPAH

For this project, sulfosuccinimidyl 6-(4'-azido-2'-nitrophenylamino)hexonate (Sulfo-SANPAH) was chosen as the "ink" which is used to pattern hydrogels. Sulfo-SANPAH is a heterobifunctional cross-linker with an amine reactive *N*-hydroxysuccinimide (NHS) ester and a photoactivate-able nitrophenyl azide (**Figure 3.7A**). This chemistry allows for easy sequential bonding of the crosslinker, first to the acrylamide gel, via the aryl azide and then to the adhesive protein of interest via the NHS ester. The aryl azide can be very quickly activated by UV to form a nitrene group that can initiate addition reactions with vinyl groups. The nitrene group can also insert into C-H and N-H sites, but will preferentially react with a primary amine if available (**Figure 3.7B**). Meanwhile, the NHS ester reacts with nucleophiles such as primary amines, such as α-amines at the N-termini of proteins and the ε-amines of lysine groups on proteins to form an amide bond. However, a competing reaction is the NHS hydrolysis. Since all proteins have primary amine groups, sulfo-SANPAH can attach any protein to acrylamide; however to attach peptides, a primary amine might not be available, and an alternate heterobifunctional crosslinkers that have one end as the aryl azide can be used, such as N-((2-Pyridyldithio)ethyl)-4-Azidosalicylamide (PEAS) or 1-(*p*-Azidosalicylamido)butane (ASIB). Both PEAS and ASIB can than react with a thiol group on cysteine.

In the context of stamping, the crosslinker can be uniformly dried on a stamp, and since PDMS attenuates very little light, one can adjust the power of the UV to accommodate for the minor attenuation, which was about 1-2 mW/cm^2 through the typically 1/8" thick glass microscope slide backed PDMS stamps). The crosslinker remains active while dried onto a stamp, and can be transferred onto a dried acrylamide surface and still chemically react.

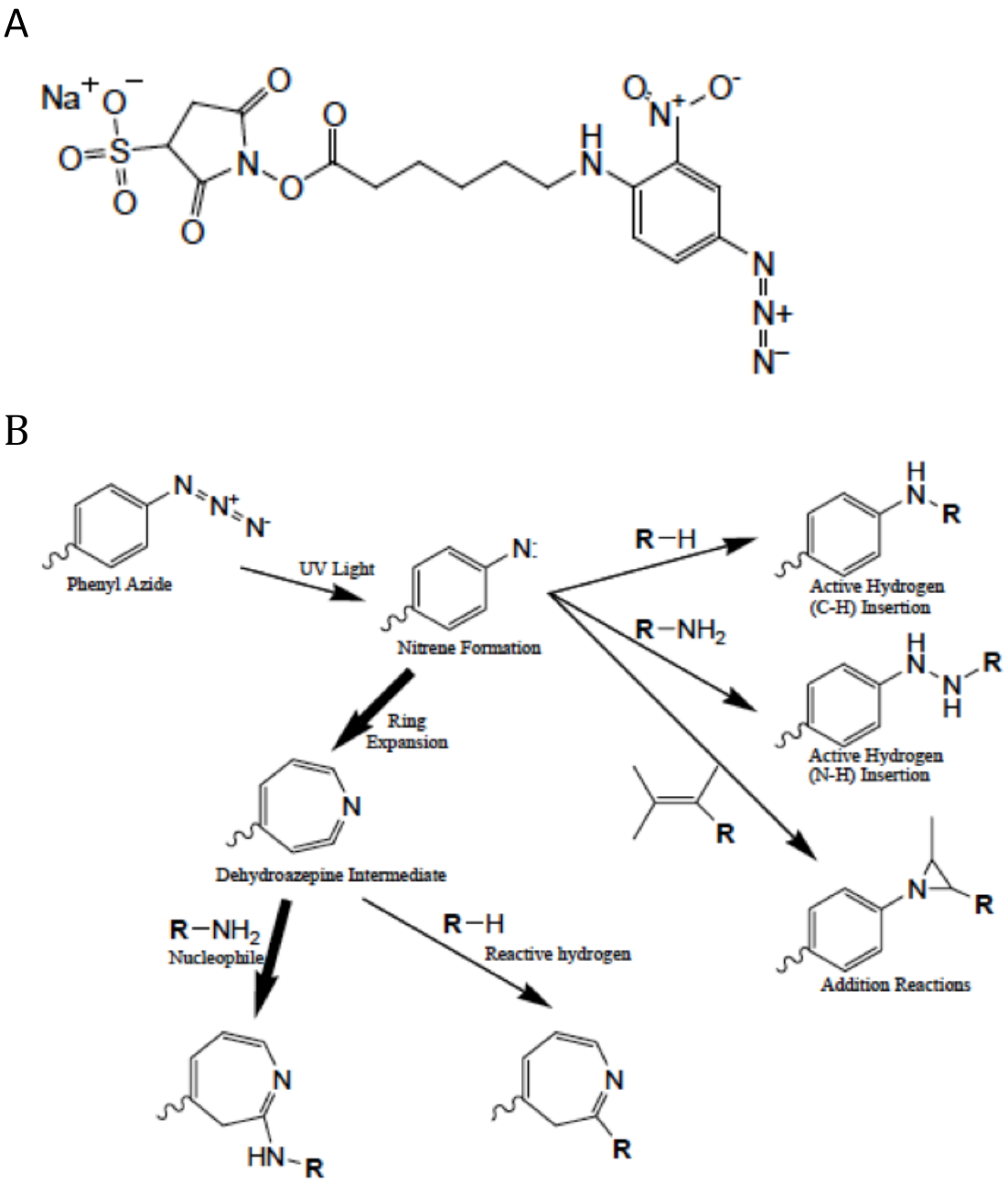

Figure 3.7 sulfo-SANPAH (A) structure. Sulfo-SANPAH has an NHS ester which can react with primary amines, and a phenyl azide which can react with many groups when exposed to UV and converted to a nitrene. (B) The possible reactions of the azide from sulfo-SANPAH upon UV activation.[84]

3.2.1.3 Adhesive Ligands

Both proteins and peptides were investigated in this work as adhesive ligands for the cell culture platform. For initial studies of proof of concept, 3T3 cells

were employed to show that cells could be patterned onto a hydrogel. The two adhesive proteins that have typically been used to conjugate cells to acrylamide gels have been collagen I and fibronectin. [12, 85, 86] Collagen I was used by Pelham and Wang in their pioneering studies of cells with the polyacrylamide system, and has since been adopted by many researchers using the polyacrylamide system, as it is the most abundant protein found in the body, and is readily available commercially as a cell culture substrate.[87, 88]

Rowlands et al.[85] however have shown that the response of a cell to the stiffness of its substrate is dependant on the adhesive ligand binding presented to the cell. Specifically, they examined collagen I, collagen IV, fibronectin and laminin coated gels. They found that mesenchymal stem cells would only differentiate into osteogenic cells on the collagen I conjugated gels at the highest stiffness examined, while myogenic differentiation occurred with all the proteins investigated with peak myoD expression levels on fibronectin conjugated 25kPa gels and collagen I coated 80 kPa gels. This finding is not surprising, as it is known that the aforementioned adhesive ligands can engage with different integrins on the cell surface, therefore leading to different cell signaling.[89] For example, while fibronectin and vitronectin both engage the RGD binding integrins $\alpha v\beta 3$ and $\alpha IIb\beta 3$, they each also engage a number of RGD binding integrins, that the other does not.[89]

Additionally, while the RGD amino acid sequence, first identified by Ruoslathi, on fibronectin (and later vitronectin) does exist on collagen, it is not clear that it is accessible to integrins for cellular attachment.[89-91] In fact, it is believed, that it is the vitronectin or fibronectin present in serum during cell culture, which binds to the collagen substrate, that actually mediates cellular adhesion.[92] I therefore chose to use fibronectin and not collagen for my proof of concept studies with 3T3 cells.

In addition to being more appropriate for the binding of 3T3s, fibronectin was selected over collagen due to the processing difficulties introduced with the use of collagen I. Collagen I gels as pH is increased, which can both affect the perceived modulus of the acrylamide substrate, and it can lead to inhomogeneous chemical presentation.[86, 93] Furthermore, since Collagen I is a fibrillar protein, it may orient on the acrylamide if it is induced to pack efficiently or more likely leave gaps if the packing is not efficient which might be expected from an entropic argument. The local fluctuations in chemical signal that may come about from using a fibrillar protein, render collagen I undesirable for the hydrogel printing technology. Lastly, since sulfo-SANPAH is used as the linking agent between acrylamide and the adhesive ligand, it is preferential to use an adhesive ligand whose pH can be raised to allow for a significant percentage of amines to be available to act as nucleophiles towards the azide on the sulfo-SANPAH.

HES cells have been shown to express all major ECM proteins and their corresponding integrins (as determined by antibody blocking experiments).[94] Braam et al. however found that while fibronectin could support hES cells in feeder-conditioned media, only Matrigel or (natural and recombinant) vitronectin could support hES cells in defined non-conditioned media.[94] At the time of this writing recombinant vitronectin is sold for nearly twenty times the prince of fibronectin, a

more common cell culture substrate protein, and therefore, the proof of principal studies were conducted with fibronectin from a cost-effectiveness standpoint.

A bone sialoprotein-based RGD peptide was also used in this work. While the affinity of RGD based peptides is about 1000 times lower than fibronectin in cell binding assays,[95] using an RGD peptide instead of fibronectin would completely eliminate the use of animal products in cell culture substrate.

3.2.2 Methods

3.2.2.1 Polyacrylamide Gels

Polyacrylamide gels were fabricated based on methodology developed in the Discher group, and more recently by Elizabeth Irwin and Kris Saha's work in the Healy lab.[19, 62, 86] For details, please see the **Appendix A.1**. Briefly, quartz discs (Quartz scientific) were cleaned with Piranha solution (3:1 Sulfuric Acid: 30% Hydrogen peroxide) and then treated with oxygen plasma at 80W and 1 Torr. The discs were then functionalized with a methacryloxypropyltrimethoxysilane (MTMS; Gelest) so that the surface had a vinyl to participate in the free radical polymerization of the polyacrylamide network. Prepolymer solutions of acrylamide were prepared from 10% acrylamide and 40% bisacrylamide stock solutions (Amersco), and then degassed. Final concentrations were chosen to yield specific target moduli. A number of groups document monomer concentration, initiator concentration and polymerization time required to yield gels with specified mechanical properties. Saha et al. determined elastic shear moduli for polyacrylamide gels, which correlated well with Young's moduli determined for polyacrylamide gels by Irwin et al. and Tse et al., so his formulations were used for this project.[19, 62, 63, 86] To perform the comparison, shear moduli were converted to elastic moduli using **Equation 3.1**:

$$G = E/[1(2+\nu)] \qquad \textbf{Eq 3.1}$$

where G is the shear modulus, E is Young's modulus, and ν is Poisson's modulus which is approximately 0.5 for polyacrylamide.[67] Right before polymerization, TEMED and APS were added and a precise amount of prepolymer solution was deposited onto the vinyl functionalized quartz disc. A coverslip glass, which was already oxygen plasma treated, and functionalized with the hydrophobic silane dichlorodimethyl silane was used to sandwich the prepolymer solution between the cover glass and the quartz so it would have a flat top surface. After 15 minutes the polymer top slip was removed by immersing the sandwich in water and sliding the cover glass off. Gels were then rinsed over night in deionized water, and sterilized in 70% ethanol prior to further modification.

3.2.2.2 Photolithography

The stamps used for this project were generated from PDMS following established standard soft photolithography procedures.[96] In order to generate PDMS stamps, negative masters were first created from the photoresist SU-8 50 (Microchem), following the recommended protocol from the manufacturer.[97] See **Appendix A.2** for detailed SU-8 protocol.

After the SU-8 master was fabricated, it was exposed to 30 seconds of oxygen plasma at ~80 W, so that it could bind to the hydrophobic silane, tridecafluoro-1,1,2,2-tetrahyrooctyl)-1-trichlorosilane (Gelest), that was used as a mold release agent for the PDMS to easily detach from the SU-8 master. Immediately after oxygen plasma treatment of the SU-8 master, it was placed in a vacuum desiccator with 200 μL of tridecafluoro-1,1,2,2-tetrahyrooctyl)-1-trichlorosilane, and left overnight, so that the vapors of the could coat and bind to the master.

PDMS (Sylgard 184, Dow Corning) was then prepared by mixing the base with curing agent at ratio of 10:1 by weight as recommended by the manufacturer. The mixture was vigorously mixed for 5 minutes and then degassed for at least half an hour. The PDMS was then poured onto the master and again degassed to ensure no remaining bubbles and that the PDMS liquid had coated all the wells in the master. PDMS was then baked at 110°C for at least 3 hours.

Prior to use, the stamps were oxygen plasma treated for 30 seconds at ~80W, as were glass microscope slides (Fischer Scientific). Immediately after plasma treating the PDMS and the glass slides, the backs of the PDMS slides were affixed to the glass microscope slides via pressure, ensuring that no air gaps formed between the PDMS and the glass. This step was necessary to prevent roof collapse of the PDMS stamp, which became a problem once features were separated by distances greater than a few hundred microns.[98, 99]

3.2.2.3 Fibronectin

Human Plasma Fibronectin (GIBCO) which came as a 5mg of lypholized powder stored at 2-8 °C, was slowly heated to room temp, and diluted to 1 mg/mL in 50 mM HEPES pH 8.5 or PBS pH 7.4, by allowing the bottle to reach room temperature and adding the HEPES buffer directly to the bottle. The Fibronectin was left for at least half an hour to fully dissolve. Vortexing or vigorous pipetting should never be performed, as this will cause the protein solution to froth, and in addition to changing the local protein concentration, can cause the protein to denature. Aliquots of 1 mg/mL Fibronectin were stored at -20°C until ready for use, at which point they were diluted with the aforementioned HEPES buffer to a final concentration of 0.1-1 mg/mL depending on the experiment.

3.2.2.4 Cell Culture

3T3 fibroblasts (ATCC) and Rat Mesenchymal Stem Cells and were used for proof of concept studies in developing the hydrogel printing technology. 3T3s were cultured as per instructions from ATCC: they were maintained in high glucose DMEM media supplemented with 10% FBS (Gibco) and 1% Pen/Strep (Life Technologies). They were passaged at a split ratio of 1:10 or higher approximately every 3 days, using 0.25% Trypsin EDTA. They were seeded onto surfaces at concentrations varying from 15,000-20,000 cells/cm^2. Rat Mesenchymal Stem Cells (rMSC) were maintained in media composted of high glucose DMEM, 15% FBS and 1% Pen/Strep. They were passaged with 0.05% Trypsin EDTA and since their growth rate was significantly slower than that of 3T3 fibroblasts, they were split at ratios closer to 1:3 or 1:5 approximately every 5 days. They were used from passage 10 until passage 20.

3.2.3 Results and Discussion

Many aspects of the patterning methodology had to be optimized, and key observations/lessons are discussed in this section, and addressed. They will be listed in chronological order of the processing steps. See **Figure 3.4** for an overview of the processing steps.

3.2.3.1 Quartz Substrate

For all experiments, the polyacrylamide hydrogel was fabricated on a quartz disc, which was then inserted into a tissue culture polystyrene culture dish, for cell culture. In their pioneering use of polyacrylamide for cell studies, Pelham and Wang used glass coverslips as the surfaces for acrylamide, and so have most subsequent researchers employing the polyacrylamide technology.[12, 86] I was interested to see whether polyacrylamide could be directly polymerized in the culture plate obviating the use of a quartz substrate, and simplifying the procedure.

Glass was chosen by Pelham and Wang,[12] as there exists chemistry to attach the polyacrylamide directly to glass. Specifically, Pelham and Wang[12] functionalized the glass with a sodium hydroxide treatment followed by the introduction of 3-aminopropyltrimethoxysilane. The silane bound to the glass and left an exposed amine group, which Pelham and Wang crosslinked to the acrylamide gel via gluteraldehyde which can react with free amines or amides in the polyacrylamide. In an improvement upon this methodology, Saha et al.[19] functionalized the glass so that it could actually participate in the free radical polymerization of the polyacrylamide gel, rather than just link to its amine and amide moieties, by using the reactive vinyl terminated, methacryloxypropyltrimethoxysilane (MTMS).

Tissue culture polystyrene plates unfortunately do not have functional groups with which to react with silanes; however, exposure to oxygen plasma can generate radical groups in the polystyrene, which can act as initiation sites for the polyacrylamide polymerization. The act of exposing polystyrene to oxygen plasma

can generate significant heat and cause the polystyrene to flow and become disfigured; therefore, there is an upper bounds to the dose of oxygen plasma one can apply to the polystyrene.[100, 101] It was determined that 6 well tissue culture polystyrene dishes could withstand up to 5 minutes of 400W of oxygen plasma prior to flowing. Solutions of 10% acrylamide 0.3% bisacrylamide with APS and TEMED in water were poured into 6-well tissue culture plates immediately after the plates were subject to 5 minutes of 400 W oxygen plasma treatment, and allowed to polymerize. They were then left over night at room temperature, and as can be seen in **Figure 3.8**, gels delaminated from the bottom of the tissue culture plates as they swelled. Clearly, the oxygen plasma treatment did not render sufficient graft points for the polyacrylamide gel to adhere to the tissue culture polystyrene dish, and the force of expansion due to swelling was therefore greater than the force associated with the bonds between the acrylamide gel and polystyrene.



Figure 3.8 Polymerizing polyacrylamide hydrogels directly in tissue culture polystyrene plates. Gels have delaminated from the bottom of the well in the course of swelling.

While it is not currently possible to attach an ~70 μm thick polyacrylamide gel to the surface of a polystyrene tissue culture plate, the use of commercially available glass-bottomed cell culture plates was also considered. Unfortunately, the glass is affixed to the plate with a glue that is soluble in methanol, which is the main solvent used for the vinyl terminated silane, MTMS, used to functionalize the glass for participation in the free radical polymerization with the polyacrylamide gel. It was therefore concluded that it was necessary to continue to fabricate the polyacrylamide gels on a quartz disc.

3.2.3.2 Acrylamide Protein Resistance

At one point during the optimization of the patterning protocol, contrary to previous results, acrylamide gels started displaying protein fouling, with fibronectin adsorbing onto the gels and supporting cell attachment, which was a troubling observation that needed to be fixed.

It has been shown that residual acrylamide monomers can react with and bind the ε-amino group of the lysine residue on proteins, in alkaline conditions.[102] Given that the fibronectin solutions used in this project are very alkaline (pH 11 for 0.1 mg/mL in PBS), there is a strong concern that this may be occurring and leading

to the less than optimal fouling properties of the polyacrylamide gel. Protein attachment, and consequently cell attachment, to the polyacrylamide gel could therefore, be controlled by minimizing the amount of unreacted monomer trapped in the gel.

It has also been shown that pH affects degree of polymer conversion for the acrylamide/bisacrylamide/TEMED/APS system. Specifically, there is a marked decrease in polymer conversion below pH 7 and, and below pH 4 there is no polymer conversion.[103] I had noticed two things in the course of my polymerization experiments that may have affected pH of the reactants, specifically the monomer storage, and the quality of deionized water.

Powder monomer had been stored as aliquots in polyethylene terephthalate or borosilicate glass scintillation vials prior to usage. The surface was of the storage container was found to statically charge the monomers, as was evidence by the clinging of the monomer to the storage container. As the vials were small, a large fraction of the monomers were getting statically charged during storage.

Additionally, the purity of acrylamide and bisacrylamide monomer can vary significantly between manufacturer[104]. Empirically it was found that acrylamide and bisacrylamide sold for electrophoresis provided consistently protein resistant gels. Specifically, the monomers used were Amersco 40% Acrylamide and 2% Bisacrylamide solutions (in deionized water), which boast an acrylic acid concentration of <0.005%. It is not surprising that reagent quality is highest for electrophoresis applications, as they require the nucleic acid or protein of interest not to bind to the gel. Once the switch was made to the Amersco monomers, polyacrylamide gels were no longer fouling.

Furthermore, it was also empirically observed that the quality of the deionized water, was affecting polymerization. Deionized water should have a pH of 7, by definition, however as it is exposed to air, it can dissolve CO_2 from the atmosphere and generate carbonic acid, lowering the pH to 5. Degassing the mixture for long periods of time prior to polymerization can allow the solution to become sufficiently acidic prior to polymerization.

3.2.3.3 Crosslinker and Buffer Properties

Before patterning could be optimized, it was necessary to optimize the bulk conjugation of adhesive ligands to the acrylamide gel via the sulfo-SANPAH crosslinker on un-patterned surfaces. Pelham and Wang[12], as discussed in section 3.2.2.1, invented the use of adhesive ligand conjugated acrylamide gels for studying the responses of cell to mechanical input. A number of researchers have adopted Pelham and Wang's protocol, which involves using sulfo-SANPAH to conjugate a cell adhesive ligand to the acrylamide gel.[20, 38, 85, 86, 105-110] In these papers there is a variety of conditions listed for the buffer used to solubilize sulfo-SANAPH, its molarity and pH, the sulfo-SANPAH concentration, total dose of UV, the adhesive ligand's buffer, and the adhesive ligands concentration. Some of the findings are summarized in **Table 3.1** below.

Table 3.1 Conditions found in the literature for conjugating an adhesive ligand to a polyacrylamide gel.

Ref.	Sulfo-SANPAH buffer properties	[sulfo-SANPAH]	Adhesive ligand	Adhesive ligand buffer properties	UV dose
[12]	200 mM HEPES pH 8.5	50 mM (24.6 mg/mL)	Collagen I 0.2 mg/mL	200 mM HEPES wash before and after conjugation. Buffer not identified	6 minute exposure 5" from UV source in sterile cabinet. 2x
[105]	50 mM HEPES pH 8.5	0.5 mg/mL	Collagen I 0.2 mg/mL or fibronectin 0.01 mg/mL	PBS	302 nm 2-3" away from two 15W tubes. 5-8 mins 2x
[110]	50 mM HEPES pH 8.5	1 mM 0.5% DMSO (0.5 mg/ml)	Collagen 1 (.2 mg/mL) fibronectin 0.015 mg/mL	PBS for collagen. HEPES for fibronectin	302 nm 2-3" away from two 15W tubes 5-8 mins 2x
[106]	1 M HEPES pH not indicated	1 mg/mL (first dissolved in DMSO to 0.025mg/μL	Collagen I 0.1 mg/mL	2x PBS wash after UV exposure. Buffer not identified	10 minutes exposure. Irradiance not indicated
[85]	Not indicated. Washed with PBS prior to sulfo-SANPAH	1 mg/mL	Collagen I .05 mg/mL Collagen IV (not given) Laminin (not given) Fibronectin (not given)	Not indicated	10 minutes. Irradiance not indicated.
[86]	Not indicated	0.2 mg/mL	Collagen I 0.1 mg/mL Fibronectin 0.01 mg/mL Laminin 0.01 mg/mL	50 mM HEPES pH 8.5	365 nm 3" from source. Irradiance not given. 10 mins. 2x if want

Ref.	Sulfo-SANPAH buffer properties	[sulfo-SANPAH]	Adhesive ligand	Adhesive ligand buffer properties	UV dose
[109]	50 mM HEPES pH 8.5	0.05% wt/vol with 0.5% DMSO	Fibronectin 0.1 mg/mL	Not indicated. 50 mM HEPES wash after UV, PBS wash after protein	2 J/cm^2 of UV +visible (from germicidal lamp). 2x
[108]	50 mM HEPES pH 8.5	0.64 mM (0.3 mg/ml)	Fibronectin 0-.032 mg/mL	50 mM HEPES pH 8.5	"UV light for 5 min at a distance of 2W"
[107]	50 mM HEPES	0.5 mg/mL	Fibronectin .01 - .016 mg/mL	HEPES	8 min. no irradiance specified. 2x

Due to the variety of conditions found in literature, it was necessary to perform some preliminary studies to determine whether the choice of buffer for reacting sulfo-SANPAH with acrylamide, the buffer's concentration, the buffer's pH, the concentration of sulfo-SANPAH, the concentration of adhesive ligand and its buffer and pH played a significant role in the conjugation efficacy.

While most authors referenced in **Table 3.1** used HEPES as the buffer for sulfo-SANPAH, I found that the high concentrations of HEPES used, greatly limited the solubility of sulfo-SANPAH. Heating the solution and then vortexing it, increased the solubility, but even at 50mM HEPES, it was difficult to fully dissolve all of the sulfo-SANPAH (0.2mg/mL). Upon sterile filtering the sulfo-SANPAH solution it was even more apparent that there were precipitates (trapped in the filter) and that were above the solubility limit of the sulfo-SANPAH. Some researchers, as can be seen from **Table 3.1**, counter this limit by adding DMSO to help solubilize the sulfo-SANPAH, but DMSO is known to be toxic to cells,[111] and DMSO is actually used to differentiate embryonic stem cells, so any remnant DMSO could interfere with the intended applications of this patterning methadology.[112, 113]

The previous researchers most likely used HEPES at pH 8.5 for the sulfo-SANPAH as the increased pH will lead to more primary amines available for conjugation, however the dominant mechanism for sulfo-SANPAH attachment to acrylamide via the UV activated azide is via insertion into C-H and N-H sites, so that having a high pH is less critical. Furthermore, NHS ester hydrolysis increases with increasing pH, and at pH 8, at 25°C the half-life of the ester is only 1 hour.

In my experiments with fibronectin conjugated in bulk to acrylamide, there was no discernable difference in cell adhesion or proliferation of rat mesenchymal stem cells to surfaces that were created with sulfo-SANPAH in PBS pH 7.4 versus those created with sulfo-SANPAH in HEPES buffer pH 8.5. Given that the NHS ester undergoes hydrolysis more rapidly as pH is increased, PBS was selected as the buffer for sulfo-SANPAH, in order to increase the number of active NHS esters

available for the subsequent conjugation to protein, which would require the additional eventual step of allowing the sulfo-SANPAH to dry onto the stamp.

Furthermore, there was no discernable difference in cell attachment or proliferation between surfaces generated with 0.2 mg/mL sulfo-SANPAH (the concentration used by Engler et al.) or any of the higher concentrations listed in **Table 3.1,** primarily because it appeared as though 0.2 mg/mL was approaching the solubility limit of sulfo-SANPAH in PBS, and even more so in HEPES.

Notably, I could not identify a HEPES buffer concentration that could properly buffer fibronectin at the concentrations of fibronectin used in this project (0.1-0.5 mg/mL). When human plasma fibronectin is reconstituted in water at a 1 mg/mL, the pH is supposed to be 11.5, according to the manufacturer (Gibco). This was too basic a solution for HEPES or PBS to buffer. Furthermore, at this high pH there would be an increased amount of primary amines available to react with the NHS ester, so for ease, PBS at pH 7.4 was used, however the pH of the solution was nearly 11.

3.2.3.4 Concentration of Fibronectin

As detailed in section 3.2.4, fibronectin was chosen as the adhesive ligand for the proof of concept experiments. The effects of fibronectin concentration were briefly investigated. On un-patterned surfaces, fibronectin was used in concentrations of 0.1-0.5 mg/mL. For gels above 1 kPa in stiffness, 3T3 cells always became confluent on the acrylamide gels regardless of initial cell seeding density (examined the range 14,000-20,000 cells/cm^2). However, once the cells became confluent, the entire cell sheet could delaminate from the surface (**Figure 3.9**). The time to delamination, from confluence was a function of initial fibronectin concentration, where the higher the concentration the longer the cell sheet remained attached to the acrylamide. In contrast, confluent cells never delaminated from tissue culture polystyrene control wells (observed up to 3 months).

For gels that were as compliant as 0.1 kPa, fibroblasts did not spread, nor did they proliferate to confluence even at the highest concentration of fibronectin examined, 1 mg/mL (**Figure 3.10**). This limits the ability of fibroblasts to be used to determine if there is a compliance of gel that cannot be patterned with the aforementioned technology, however as detailed in chapter 4, polyacrylamide gels as soft as 140Pa could be patterned with fibronectin of Matrigel and support hES cells in the short term. The observation of diminishing fibroblast response to adhesive ligand concentration as the gel compliance increases is consistent with observations from Engler et al.[17]

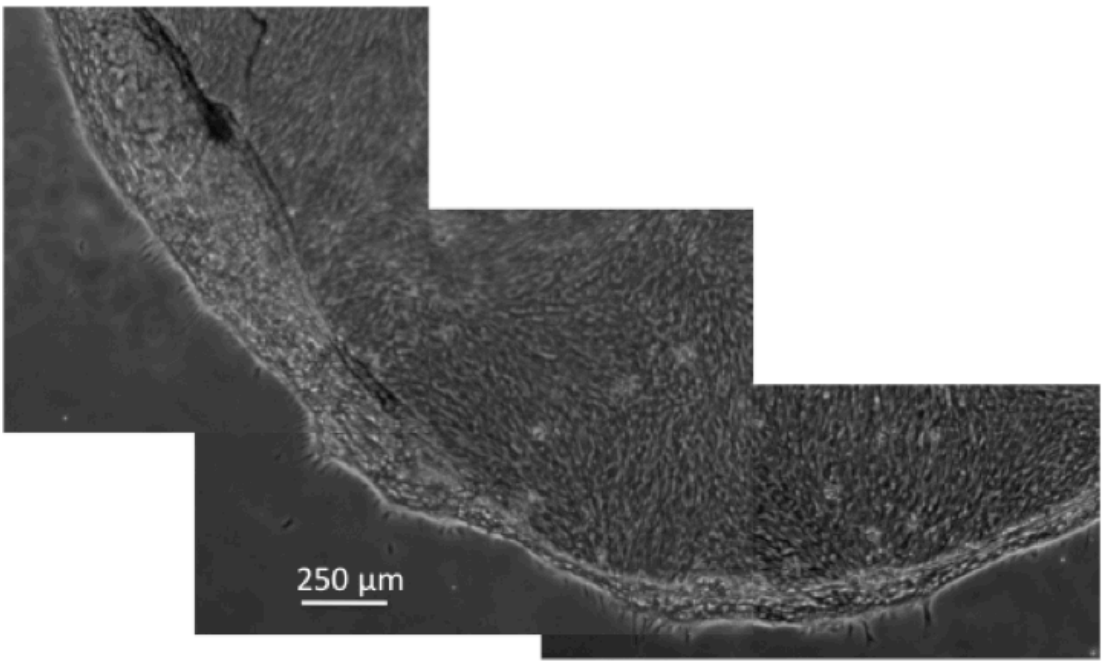

Figure 3.9 Delamination of a 3T3 cell sheet from a fibronectin conjugated 10 kPa polyacrylamide gel, which occurs once the cell sheet has become confluent. Time to delamination is a function of the adhesive ligand concentration, with higher concentrations increasing the time to delamination.

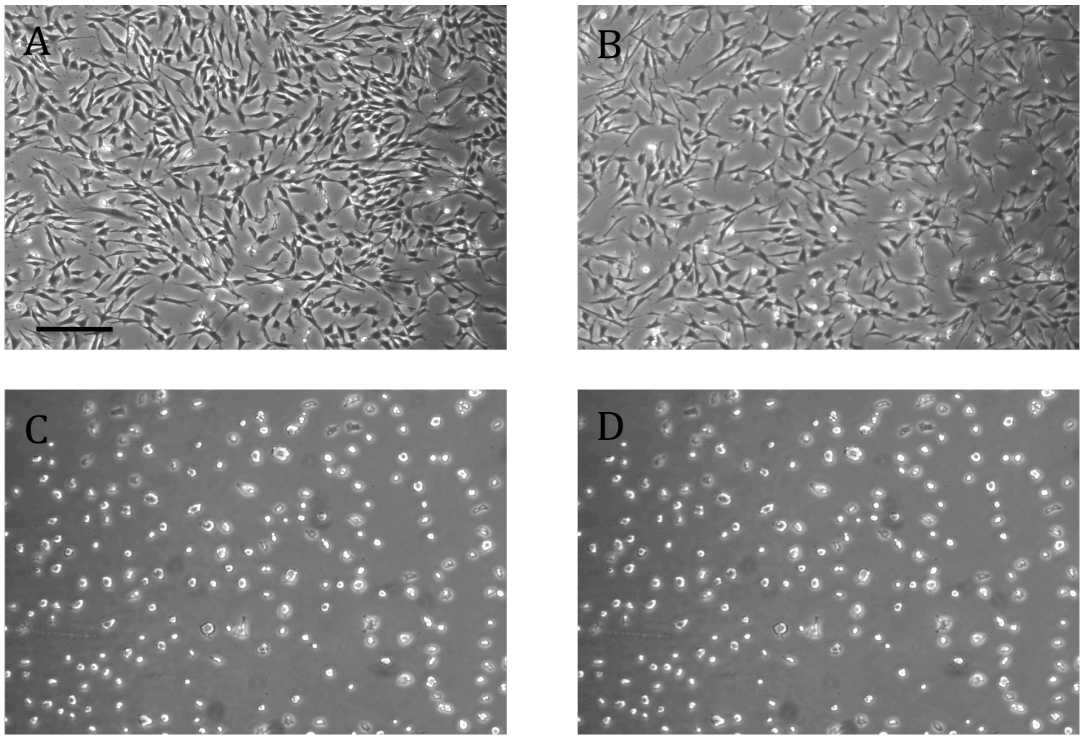

Figure 3.10 On sufficiently compliant fibronectin conjugated gels (< 0.1 kPa), 3T3 cells cannot spread or proliferate. For all gels, 1 mg/mL fibronectin was used. On all gels, 3T3 cells were seeded at 15,000 cells/cm^2. Scale bar = 250µm. 3T3 cells on fibronectin conjugated polyacrylamide gels: (A) 10 kPa gel 24 hours after seeding; (B) 1 kPa gel 24 hours after seeding; (C) 0.1 kPa gel 24 hours after seeding; (D) 0.1 kPa gel 72 hours after seeding. After 72 hours, cell number does not appear to have increased.

3.2.3.5 Photolithography and Stamping

One important design criteria in fabricated stamps for hydrogel patterning is stamp height. As discussed in **Section 3.2.2.1**, the hydrogel should be at least 70 μm thick so that cell does not sense the stiffer glass substrate. Even though the acrylamide and bisacrylamide compositions chosen in this work lead to a maximum swelling value of 1.2, and the stamping was performed while the gel was dehydrated, the stamp height should be sufficiently large such that any hydrogel compressed into the grooves between features would be too short to contact the roof of the stamp. Therefore, the larger the stamp height, the cleaner the stamping; however, there are two factors limiting the maximum size of the stamp height: 1) the bending stiffness of the features on the PDMS stamp and 2) the ability to process a master with high aspect ratio features. Biebuyck et al.[114] have experimentally shown that when the aspect ratio of the stamp features is too large the features will buckle. Furthermore, when the aspect ratio is high, features can fuse into contact by surface forces, and especially by capillary forces when exposed to the inking solution.[99, 115, 116] A 100 μm feature height was chosen as it was expected to be sufficiently tall for the hydrogels and it was constructible with SU-8 50 a low viscosity epoxy formulation for PDMS masters. 250 μm tall feature stamps were also fabricated, as that height would still render a low aspect ratio features (the minimum stamp feature diameter was 200 μm). In order to construct features of the height, a higher viscosity master formulation (SU-8 100) was required. Due to the high viscosity it was difficult to get uniform films in the spin casting step, even when the formulation was preheated to increase flow. More problematic was the inability of the developer to completely removed uncured SU-8 due to the depth of the features in the master. Therefore, stamps were only produced with SU-8 50, and it became apparent that 100 μm were sufficient for stamping, as detailed below.

Another problem encountered with the construction of the PDMS stamps was that of roof collapse, or the ability of the non-featured areas of the stamp to collapse onto the surface being stamped, due to the compliance of the stamp and the spacing between features. As features were the size of desired colonies, (at least 200 μm), it became apparent that one could use an ink-pad to actually test the resistance of the stamps to roof collapse. The thicker the stamp, or the stiffer the stamp, the less susceptible the stamp should be to roof collapse. Increasing the thickness of the total stamp was not very feasible, as this prevented the stamp from releasing from the SU-8 mold without fracturing. PDMS of two different compositions were tested, namely the standard 10:1 (base:curing agent) and 5:1. The stamps were then inked with an inkpad and stamped onto a piece of paper. Stamping was performed by manually pressing the stamp into the paper. From **Figure 3.11** it is evident that pressure that is not distributed over a wide enough area prevents all features from transferring, and that very high pressure (high force per area) leads to roof collapse even in the stiffest PDMS stamp formulation. Once the PDMS stamp was backed with a 1 mm microscope glass slide, roof collapse was completely avoided (**Figure**

3.12D) It was therefore determined, that a glass backing was absolutely necessary for stamping.

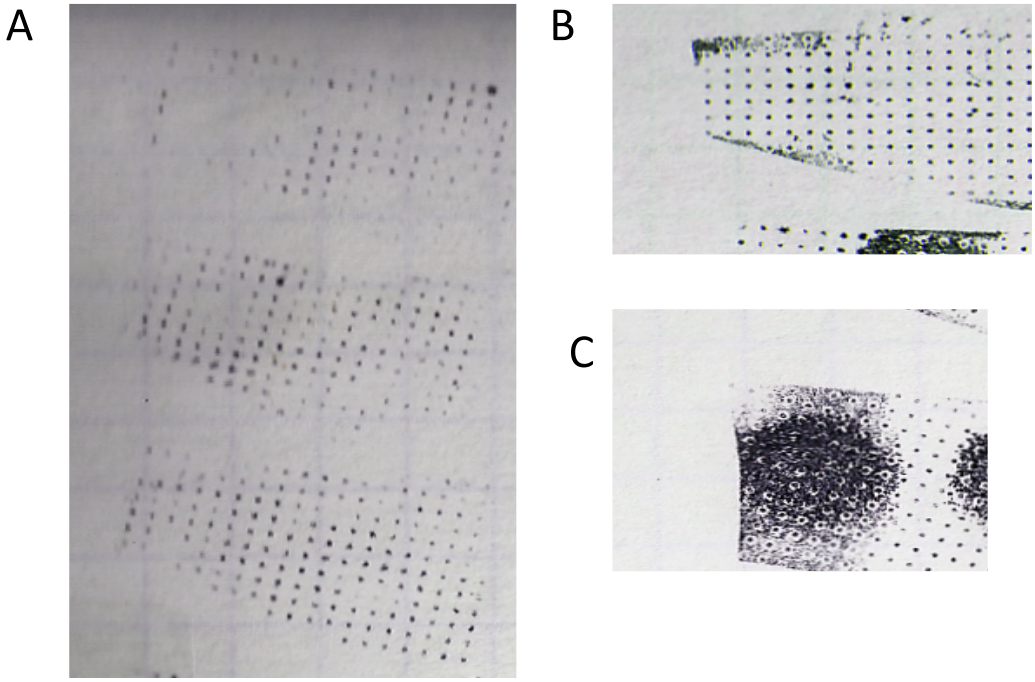

Figure 3.11 Inking PDMS stamps with a standard inkpad and testing pattern transfer onto a stiff, less diffusive surface than acrylamide, namely paper. Stamp posts were 400 μm in diameter. (A) PDMS was prepared with the typical 10:1 (base: curing agent) formulation, and was manually pressed onto paper without a glass backing on the stamp. Insufficient and non-homogeneous pressure limit the ability of the pattern to transfer over the entire area. (B) Extreme localized pressure leads to roof collapse when there is no glass backing for the 10:1 PDMS stamps. C) Roof collapse is also evident in the stiffer 5:1 PDMS formulation when the stamp is subjected to highly localized pressure.

Polyacrylamide drying times, were also investigated (using an inkpad) to determine minimum drying time to prevent diffusion of ink. Two drying methods were examined. Initially a nitrogen gun was employed to dry the quartz disc backed acrylamide gels. If the nitrogen pressure was too high, the films damaged easily. Film drying time was not easily quantifiable with the nitrogen flow, as the orifice of the gun was smaller than the acrylamide gel, and the gun had to therefore be rastered over the sample to dry it, leading to spatially and temporally inhomogeneous drying. Instead, films were dried by placing them in a sterile biosafety cabinet with a known air flow rate and pattern, dependent, on the sash height. The sash height was left at the highest position recommended by the manufacturer for safe use of the biosafety cabinet, yielding a flow rate of 100 ft/min at the face and nearly zero flow rate at the center of the hood where the polyacrylamide was left to dry. At short drying times (i.e. less than 5 minutes), the ink diffused through out the surface (**Figure 3.12**). After 1 hour, the polyacrylamide was sufficiently dry to prevent gross ink diffusion (**Figure 3.12**). It should also be noted that this was conducted with inkpad ink, which was not allowed to dry on the stamp prior to stamping, in contrast to the crosslinker "ink" (sulfo-SANPAH) which

was left to dry on the stamp surface prior to stamping. Thus, the diffusion would be even lower for sulfo-SANPAH for the same stamping times.

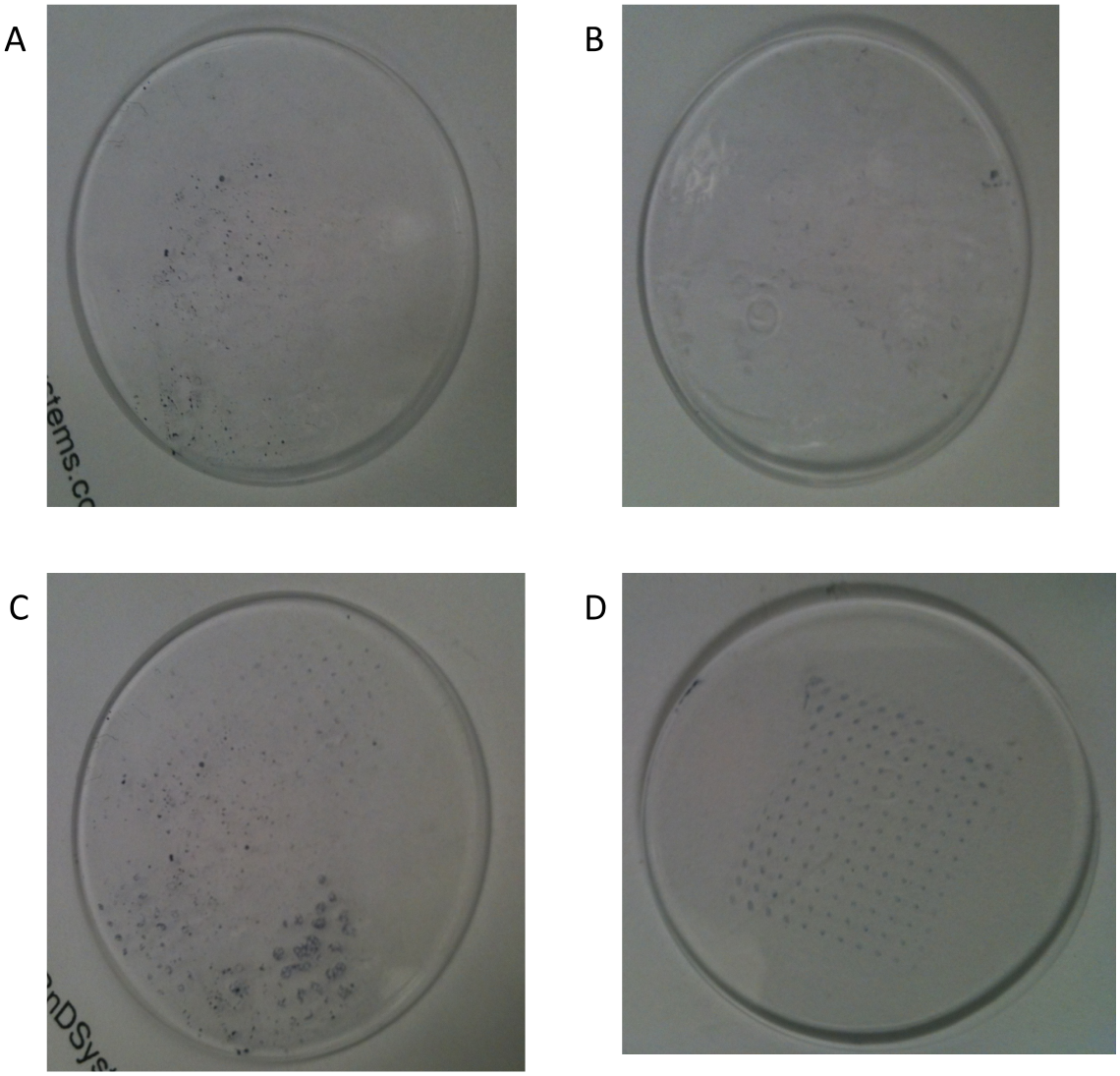

Figure 3.12 Determining an acrylamide gel drying time that can sufficiently prevent gross ink diffusion. PDMS stamps were backed with glass to prevent roof collapse. Polyacrylamide gel drying times prior to stamping: (A) 1 minute (B) 5 minutes (C) 10 Minutes (D) 1 hour.

Additionally, the effects of the solvent of the polyacrylamide gel on gel drying were examined. Polyacrylamide gels were either hydrated in deionized water, or PBS pH 7.4 after 70% ethanol sterilization. Gels in PBS consistently left inhomogeneous salt aggregates, which can interfere with the stamping, as can be seen in **Figure 3.13**. PBS was initially examined as a solvent as it was thought that pH control would be important for covalently reacting the crosslinker "ink" to the acrylamide gel. However, subsequent experiments showed that the reaction was possible in DI water, so PBS was no longer used as the solvent for the acrylamide gel during the stamping process.

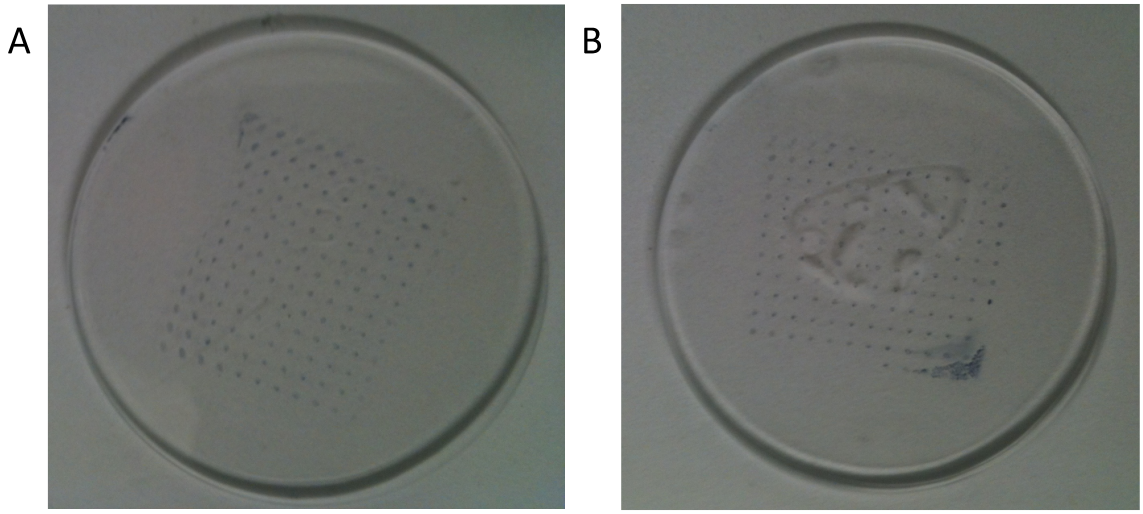

Figure 3.13 Comparing polyacrylamide gel drying as a function of polyacrylamide gel storage solution: (A) Deionized water and (B) PBS. Both gels were dried for 1 hour prior to stamping. The drying process leaves dense areas of high salt concentration in the polyacrylamide gel which was stored in PBS.

Another parameter considered was the time allotted for ink adsorption onto the PDMS stamp. If insufficient time is allotted, most of the ink will be displaced in the nitrogen drying step; however, since the ink this project was a crosslinker with an NHS ester, with limited half life at pH 7, there was an upper bounds to the allowable "ink" incubation time. Consulting microcontact printing literature, it became evident, that regardless of the "ink" used (i.e. polymer, small molecule, or protein) "inks" were always adsorbed onto the PDMS stamp for 1 hour prior to a deionized water rinse and nitrogen drying.[117-121] Testing the crosslinker after 1 hour adsorption onto a PDMS stamp in a dark room showed that the crosslinker was still active. This was tested by examining 3T3 cell attachment to these surfaces after they were conjugated with fibronectin, and it was shown that 1 hour "ink" incubation time on the PDMS stamp does not diminish the reactivity of the crosslinker to an unacceptable level, such as one in which the ester could not react with fibronectin which was necessary for cell attachment.

3.2.3.6 Sterility

In order to use stamped hydrogel surfaces for cell culture, it was necessary to ensure that the gels were sterile after processing. Analysis of the literature cited earlier in this dissertation (such as **Table 3.1**) as for protein conjugated acrylamide cell substrates, it was clear that many authors did not indicate whether they sterilized their surfaces, however the authors may have not considered sterilization necessary as all the cells used were grown in media with antibiotics. For hES cells this was not feasible as they are grown in the absence of antibiotics. Some authors used UV to sterilize the surfaces after protein conjugation; however, this option was dismissed as UV can degrade proteins.[122] Furthermore, if the UV dose was low enough to prevent significant destruction to the structure of the protein, it is not clear that it was high enough to significantly destroy the DNA in bacteria and render

the surface sterile. In fact, work in the Healy group has shown that UVC, at the laboratory dose of 400 mW/cm^2 for 15 hours does not eliminate E. Coli to below detectable amounts, and furthermore, degrades RGD peptides.[123] Sterilizing from then on in the Healy lab was accomplished by treating gels with 30 minute UV incubation prior to peptide functionalization.[19]

Initially I attempted to sterilize the surfaces after they were completely fabricated, using a 30 minute 70% ethanol incubation followed by copious PBS rinses prior to cell seeding. However, on one occasion 3T3 cell contamination occurred and it was clear that this method was not sufficient. Additionally, there was concern that the ethanol can potentially irreversibly denature the adhesive protein of interest. Moreover, 3T3 cell media contains the antibiotic combination penicillin and streptomycin, which most hES cell culture does not contain, due to the fear that it can affect proliferation and differentiation. Therefore, it was necessary to find an alternate sterilization procedure.[124]

Since 30 minute 70% Ethanol incubation is more effective at killing bacteria, and polyacrylamide polymers can degrade via chain scission from UV exposure, I opted to sterilize the polyacrylamide gels in 70% Ethanol, prior to stamping, and to sterile filter all subsequent reagents with a low protein adsorbing 0.22 μm filter, and to conduct all work after the polyacrylamide polymerization in a sterile hood.[125]

An unexpected benefit of this sterilization process was the added ease of quality control of the polyacrylamide gels afforded by ethanol sterilization. Since ethanol is not a good solvent for polyacrylamide gels, gels in ethanol will collapse and become opaque, which allows for increased visibility of defects, such as holes in the gel caused by air bubbles trapped either in the prepolymer solution or by the sandwiching of the top cover slip.[126] Some defects cannot be seen when the polymer is hydrated and can only been seen upon dehydration/sterilization with ethanol, such as gradations in height of the gel which can be seen as gradations in opacity. The non-uniform gel height is a result of the non-level surfaces in the hoods used for polymerization, and one way to mitigate the problem is to decrease the polymerization time.

Since adopting the ethanol sterilization protocol for the polyacrylamide gel, and proceeding sterile for all subsequent steps, no contamination occurred in any 3T3 or hES cell experiments.

3.2.3.7 Summary of Patterning Protocol

Optimal parameters involved in the patterning process discussed in the preceding sections are summarized in this section in the order in which they were presented.

Quartz Substrate: It was found that polyacrylamide gels had to be prepared on quartz substrates with a silane mediating attachment to the quartz. A strong attachment to the substrate was necessary to prevent the polyacrylamide buckling or delamination from the surface due to swelling forces. TCPS did not offer sufficient grafting points for the polyacrylamide gel, and the polyacrylamide gel was able to delaminate from the surface upon swelling. Exposing TPCS to oxygen plasma at

levels that would not induce flow and deformation of the TCPS did not ameliorate the problem of insufficient graft sites, and polyacrylamide gels still delaminated as they swelled and buckled. It was therefore concluded that a quartz backing was necessary to maintain a flat topography with the polyacrylamide gels.

Crosslinker and Buffer Properties: Buffer identity and concentration for both the crosslinker (sulfo-SANPAH) and the adhesive ligand (fibronectin) were examined. It was found that while HEPES buffers at pH 8.5 at various concentrations were historically used to conjugate proteins via sulfo-SANPAH to polyacrylamide gels, PBS was a better solvent for both sulfo-SANPAH, in terms of solubility and increasing the half life of the NHS ester. It was also found that fibronectin at the concentrations used was too alkaline to be buffered by either PBS or HEPES, so PBS was used as its solvent due to ease of access of the reagent.

Sterilization: Sterilization procedures were also optimized. While other researchers have used UV to sterilize protein conjugated polyacrylamide gels, after protein conjugation, this was not deemed appropriate, as the UV could denature proteins, and if the UV was used at a sufficiently low enough power so as to prevent denaturation, how was that guarantee of sufficient bacterial DNA damage? Additionally, these researchers used media formulations with antibiotics, which is not a typically exercised option with hES cell culture. Sterilizing with ethanol after protein conjugation was also not deemed as an appropriate option as that could too denature proteins. Therefore, polyacrylamide gels were sterilized with ethanol prior to any conjugation or stamping steps. All subsequent reagents were sterile filtered, and once the PDMS stamp was backed with glass, it was sterilized with ethanol and all subsequent procedures were performed in a sterile biosafety cabinet. Using ethanol to sterilize the polyacrylamide gels prior to protein/peptide conjugation, also allowed one to visualize the quality of the polyacrylamide gels, as ethanol dehydrated the gel to an opaque white mass where holes or inconsistencies in height which were not visible in the swollen state, became visible.

Photolithography and Stamping: In order to have features separated by long distance, on the patterned hydrogels, it was necessary to fuse the PDMS stamps to a glass backing to prevent roof collapse. Roof collapse experiments were easily first carried out by using the PDMS stamp on paper with an actual inkpad, as desired the feature sizes that correspond to meaningful colony sizes (400-1200μm diameter) are visible to the naked eye. The glass backing was found to barely attenuate the UV light through the stamp, and the attenuation could easily be compensated for by increasing total UV exposure time. Additionally, polyacrylamide gel drying times under specific airflow conditions were determined to allow for pattern transfer but to minimize diffusion of the ink.

Acrylamide Protein Resistance: It was observed that storage conditions of the acrylamide and bisacrylamide monomer and the use of DI water could affect the protein resistance of the polyacrylamide gel. In order to decrease protein adsorption, it was necessary to minimize the presence of uncreated monomers trapped in the final gel via selection of very pure reagents and a non-acidic solvent.

3.2.3.6 Patterning with 3T3 cells

Using the UV activated microcontact printing technique detailed herein, it was possible to create long range patterns of 3T3 cells on very compliant surfaces (as compliant as 1 kPa) (**Figure 3.14**).

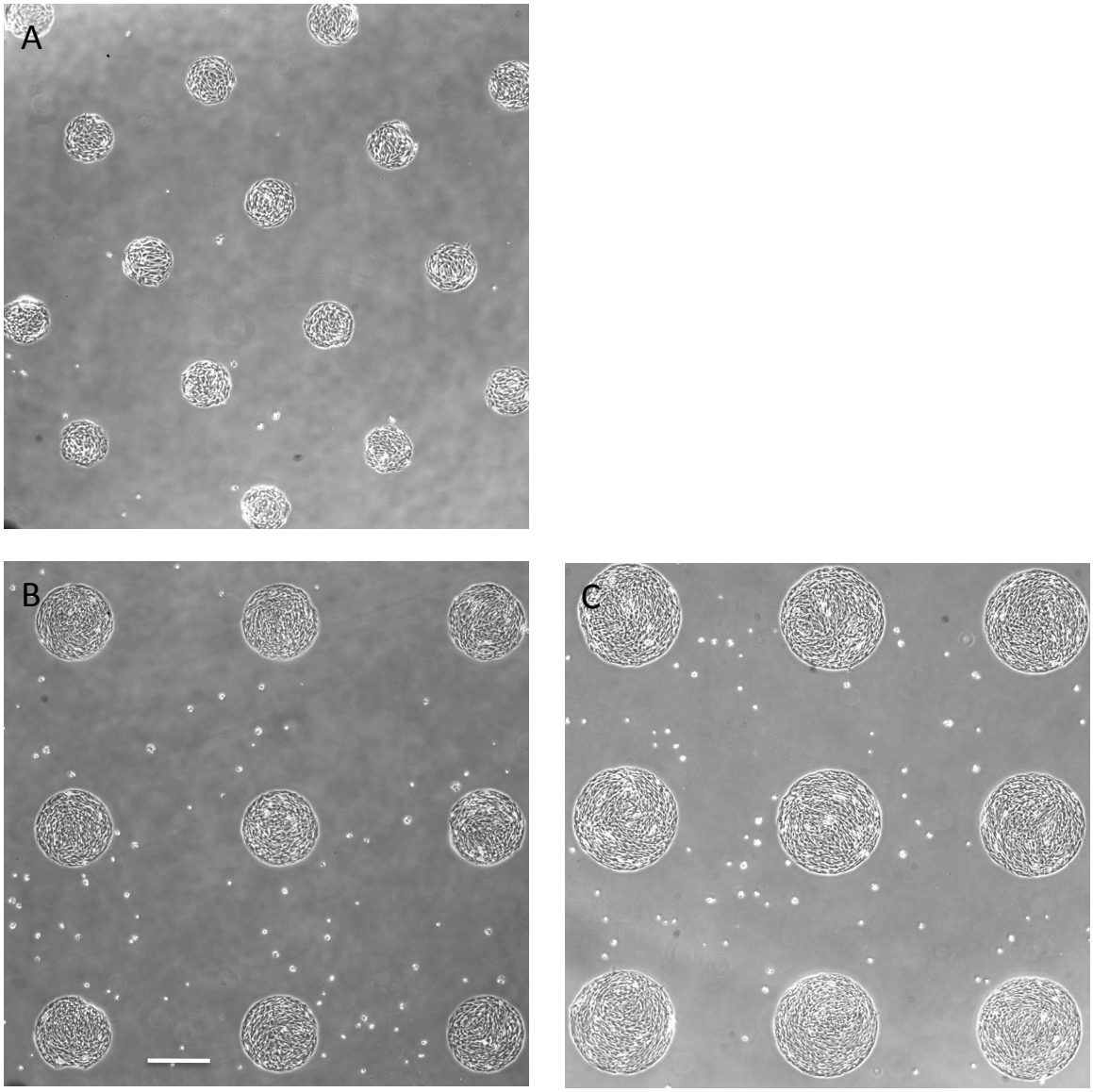

3.14 3T3 cells patterned on fibronectin (.5 mg/mL) conjugated polyacrylamide gels (1 kPa), day 2. Scale bar = 500 μm. PDMS stamps with post diameters: (A) 400 μm, (B) 600 μm, and (C) 800 μm were used to generate these patterns.

It was possible to print the entire area of the well of a 6 well plate (~35 mm^2). More compliant gels were not examined with 3T3 cells, as the fibroblasts could not proliferate or spread on gels more compliant, regardless of adhesive ligand concentration (see **Section 3.2.3.4**). However, the technology is still employable on gels as compliant as 140 Pa, as demonstrated with hES cells in **Chapter 4**. The UV

activated microcontact printing technique is not likely to be constrained by the compliance of the hydrogel but rather, by the swelling ratio of the hydrogel. Furthermore, there is no biological reason to pattern surfaces more compliant than 100Pa, which corresponds to the stiffness of the most compliant tissues in the human body, fat and brain.

Interestingly, as 3T3 cells proliferated, they generated forces on the underlying polyacrylamide gels that allowed the cellular island to contract (**Figure 3.15**). In contrast, on TCPS, or other stiff culture surfaces, cellular islands cannot deform the surface, and they are unable to contract, if attached directly to the surface. The ability for the cellular islands to contract is particularly appealing for applications with beating cells such as the derivation of cardiac cells from induced pluripotent stem cells (iPS) as discussed in **chapter 5**.

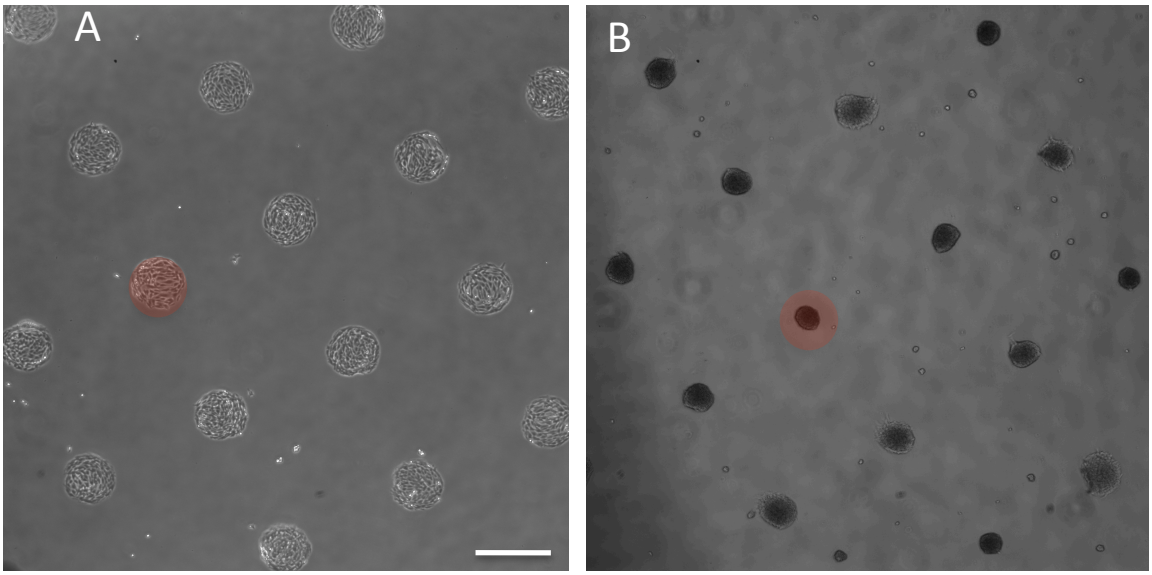

Figure 3.15 3T3 cellular islands can contract on fibronectin patterned polyacrylamide gels. 1 kPa gels. Scale bar = 500 μm. (A) day 1 after seeding (B) 5 days after seeding. The red circle is a visual guide to show cell island contraction, and it represents the area of a cell island at day 1

3.3 Modulating the Fouling Behavior of Acrylamide with PEG

3.3.1 Introduction

Even though we achieved excellent cell patterning results on variable moduli polyacrylamide gels, preliminary studies, in the presence of serum containing media, such as those used for 3T3 fibroblasts and rat mesenchymal stem cells, a few poorly spread, balled up cells became adherent to the polyacrylamide gel. It was also observed that when conjugating sulfo-SANPAH to the polyacrylamide gel, and then adding cells in serum containing media, even more cells could attach and remain adherent (**Figure 3.16**). For stem cell applications, it was critical to

minimize cell attachment to background regions, as these cells would confound proposed paracrine signaling studies.

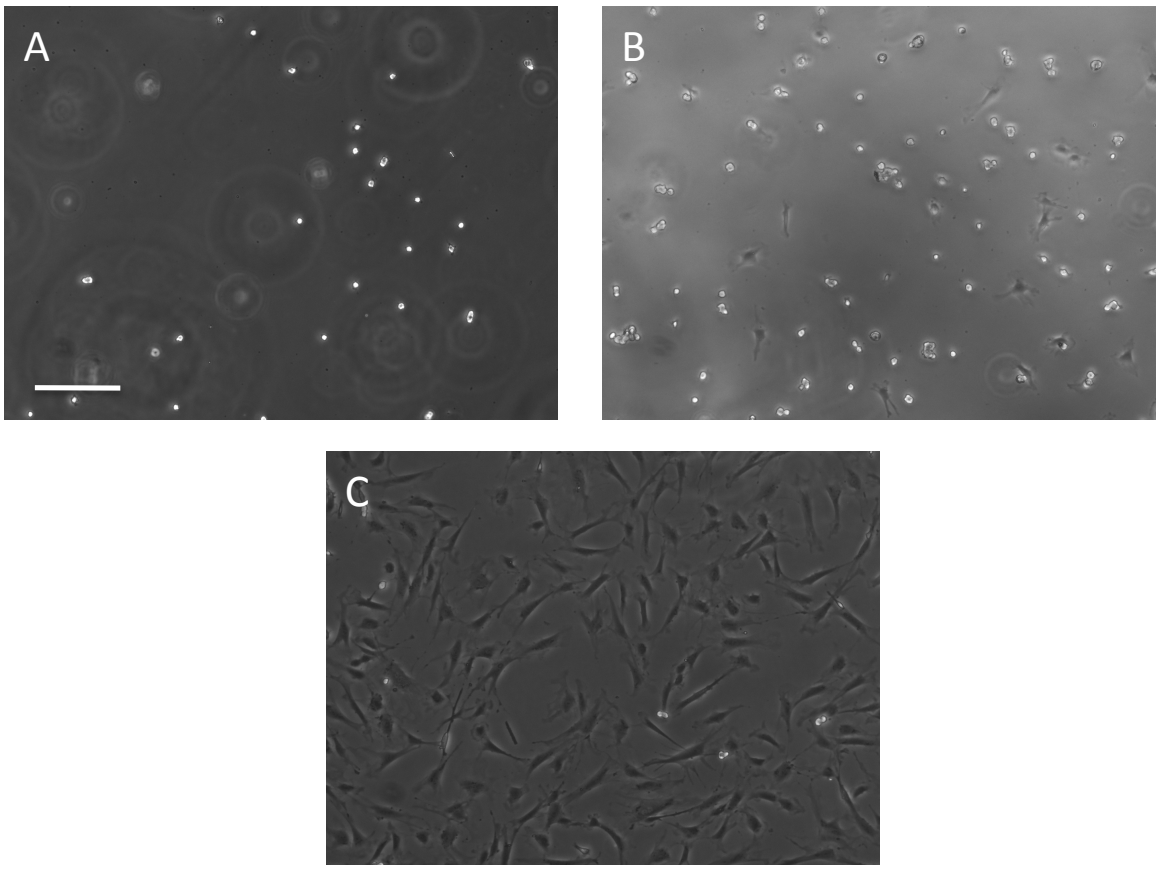

Figure 3.16 The ability of polyacrylamide gels to support rat mesenchymal stem cell adhesion 1 day after seeding at 20,000 cells/cm^2 in the presence of serum. (A) 10 kPa acrylamide; (B) 10 kPa acrylamide conjugated to sulfo-SANPAH; (C) 10 kPa acrylamide conjugated to fibronectin via sulfo-SANPAH.

A number of molecules and polymers were therefore investigated that could bind to any excess sulfo-SANPAH that was not bound to an adhesive ligand, that may have strayed from the patterned region. The small molecules examined in this work were tris(hydroxymethyl)aminomethane (TRIS), and 2-(2-aminoethoxy)ethanol (AEOE), which are depicted in **Figure 3.17**. TRIS was chosen as it had been used in previous research to quench any unreacted sulfo-SANPAH. TRIS has a primary amine, which can react with sulfo-SANPAH, leaving 3 hydroxyl groups on the surface to as act as a protein repellent layer. Similarly, AEOE was used by Yang et al.[120] to quench unreacted pentaflourphenol (PFP) in their MAPS (Microcontact printing on Activated Polymer Surfaces) technology, and it has been used by Semler et al.[108] specifically to neutralize unreacted sulfo-SANPAH. Based on research by Whitesides' group[80], it was expected that ether and hydroxyl groups could limit protein adsorption, as they are the minimal units of ethylene glycol, a molecule extensively studied by Andarade et al. due to poly(ethylene glycol)'s (PEG) noted protein film resistance.[80, 127-129]

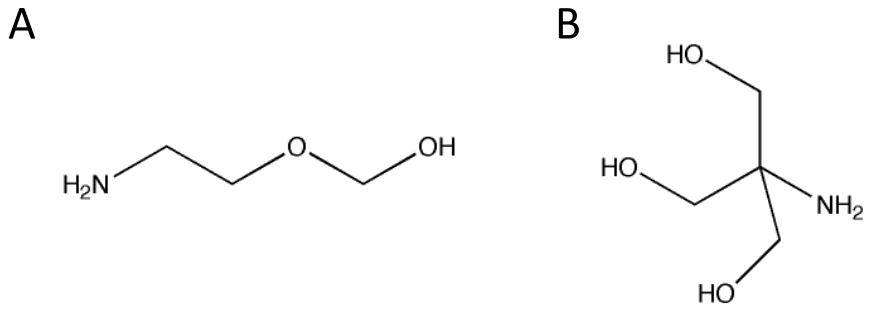

Figure 3.17 Two small molecules investigated as backfillers to minimize adsorption of proteins and cells onto residual unconjugated sulfo-SANPAH. (A) Aminoethoxyethanol (AEOE) (B) tris(hydroxymethyl)aminomethane (TRIS)

However, it has been shown that the polyethylene glycol chains, need to be of a certain minimum length (2-6 monomers) to prevent protein adsorption, which may limit the ability of the small molecules AEOE and TRIS to adequately prevent protein adsorption.[130, 131] Longer PEG chains have proven to be remarkably efficacious in preventing cellular adhesion, so they too were examined as agents to decrease the fouling of acrylamide gels.[81, 132 133] Two parameters that were explored for the PEG chains were chain length, and terminal chemical group. It is expected that a chain length above about 6 units of PEG should prevent protein adsorption[131] as long as the PEG is grafted at the maximum possible density.[81] However, the length of the chain can affect the likelihood of a terminal chain end being available for reaction. At least one chain end needs to have the reactive amine group, and the other chain end can be selected to either minimize protein adsorption (methoxy or hydroxyl)[131], or have an amine termination to increase the likelihood of the chain reacting with the surface.

The molecular weights (MW)s of the PEG chains explored herein were chosen based on the work of Sofia et al.,[81] who studied protein fouling of PEG grafted surfaces, and the work of Greg Harbers in the Healy lab, who studied the protein fouling of PEG grafted interpenetrating polymer networks (IPN)s composed of acrylamide and PEG networks.[134] Sofia et al. covalently grafted PEG chains of MW: 3,400, 10,000 and 20,000 g/mol to silicon surfaces and determined the solution concentration and the consequent surface concentration, or grafting density, required for a specific PEG chain length to prevent protein adsorption. Prior to Sofia's study, PEG's nonfouling had been studied in the context of self assembled monolayers on gold, which allow for extremely high grafting densities. Sofia's work was the first to study the behavior of much longer randomly coiled chains covalently attached to a surface. The assumption was that for such longer randomly coiled chains examined by Sofia, the maximum grafting density would occur at the brush regime, where chain spacing is approximately equal to the radius of gyration, forcing chains to stretch away from the surface, and adopt a longer conformation than they would in solution.[135-138] Using ellipsometry to determine the dry thickness of the PEG films, Sofia et al. were able to correlate the input concentration of PEG with the grafting density, and they observed that the highest grafting density was obtained for the shortest PEG chain (3,400 g/mol), which is to be expected as the

larger the PEG chain, the larger the excluded volume effects which prevent tight packing of the chains at the interface. They also noticed that the grafting density plateaued at input concentration equivalent to the critical overlap concentration C* where

$$C^* = \frac{MW}{N_A \frac{4}{3}\pi R_G^{\,3}} \qquad \textbf{Eq. 3.2}$$

MW is the molecular weight, Rg is the radius of gyration, and N_A is Avogadro's number. Lastly, they showed that at PEG grafting densities achieved with solution concentrations slightly below the overlap concentration, the PEG surfaces were resistant to protein adsorption (as measured by protein film thickness with x-ray photoelectron spectroscopy (XPS)).

One thing to note, was that in Sofia's work, there was as very high number of grafting sites available for the PEG chains, even if it was not as high as that available with self assembled monolayers. In Sofia's work, the silicon substrate was coated with trimethoxysilylpropyldiethylenetriamine to create reactive amines on the surface. They concluded that the surface amine concentration was four secondary amines and two primary amines per square nanometer with an average amine spacing of 7 Å. The radius of gyration, of 3,400 MW PEG, in comparison is about 25 Å (as calculated from light scattering data obtained by Devanand et al.[139]). One would expect potentially fewer grafting sites when binding to a polymer network. However, Harbers et al.[134] found that highest conjugation of 3,400 MW PEG to his poly(AAm-co-PEG/Aac) IPN occurred with PEG chain input concentrations equivalent to the critical overlap concentration, and he found that these surfaces resisted protein adsorption.

Sofia's work also demonstrated that for the same solution concentration, a shorter PEG chain could attain a higher grafting density than a longer PEG chain. Longer chains; however, required a lower solution concentration to reach the critical overlap concentration. Longer chains could also extend further away from the interface. However the disadvantage of using a longer chain is that as the chain gets larger, the volume occupied by the polymer increases, which decreases the chance of the chain ends being available for a chemical reaction. I therefore decided to investigate three molecular weights of PEG chains, including the 3,400 g/mol used by Sofia et al.[81] and Harbers et al.,[134] and one shorter chain (2,000 g/mol) and one longer chain(5,000 g/mol).

3.3.2 Methods and Materials

10 kPa polyacrylamide gels were constructed as described in section **3.2.1.1.** Quartz backed gels were then sterilized with 70% ethanol overnight and washed three times with PBS (Life Technologies), and then paced into BD Falcon 6 well tissue culture plates, where 1 ml of 0.2 mg/ml sulfo-SANPAH, was added to each well. Plates were placed in a UV flood illuminating chamber (Dymax, Dymax Corporation, Torrington CT), and exposed to 1.25 J/ cm^2 of UV (99 seconds at 1.25

mW/cm^2) (with lid on) to activate the azide of the sulfo-SANPAH. The plates were then rinsed with PBS to remove any unbound sulfo-SANPAH, and 1ml of either Tris (1 M), AEOE (1 M at pH 8.5 in HEPES), or a PEG chain was added to each well and allowed to react for for 4 hours at room temperature. The gels were then rinsed with PBS three times, and rat mesenchymal stem cells were seeded on the surfaces as described in section **3.2.4.4** at 20,000 cells/cm^2 in 10% FBS media.

The PEG chains used were of the form NH_2-PEG_x-Y where Y= NH_2, CH_3 or OH. The molecular weights selected were 2,000, 3,400, and 5,000 g/mol. In order to graft at the maximum possible density, the concentration of PEG used for each was the critical concentration as defined in **Equation 3.3**. The radius of gyration (needed to calculate the overlap concentration) was calculated using **Equation 3.3**, obtained from Devanand et al.[139] from static light scattering experiments:

$$Rg = 0.215(MW)^{0.583} \qquad \textbf{Eq 3.3}$$

The equation was derived from higher molecular weight PEG chains, but the exponent is very close to 0.588 expected from the Flory model for a good solvent, lending legitimacy to the use of this equation for short PEG chains. **Table 3.2** shows the actual concentrations used for the experiments as a function of PEG chain length.

Table 3.2 Radius of Gyration and Critical Concentration C* as a function of PEG chain molecular weight. The Critical Concentration C* was used as the input concentration for reactions.

PEG chain (g/mol)	Radius of Gyration (Å)	Critical Concentration C* (g/ml)
2,000	18	0.136
3,400	25	0.086
5,000	31	0.068

3.3.3 Results and Discussion

TRIS and AEOE did not appear to reduce the fouling of sufo-SANPAH conjugated acrylamide (**Figure 3.18**), in that for all three conditions, some cells attach and a few even spread, rendering those surfaces indistinguishable from the sulfo-SANPAH conjugated acrylamide surface.

The two shorter length PEG chains examined (MW=2,000, and 3,400, both diamino) were able to significantly reduce the fouling of the acrylamide gel as was evidenced by the near complete lack of cell adhesion on those surfaces (**Figure 3.19**). In contrast, the largest PEG chain examined (MW=5,000) allowed for significant cellular attachment, demonstrating that a MW of 5,000 was too large to allow chain ends to reach acrylamide for conjugation. Since the diamino PEG chains were able to prevent cell attachment to the polyacrylamide gels, the PEG chains that had methyl and hydroxyl groups were not tested.

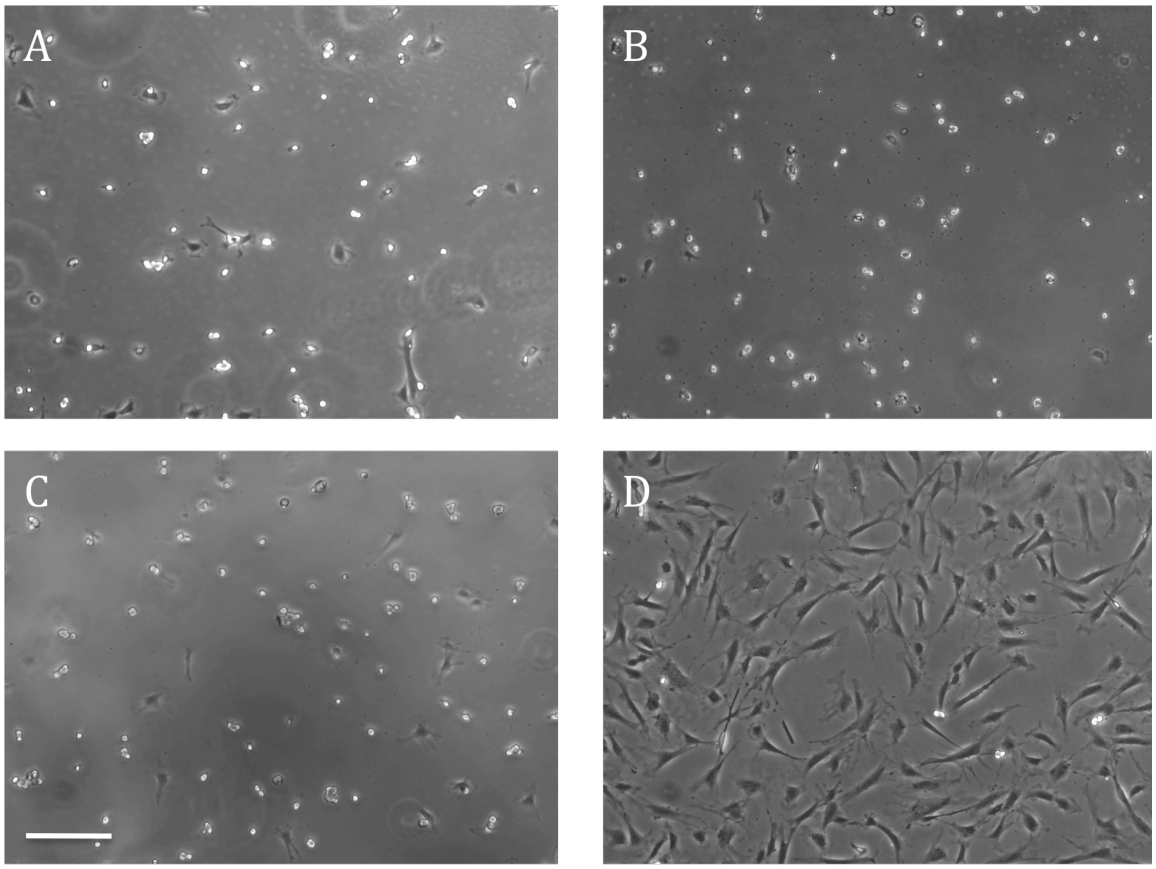

Figure 3.18 Exploring the use of backfillers to decrease the fouling of suflo-SANPAH conjugated acrylamide gels, by observing cellular adhesion of rat mesenchymal stem cells to the surface 1 day after they were seeded at 20,000 cells/cm^2 in the presence of serum on 10 kPa gels (after rinsing with PBS). (A) TRIS conjugated to acrylamide via sulfo-SANPAH; (B) AEOE conjugated to acrylamide via sulfo-SANPAH; (C) sulfo-SANPAH conjugated polyacrylamide; (D) fibronectin conjugated to polyacrylamide via sulfo-SANPAH. Scale bar = 250 μm

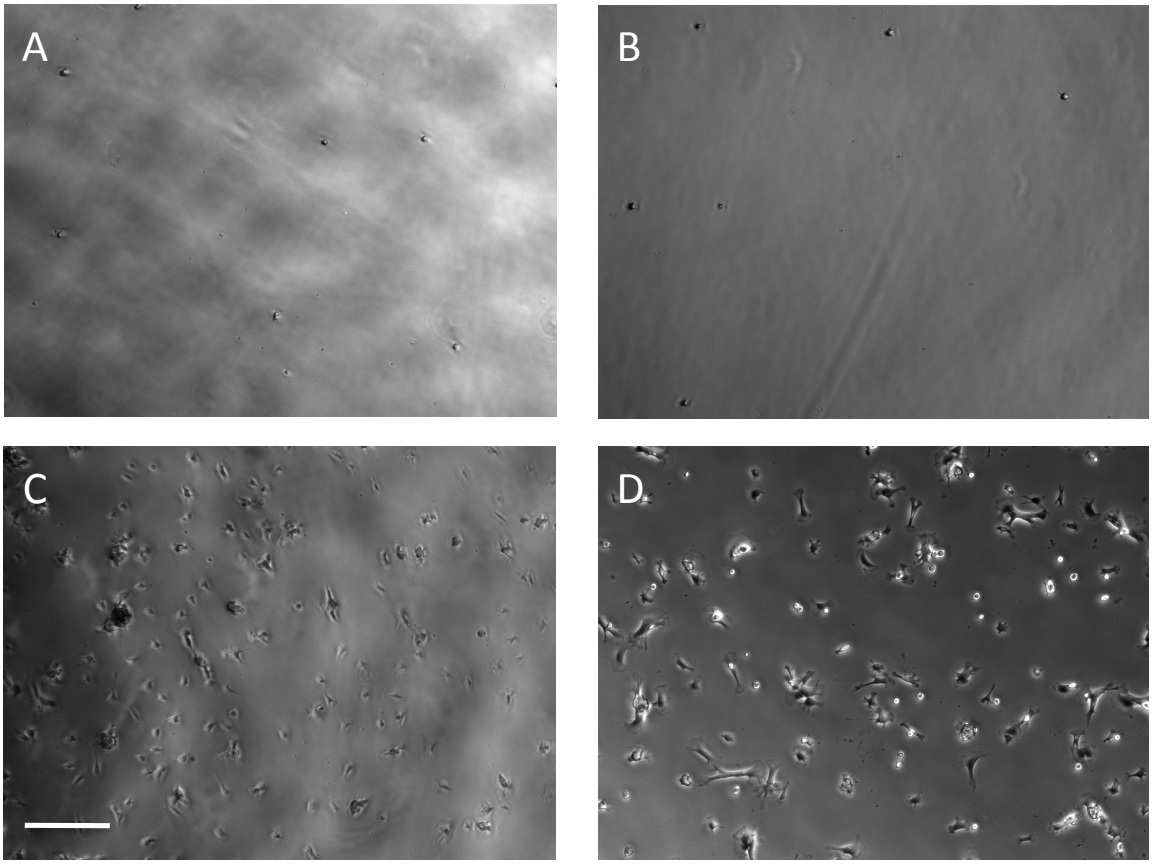

Figure 3.19 Diamino-PEG chains of varying length affect the ability of cells to attach to 10 kPa polyacrylamide gels. Images taken 3 days after rat mesenchymal stem cells were seeded on the surfaces at 20,000 cells/cm^2 (after rinsing with PBS). (A) PEG chain MW= 2,000 (B) PEG chain MW=3,400 (C) PEG chain MW= 5,000 (D) control without PEG chain: 10 kPa polyacrylamide gel. Scale bar = 250 μm.

In conclusion, it was found that, if necessary, PEG chains be conjugated to polyacrylamide to reduce protein adsorption, by using a solution concentration at the critical overlap concentration of the chain, and using PEG chains sufficiently short to allow the end groups to be accessible for reaction (in this work MW < 5,000 g/mol)

3.4 Patterning Acrylamide with Adhesion Peptides

3.4.1 Introduction

As discussed in **Section 3.2.2.3**, the RGD peptide is the minimum necessary unit for cellular adhesion, as discovered by Ruoslahti.[91]. While, fibronectin can now be purchased in recombinant format, the use of peptides can significantly reduce the cost of the proposed cell culture substrate relative to recombinant fibronectin. Additionally, the covalent binding of fibronectin via sulfo-SANPAH can occur at any or multiple free primary amines, which may alter the number of active binding sites available to cell surface receptors, or denature and expose cryptic sites on the

protein. A peptide in contrast is short enough that it can be designed to only react covalently at one specific site, leaving the cell binding motif (RGD) unaltered.

As discussed in **section 3.2.2.3**, while RGD is the minimum peptide sequence required for cellular adhesion, the flanking amino acids modulate the strength of the adhesion and subsequent cellular behavior. For example, it has been shown that GRGDSP has a higher binding affinity than RGDS.[140] In addition to the studies that have shown that altering a peptide in the RGD can diminish or completely abolish binding affinity[141], numerous studies have also shown that changing amino acids in the flanking region can significantly affect binding affinity.[95, 141-143] In this work, the RGD sequence used was that derived from bone sialoprotien. The peptide was aceylated and amidated at the ends for stability and contained a cysteine group for conjugation, and specifically had the sequence: Ac - Cys - Gly - Gly - Asn - Gly - Glu - Pro - Arg - Gly - Asp - Thr - Tyr - Arg - Ala - Tyr - NH_2. This peptide was explored in the Healy lab by Ali Rezania and he found that interacts with the $\alpha_v\beta_3$ and $\alpha_5\beta_1$ integrins. [144-146] Subsequently, Healy lab members have also used this peptide sequence to engage adult and neural stem cell populations.[3, 19, 147]

In order to pattern an RGD peptide on the acrylamide hydrogel, preliminary studies were conducted to determine optimal conjugation of the RGD peptide unpatterned, to the acrylamide gel. The peptide was conjugated with the crosslinker N-((2-pyridyldithio)ethyl)-4-azidosalicylamide) (PEAS) which has a UV activated azide on one end, and a thiol reactive group on the other end, which can react with the thiol of the terminal cysteine on the peptide (**Figure 3.20**). In this work, a number of concentrations of crosslinker and RGD were examined and fibroblast adhesion was used to test conjugation efficacy.

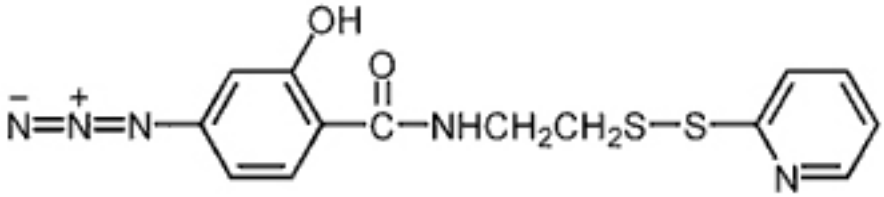

Figure 3.20 PEAS structure has a UV activate-able azide group, like sulfo-SANPAH, on one end, and a thiol reactive group on the other end.

Since cell response was expected to be a function of RGD surface concentration, it was necessary to choose appropriate concentrations of RGD for the experiment. Hubbell's group[148] had shown that below an RGD surface concentration of 10 fmol/cm^2, fibroblasts failed to spread, and that a surface density of 1fmol/cm^2 was required for the formation of focal contacts. Rezania et al.[146] found that .01 pmol/cm^2 of the bone sialoprotein RGD sequence was necessary for cellular attachment of rat calvarial osteoblasts. At 0.01 pmol/cm^2 , cells attached at the same percentage relative to the positive control (TCPS with 15% FBS media), as they did on the negative RGE control surface. At that concentration they also spread to the same extent as they did on the negative RGE control. They found that at 0.62 pmol/cm^2, cells not only attached, but spread to the same size as they spread when plated with 15% FBS on TCPS. However, above 4 pmol/cm^2, there was significant

cellular attachment with the percentage of cells attaching reaching 88% of the number attached to the positive control (TCPS with 15% FBS media).

In the aforementioned papers, both Hubbell and Rezania attached their RGD peptides to solid supports (glass and silicon respectively), and not to swollen polymers. RGD peptides have also been successfully grafted onto very thin (~10-100 nm) swollen polymers, and they were capable of supporting cellular adhesion and long term proliferation.[149, 150] For example, Hubbell's group conjugated GRGDS to a semi-interpenetrating polymer network (sIPN) of polyethylene glycol and acrylic acid (PEG-co-AA), and demonstrated that the human foreskin fibroblast cells (at concentrations as high as 100,000 cells/cm^2 and in the presence of serum) would not attach to the polymer network when not conjugated with peptide, however in the sIPN was conjugate to peptide cells could attach, spread and proliferate robustly. In contrast, when Hubbell's group attempted to attach cell adhesive peptides to PEG-surface-modified-PET (polyethylene terephthalate), they were not able to attain a surface density above 20 fmol/cm^2, and as a consequence there was limited cell spreading of the cells that were able to attach, which underscores the potential difficulty of conjugating the peptides to a swollen polymer instead of a solid support, as was attempted in this manuscript.[151] Using the sIPN, Hubbell's group was able to achieve peptide surface density of 40 pmol/cm^2.[149] Even higher RGD densities were achieved by Brandley and Schnaar[152] who incorporated an RGD peptide into an polyacrylamide gel by copolymerizing an acrylate conjugated peptide with the acrylamide and bisacrylamide. In this fashion, they were able to obtain surface RGD densities as high as 15 nmol/cm^2. Interestingly in their work, with 3T3 cells, they found that surface densities on the order of 150 nmol/cm^2 were required for the cells to attach and spread in a comparable fashion to their attachment and spreading on a TCPS control surface. At concentrations of 4 nmol/cm^2, cells could barely attach, spread or proliferate, in seemingly sharp contrast with Hubbell and Rezania's observation for minimum RGD surface density on the order of femto or picomols/cm^2. However, one must recall that cellular behavior on soft surfaces is a function of both ligand density and modulus of underlying substrate. The gels made by Brandley and Schnaar[152] were 0.6 mm thick, and while their modulus was not determined, it is expected that they are significantly more compliant than Hubbell's sIPNs[149], or the peptide conjugated interpenetrating polymer networks (IPNs) in the Healy lab[150] whose thickness is ~100nm, and therefore effectively presents a surface as stiff as the substrate below the IPN. The fact that RGD peptide surface concentration necessary to elicit specific cellular behavior varies by surface, with more compliant surfaces requiring higher ligand density, is not surprising and is consistent with results from Engler et al.[17]

It was therefore the aim of this section to determine if an RGD peptide could be covalently attached to a polyacrylamide hydrogel via UV-activatable crosslinker, for use in a patterned substrate, and to determine which range of concentrations of crosslinker and peptide should be used.

3.4.2 Methods and Materials

10 kPa polyacrylamide gels were constructed as described in section **3.2.1.1.** Quartz backed gels were then sterilized with 70% ethanol overnight and washed three times with PBS, and then paced into BD Falcon 6 well tissue culture plates.

The RGD peptide used had the following sequence:
Ac - Cys - Gly - Gly - Asn - Gly - Glu - Pro - Arg - Gly - Asp - Thr - Tyr - Arg - Ala - Tyr - NH2 (American Peptides) and was purchased from American Peptides.

In order for the crosslinker PEAS to bind a thiol it must be reduced, and not in disulfide format. Furthermore, the RGD peptide itself needs to be reduced as the thiol on its cysteine group can become oxidized during storage from exposure to air.

Since two new components (crosslinker and adhesive ligand) were added to the system they were tested separately before being combined. That is to say the PEAS was first evaluated with the protein fibronectin at 0.5 mg/ml in PBS, in order to determine optimal concentration and processing conditions.
Both the peptide and the crosslinker PEAS were reduced using the (Tris[2-carboxyethyl] phosphine (TCEP), following protocol developed by Jacob Pollock, in the Healy lab.[153] In that protocol a solution of 3 mg NaOH and 5.7 mg TCEP per ml water is prepared. 50 uL of that solution is then added for every 1mg of peptide and allowing to react at 4°C for thirty minutes.

The minimum PEAS input concentration evaluated was 100uM, which is the same concentration of sulfo-SANPAH used in the patterning project.

Triplicate surfaces were prepared for each reaction condition. 3T3 cells were seeded on the surfaces at 14,000 cells/cm^2, and were used to visualize efficacy of reaction 1 day and 3 days after cell seeding. Cells were seeded in serum free media, and media was exchanged at 4 hours to media with 15% FBS for peptide surfaces.

3.4.3 Results and Discussion

Fibronectin was used to determine appropriate concentrations to use of the PEAS crosslinker, and to validate the reducing protocol, as the response of 3T3 cells on fibronectin conjugated to polyacrylamide gels has already been established in the earlier parts of this dissertation. At 100 uM input concentration of PEAS, fibronectin conjugation to 10 kPa polyacrylamide is comparable to fibronectin conjugation when using sulfo-SANPAH, as can be seen by the equivalent cell attachment to both surfaces (**Figure 3.21**). As expected, when fibronectin is physiosorbed onto polyacrylamide, few if any cells stick, and they are not spread (**Figure 3.21A**). In contrast, cells on 10 kPa acrylamide conjugated with 0.5 mg/ml fibronectin show greater cell density than cells grown on TCPS (**Figure 3.21**). When PEAS was not reduced with TCEP, prior to conjugation with fibronectin, no cells attached (data not shown), indicating that PEAS was successfully reduced with TCEP, and that the reduction was necessary for the crosslinker to react with a free thiol in the fibronectin protein.

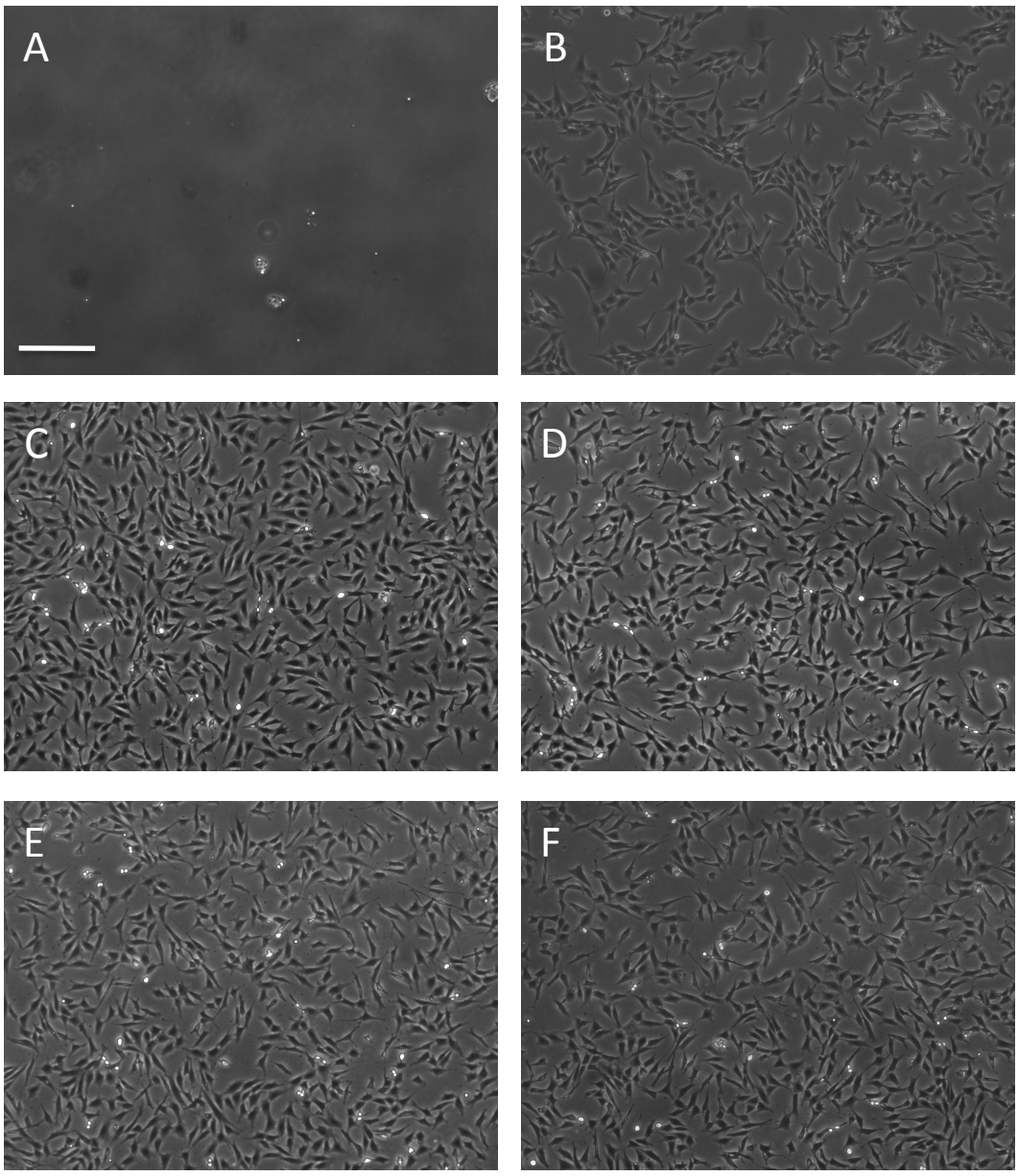

Figure 3.21 Using fibronectin to determine sufficient concentrations of PEAS crosslinker, and to validate reducing protocol for PEAS. Scale bar = 250 μm. Day 1 after 3T3 cells were seeded at 14,000 cells/cm^2 onto 10 kPa polyacrylamide surfaces that had fibronectin conjugated to them via the crosslinker PEAS. (A) fibronectin adsorbed onto polyacrylamide (no PEAS); (B) TCPS control; (C) TCPS control with pre-adsorbed fibronectin; (D) fibronectin conjugated to polyacrylamide via sulfo-SANPAH; (E)fibronectin conjugated to polyacrylamide via PEAS (100uM PEAS input); (F) fibronectin conjugated to polyacrylamide via PEAS (200uM PEAS input)

RGD peptide conjugation was attempted with the input concentration range of 100-400 uM, notably higher than what has been used in the Healy lab for conjugating to thin IPNs of poly(AAm-co-EG/AAc), or variable modulus poly(AAm-co-EG/AAc) (which has been ~ 20 uM).[19, 150, 154] However, cellular attachment onto these surfaces did not appear to differ between surfaces in which the peptide was conjugated with PEAS to 10 kPa acrylamide and surfaces in which serum and no

peptide were allowed to react with PEAS (**Figure 3.22**). The peptide did appear to be active as other students in the laboratory used peptide from the same batch, which was reduced using the same TCEP protocol.

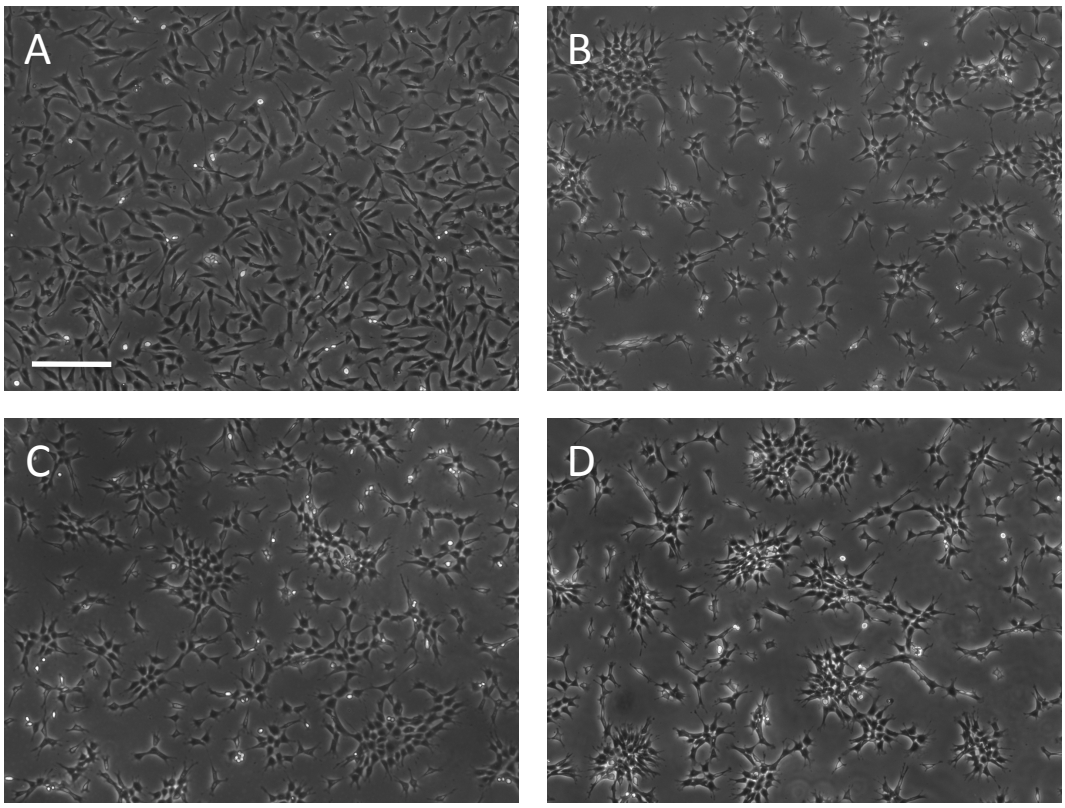

Figure 3.22 3T3 cells 1 day after seeding at 14,000 cells/cm^2 on surfaces created by conjugating adhesive ligands to 10 kPa polyacrylamide via 200 uM PEAS. Scale bar = 250 μm (A) adhesive ligand = fibronectin (B) adhesive ligand = serum (C) adhesive ligand = 100 uM RGD (input concentration) (D) adhesive ligand = 400 uM RGD (input concentration)

There are a few possible explanations for the observed RGD results, including insufficient peptide attachment, excess peptide getting trapped in the gel and eluting over time, and reduction of the peptide – PEAS bond due to processing conditions. Each of those potential explanations will be addressed below.

As detailed in **Section 3.4.1,** a number of papers have claimed different minimum surface densities of RGD peptides required for fibroblasts and similar cells to attach and spread on surface to the same extent that they would on TCPS in the presence of media with serum. Brandley et. al[152], using a polyacrylamide gel required surface densities nmol/cm^2 to maintain the same cell behavior as the positive TCPS control, while Rezania et. al[146] and Hubbell[148] required surface concentrations orders of magnitude lower, such as the fmol/cm^2 and pmol/cm^2 range when covalently attaching the RGD peptide to a solid support. As mentioned in the **Section 3.4.1** it is to be expect that a higher surface density of ligand is required to elicit the same cellular spreading, as the surface becomes more compliant. Brandley et al.[152] did not measure the stiffness of their surface, but it

would be expected to be within 1 order of magnitude of the 10 kPa gels discussed herein.

When the RGD surfaces were examined after three days, the cells had balled into large aggregates and were able to pull up from the acrylamide surfaces (**Figure 3.23**) in contrast to cells grown on polyacrylamide surfaces with fibronectin conjugated with the same crosslinker (PEAS). This would indicate that insufficient amounts of peptide were conjugated to the surface, or more likely that unreacted peptide was getting trapped in the gel, and slowly eluting over time to competitively bind with acrylamide bound peptide. In support of the later theory, on day 1 there did not seem to be a difference in the number of cells attached or their spreading as a function of input RGD peptide concentration (100 uM or 400 uM) (**Figure 3.22**), however by day 4 there were fewer cells attached on the 400 uM surfaces (in all 3 wells prepared for that condition (data only shown from 1 well) (**Figure 3.23**). Additionally, the serum wells had higher cellular attachment on day 3 than either of the RGD surfaces. In order to definitively determine which of these two scenarios were more likely (insufficient RGD surface density, or excess RGD getting trapped in the hydrogel and eluting over time), one would have to be able to quantify the surface density of RGD peptide on the polyacrylamide gels.

Barber et. al[154] pioneered a technique to quantify RGD peptides conjugated to a surface which involved the use of chymotrypsin, an enzyme which cuts peptides after the amino acids tyrosine, tryptophan, and phenylalanine, if they are not followed by proline. Incubating chymotrypsin with an appropriately designed FITC conjugated RGD peptide that was attached to the thin IPN, poly(AAm-co-EG/AAc). The FITC fragment of the peptide was cleaved, and the fluorescent intensity of the solution was then quantified to determine peptide concentration. Unfortunately, this novel technique does not work well with thicker gels, which can trap the cleaved peptides and chymotrypsin. There have been attempts in our group to overcome this problem by using chymotrypsin attached to micron sized beads, however the fluorescent intensity of the signal kept increasing in time and never became steady. Therefore, no attempt was made to quantify the amount of RGD on the surfaces described herein.

An alternate explanation for the observed results, was that any remnant TCEP could have reduced the bond between PEAS and the RGD peptide. In order to minimize that possibility, this experiment was also attempted without using TCEP to reduce the peptide, prior to conjugation, while keeping the PEAS TCEP reducing step. Prior to peptide addition, the polyacrylamide gel was rinsed in PBS 5 times to remove any residual TCEP. Even under those conditions, cellular binding did not differ from its behavior with serum, and was never as robust as it was on TCPS controls (data not shown). Additionally, reduction of the peptide was attempted with TCEP bound to agarose beads (commercially available from Thermo-Scientific), following manufacturer's protocol, however results still did not differ from **Figure 3.22**. Another option would have been to use a crosslinker with a UV activate-able azide linkage on one end, and thiol reactive group on the other end that would not require reduction prior to conjugation, such as 1-(p-azidosalicylamido)-4-(iodoacetamido) butane (ASIB). Unfortunately, at the time of this research, that molecule was no longer commercially available, however it does appear to be

commercially available from one vendor at the time of this writing (Biocompare.com).

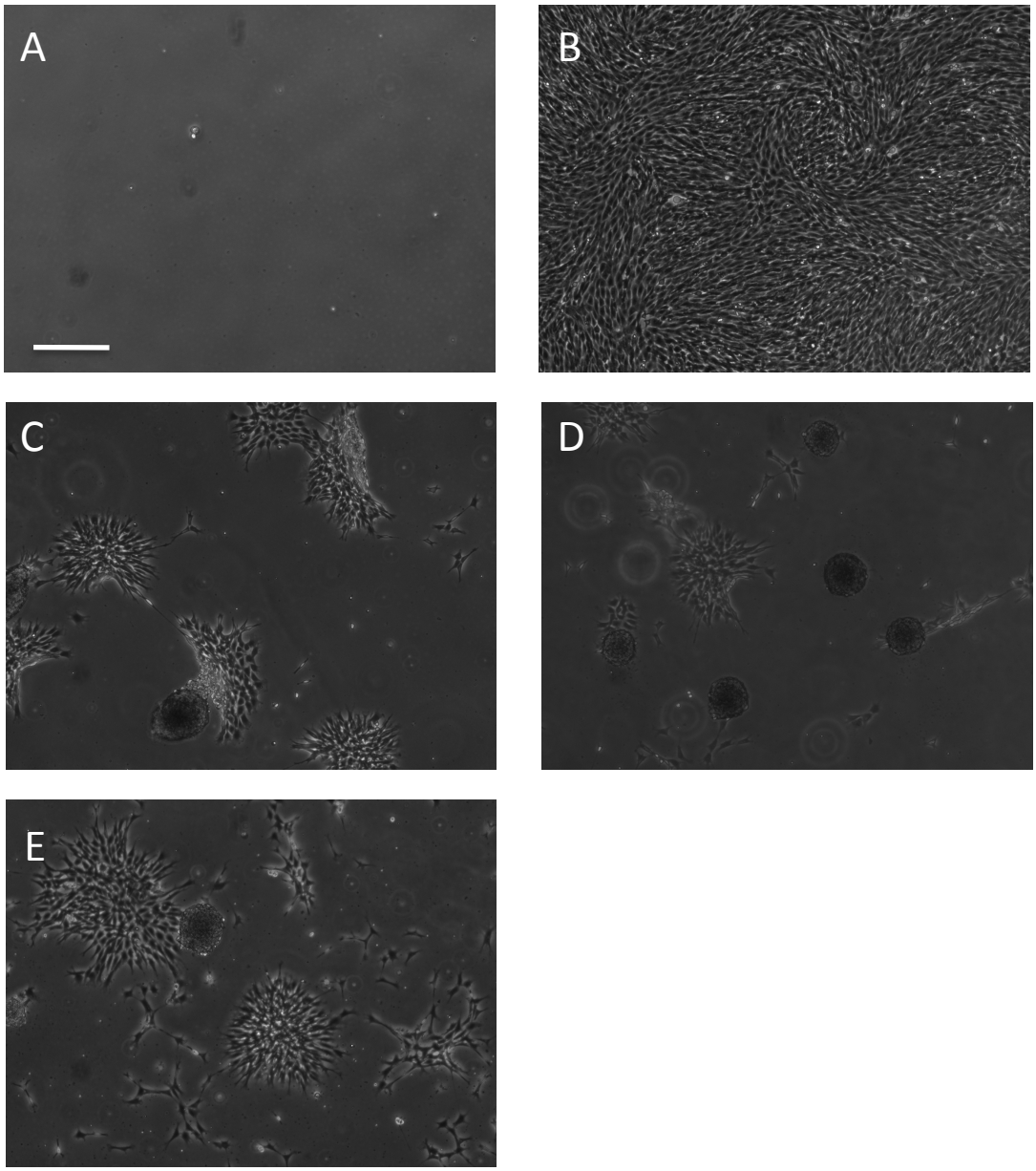

Figure 3.23 3T3 cells 3 days after seeding on surfaces created by conjugating adhesive ligands to 10 kPa polyacrylamide via 200 μM PEAS. Scale bar = 250 μm (A) no adhesive ligand; (B) adhesive ligand = 0.5 mg/mL fibronectin; (C) adhesive ligand = 100 μM RGD; (D) adhesive ligand = 400 μM RGD; (E) adhesive ligand = DMEM media with 15% FBS

Since a suitable method to attach sufficient RGD peptide to polyacrylamide hydrogel surfaces was not found, no attempt was made to pattern the peptide onto the polyacrylamide hydrogels. It is however my belief that the bond between the crosslinker and the peptide was not stable enough in the possible presence of any unwashed reducing agent. Therefore, this experiment should be tried again with the

ASIB crosslinker, which does not require a reducing step prior to peptide conjugation.

3.5 Alternate Patterning Methodologies Explored

In addition to the main patterning methodology described herein, a number of other methodologies were explored, that were less successful. However, I feel that it is informative to point out those techniques and to elucidate their failure mechanisms. For example, when microcontact printing the sulfo-SANPAH crosslinker and then UV illuminating in two separate steps, instead of illuminating through the stamp while printing, the features were significantly messier and a an appreciable amount of background fouling was visible (compare **Figure 3.24** to **Figures 3.14 and 3.15**. A likely explanation for the difference in pattern fidelity between the two techniques is that exposing to UV while printing decreases the time the stamp is in contact with polyacrylamide gel, therefore decreasing the time available for the ink to diffuse away from the patterned region.

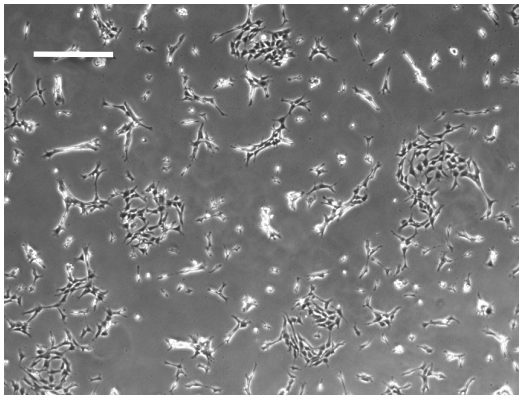

Figure 3.24 Microcontact printing the crosslinker sulfo-SANPAH and then exposing to UV, yields messy patterns that are not well defined, and show a significant amount of background fouling. Scale bar = 250 µm. Compare with figures **3.14 and 3.15** in which UV exposure occurred during printing.

3.5.1 Photomask

Another technique examined was the use of a photomask to selectively activate sulfo-SANPAH that was applied in bulk to the whole hydrogel (illustrated in **Figure 3.25**). The photomask was a transparency printed at a 10,000 DPI, which had ink where the sulfo-SANPAH should not get conjugated. It had the exact opposite polarization of the photomasks used to generate SU-8 masters which were used to fabricate PDMS stamps for printing polyacrylamide gels. The assumption was that sulfo-SANPAH not exposed to UV would not have an activated azide group, and would therefore not bind to the polyacrylamide gel, and would wash away in a subsequent rinse step. This method was appealing as it shortened the patterning procedure by eliminating the time consuming PDMS stamp creation step.

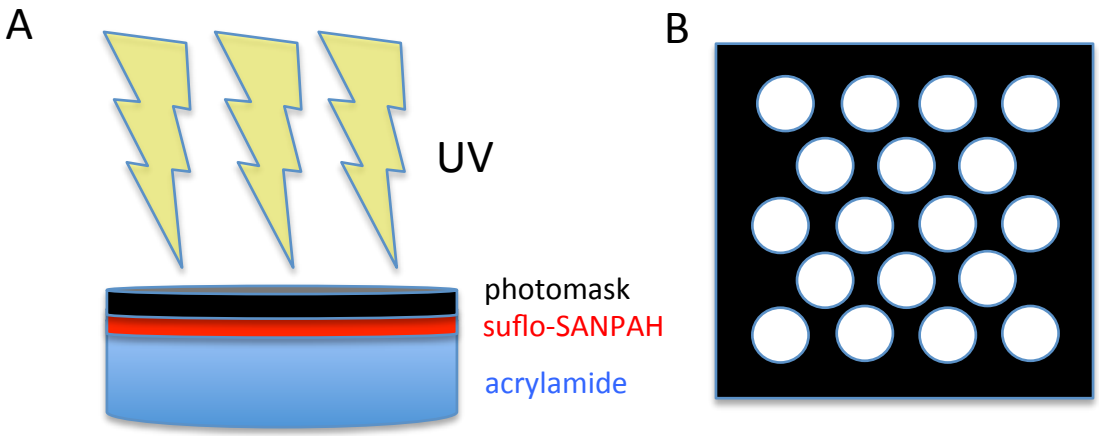

Figure 3.25 Schematic of using a photomask to selectively illuminate sulfo-SANPAH, as a patterning methodology. (A) Sulfo-SANPAH is applied in bulk to the polyacrylamide gel, and a photomask is placed directly on top of the sulfo-SANPAH covered polyacrylamide gel. The setup is the exposed to UV. (B) Top view of photomask. UV is blocked from all black regions, and is transmitted in the blank regions. The photomask is a transparency printed at a 10,000 DPI.

3.5.1.1 Methods and Materials

Polyacrylamide gels were prepared as detailed in **Section 3.2.1.1**, but instead of inking sulfo-SANPAH onto the PDMS stamps, 1 mL of the sulfo-SANPAH solution (0.2 mg/mL in PBS) was poured onto the gel. A photomask was then applied to the gel inkside down under a UV flood illuminator (EXFO Omnicure 1500W light source (with a 365 nm bandpass filter)) and exposed to 365 nm light at $1.25 * 10^{-2}$ W/cm^2 for varying times (5 seconds, 10 seconds, 1 minute). After exposure, the photomask was then removed and the gels were washed three times in copious amounts of PBS, in order to remove any unconjugated sulfo-SANPAH. The samples were then incubated with 1 mL of 0.2 mg/mL fibronectin and placed on a rocker for 1 hour at room temperature. The gels were then rinsed three times in PBS. 3T3 cells were then seeded on the surfaces at 15,000 cells/cm^2.

3.5.1.2 Results and Discussion

A photomask was used to selectively activate sulfo-SANPAH, which had been applied in bulk to the acrylamide hydrogel, and regardless of exposure time, cells stuck to the entire pattern (**Figure 3.26**). Illuminating for less than 5 seconds was not attempted as it was determined that this would not allow for sufficient azide activation. Minimum azide activation time was determined empirically using a second UV source, at the same power, namely the Dymax curing system, which has a clear window, and allowed one to observe the color change (red to brown) as the UV interacted with sulfo-SANPAH. Using the Dymax UV system, it was observed that it took about 5 seconds for the solution color to fully change.

When sulfo-SANPAH is applied in bulk there exist significantly more sulfo-SANPAH molecules than can react with the surface of the polyacrylamide gel than when sulfo-SANPAH is applied via a stamp, with only approximately a monolayer available to react. Even if there was no diffraction through the photomask, creating active azide groups in excess of what can react with the surface, prevents patterning, as all the excess unconjugated sulfo-SANPAH molecules will react with previously masked polyacrylamide gel regions during the post-exposure wash step. It was therefore determined that using a photomask to selectively activate sulfo-SANPAH applied in bulk to a polyacrylamide gel was not a feasible method to pattern a hydrogel.

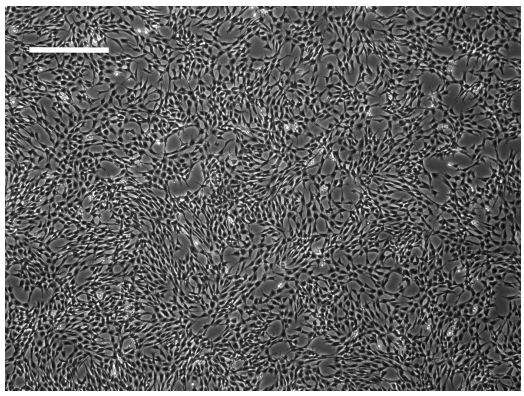

Figure 3.26 3T3 cells stuck to the entire polyacrylamide gel surface, when the gel was patterned with fibronectin via a photomask, illustrating the failure of this technique, which allows for sufficient mobility of the ink (sulfo-SANPAH crosslinker) to cover the entire surface. Scale bar = 250 μm

3.5.2 Stamping with Protein Ink

Another patterning method explored was the use of the adhesive ligand protein as the ink, with the crosslinker applied in bulk to the whole surface, and PEG chains used as backfillers to quench all unreacted crosslinker. The largest hurdle with that approach was successful inking of the stamp, which implied a uniform protein film on the stamp that could retain proper functionality of the protein after transfer.

Fibronectin solutions at a variety of concentrations were prepared with a variety of buffers (PBS and HEPES), with the concentration of the buffers also varied, in order to control the drying patterns of the protein. Ink was left on the stamp in a sterile biosafety hood to for 1 hour to allow the ink to adsorb, which is common practice for microcontact printing of proteins.[121, 155] Macroscopically, it was apparent that the air flow in the sterile hoods caused non-uniform drying (**Figure 3.27A**). Even with the sash closed, to eliminate air flow, and all drying accomplished with a nitrogen gun, inhomogeneous films were visible on the stamps (**Figure 3.27B-C**). Even worse, at higher protein concentration (0.5 mg/mL), the stamp never appeared dry after prolonged drying times with a nitrogen gun (~5 minutes).

In fact it was possible to dry the films in such a manner that all of the protein clung to the edges of the PDMS posts, and to the roof, and no protein was present on the tops of the post, creating cell patterns that were the inverse of the PDMS stamp (**Figure 3.27D**).

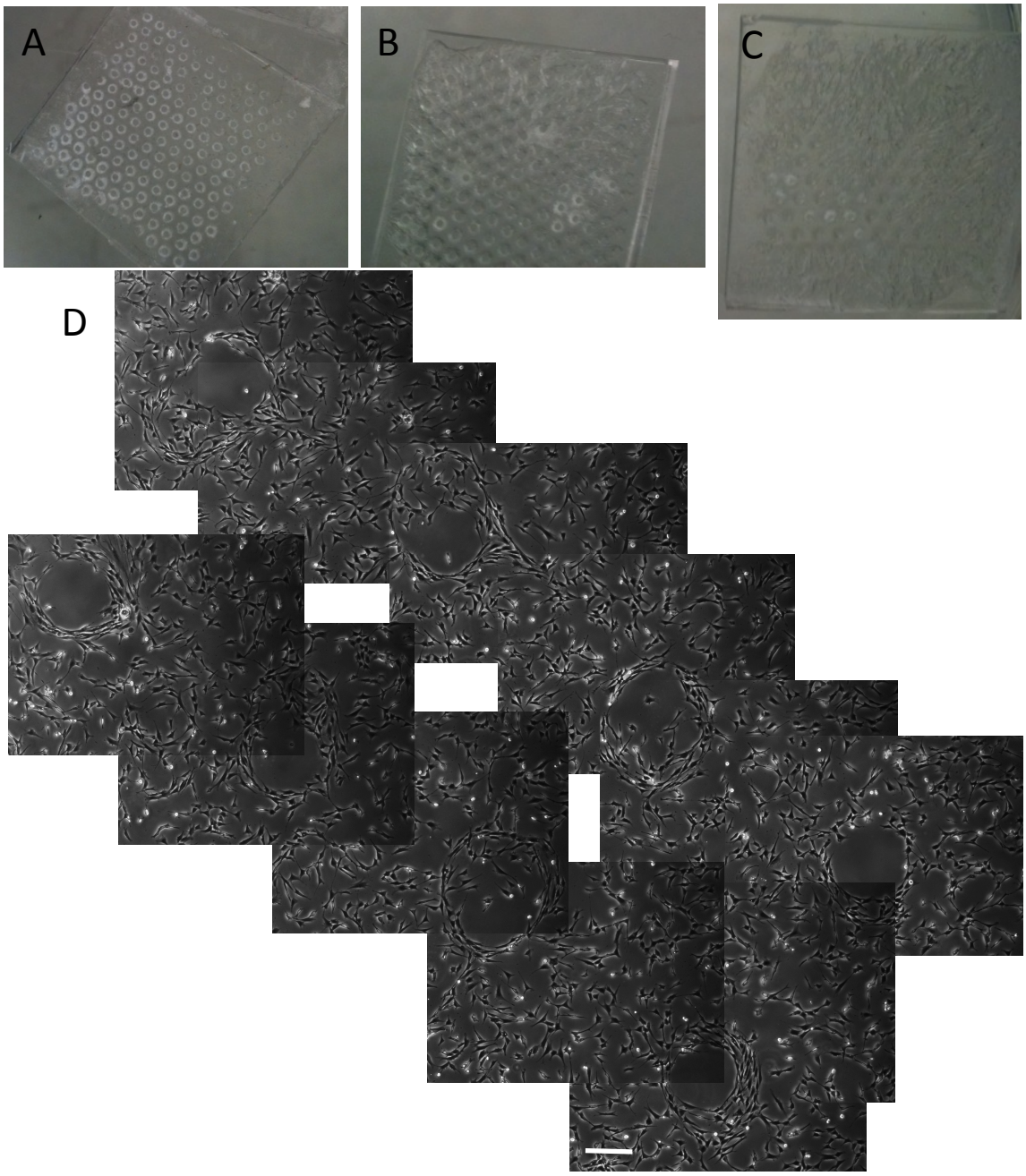

Figure 3.27 The difficulty in preparing uniformly coated protein stamps. At high protein (0.1 mg/mL) and buffer concentrations (200mM HEPES), protein does not dry uniformly onto PDMS stamp (A) and the film can be seen leaving rings around the PDMS posts. Protein films never fully dry when (A) left to air dry for 1 hour or (B) & (C) dried with a nitrogen gun for 5 minutes, as salt in buffer can be acting as kosmotrope. (D) Cells patterned using protein stamps, can show an inverse pattern to the stamp with cells only binding where the PDMS posts did not contact the polyacrylamide gel. Scale bar = 250μm.

The protein drying patterns were reminiscent of coffee rings, and the coffee ring effect. The coffee ring effect was first formally described by Deegan et al.[156] in 1997, when Deegan theorized that the ring pattern that can be observed in coffee cups, is due to a pinned contact line of the evaporating fluid. Evaporation occurs most quickly at the edges of a droplet due to the decreased height of the fluid at the edge relative to the interior of the droplet. Since the edge of drop is constrained by its attachment to the surface, fluid from the interior of a drop is pushed outward toward the edges to compensate for evaporative losses, and solute is pushed along with that fluid as it moves to the edges, thus solute is constantly transported to the edges of the drop, forming a ring when all the fluid has evaporated.

The coffee ring phenomena would lead one to suspect that it is not possible to create a uniform protein film on a PDMS stamp. However, the coffee ring phenomenon can be completely counteracted by Marangoni flow, which is mass transfer due to a surface tension gradient.[157] During evaporation, there is non-uniform cooling along the surface of a drying droplet creating a temperature gradient, which creates a surface tension gradient along the droplet's free surface. Marangoni flow carries particles that are near the free liquid surface of the droplet inward toward the top of the droplet and then plunges them down to the substrate near the center of the droplet, where the solute particle can stick to the substrate. If the solute particles do not stick to the substrate they are the carried along the substrate to the edge, where they are recirculated along the free surface back toward the top of the droplet. Hu et al.[157] have been able to use solvents with high evaporation to increase Marangoni flow and force particles to dry in the center of the droplet, rather than in a ring around the edge.

Solvents more volatile than PBS and HEPES were therefore also examined for preparing uniform films of fibronectin on PDMS stamps. Specifically, IPA, methanol, ethanol, and acetone were examined. PDMS was also exposed to various degrees of oxygen plasma, so as to modify the wetting properties of the aforementioned solvents, and therefore the contact line pinning and the Marangoni flow. Fibronectin at 0.5 mg/mL was not soluble in acetone and completely precipitated, whereas it formed a cloudy solution in IPA, was fully soluble in methanol and ethanol. Neither methanol nor ethanol yielded uniform protein films on PDMS regardless of oxygen plasma treatment or drying technique. Additionally, the aforementioned solvents have organic character and can dehydrate and therefore denature proteins, so their use should be avoided.

While functional microcontact protein transfer has been demonstrated by Chris Chen's group for a number of years, and most recently with a double printing technique, the protein concentrations used in those reports were an order of magnitude lower than what is used herein.[158] In Chris Chen's applications, the proteins were transferred onto solid supports and were left deposited on the solid support in a physiosorbed manner. Fibronectin used for patterning polyacrylamide hydrogels in this project was never used at a concentration lower than 0.1 mg/mL, and often used at concentration as high as 0.5 mg/mL. Larson et al.[159] have shown that the structure of protein films created by evaporative drying is strongly influenced by protein concentration and buffer properties such as the concentration

of the buffer and whether the buffer is chaotropic or kosmotropic. For example they found that for a specific protein, changing the buffer concentration changed the drying pattern from coffee ring & internal soccer ball to coffee ring only. It is therefore possible that at the protein concentrations used for a patterning application it is not possible to form uniform films, however at the lower concentrations used by Chris Chen's group more uniform patterns could be achieved. However, using concentrations of protein too low would limit the attachment and spreading of the cells on the compliant polyacrylamide surfaces. Therefore, I decided to use the crosslinker as the ink, instead of using the protein as the ink in the patterning of hydrogels.

3.6 Conclusions and Future Work

This chapter detailed the successful development of a methodology to pattern mechanically tunable polyacrylamide gels, via UV activated microcontact printing. Alternate less successful printing methodologies were also discussed in comparison, and their failures were explicated, highlighting the benefits of the UV activated microcontact printing technology. Parameters for printing were optimized such as buffer and crosslinker identity and concentration, photolithography, stamping parameters, gel drying, the protein resistance of the gel, and sterilization. The use of peptides instead of proteins was also explored in the context of the patterning methodology, and a better crosslinker needs to be used for such an application such as the ASIB crosslinker, which does not require a reduction step prior to peptide conjugation.

With the protein printing technology developed herein, large area patterns of 3T3 cells on fibronectin conjugated 1 kPa polyacrylamide gels were successfully generated. Cell colonies contracted on the compliant surfaces, which is a feature that can be particularly interesting for applications with beating cells such as cardiac cells (as discussed in **Chapter 5**). The patterned hydrogels will also be used in **Chapter 4** with human embryonic stem cells.

Chapter 4
The Influence of Modulus on Human Embryonic Stem Cells

4.1 Introduction
4.2 Methods and Materials
    4.2.1 Human Embryonic Stem Cell Culture
    4.2.2. Polyacrylamide Substrates
    4.2.3 Proliferation
    4.2.4 Quantitative RT-PCR
    4.2.5 Immunocytochemistry
    4.2.6 Statistical Analysis
4.3 Results and Discussion
    4.3.1 Proliferation
    4.3.2 Pluripotent Gene Expression
    4.3.3 Patterning
4.4 Conclusions

4.1 Introduction

As detailed in the previous chapters of this dissertation, numerous researchers have demonstrated that the behavior of terminally differentiated cells and adult stem cells can be influenced by the mechanical environment surrounding the cells. To date, little work has been done to investigate the effects of mechanical properties on the fate of embryonic stem cells, and in fact the only work in that field has been with mouse embryonic stem (mES), and not with human embryonic stem cells.[1-3] Therefore, in this chapter, proliferation and gene expression were assayed to determine the influence of substrate stiffness on hES cells.

There are key differences in the regulatory pathways of mouse embryonic stem cells and human embryonic stem cells, necessitating this chapter's exploration of the influence of substrate stiffness on hES cell behavior.[4-7] Chromatin immunopercipitation assays have shown that the transcription factors required for pluripotency maintenance, OCT4 and Nanog, do not bind to the same target genes for mice and humans. For example, in humans, but not in mice, Oct4 and Nanog bind to the genes *heart and neural crest derivatives expressed 1 (HAND1)* and MYST3, while in mice but not humans, OCT4 and Nanog bind to the gene *Estrogen-related receptor b (Esrrb).*[8] In terms of epigenetics, mES cells also differ from hES cells, where hES cells only show approximately 35% DNA methylation, significantly lower than what has been found in mES cell lines.[9-11] Moreover, while LIF is required to maintain pluripotency in mES cells, this is not the case of hES cells. Daheron et al.[12] have shown that while hES cells express LIF receptor β and the signaling subunit gp130, and that human LIF can induce STAT3 phosphorylation and nuclear translocation, LIF is unable to maintain the pluripotency of hES cells, and they found that hES cells do not show STAT3 activation in feeder free culture. It is therefore clear from the protein level to the epigenetic level that while embryonic stem cells may share traits across species, it is not appropriate to translate results reported for mES to hES cells.

In this chapter, the proliferation and pluripotent gene expression of hES cells during short term culture is explored. Due to the high variability seen in the data the use of the patterned hydrogels in **Chapter 3** to reduce some of the variability is proposed, and preliminary data on the ability to pattern hES cells onto the patterned hydrogels is presented.

4.2 Methods and Materials

4.2.1 Human Embryonic Stem Cell Culture

Feeder independent H1 hES cells from the cell line WA01-FI lot# WA01-DDL-17 (WiCell, Madison, Wisconsin) were maintained as recommended by WiCell. These cells are defined by WiCell as feeder independent and were obtained at passage 30 (WiCell indicates that they were grown on MEFs until passage 18 and then cells were transitioned to Matrigel for all subsequent passages). Once obtained, cells were maintained on hESC-qualified Matrigel (BD Bioscience) and with mTeSR

media (StemCell Technologies, Vancouver, Canada), which was exchanged daily. Prior to cell passaging, Matrigel which was stored at -20°C was thawed to 4°C in a refrigerator, and was then diluted ~ 1:75 with 4°C KO-DMEM. Note, Matrigel is sold by volume, so the concentration of proteins varies by lot, and for each lot, BD Bioscience recommends a specific Matrigel aliquot volume (~300 uL) to be used for hES cell culture, which is then diluted in 25 mL KO-DMEM. 1.5 mL of diluted Matrigel was added to each well of a 6 well tissue culture plate (Costar), and allowed to adsorb for 1 hour. After 1 hour, Matrigel was aspirated from the wells, and 1 mL media was added to each well. Cells were passaged every 4-5 days at split ratios 1:6-1:12, using StemPro Accutase (Life Technologies). Specifically, cells were rinsed with PBS (Life Technologies) and then incubated with Accutase at 0.5 mL/well for 3 minutes at 37°C. At this point, cells were no longer attached to the well and 5 ml PBS was added to each well to dilute the Accutase. The cell solution was then removed from the well and centrifuged at 500 rpm for 2 minutes, after which the supernatant was then aspirated and cells were resuspended in mTeSR with 5 μM ROCK Inhibitor (Calbiochem EMD Chemicals), and then seeded onto the Matrigel plates. ROCK inhibitor was only kept for 1 day after passaging and removed during the first media exchange. Cells used were under passage 50 for all experiments detailed in this chapter. Cells were intentionally not passaged with Collagenase IV or other enzymes such as Dispase, which require manual mechanical scraping to detach cells, which can be inconsistent between passages. Cells were periodically karyotyped at Children's Hospital Oakland Research Institute (CHORI), and were always found to have a normal karyotype. Cells were seeded onto surfaces at the same ratios at which they were split for passaging.

4.2.2 Polyacrylamide Substrates

Quartz-supported acrylamide gels were prepared as described in **Chapter 3** and in more detail in **Appendix A.1**. Specifically, to make 10 kPa polyacrylamide gels, a prepolymer solution of 10% acrylamide 0.3% bisacrylamide was used. To make 1 kPa polyacrylamide gels a prepolymer solution of 5% acrylamide and 0.2% bisacrylamide was used. To make 140 Pa gels, a prepolymer solution of 3% Aam and 0.2% was used. APS and TEMED were used for as initiators.

To make uniformly coated gels, gels were sterilized in 70% ethanol, rinsed 5 times in PBS, and then paced into BD Falcon 6 well tissue culture plates, where 1 ml of 0.2 mg/mL sulfo-SANPAH was added to each well. The plates were then placed in a UV flood illuminating chamber (Dymax, Dymax Corporation, Torrington CT), and exposed to 1.25 J/ cm^2 of UV (99 seconds at 1.25 mW/cm^2) (with lid on) to activate the azide of the sulfo-SANPAH. The plates were then rinsed with PBS to remove any unbound sulfo-SANPAH, and the adhesive protein or protein mixture of choice (Matrigel, fibronectin, vitronectin) was immediately added to the plates and incubated for 1 hour at room temperature. Wells were then rinsed with PBS and cells were then seeded as detailed in the cell culture section. The Matrigel (BD Bioscience) concentration used was that recommend by WiCell and BD bioscience for hES cell growth (1:75 dilution of hESC qualified Matrigel). Fibronectin (Sigma

Aldrich) was used at 0.017 or 0.5 mg/mL and recombinant vitronectin (Sigma Aldrich) was only used at 0.017 mg/ml, due to the expense of the reagent. Additionally according to the manufacturer, Sigma Aldrich, the maximum surface coverage of vitronectin is 0.0001 mg/cm^2, and given that the well of a 6 well plate is 9.6 cm^2, using 1 mL/well of 0.017 mg/mL of vitronectin solution is an order of magnitude in excess of the maximum anticipated coverage. Meanwhile, the same manufacturer lists the surface coverage, and suggested use surface concentration of fibronectin as 0.001-0.005 mg/cm^2, which is clearly larger than that recommended for vitronectin.

Fibronectin and Matrigel patterned polyacrylamide gels were prepared as described in detail in **Appendix A.3.** Briefly, polyacrylamide gels were sterilized in 70% ethanol and then rinsed 5 times in PBS. Glass microscope slides and PDMS stamps with post diameters corresponding to desired colony sizes, were fabricated and exposed to oxygen plasma at 1 Torr and 80W for 30 seconds. The backs of the PDMS stamps were affixed to the glass microscope slides immediately after the plasma treatment. Stamps were then sterilized with 70% ethanol and allowed to dry in a sterile hood. 0.2 mg/mL sterile filtered sulfo-SANPAH in PBS was added to the top of each stamp, and allowed to incubate on the stamp, in darkness, for 30 minutes. Subsequently, stamps were dried with a nitrogen gun. Stamps were then placed in conformal contact with dehydrated acrylamide gels, and 0.125 J/cm^2 UV was shone through the stamp. The stamps were then removed and the acrylamide gels were wash three times in PBS, and then incubated with 0.25 mg/mL fibronectin in PBS for 1 hour. The gels were then rinsed thee times in PBS, and were then ready for cell seeding. Cells were seeded on the same day that fibronectin was patterned.

4.2.3 Proliferation

For each desired time point, three repeat wells were created for each surface type: adhesive ligand attached to TCPS, adhesive ligand conjugated to 10 kPa polyacrylamide, and adhesive ligand conjugated to 1 kPa polyacrylamide. The adhesive ligands used where Matrigel (at concentration used for hES culture: 1:75 dilution in KO-DMEM – see **Section 4.2.1.1**), and fibronectin at 0.5 mg/mL in PBS.

Due to the limitations of the Cyquant assay, and techniques based on processing images of cells during culture (expounded upon in **Appendix A.5**), the propidium iodide based NucleoCounter (Chemometec) was used to count cells. The NucleoCounter itself is composed of a fluorescent microscope with a CCD camera, which uses thresholding software to detect fluorescently stained nuclei, and error correction options to account for bubbles, ultimately producing an output of cell concentration.

At the designated time point (day 1, 2 or 3) wells were gently washed once with PBS, and cells were then detached from well surfaces by incubating with 0.5 mL/well (6 well plates) 0.25% Trypsin EDTA at 37°C for ten minutes. Wells were inspected with an optical microscope to confirm that cells had detached from the surfaces. 2 mL of PBS was added to each well to allow for easier trituration, as at this point cells were detached from the surface, but they were present in large

clumps clumps. After trituration, cells were again inspected with an optical microscope to confirm that the cells were present as single cells, and not cell clumps, which would confound cell quantification. The single cell suspension was then transferred into a falcon tube, from which 200μL were removed and combined with the 200μL of NucleoCounter cell lysis buffer (Chemometec) and inverted 20 times in a 1.5 ml Eppendorf tube to mix, as recommended by Chemometec. The cell mixture was then combined with a 200μL of NucleoCounter propidium iodide buffer, inverted 20 times and immediately loaded into the NucleoCounter cell counting cassette. The cassette was then immediately placed into the NucleoCounter, and cell concentrations were obtained. Three separate readings were made for each well by taking three separate samples from each well.

4.2.4 Pluripotent Gene Expression

Three biological replicates were created for each surface type examined (Matrigel adsorbed onto TCPS, Matrigel conjugated to 10 kPa polyacrylamide, and Matrigel conjugated to 1 kPa polyacrylamide). 4 days after seeding hES cells onto Matrigel conjugated polyacrylamide gels, hES cells were exposed to Trypsin (Life Technologies) to detach them from the surfaces. Cells were resuspended in DMEM (Life Technologies) media with 10% FBS (Life Technologies). Cells were then centrifuged to remove media and resuspended in 1ml of PBS. RNA was then extracted using the Qiagen RNAse mini kit with Qiashredder (Life Technologies) following manufacturer's instructions. RNA purity and concentration were determined with a NanoDrop 2000 spectrophotometer (Thermo Scientific) where 260:280 was 2.07-2.1 for all samples and 260:230 was 1.67-1.8 for all samples. cDNA was prepared using the Taqman Fast Cells-C_T kit (Applied Biosystems) according to the manufacturer's instructions. Again, cDNA purity and concentration were determined with a NanoDrop 2000 spectrophotometer, and 260:280 was 1.8-1.81 for all samples, and 260:230 was 2.28-2.35 for all samples. cDNA and qRT-PCR reactions were performed with a StepOnePlus instrument (Applied Biosystems) using TaqMan Fast Universal PCR Master Mix, and TaqMan Gene Expression Assays (GAPDH HS9999905_m1; Oct4 Hs00742896_s1; Nanog Hs02387400_g1; Sox2 Hs00602736_s1) according to the manufacturer's instructions.

The comparative C_T (threshold cycle) method was used to analyze qRT-PCR data.[13, 14]

4.2.5 Immunocytochemistry

At day 4 after seeding, cells were fixed with 4% Paraformaldehyde (PFA) in PBS for twenty minutes at room temperature. Cells were then gently washed three times with PBS. Cells were permeabilized with 0.1% TritonX, followed by a one rinse with PBS, and followed by a block with 10% goat serum in PBS, with 0.1% Triton for 1 hour at room temperature. Cells were then incubated overnight at 4°C in primary antibodies diluted 1:100 in 2% goat serum, 0.1% Triton PBS. The primary antibodies used were OCT4 mouse antihuman monoclonal (Abcam ab91194), SOX2 rabbit antihuman polyclonal (Abcam ab59776), and Nanog rabbit

antihuman polyclonal (Abcam ab21624). Cells are then washed three times in PBS with 0.1% Triton for half an hour per wash and then incubated with the secondary antibodies at 1:500 dilution. The secondary antibodies used were goat anti-Rabbit alexaflour 488 (Abcam) and goat anti-mouse alexaflour 568 (Abcam). Finally, cells were rinsed three times gently with PBS and incubated with 300nM 4',6-diamidino-2-phenylindole (DAPI; Life Technologies) for 5 minutes.

4.2.6 Statistical Analysis

Statistically significant differences were determined using ANOVA between samples with Tukey-Kramer *post hoc* test with $p < 0.05$ using JMP software. C_T values obtained from qRT-PCR were converted to $2(-\Delta C_T)$, prior to any statistical analysis (ΔC_T is the difference between C_T for the gene of interest and C_T of the housekeeping gene, which was GAPDH in this work), as C_T is an exponential term and therefore must be linearized before statistical analysis. [13]. Means and standard deviations for relative quantification plots were calculated following the methodology detailed in Bookout et al. for the Nuclear Receptor Signaling Atlas (NURSA)[15]

4.3 Results and Discussion

4.3.1 Proliferation

Proliferation of H1 hES cells was assessed for cells seeded on Matrigel conjugated polyacrylamide surfaces with elastic moduli 1 kPa and 10 kPa and for Matrigel adsorbed onto TCPS (~ 3 GPa) (**Figure 4.1**). There was no statistical difference as assessed by ANOVA and Tukey-Kramer *post hoc* test between surfaces on day 1 for cell attachment (**Figure 4.1A**) at $p < 0.05$ ($p = .2259$ for the difference between TCPS and 1 kPa). Only at day 3 was there a statistically significant difference between the surfaces, with 1 kPa surfaces having significantly fewer cells than either the 10 kPa or TCPS surfaces. The variability observed in the proliferation data may be due to the fact that Matrigel is composed of thousands of proteins, and it is unclear which proteins are binding to the polyacrylamide gel, and whether the same proteins are binding to each gel.

In order to limit the complications of a poorly defined conjugated ligand, as is present with the Matrigel surfaces, proliferation was also assessed for cells seeded on fibronectin conjugated polyacrylamide surfaces with elastic moduli 1 kPa and 10 kPa, and for fibronectin adsorbed onto TCPS (~ 3 GPa) (**Figure 4.2**). While there was no statistical difference as assessed with ANOVA and Tukey-Kramer *post hoc* test between surfaces on day 1 for cell attachment (**Figure 4.2B**) at $p < 0.05$, the p-value for the ANOVA was 0.0690, with $p = 0.0892$ for the difference between 1 kPa polyacrylamide and TCPS, and $p = 0.1053$ between 10 kPa polyacrylamide and TCPS. Tukey-Kramer is conservative and may underestimate differences populations that are highly heterogeneous such as stem cells. By day 2 the cell number did display

statistically significant difference between 1kPa polyacrylamide and TCPS, and between 10 kPa and TCPS, with both gels having significantly fewer cells than TCPS.

Comparing the Matrigel surfaces with the fibronectin surfaces, it is interesting to note, that at day 1 there is little difference in cell attachment to Matrigel surfaces, but on fibronectin there is increased cell attachment onto the compliant gels relative to TCPS. However, for both Matrigel and fibronectin surfaces, cells proliferate more quickly on the stiffer surface, TCPS, an observation consistent with the other cells types.[16-18] Interestingly, after day 1, for Matrigel surfaces, the 10 kPa gels showed behavior similar to the TCPS surfaces and different from the 1 kPa gels in terms of cell proliferation, whereas for the fibronectin surfaces the 10 kPa gels showed behavior similar to the 1 kPa gels, and different from the TCPS surfaces. The observation that 10 kPa gels can be presenting a relatively stiff substrate (behavior similar to TCPS), and also a relatively compliant substrate (behavior similar to 1 kPa gels) may be explained by the fact that the degree to which substrate modulus affects cellular behavior is a function of ligand density.[19] Since there is no way to ensure that the same amount of surface adhesive ligands were presented with the fibronectin surfaces as the Matrigel surfaces, it is likely the adhesive ligand concentration was not the same for Matrigel conjugated 10 kPa and fibronectin conjugated 10 kPa, leading to the disparate behavior of those gels.

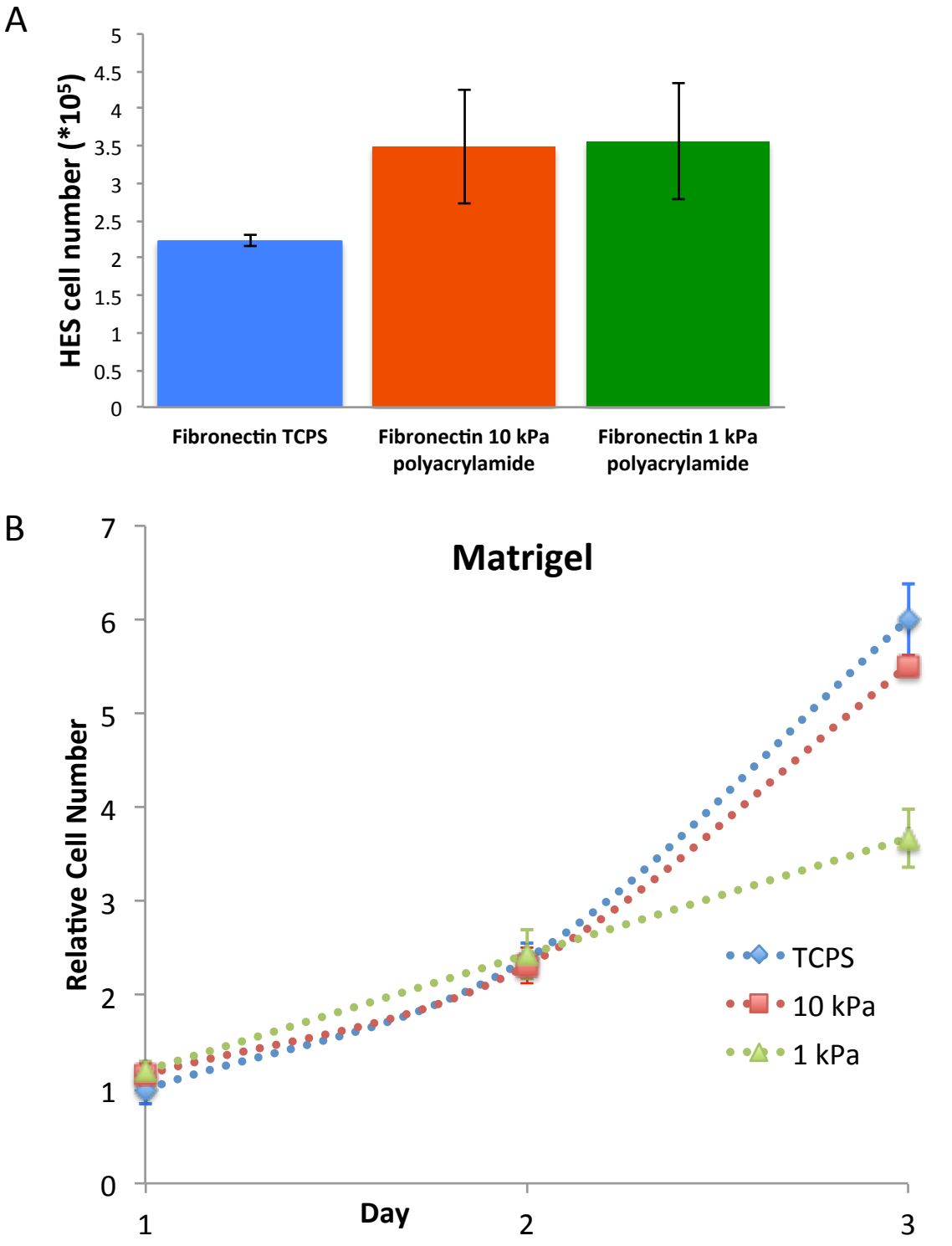

Figure 4.1 H1 hES cell proliferation on Matrigel conjugated surfaces. (A) Cell attachment on day 1 and (B) proliferation normalized to Matrigel on TCPS at day 1. Values shown are mean and standard deviation. No statistically significant differences were seen between surfaces on day 1 or day 2. At day 3, The 1 kPa surfaces had fewer cells than both the 10 kPa and the TCPS surfaces ($p < 0.05$)

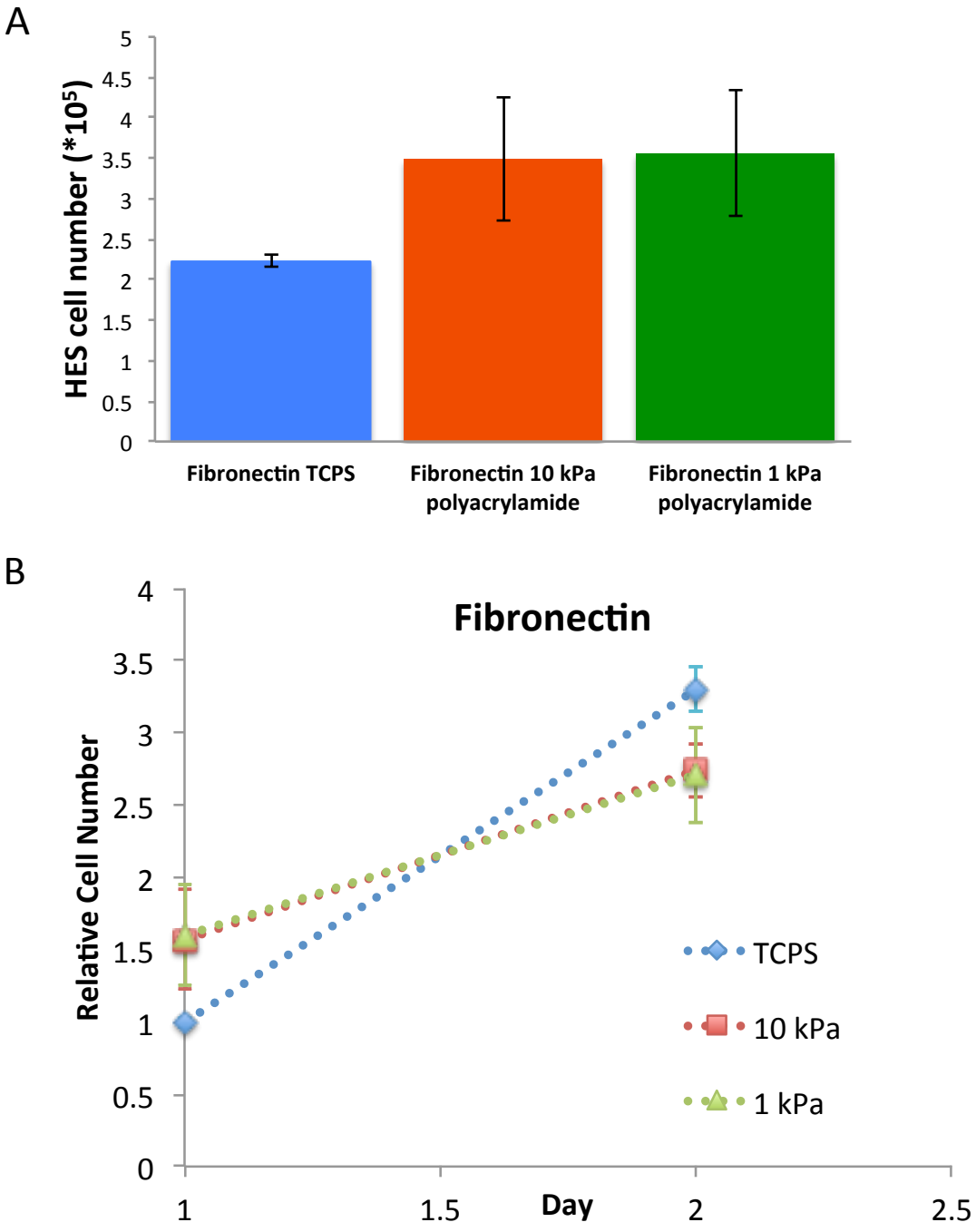

Figure 4.2 H1 hES cell proliferation on fibronectin conjugated surfaces. (A) Cell attachment on day 1 and (B) cell proliferation normalized to fibronectin on TCPS at day 1. Values shown are mean and standard deviation. Statistically significant differences in attachment on day 1 were only seen at $p < 0.1$. At day 2 both 10 kPa and 1 kPa gels had fewer cells than TCPS ($p < 0.05$).

4.3.2 Pluripotent Gene Expression

The expression of the pluripotency factors OCT4, Nanog, and SOX2, of H1 hES cells grown on Matrigel conjugated compliant polyacrylamide gels was assessed 4 days after seeding cells (**Figure 4.3**), using qRT-PCR. For each gene, no statistical difference was found between the three surfaces assessed (Matrigel adsorbed onto TCPS, Matrigel conjugated to 10 kPa polyacrylamide, and Matrigel conjugated to 1 kPa polyacrylamide) using a Tukey-Kramer *post hoc* test. ANOVA p-values are listed in **Table 4.1**

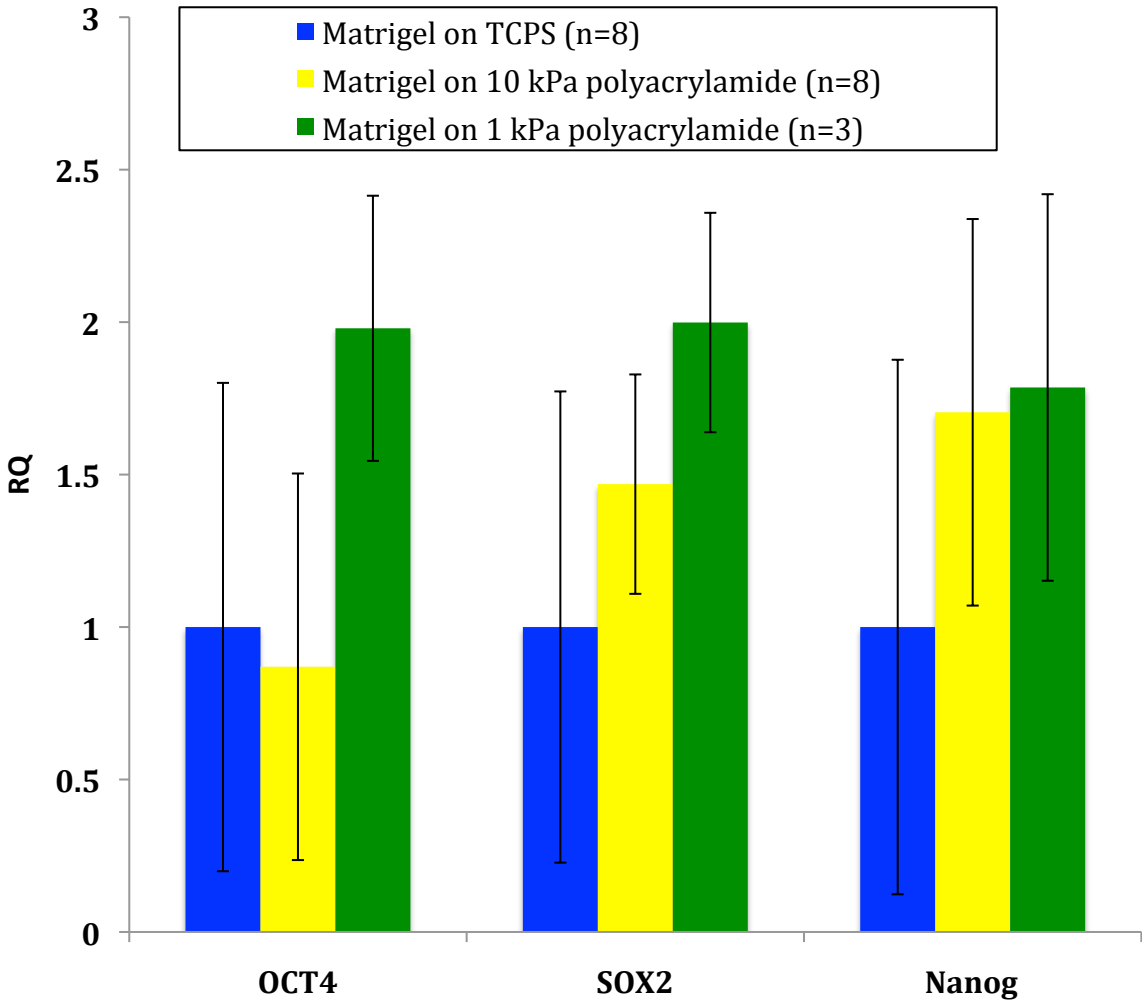

Figure 4.3 Expression of pluripotency genes at day 4 for H1 hES cells grown on substrates of varying stiffness. Values presented are mean and standard deviation. None of the genes showed statistically significant differences between the substrates examined.

Table 4.1 ANOVA p-values for pluripotency genes of H1 hES cells cultured on surfaces with variable moduli

Gene	ANOVA P-value
OCT4	0.5909
SOX2	0.2796
Nanog	0.7307

These results were surprising as they seem to contradict the observations of Chowdhury et al.[20] regarding compliant surfaces increasing the expression of the same pluripotency genes for mES cells when they were cultured on collagen conjugated polyacrylamide gels (0.6 KPa) relative to collagen coated TCPS. The main finding of the paper was that in the absence of LIF, a factor required to maintain pluripotency in mES cells, but not hES cells,[12] a compliant gel (0.6 KPa) was able to maintain the pluripotency of the mES cells in contrast to the rigid TCPS culture surface. In our experiment, no soluble factors required to maintain pluripotency were removed from the culture media, which may explain the lack of observed effect of substrate modulus in the hES experiment.

However, in that same article, Chowdhury et al.[20] do provide some evidence that substrate stiffness affects pluripotent gene expression in mES cells. They presented immunostaining evidence of a small area of cell colonies, showing that in the presence of LIF, more colonies on collagen conjugated polyacrylamide showed OCT4 expression, as compared to colonies on collagen adsorbed onto rigid TCPS dishes, implying that even in the presence of LIF a compliant substrate increases pluripotency. Additionally, they showed that in the presence of LIF, OCT4 expression was lower for cells on polyacrylamide surfaces that were stiffer than 0.6 kPa (3.5 kPa and 8 kPa), as demonstrated by fluorescence of the colonies which were comprised of mES cells transfected to express GFP under the OCT4 promoter. However, their FACS data did not show a significant difference between OCT4 expression of cells on the polyacrylamide surface and TCPS. Therefore, from their manuscript it is not clear whether substrate stiffness makes a difference in the expression of pluripotent genes for mES cells, in the presence of all the chemical signals required to maintain pluripotency, which may be consistent with our observation reported herein.

While LIF was a logical choice to remove from mES culture, it is not clear what could be comparatively removed from hES culture to try to emulate Chowdhury ’s experiment. One possible factor to remove from hES cell culture is Rho kinase (ROCK) inhibitor, which is used during hES cell passaging in order to decrease apoptosis.[21] ROCK, and consequently its inhibitor, affect actin filament organization and contractility, and therefore the mechanical properties and mechanical responses of cells. It would therefore be interesting to see whether using soft surfaces during hES cell passaging could eliminate the need for ROCK inhibitor in hES cell culture.

An alternate plausible explanation for substrate stiffness seemingly not affecting pluripotency gene expression in hES cells is that the biological variability within hES cells may be too large for differences between groups of hES cells cultured under different conditions to be discernable. Numerous researchers have already demonstrated that there is considerable heterogeneity in mES and hES cell culture.[22-31] Willems et al.[32] have interestingly shown that the statistical methods used to analyze qRT-PCR data can lead to the incorrect conclusion that there are no statistical differences present in experiments with highly heterogeneous populations such as mouse embryonic stem cells. Specifically, they induced Brachyury expression in mES cells by Acitivin A at specific concentrations, and using immunostaining, showed that at low Activin A concentrations, Brachyury expression was highest compared to no Acivitin A, and to high Acitivin A concentration. However, the qRT-PCR data indicated that the were no significant differences for Brachyury expression amongst the groups: no Activin A, low Activin A concentration, and high Activin A concentration, in contrast to the immunostaining results. They contend that the high biological variability in each sample obscures meaningful differences in means, and they detail a method including steps of log transformation, mean centering about experiments, and autoscaling to decrease 95% confidence interval to reveal differences in gene expression for populations that are highly variable. Prior to transformation steps, their ANOVA $p = 0.7986$, which is higher than the p values determined for our experiment of gene expression of hES cells on surfaces of with different elastic moduli (**Table 4.1**), indicating that it is possible that there are significant differences in the hES pluripotency gene expression presented in this chapter.

For the variance and effect seen in the expression of pluripotent genes in the hES cell experiment, a sample size of about 35 would be required to have an analysis power of 0.8. However, it is not practically feasible to use a sample size that large when working with hES cells. Since the sample size cannot be significantly increased, we would have to reduce the variability within the population, if possible, to determine whether surface stiffness affects pluripotent gene expression.

One manifestation of cell population heterogeneity is the spread of colony sizes during typical cell culture with Matrigel on TCPS (**Figure 4.4A**). Using imageJ to determine area and perimeter of colonies in three wells at day 4 of culture on Matrigel on TCPS, it was found that the variability of the area and perimeter were comparable to the means themselves (area = 52,243 ± 60,790 and perimeter = 1,303 ± 1,004 μm (mean ± standard deviation)) (**Figure 4.5**). It has been shown that adult stem cells on edges are subjected to different stress than internal cells on patterns, which affect their differentiation trajectory, so it would be expected that edge effects are also present in hES cell colonies.[33]

We had anticipated that gene expression would vary with substrate stiffness, as cell colonies appeared morphologically different depending on the stiffness of the underlying substrate (**Figure 4.4**), with more spread cells at the edges of colonies on TCPS than on polyacrylamide gels, and in other cell lines, cell spreading has been shown to effect gene expression.[33-37]

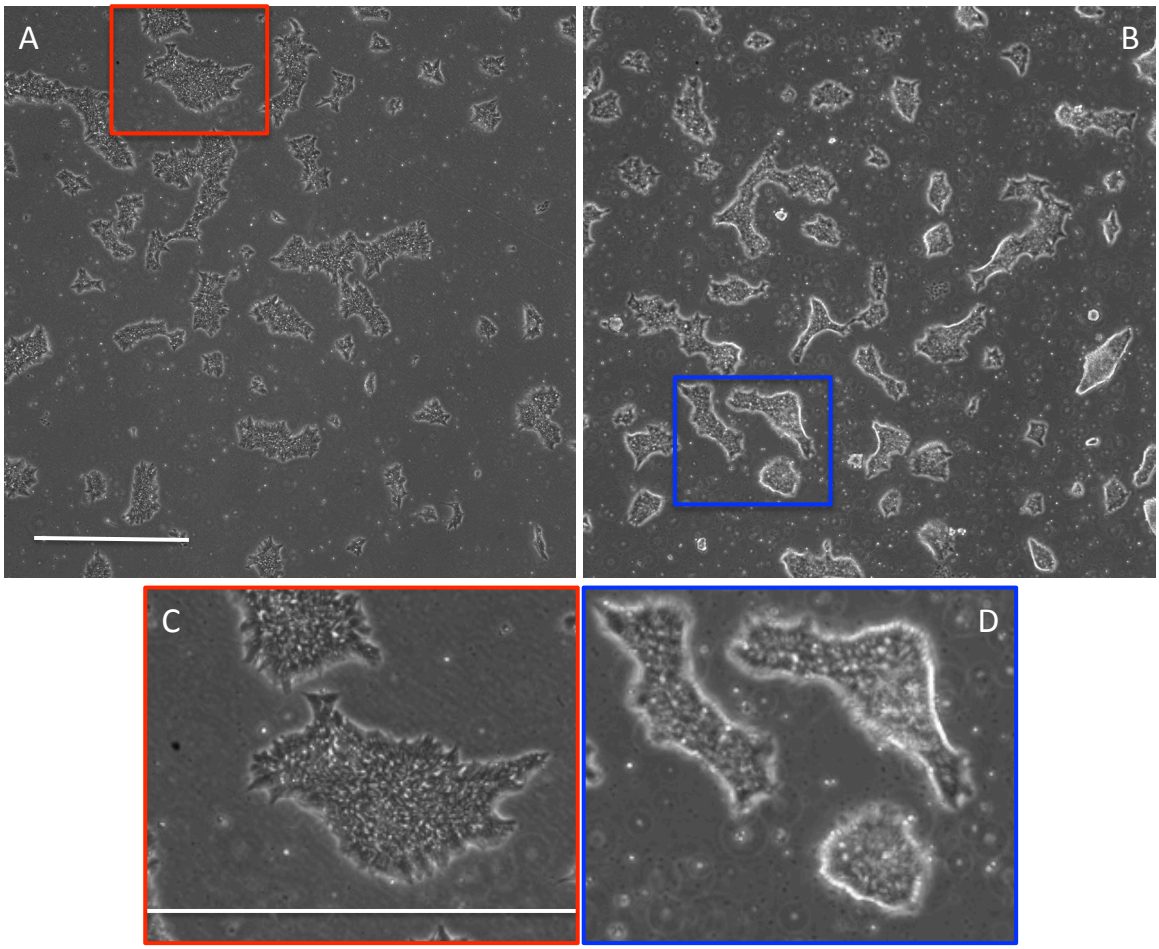

Figure 4.4 H1 hES cells on (A) Matrigel on TCPS and (B) Matrigel conjugated to 10 kPa polyacrylamide. (C) and (D) are magnifications of (A) and (B). Scale bar = 1 mm. Cells on Matrigel on TCPS are more spread and less dense than cells on Matrigel on 10 kPa polyacrylamide. Additionally, colonies on 10 kPa polyacrylamide are more phase bright at their edges, with cells less likely to spread to the same extent on colony edges as they do on Matrigel on TCPS.

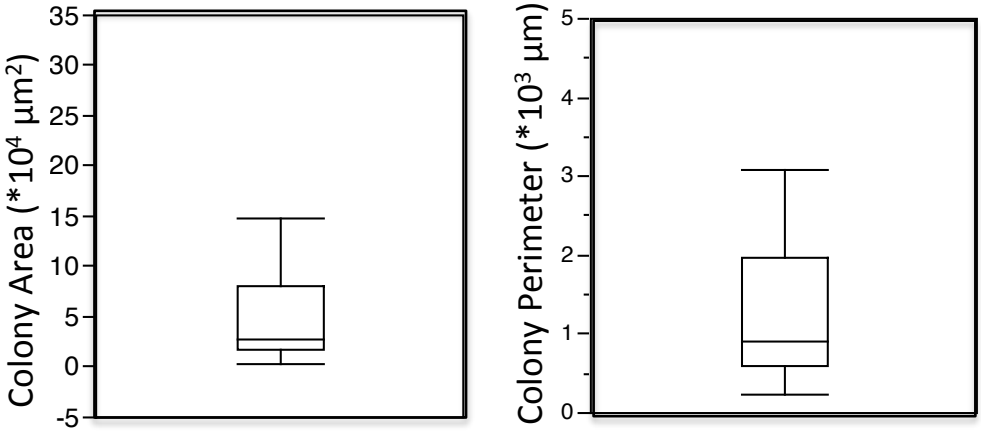

Figure 4.5 Colony area and perimeter distribution for H1 hES cells grown on Matrigel on TCPS at day 4 (from 3 wells). Area = 52,243 ± 60,790 and perimeter = 1303 ± 1004 µm (mean ± standard deviation)

4.3.3 Patterning

In the absence of a profound effect, we therefore hypothesize that by using our patterned hydrogels detailed in **chapter 3**, we can decrease some of the heterogeneity in the cell population by controlling colony area, perimeter and spacing, thereby helping us determine whether there is an effect of substrate modulus on pluripotency gene expression that is obscured by cell population heterogeneity, or whether there is no effect of substrate stiffness on pluripotent gene expression.

Towards that end, we first sought to show that hES cells could attach to and maintain pluripotency on the patterned polyacrylamide hydrogels. HES cells could be patterned onto Matrigel patterned polyacrylamide gels, as soft as 140 Pa (**Figure 4.6**). Additionally, hES cells could be patterned onto fibronectin patterned 140 Pa gels and maintain pluripotency at day 4, as indicated by the positive staining for pluripotency markers OCT4 and Nanog, (**Figure 4.7**).

The fibronectin results are interesting since Braam et al.[38] have claimed that while fibronectin could "support" hES cells in MEF conditioned media, only Matrigel or (natural and recombinant) vitronectin could "support" hES cells in defined non-conditioned media (mTeSR). In our work, mTeSR was used to maintain the cells. Upon closer inspection, Braam et al.[38] did not dismiss fibronectin for its inability to maintain pluripotency in hES cells (this was not tested), but rather they examined cell attachment and proliferation only. Interestingly, fibronectin and vitronectin both engage the RGD binding integrins $\alpha v\beta 3$ and $\alpha IIb\beta 3$, but they each also engage a number of other RGD binding integrins, that the other does not.[39] While fibronectin was used in these experiments due its cost efficiency relative to vitronectin, our short term passage results indicate that fibronectin may be used as a suitable adhesive ligand for hES cell culture, especially when coupled with a compliant substrate. Due to its relative expense, recombinant vitronectin patterned surfaces were not generated for proliferation or pluripotency assays; however, preliminary experiments with uniformly coated vitronectin and fibronectin indicated that a much lower quantity of vitronectin was required compared to fibronectin to elicit a similar cell response in terms of attachment area and proliferation (**Figure 4.8**). As the cost of recombinant proteins decreases, it may be feasible to use vitronectin for patterned hydrogels applications. It would also be interesting to see whether on vitronectin there is a statistically significant effect of substrate stiffness on hES cell pluripotency.

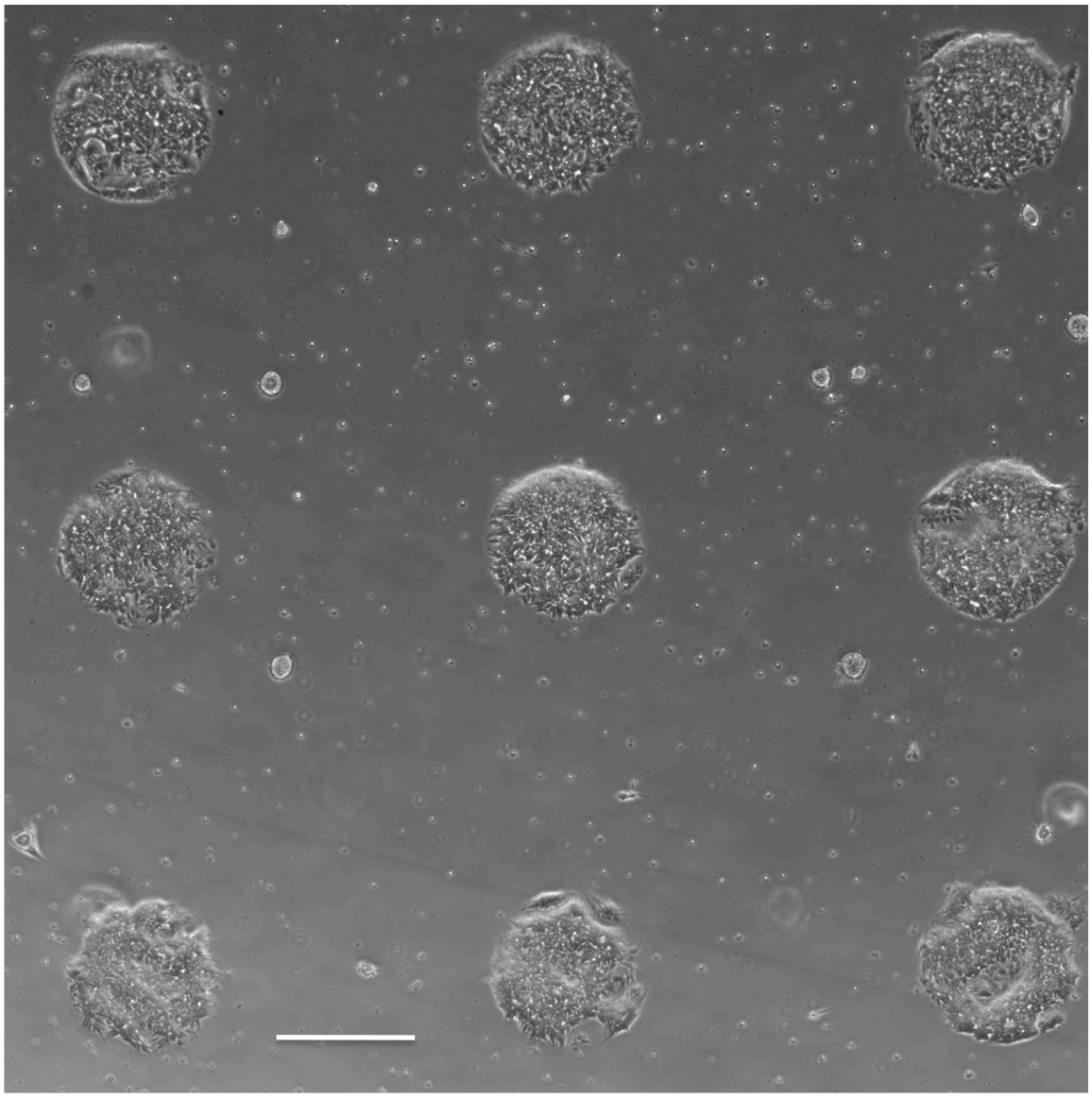

Figure 4.6 H1 hES cells attach and display typical morphology on a 140 Pa polyacrylamide gel patterned with Matrigel (day 3 after passaging). Scale bar = 500 μm.

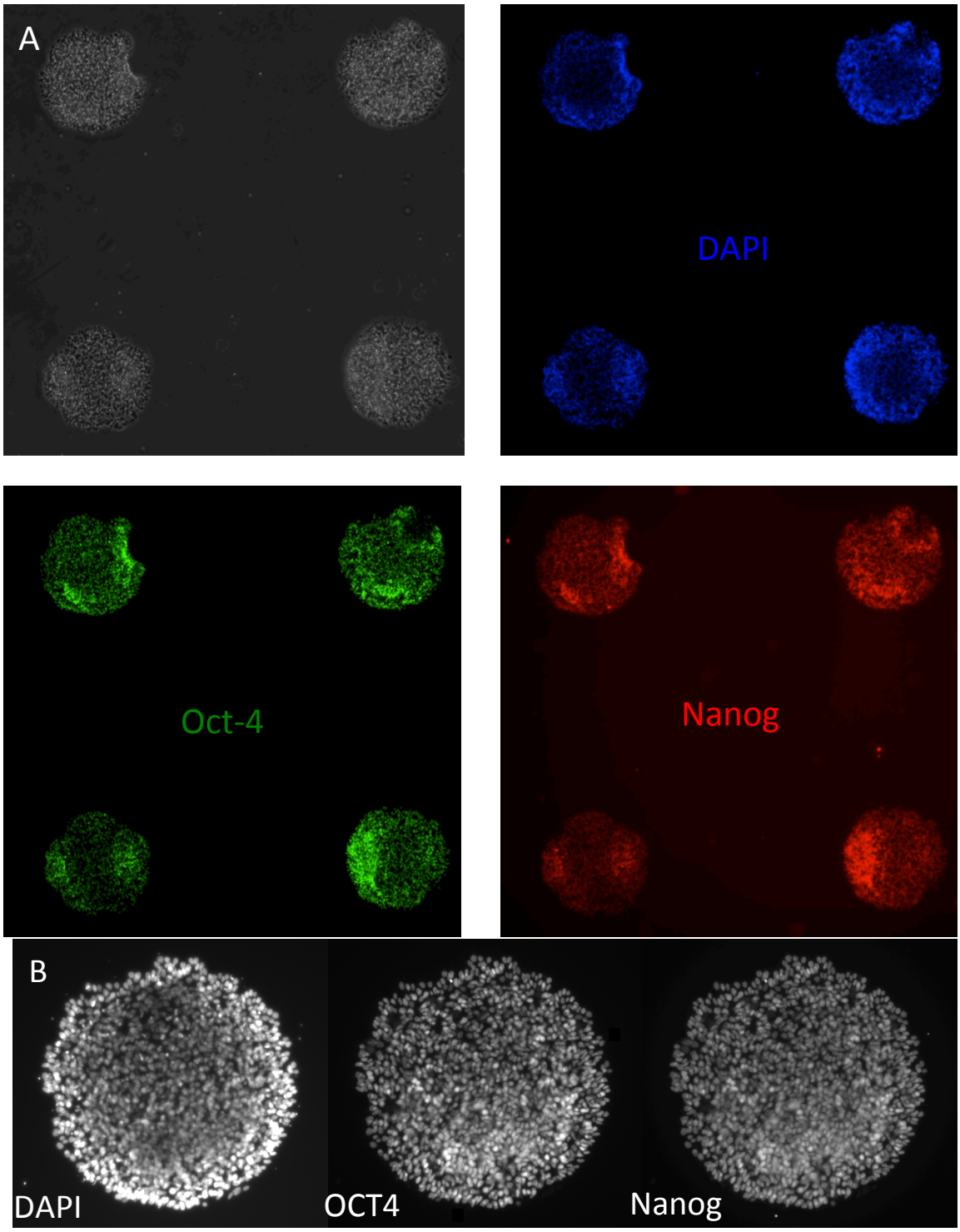

Figure 4.7 H1 hES cells co-stained for pluripotency markers OCT4 and Nanog on fibronectin patterned 140 Pa polyacrylamide gels on day 4 after passaging at (A) 4x magnification showing 4 cell islands and (B) 10x magnification focusing on one island, demonstrating the ability of H1 hES cells to remain pluripotent on the patterned surface.

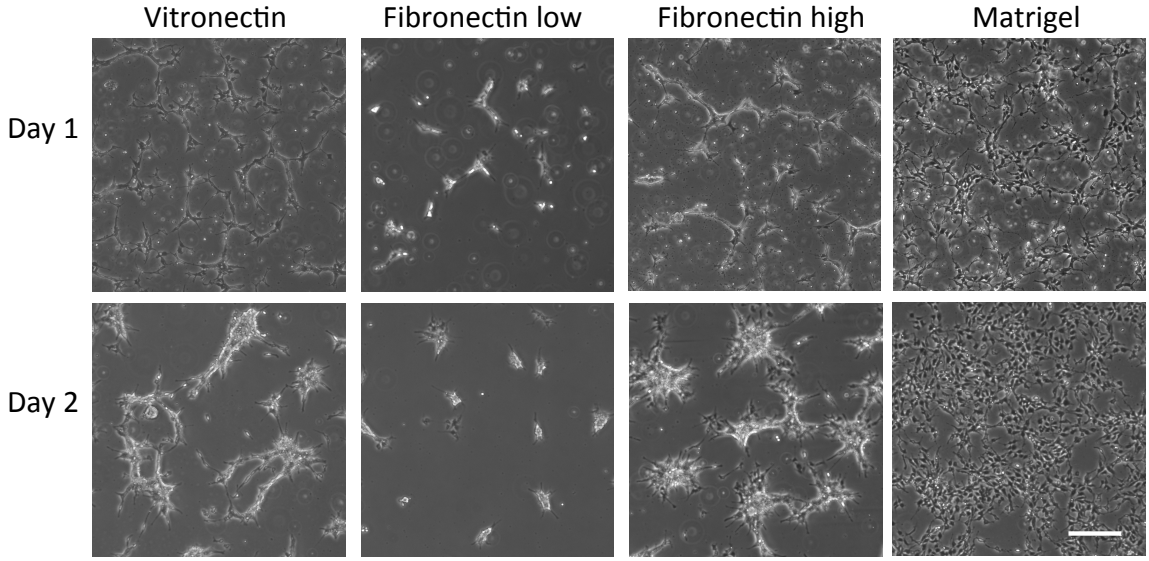

Figure 4.8 H1 hES cells on 1 kPa polyacrylamide gels uniformly conjugated with fibronectin, vitronectin, or Matrigel, 1 day and 2 days after passaging with Accutase and ROCK inhibitor. Matrigel was used at concentration specified by BD bioscience and WiCell for hES culture (~1:75 dilution). Vitronectin was used at 0.017 mg/ml, and fibronectin was used at 0.017 mg/ml or 0.5 mg/ml. When used at the same concentration, vitronectin supports more hES cells than fibronectin. All images are taken after media exchange. Scale bar = 250 μm.

4.4 Conclusions

In this chapter, the hypothesis that hES cell behavior is influenced by substrate modulus by examining hES cell proliferation and gene expression on polyacrylamide surfaces of varying moduli and TCPS. While proliferation was seen to increase with increasing substrate stiffness, as is typical with other cell types, there was no statistically significant difference in pluripotent gene expression for hES cells grown on surfaces with different moduli. We presented arguments that a difference may exist, but is obscured by the large biological variability present in the hES cell population, and we suggest that repeating the pluripotency gene expression assay on our patterned surfaces may help reduce the variability so that we can determine whether substrate stiffness does indeed affect pluripotency gene expression for hES cells. Towards that end, we showed hES cells could be patterned onto gels as soft as 140 Pa, with both Matrigel and fibronectin, and in the short term, immunostaining indicated that the cells could maintain pluripotency on the patterned surfaces. In the future we will perform pluripotent gene expression tests on hES cells on patterned polyacrylamide surfaces.

Chapter 5
Use of Substrates for Long QT Induced Pluripotent Stem Cells

5.1 Introduction
5.2 Methods and Materials
    5.2.1 Cell Culture
    5.2.2 Patterned Surfaces Preparation
    5.2.2 Immunocytochemistry
    5.2.3 Electrophysiology
5.3 Results and Discussion
5.4 Conclusions

5.1 Introduction

Holding even more therapeutic promise than hES cells, are induced pluripotent stem (iPS) cells, which are somatic cells that have been returned to a pluripotent state, similar to that of hES cells in terms of differentiation potential and epigenetic signature. In his Nobel Prize earning work, Yamanaka first created iPS cells by introducing the genes for the transcription factors: OCT4, SOX2, KLF4 and MYC via retroviral vectors into terminally differentiated human skin fibroblasts, after showing successful generation of mouse iPS cells with the same four transcription factors.[1, 2] In the same year, Yu et. al also created iPS cells by introducing the genes for the transcription factors: OCT4, SOX2, Nanog and LIN28 via retroviral vectors into human primary diploid fibroblast cells.[3] Since then, a number of methods have been developed to generate human iPS cells,[4-6] including non-viral methods such as transfection with synthetic mRNA,[7] microRNA,[8] and episomal vectors[9], and the introduction of the transcription factors via cell penetrating peptides[10] and cell penetrating recombinant proteins.[11]

iPS cells are particularly appealing because they can be taken from a patient to generate a large amount of patient specific cells that can be used to study disease progression or used for the development of patient specific drug therapies. Cells from certain tissues are particularly inaccessible from live patients such as brain and heart tissues, making it nearly impossible to generate patient specific disease tissue models or patient specific drug tests. Using iPS cells instead of terminally differentiated disease cells can circumvent that limitation, since iPS lines can be maintained for many passages, and they can be expanded, so that only a small, often ectopic, sample is required. In order to generate sufficient numbers of cells from inaccessible tissues such as heart and brain, skin cells can be reprogrammed into iPS cells, and then expanded, and then directly differentiated into cardiac or nerve cells.

Park et al. have demonstrated that cells from disease specific tissues, while reprogrammed to a pluripotent state, still maintain genetic markers of the disease state, rendering them an attractive tool for studying genetic diseases.[12] Ebert et al. have even been able to direct the differentiation of iPS cells from a patient with spinal muscular dystrophy and from his healthy mother into motor neurons, demonstrating that the cells showed differing behavior owing to the genetic disease.[13]

Of great significance, iPS based models can be more relevant than animal models for disease modeling. Animal models require complicated and expensive knockout strategies, and the genes responsible for the disease in humans do not always lead to the disease in other species. For example, cystic fibrosis in humans is caused by mutations in the CFTR gene, however mice with the missing gene do not develop cystic fibrosis.[14] A currently used disease model for cystic fibrosis employs a mouse with completely normal cystic fibrosis gene and overexpression of a second gene (not implicated in the human disease) SCNNI that controls transmembrane sodium ion flow. [15] Clearly, this is not the best mimic of the cystic fibrosis in humans, and this underscores the limitations of animal models for studying disease progression. Cardiac diseases are particularly difficult to recapitulate with animal models due to inherent physiological differences between humans and mice, such as

their vastly differing heart rates (60 beats per minute (bpm) in humans and 500 bpm in mice), and their differing composition: fetal mouse hearts are predominantly comprised of βMHC (myosin heavy chain), while the adult mouse hearts are predominantly comprised of αMHC; whereas human fetal hearts predominantly express αMHC and adult hearts are mainly comprised of βMHC.[16]

Amongst the first diseases to be studied with iPS cells were heart diseases, such as the long QT syndrome diseases.[17] The QT interval refers to the time between Q and T peaks, which correspond to the opening and closing of the left ventricle (**Figure 5.1**). The disease is caused by mutations in ion channel genes, and currently there are 13 genetic variants known.[18]. Some examples include mutations of potassium channel genes (which lead to LQT1 and LQT2 syndromes), mutations of a sodium channel gene (which leads to LQT3), and mutations of a calcium gene (which lead to LQT8). All forms of the disease involve abnormal repolarization of the heart, which leads to arrhythmias, and other clinical manifestations such as palpitations, syncope, seizures, and sudden cardiac death.

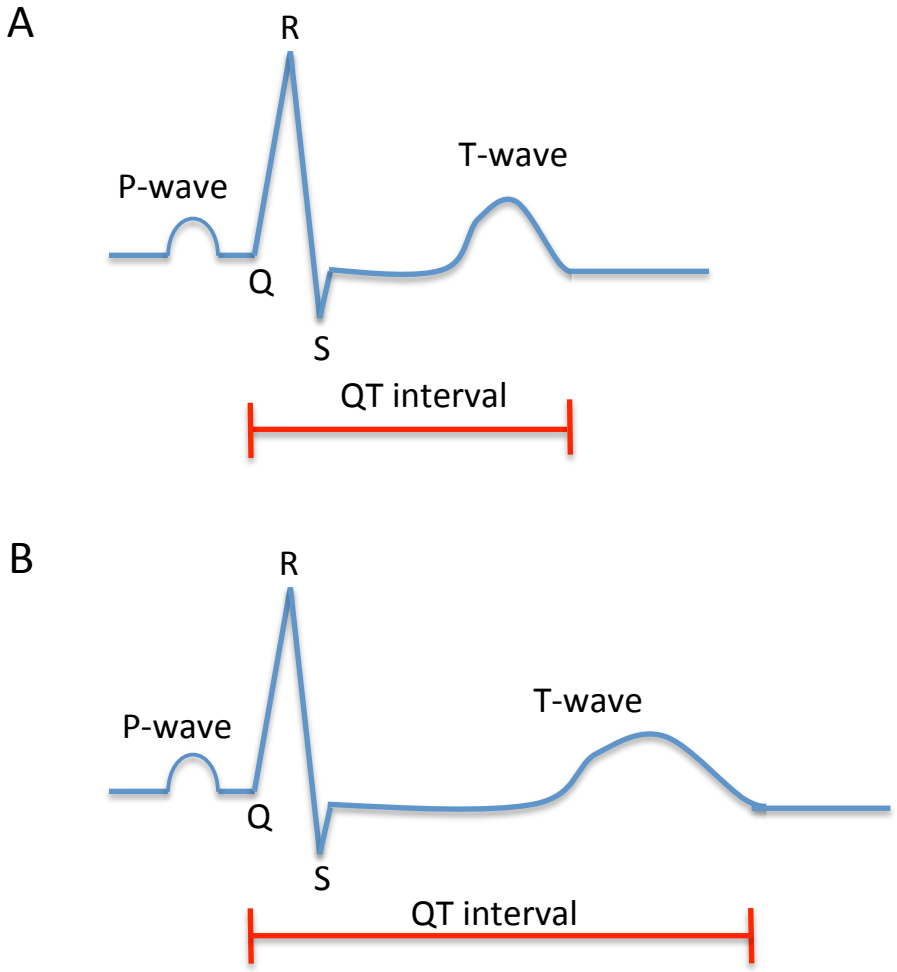

Figure 5.1 Schematic electrocardiogram of (A) normal heart and (B) long QT syndrome heart. The P-wave corresponds to atrial depolarization, the QRS segment corresponds to ventricular depolarization, and the T-wave corresponds to ventricular repolarization. The QT interval therefore corresponds to the time for ventricular depolarization and repolarization.

iPS cells have been successfully derived from patients with long QT syndromes, and those cells mimicked the electrophysiological characteristics of the disease such as a prolonged action potential, and irregular beating rates under regular conditions and under β-adrenergic stimulation.[19-22] Human iPS derived cardiomyocytes from patients with LQT2 syndrome, have already been used for drug screening and have shown arrhythmogenicity after exposure to repolarization-prolonging chemicals and sensitivity to HERG (human ether-ago-go).[19, 22-25] β-adrenergic blocking agents, which are already in clinical use for patients with cardiac arrhythmias, were shown to attenuate catecholamine-induced tachyarrhythmia in single cardiomyocytes derived from iPS cells of patients with long QT syndromes.[19, 24] Additionally, drugs that are not yet in clinical use have also been evaluated with cardiomyocytes derived from iPS cells of patients with long QT syndromes (specifically LQTS2), such as ion channel blockers (nifedipine and ranolzaine), ion channel openers (pinacidil and nicorandil), and a potassium current channel enhancer (PD-118057), and they have been shown to prevent arrhythmias.[23, 24]

Despite the aforementioned advances with cardiac cells derived from iPS cells from patients with cardiac diseases, such as the long QT diseases, there is much room for improvement in the differentiation of iPS cells into cardiac cells, which can be addressed with our patterned hydrogel surfaces. A brief summary of cardiac differentiation techniques and their limitations will be presented below, in order to motivate the use of our patterend hydrogel surfaces.

Cardiomyocytes were first derived from hES cells (the H9) line by Kehat et. al who noticed the spontaneous beating of the cells when they were turned into embryoid bodies (EBs) (by culturing in suspension with a nonadhesive cultureware) and then replated as embryoid bodies onto adherent gelatin surfaces.[26] Only about 8% of the EBs showed spontaneous contracting areas, but the cells in those areas stained positively for cardiac cell markers such as cardiac myosin heavy chain, α-actinin, desmin, and cardiac troponin I (anti-cTnI). The cells cardiac lineage was further corroborated with gene expression, electron microscopy to show sarcomeric structures, and electrophysiological testing. Similar spontaneous differentiation protocols using EBs were then published using other hESC and hiPS lines.[27-29] While ~8% of EBs showed areas that were beating, the actual percentage of cells contracting was very low, and significant cell line to cell line variability was found for the efficiency of cardiomyocyte generation.[30] More problematic was the limited reproducibility of these protocols due to the heterogeneity of the EB sizes and the use of undefined component such as serum, which have significant lot to lot source variability.

Towards that end, researchers have been trying to systemize cardiomyocyte derivation from human pluripotent stem cells by eliminating or limiting the use of undefined components and controlling the size of the EBs used, or eliminating the use of EBs all together. While the use of centrifuge-spin-aggregating wells, microwells, and micropatterning have been shown to control the size EBs and optimal EB sizes for cardiomyocyte differentiation were reported for each

method,[31-35] avoiding the generation of EBs and instead differentiating from a monolayer of cells can allow for a more uniform and reproducible presentation of signals such as growth factors, due to the less complex diffusion present in monolayer culture.

In the absence or serum, new protocols were developed relying on growth factors implicated in *in vitro* cardiogenesis such as BMP4, activin A, FGF2, Wnt agonists and antagonists, and vascular endothelial growth factor (VEGF).[36-43] However these protocols require monitoring steps, such as monitoring the kinase domain receptor/c-kit[36] or Flk1/PDGF receptor α[43] expression to determine optimal time and concentration of growth factor addition, which will be differ by cell line. Another recent directed differentiation protocol requires cell sorting with an antibody against signal-regulatory protein α (SIRPA), in order to get high percentage of cardiomyocytes, but this sorting is not amenable to scale up.[44]

Notably, Laflamme et. al. have used sequential addition of activin A and BMP4 in defined RPMI/B27 medium on monolayer culture of H7 hESC cells (on Matrigel in the presence of MEF conditioned media) to obtain 30% cardiomyocytes, or >70% after a Percoll gradient centrifugation step, significantly higher than the percentages achieved with EB methods.[45] However, the use of Matrigel and MEF conditioned media in Laflamme's protocol pose the same lot to lot variability problems as the serum protocols, which have made that protocol difficult to reproduce, with high variability seen between cells lines and experimental repeats.[46, 47] Most recently, Lian et. al have developed a directed differentiation protocol based on temporally modulating canonical Wnt signaling (inducting of canonical Wnt signaling early in the differentiation and suppressing it later in the protocol), which they were able to perform, not only on Matrigel, but on the synthetic surface Synthemax (manufactured by Dow Corning), to yield >95% cardiomyocytes.[48] Synthemax, a peptide displaying polymer hydrogel, however is proprietary and its exact composition is not known, making it an undefined component in the system.

We hypothesize that patterned hydrogels may increase the efficiency of cardiomyoctye generation from pluripotent cells during directed differentiation, by both decreasing the variability introduced from using poorly defined surfaces such as Matrigel, and by introducing signals not present in the current methodologies, such as mechanical cues, alignment due to the confinement from patterns, and control over paracrine signaling via control over pattern size and spacing.

As a preliminary study, we wanted to see whether patterned hydrogels could support cardiomyocytes derived from from iPS cells. This chapter therefore focuses on the ability of patterned hydrogels to support cardiomyocytes derived from iPS cells from patients with the LQT3 syndrome.

5.2 Methods and Materials

5.2.1 Cell Culture

iPS cells derived from a LQT3 patient were kindly donated by Bruce Conklin's lab at the Gladstone institute. The cells were maintained on hESC-qualified Matrigel

(BD Bioscience) and with mTeSR media (StemCell Technologies, Vancouver, Canada), which was exchanged daily. Prior to cell passaging, Matrigel which was stored at -20°C was thawed to 4°C in a refrigerator, and was then diluted ~ 1:75 with 4°C KO-DMEM. Note, Matrigel is sold by volume, so the concentration of proteins varies by lot, and for each lot, BD Bioscience recommends a specific Matrigel aliquot volume (~300 uL) to be used for hES cell culture, which is then diluted in 25 mL KO-DMEM. 1.5 mL of diluted Matrigel was added to each well of a 6 well tissue culture plate (Costar), and allowed to adsorb for 1 hour. After 1 hour, Matrigel was aspirated from the wells, and 1 mL media was added to each well. Cells were passaged every 4-5 days at split ratios 1:6-1:12, using StemPro Accutase (Life Technologies). Specifically, cells were rinsed with PBS (Life Technologies) and then incubated with Accutase at 0.5 mL/well for 3 minutes at 37°C. At this point, cells were no longer attached to the well and 5 ml PBS was added to each well to dilute the Accutase. The cell solution was then removed from the well and centrifuged at 500 rpm for 2 minutes, after which the supernatant was then aspirated and cells were resuspended in mTeSR with 5 μM ROCK Inhibitor (Calbiochem EMD Chemicals), and then seeded onto the Matrigel plates. ROCK inhibitor was only kept for 1 day after passaging and removed during the first media exchange. Cells used were under passage 50 for all experiments detailed in this chapter. Cells were intentionally not passaged with Collagenase IV or other enzymes such as Dispase, which require manual mechanical scraping to detach cells, which can be inconsistent between passages. Cells were periodically karyotyped at Children's Hospital Oakland Research Institute (CHORI), and were always found to have a normal karyotype. Cells were seeded onto surfaces at the same ratios at which they were split for passaging

iPS cells were directly differentiation into cardiac cells using a protocol, based on the Matrigel sandwich method,[49] which will be described below. When undifferentiated iPS cells reached 80% confluence, the cells were overlaid with Matrigel diluted in mTeSR (1 mg/15 ml). When cells reached 100% confluence, medium was changed to RPMI 1640 medium (Life Technologies) containing B27 complete supplement (with insulin) (Invitrogen) and100 ng/mL Activin A (R&D Systems), and this day is designated as day 0. On day 1 medium was replaced with RPMI 1640 medium containing B27 supplement without insulin (Invitrogen), 10 ng/mL BMP-4 (R&D Systems) and 5 ng/mL bFGF. On day 5, medium was replaced with RPMI 1640 medium containing B27 complete supplement (with insulin). Medium was then changed every 3 days with RPMI 1640 medium containing B27 complete supplement (with insulin). Cells would typically begin beating by day 12, and they would continue beating for months, if not longer.

After beating cell sheets were formed, cells were detached and plated onto fibronectin patterned acrylamide surfaces by detaching with 0.25% Trypsin EDTA (Life Technologies) using the same method described in **Section 3.2.2.4** for passaging RMSC and 3T3 fibroblasts, with the noted difference that the media used for the cardiac cells during passage was RPMI 1640 medium containing B27 complete supplement (with insulin).

5.2.2 Patterned Surfaces

Quartz-supported acrylamide gels were prepared as described in **Appendix A.1**. Gels were sterilized in 70% ethanol and then rinsed 5 times in PBS. Glass microscope slides and PDMS stamps with post diameters corresponding to desired colony sizes, were fabricated and exposed to oxygen plasma at 1 Torr and 80W for 30 seconds. The backs of the PDMS stamps were affixed to the glass microscope slides immediately after the plasma treatment. Stamps were then sterilized with 70% ethanol and allowed to dry in a sterile hood. 0.2 mg/mL sterile filtered sulfo-SANPAH in PBS was added to the top of each stamp, and allowed to incubate on the stamp, in darkness, for 30 minutes. Subsequently, stamps were dried with a nitrogen gun. Stamps were then placed in conformal contact with dehydrated acrylamide gels, 0.125 J/cm^2 UV was shone through the stamp. The stamps were then removed and the acrylamide gels were washed three times in PBS, and then incubated with 0.25 mg/mL fibronectin in PBS for 1 hour. The gels were then rinsed thee times in PBS, and were then ready for cell seeding. Cells were seeded on the same day that fibronectin was patterned.

5.2.3 Immunocytochemistry

At day 3 after seeding, cells were fixed with 4% Paraformaldehyde (PFA) in PBS for twenty minutes at room temperature. Cells were then gently washed three times with PBS. Cells were permeabilized with 0.1% TritonX, followed by a one rinse with PBS, and followed by a block with 10% goat serum in PBS, with 0.1% Triton for 1 hour at room temperature. Cells were then incubated overnight at 4°C in primary antibodies diluted 1:100 in 2% goat serum, 0.1% Triton PBS. The primary antibodies used were Cardiac Troponin T mouse antihuman monoclonal (Thermo Scientific, MS-295) and SM22 (smooth muscle myosin) rabbit antihuman polyclonal (Abcam ab21624). Cells were then washed three times in PBS with 0.1% Triton for half an hour per wash and then incubated with the secondary antibodies at 1:500 dilution. The secondary antibodies used were goat anti-Rabbit alexaflour 488 (Abcam) and goat anti-mouse alexaflour 568 (Abcam). Finally cells were rinsed three times gently with PBS and incubated with 300nM 4',6-diamidino-2-phenylindole (DAPI; Life Technologies) for 5 minutes.

5.2.4. Electrophysiology

The electric properties of the beating cells were also investigated with the ANEP (aminonaphthylethenylpyridinium) voltage sensitive dyes Di-4-ANEPPS and Di-8-ANEPPS (Invitrogen), which fluoresce in response to changes in electrical field surrounding the dyes. The dyes are lipophilic, and do not fluoresce in water, however they bind strongly to the phospholipid cell membrane, where they fluoresce. The excitation spectra of the ANEP dyes display a potential dependant shift, which therefore allows excitation ratio measurements to quantify a change in cell membrane potential. A sCMOS camera recording at 200 fps was used to image

cells treated with the ANEP dyes, and the BrainVision MiCAM Analysis software was used for analysis. Stock solutions of the dye at 1 mg/ml in DMSO were diluted to 0.2–2 μM with Pluronic® F-127 (0.05%) and then added to live cells for 10 minutes. Cells were then gently washed with PBS to remove any unbound dye.

5.3 Results and Discussion

Beating cardiomyocytes directly differentiated from iPS cells from a long QT patient, (hiPS-CM) were replated onto fibronectin patterned, 1 kPa hydrogels. Prior to replating, it was observed that the directly differentiated cells seemed to compromise at least two morphologically and behaviorally distinct cell subtypes (FACs data from Zhen Ma in the Healy laboratory indicated that only 50.3% of cells were positive for cardiac troponin T). One population resembled fibroblasts in morphology and in strong adhesion to the cell culture surface. The second population was comprised of the beating cells, which were usually less elongated, and sometimes rounder than the fibroblast like cells. The beating cells were found in sheets or large masses on top of the fibroblast like cells, and with loose adhesions to the fibroblast cells, which was concluded based on the observation that the fibroblasts cells remained stationary, while the overlying beating cells moved as part of their beating. Having a mixed population of cells from cardiac differentiation is not surprising, as the heart itself is compromised of a number of cardiac cell types: cardiomyocytes, vascular smooth muscle cells, and endothelial cells. Even within the cardiomyocyte lineage there are atrial, ventricular, and pacemaker cells. The observations are consistent with those for the cardiac differentiation protocols described in **Section 5.1.**

The patterned fibronectin surfaces were capable of supporting hiPS-CM as confirmed by cells staining positive for markers of cardiac lineage such as smooth muscle myosin SM22, and cardiac troponin T (**Figure 5.2**), but it is clear, as was the case for the hiPS-CM in typical culture conditions that there is a heterogeneous cell population. Time lapse imaging of cells revealed that cells were beating synchronously within the islands, but various islands did not beat at the same rate. Images from the videos **Figure 5.3** where it is the rounder phase bright cells that beat, and the fibroblast looking cells that do not beating.

Voltage sensitive dyes were used to study electrophysiological properties of hiPS-CM, such as the action potential duration. While the dyes are particularly time sensitive in that they can detect and respond to potential changes that occur on the order of milliseconds, their change in fluorescence is only about 2–10% fluorescence change per 100 mV. Even though cells were seen beating on the patterned islands, they did not generate a large enough change in potential for the fluorescence signal of the voltage sensitive dye to be detectable above noise. It was observed that fluorescent signals above noise could only be generating in large clusters of beating cells of what appeared to be tens to hundreds of beating cells as were present inhomogeneously on the unpatterned surfaces on which the cells were directly differentiated. In these larger clusters, action potential duration was seen to be a function of location within the mass of beating cells, and not constant for all cells in the same beating mass (unpublished data from Zhen Ma and Or Gadish in the

Healy lab). When higher concentrations of the voltage sensitive dyes were used with the live hiPS-CM, in an attempt to increase the signal, the cells died, as the dye is toxic. It is therefore recommended that a patch clamp be used to assess the electrophysiology of the hips-CM cells, as the voltage sensitive dyes and sCMOS camera combination are not sensitive enough to detect the changes in membrane potential of beating hiPS-CM at low cell densities.

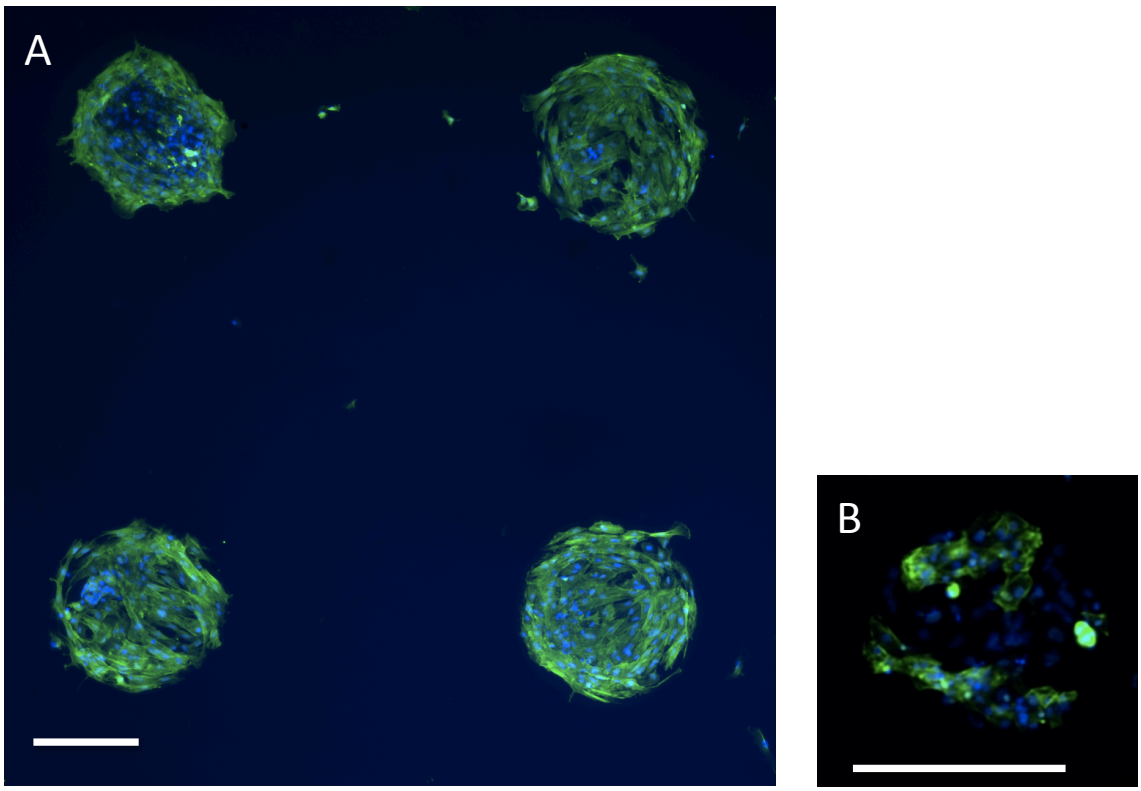

Figure 5.2 1 kPa fibronectin patterned acrylamide gels can support cardiac cells directly differentiated from long QT patient iPS cells, as indicated by protein expression (green) of cardiac lineage (A) smooth muscle myosin (B) cardiac troponin T. The blue stain is DAPI and scale bar = 500 μm.

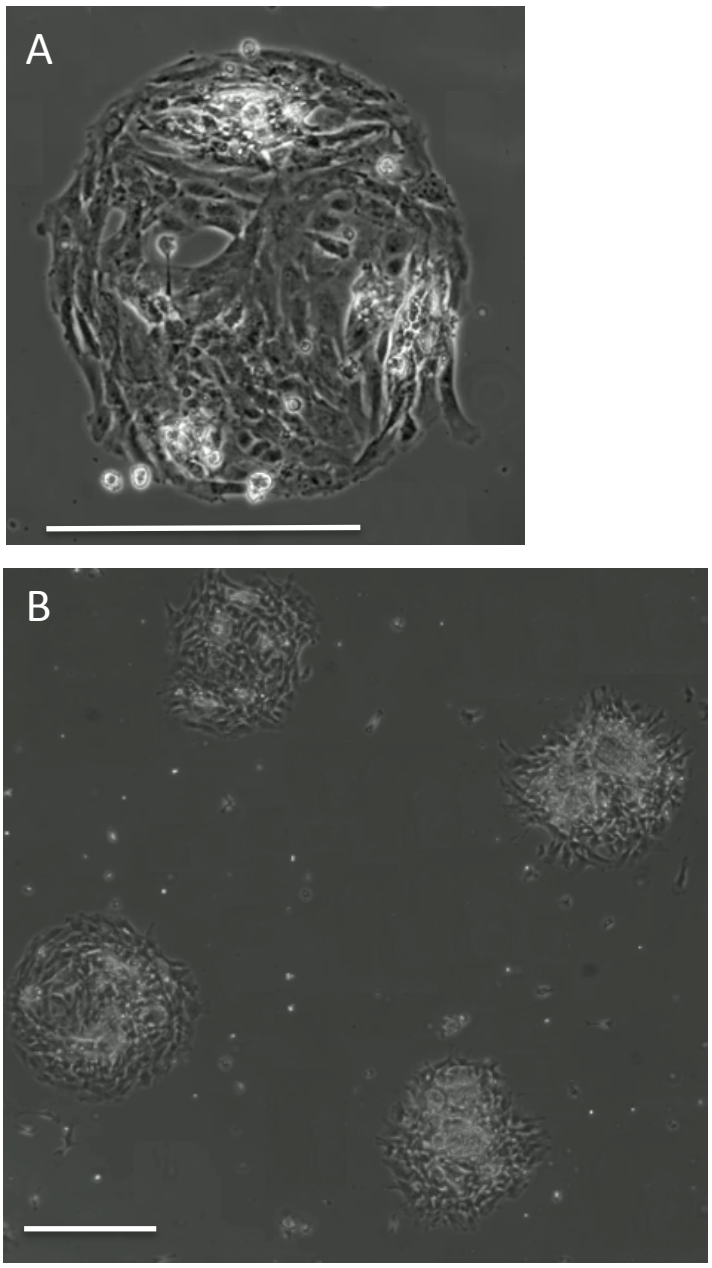

Figure 5.3 Stills from videos of beating hiPS cardiac cells (A) and (B). The phase bright cells in the islands were the beating cells, while the cells that looked more fibroblast-like did not beat. Islands had mixed populations of beating and non-beating cells, with cells in the same island beating synchronously. Contracting cells in the colony could ultimately deform the colony from its original shape (B). Scale bar = 500 μm.

The cells used herein where directly differentiated on Matrigel surfaces into cardiac lineage, prior to being placed on the patterned hydrogel surface. However, in the future, we envision using the patterned hydrogels for the directed differentiation of hiPS into cardiac cells. We hypothesize that patterned hydrogels may increase the efficiency of cardiomyocyte generation from pluripotent cells during directed differentiation, by both decreasing the variability introduced from

using poorly defined surfaces such as Matrigel, and by introducing signals not present in the current protocols, such as mechanical cues, alignment due to the confinement from patterns, and control over paracrine signaling via control over pattern size and spacing.

Engler et. al have already demonstrated that embryonic cardiomyocytes can beat for longer on more compliant surfaces (1-10 kPa gels) versus stiff culture surfaces, and that on the more compliant gels a larger fraction of the cardiomyocytes were striated (as visualized by α-actinin staining).[50] McDevitt et al. also have shown that patterning cardiomyocytes on laminin lanes aligned the cells into rod shapes, parallel to the lanes and localized the junction molecules N-cadherin and connexin43 at the edges of the rods, allowing for cells to beat synchronously within a lane when the lanes were spread far apart, and synchronously over a sheet when the lane spacing was so small as to allow cells to bridge between lanes.[51] Combining these two strategies, as the patterned hydrogel described herein does, may lead to more homogenous cardiac populations during directed differentiation.

Additionally, it is possible that the use of adhesive ligands other than fibronectin in the patterned hydrogel system may lead to different subpopulations binding and supporting the beating cells. However, on a compliant surface, the fibroblast-like cells required to serve as a flexible substrate for the beating cells in typical culture, may no longer be required.

In addition to producing cardiomyocytes, one would also like to control the maturity of the cardiomyocytes. It is often important to induce proper maturity in cell types for accurate disease modeling with iPS cells. For example, conditions such as hypertrophy (cell enlargement) occur in adult cardiac cells but rarely occur in fetal cardiomyocytes.[52] For diseases of the sarcomere contractile apparatus, the difference in force of contraction between healthy and myopathic cells is significantly smaller in fetal cardiomyocytes than in adult cells.[52] Consequently, many groups are trying to get more homogenous populations of mature atrial, ventricular and conduction system cells. Our platform could potentially provide more homogenous populations of mature atrial, ventricular and conduction system cells.

5.4 Conclusion

We have shown that fibronectin patterned acrylamide hydrogels can support hiPS-CM, and that when confined to islands, beating cells in an island beat synchronously. Voltages sensitive dyes combined with sCMOS cameras are not sensitive enough to report electrophysiology from such small clusters of cells, as the islands investigated herein. We anticipate that the patterned hydrogel platform can be used as part of a cardiac directed differentiation protocol to increase homogeneity and yield of cardiac lineage cells due to the inputs of a compliant deformable surfaces, and geometric constraint which forces cells to beat synchronously.

Chapter 6
Conclusions and Future Directions

6.1 Results Summary
- 6.1.1. Matrigel Characterization
- 6.1.2 Chemically Patterned Hydrogels
- 6.1.3 Effect of Substrate Modulus on Human Embryonic Stem Cells
- 6.1.4 Pluripotent Cells on Patterned Hydrogels

6.2 Future Work

6.1 Results Summary

Creating synthetic human embryonic stem (hES) cell culture systems is crucial for the future of regenerative medicine. Current hES cell culturing techniques are limited because of the use of animal products, which can introduce pathogens as well as limit the scalability and reproducibility of these platforms. While media formulations have been optimized to include only human or recombinant proteins, the current gold standard for stem cell culture substrate is still Matrigel, an excretion from a mouse tumor that resembles the extra cellular matrix.

In this dissertation I studied the physiochemical properties of Matrigel, and I then developed a synthetic platform on which to culture human pluripotent cells, to both try and replace Matrigel, and to offer a platform on which to conduct fundamental scientific studies on human pluripotent stem cells. The platform, which was comprised of a chemically patterned hydrogel, allowed for the control of the mechanical environment of the cells and their paracrine signaling. The mechanical environment was controlled by tuning the modulus of the hydrogel, and paracrine signaling could be controlled by regulating cell colony size and spacing via the chemical patterning.

6.1.1 Matrigel Characterization

Differences in attachment, proliferation, and differentiation were measured for hES cells cultured on various substrata coated with Matrigel. It was observed that hES cells attach and grow poorly on Matrigel adsorbed onto polystyrene, while they proliferate when exposed to Matrigel adsorbed onto glass or oxygen plasma treated polystyrene e.g., "tissue culture" treated polystyrene. Furthermore, hES cells grown on the Matrigel coated tissue culture polystyrene are less likely to differentiate than those grown on the Matrigel coated glass. To assess the mechanism for these observations, I replicated the cell culture interface in a quartz crystal microbalance with dissipation monitoring. In addition, I used ellipsometry and scanning electron microscopy to determine the thickness and topography of Matrigel on the varying surfaces. Matrigel formed a viscoelastic multilayer with similar thickness on all three surfaces; however, the network structure was different, where the adsorbed proteins formed a globular network on polystyrene, and fibrillar networks on the hydrophilic substrates. Matrigel networks on glass were denser than on oxygen plasma treated polystyrene, suggesting that the density and structure of the Matrigel network affects stem cell differentiation, where a denser network promoted uncontrolled hES cell differentiation and did not maintain the self-renewal phenotype

6.1.2 Chemically Patterned Hydrogels

A technique for patterning low swelling hydrogels was presented and compared to less successful patterning methodologies. In this technique, a UV activated ink was transferred to a low swelling polyacrylamide hydrogel via simultaneously microcontact printing and UV illuminating through the stamp. The

ink had an NHS ester, which could then react with proteins of interest. 3T3 cells could be patterned onto polyacrylamide gels as compliant as 1 kPa, in patterns that spanned the entire area of a well of a 6 well plate (35 mm^2). Below 1 kPa, fibroblasts could not spread nor proliferate; however, more compliant patterned gels (140 Pa) could support hES cells (chapter 4). Parameters for the pattern transfer were optimized and documented in this chapter, and key findings will briefly be summarized here.

It was found that a quartz backing was requisite for the polyacrylamide gels, as an insufficient amount of graft sites were generated on TCPS, even when exposed to oxygen plasma, which allowed the polyacrylamide gel to buckle and delaminate from the confined swelling. In contrast, a sufficient number of graft sites for the polymer could be generated on quartz by attaching a vinyl terminated silane to the quartz.

The protein fouling of polyacrylamide was seen to be a function of reaction and solvent pH, which affected degree of conversion, and could be controlled by monomer storage and solvent choice.

Sterilization had to be performed once the gel was prepared, and all subsequent work was performed with sterile filtered reagents in a sterile biosafety cabinet, as typical sterilizing procedures such as exposure to ethanol or UV, can degrade proteins. Polyacryalmide gels were sterilized with 70% ethanol, a nonsolvent for the gel, which provided a quality control step by turning the gel opaque, making apparent any inhomogeneities in the gel that were invisible in the swollen state.

Buffer identity and concentration and crosslinker concentration were optimized, and it was found that PBS at pH 7.4 and not HEPES at pH 8.5 was the best buffer for all steps of the reaction, and that when using proteins as alkaline as fibronectin, at concentrations above 0.1 mg/mL, neither PBS nor HEPES could adequately buffer the reaction. However, the high pH of the fibronectin solutions was a benefit, as it guaranteed that many primary amines were available for reaction with the NHS ester of the crosslinker.

Lastly, parameters regarding the stamping were optimized. It was found that glass backing was required to pattern on the length scale of colony dimensions (at least 400 μm) spaced at least one colony dimension apart, to prevent roof collapse of the stamp. Hydrogel drying times and stamp contact times were also optimized to prevent ink diffusion, but to allow for the conjugation reaction.

An exploration into the ability of PEG to modify the fouling properties of polyacrylamide was also performed. It was found that, if necessary, PEG chains can be conjugated to polyacrylamide to reduce protein adsorption, by using a solution concentration at the critical overlap concentration of the chain, and using PEG chains sufficiently short to allow the end groups to be accessible for reaction (in this work MW < 5,000 g/mol).

Finally, preliminary work was carried out to investigate the use the patterning methodology for an RGD peptide, rather than fibronectin, using a UV-activated crosslinker that could react with the peptide's with free thiol group. The limited cell spreading and proliferation on these surfaces indicated that either an

insufficient amount of peptide was present on the surface, or that excess unreacted peptide was competitively binding with the cells, or that the peptide-crosslinker bond was getting reduced. A more suitable crosslinker for peptide conjugation is the ASIB crosslinker, which has a UV activated end to react with the polyacrylamide and a maleimide end to react with a thiol containing peptide. In contrast to the crosslinker used in this work, ASIB would not require reduction prior to conjugation, and would not be affected by residual reducing agent from the peptide reduction step. However, at the time of this dissertation, ASIB was not commercially available.

6.1.3 Effect of Substrate Modulus on Human Embryonic Stem Cells

The hypothesis that hES cell behavior is influenced by substrate modulus was addressed by examining hES cell proliferation and gene expression on polyacrylamide surfaces of varying moduli and TCPS (functionalized with either fibronectin or Matrigel). While proliferation was seen to increase with increasing substrate stiffness, regardless of adhesive ligand (fibronectin or Matrigel), as is typical with other cell types, there was no statistically significant difference in pluripotent gene expression for hES cells grown on surfaces with different moduli.

6.1.4 Pluripotent Cells on Patterned Hydrogels

HES cells were successfully attached onto Matrigel and fibronectin patterned polyacrylamide gels as compliant as 140 Pa, with pluripotency maintained at day 4 of patterning as determined by immunostaining of the pluripotency genes OCT4 and Nanog. Additionally, cardiomyocytes directly differentiated from iPS cells from a patient with long QT3 syndrome were also seeded onto fibronectin patterned 1 kPa gels, and cells beat synchronously within an island, but they did not necessarily beat synchronously between islands. Electrophysiological measurements were attempted on the beating cells in the islands using voltage sensitive dyes and sCMOS camera, however signal above noise was not detected for the dye used at doses that would not kill the cells.

6.2 Future Work

Having developed a methodology to chemically pattern very compliant hydrogels, and having preliminarily demonstrated the ability of the patterned hydrogels to support pluripotent cells, there remain a number of interesting experiments to explore with this platform.

As demonstrated in chapter 4, it is unclear whether substrate stiffness affects pluripotent gene expression in hES cells, as no statistically significant difference was observed, potentially due to the high variability inherent in the data. I am therefore particularly interested in seeing whether the patterned hydrogels can reduce that variability by controlling colony area, perimeter and spacing, and ultimately answer the question of whether substrate stiffness affects pluripotent gene expression. Since the pluripotent gene expression assay performed in chapter 4 was done at 1 passage, it would also be very interesting to see with both patterned and un-

patterned hydrogels whether gene expression would eventually become a function of substrate stiffness during long term culture, involving many passages. I would also like to test the hypothesis that compliant hydrogels may abrogate the need for ROCK inhibitor in hES culture. Also, as mentioned in this work, fibronectin was used instead of recombinant vitronectin for patterned surfaces, but as the cost of recombinant proteins decline, the role of vitronectin as a function of substrate modulus could be explored for hES cells. In terms of iPS cells, I am particularly interested in combining the patterned hydrogels developed herein with directed differentiation protocols to increase efficiency and homogeneity of target cell types, such as the cardiac lineage cells described in chapter 5. However, the patterned hydrogel can find use in directed differentiation of any cell type, and not only for contracting cell types.

References

Chapter 1

1. Evans, M. J.; Kaufman, M. H., Establishment in culture of pluripotential cells from mouse embryos. *Nature* **1981,** 292, (5819), 154-6.
2. Thomson, J. A.; Itskovitz-Eldor, J.; Shapiro, S. S.; Waknitz, M. A.; Swiergiel, J. J.; Marshall, V. S.; Jones, J. M., Embryonic stem cell lines derived from human blastocysts. *Science* **1998,** 282, (5391), 1145-1147.
3. Takahashi, K.; Tanabe, K.; Ohnuki, M.; Narita, M.; Ichisaka, T.; Tomoda, K.; Yamanaka, S., Induction of pluripotent stem cells from adult human fibroblasts by defined factors. *Cell* **2007,** 131, (5), 861-872.
4. Yu, J.; Vodyanik, M. A.; Smuga-Otto, K.; Antosiewicz-Bourget, J.; Frane, J. L.; Tian, S.; Nie, J.; Jonsdottir, G. A.; Ruotti, V.; Stewart, R.; Slukvin, I. I.; Thomson, J. A., Induced pluripotent stem cell lines derived from human somatic cells. *Science* **2007,** 318, (5858), 1917-1920.
5. Harrison, R. G., Observations on the living developing nerve fiber. *Anatomical Record* **1907,** 1, (5), 116-118.
6. CorningLifeScience Cell Culture History. http://www.corning.com/lifesciences/us_canada/en/about_us/cell_culture_history.aspx (December 2012),
7. Skloot, R., *The Immortal Life of Henrietta Lacks*. Random House: 2010.

Chapter 2

1. Thomson, J. A.; Itskovitz-Eldor, J.; Shapiro, S. S.; Waknitz, M. A.; Swiergiel, J. J.; Marshall, V. S.; Jones, J. M., Embryonic stem cell lines derived from human blastocysts. *Science* **1998,** 282, (5391), 1145-1147.
2. Reubinoff, B. E.; Pera, M. F.; Fong, C. Y.; Trounson, A.; Bongso, A., Embryonic stem cell lines from human blastocysts: somatic differentiation in vitro. *Nature Biotechnology* **2000,** 18, (4), 399-404.
3. Fletcher, J. M.; Ferrier, P. M.; Gardner, J. O.; Harkness, L.; Dhanjal, S.; Serhal, P.; Harper, J.; Delhanty, J.; Brownstein, D. G.; Prasad, Y. R.; Lebkowski, J.; Mandalam, R.; Wilmut, I.; De Sousa, P. A., Variations in humanized and defined culture conditions supporting derivation of new human embryonic stem cell lines. *Cloning Stem Cells* **2006,** 8, (4), 319-34.
4. Richards, M.; Fong, C. Y.; Chan, W. K.; Wong, P. C.; Bongso, A., Human feeders support prolonged undifferentiated growth of human inner cell masses and embryonic stem cells. *Nat Biotechnol* **2002,** 20, (9), 933-6.
5. Cheng, L.; Hammond, H.; Ye, Z.; Zhan, X.; Dravid, G., Human adult marrow cells support prolonged expansion of human embryonic stem cells in culture. *Stem Cells* **2003,** 21, (2), 131-42.
6. Genbacev, O.; Krtolica, A.; Zdravkovic, T.; Brunette, E.; Powell, S.; Nath, A.; Caceres, E.; McMaster, M.; McDonagh, S.; Li, Y.; Mandalam, R.; Lebkowski, J.; Fisher, S.

J., Serum-free derivation of human embryonic stem cell lines on human placental fibroblast feeders. *Fertil Steril* **2005,** 83, (5), 1517-29.
7. Martin, M. J.; Muotri, A.; Gage, F.; Varki, A., Human embryonic stem cells express an immunogenic nonhuman sialic acid. *Nat Med* **2005,** 11, (2), 228-32.
8. Chase, L. G.; Firpo, M. T., Development of serum-free culture systems for human embryonic stem cells. *Curr Opin Chem Biol* **2007,** 11, (4), 367-72.
9. Xu, C.; Inokuma, M. S.; Denham, J.; Golds, K.; Kundu, P.; Gold, J. D.; Carpenter, M. K., Feeder-free growth of undifferentiated human embryonic stem cells. *Nat Biotechnol* **2001,** 19, (10), 971-4.
10. Li, P., Brunette, Lebkowski, Mandalam, Expansion of Human Embryonic Stem Cells in Defined Serum-Free Medium Devoid of Animal-Derived Products. *Biotechnology and Bioengineering* **2005,** 91, (6).
11. Yao, S.; Chen, S.; Clark, J.; Hao, E.; Beattie, G. M.; Hayek, A.; Ding, S., Long-term self-renewal and directed differentiation of human embryonic stem cells in chemically defined conditions. *Proc Natl Acad Sci U S A* **2006,** 103, (18), 6907-12.
12. Beattie, G. M.; Lopez, A. D.; Bucay, N.; Hinton, A.; Firpo, M. T.; King, C. C.; Hayek, A., Activin A maintains pluripotency of human embryonic stem cells in the absence of feeder layers. *Stem Cells* **2005,** 23, (4), 489-95.
13. Ludwig, T. E.; Levenstein, M. E.; Jones, J. M.; Berggren, W. T.; Mitchen, E. R.; Frane, J. L.; Crandall, L. J.; Daigh, C. A.; Conard, K. R.; Piekarczyk, M. S.; Llanas, R. A.; Thomson, J. A., Derivation of human embryonic stem cells in defined conditions. *Nat Biotechnol* **2006,** 24, (2), 185-7.
14. Kleinman, H. K.; McGarvey, M. L.; Liotta, L. A.; Robey, P. G.; Tryggvason, K.; Martin, G. R., Isolation and characterization of type IV procollagen, laminin, and heparan sulfate proteoglycan from the EHS sarcoma. *Biochemistry* **1982,** 21, (24), 6188-93.
15. Biosciences, B. D. http://www.bdbiosciences.com/discovery_labware/products/display_product.php?keyID=230
16. Barker, L., Method of production and control of a commercial tissue culture surface. *Journal of Tissue Culture Methods* **1994,** 16.
17. Curtis, A. S. G.; Forrester, J. V.; McInnes, C.; Lawrie, F., Adhesion of cells to polystyrene surfaces. *Journal of Cell Biology* **1983,** 97, (5), 1500-1506.
18. Fletcher, M.; Marshall, K. C., Bubble contact-angle method for evaluating substratum interfacial characteristics and its relevance to bacterial attachment. *Applied and Environmental Microbiology* **1982,** 44, (1), 184-192.
19. Englander, T.; Wiegel, D.; Naji, L.; Arnold, K., Dehydration of glass surfaces studied by contact angle measurements. *Journal of Colloid and Interface Science* **1996,** 179, (2), 635-636.
20. Irwin, E. F.; Ho, J. E.; Kane, S. R.; Healy, K. E., Analysis of interpenetrating polymer networks via quartz crystal microbalance with dissipation monitoring. *Langmuir* **2005,** 21, (12), 5529-5536.
21. Munro, J. C.; Frank, C. W., Polyacrylamide adsorption from aqueous solutions on gold and silver surfaces monitored by the quartz crystal microbalance. *Macromolecules* **2004,** 37, (3), 925-938.

22. Foose, L. L.; Blanch, H. W.; Radke, C. J., Immobilized protein films for assessing surface proteolysis kinetics. *J Biotechnol* **2007,** 132, (1), 32-7.
23. Brandrup; Immergut, *Polymer Handbook*. 2nd ed.; John Wiley & Sons: 1975.
24. Lockwood, N. A.; Mohr, J. C.; Ji, L.; Murphy, C. J.; Palecek, S. R.; de Pablo, J. J.; Abbott, N. L., Thermotropic liquid crystals as substrates for imaging the reorganization of matrigel by human embryonic stem cells. *Advanced Functional Materials* **2006,** 16, (5), 618-624.
25. Foose, L. L.; W. Blanch, H.; J. Radke, C., Kinetics of Adsorption and Proteolytic Cleavage of a Multilayer Ovalbumin Film by Subtilisin Carlsberg. *Langmuir* **2008,** 24, (14), 7388-7393.
26. Yi Wei Zhang, J. D., R. Scott Thies, Oligodendrocyte Progenitor Cells Derived from Human Embryonic Stem Cells Express Neurotrophic Factors. *Stem Cells and Development* **2006,** 15, (6), 943-952.
27. Balamurugan, S.; Ista, L. K.; Yan, J.; Lopez, G. P.; Fick, J.; Himmelhaus, M.; Grunze, M., Reversible protein adsorption and bioadhesion on monolayers terminated with mixtures of oligo(ethylene glycol) and methyl groups. *J Am Chem Soc* **2005,** 127, (42), 14548-9.
28. Sauerbrey, G., Verwendung Von Schwingquarzen Zur Wagung Dunner Schichten Und Zur Mikrowagung. *Zeitschrift Fur Physik* **1959,** 155, (2), 206-222.
29. Hook, F.; Rodahl, M.; Kasemo, B.; Brzezinski, P., Structural changes in hemoglobin during adsorption to solid surfaces: Effects of pH, ionic strength, and ligand binding. *Proceedings of the National Academy of Sciences of the United States of America* **1998,** 95, (21), 12271-12276.
30. Voinova, M. V.; Rodahl, M.; Jonson, M.; Kasemo, B., Viscoelastic acoustic response of layered polymer films at fluid-solid interfaces: Continuum mechanics approach. *Physica Scripta* **1999,** 59, (5), 391-396.
31. Fang, F.; Satulovsky, J.; Szleifer, I., Kinetics of protein adsorption and desorption on surfaces with grafted polymers. *Biophysical Journal* **2005,** 89, (3), 1516-1533.
32. Fredrik Hook, B. K., Variations in Coupled Water, Viscoelastic Properties, and Film Thickness of a Mefp-1 Protein
Film during Adsorption and Cross-Linking: A Quartz Crystal Microbalance with Dissipation
Monitoring, Ellipsometry, and Surface Plasmon Resonance Study *Analytical Chemistry* **2001,** 73, 5796-5804.
33. Hansen, K. C.; Kiemele, L.; Maller, O.; O'Brien, J.; Shankar, A.; Fornetti, J.; Schedin, P., An In-solution Ultrasonication-assisted Digestion Method for Improved Extracellular Matrix Proteome Coverage. *Molecular & Cellular Proteomics* **2009,** 8, (7), 1648-1657.
34. McBeath, R.; Pirone, D. M.; Nelson, C. M.; Bhadriraju, K.; Chen, C. S., Cell shape, cytoskeletal tension, and RhoA regulate stem cell lineage commitment. *Developmental Cell* **2004,** 6, (4), 483-495.
35. Bhadriraju, K.; Yang, M.; Ruiz, S. A.; Pirone, D.; Tan, J.; Chen, C. S., Activation of ROCK by RhoA is regulated by cell adhesion, shape, and cytoskeletal tension. *Experimental Cell Research* **2007,** 313, 3616-3623.

36. Maheshwari, G.; Brown, G.; Lauffenburger, D. A.; Wells, A.; Griffith, L. G., Cell adhesion and motility depend on nanoscale RGD clustering. *Journal of Cell Science* **2000,** 113, (10), 1677-1686.
37. Elbert, D. L.; Hubbell, J. A., Conjugate addition reactions combined with free-radical cross-linking for the design of materials for tissue engineering. *Biomacromolecules* **2001,** 2, (2), 430-441.
38. Arnold, M.; Cavalcanti-Adam, E. A.; Glass, R.; Blummel, J.; Eck, W.; Kantlehner, M.; Kessler, H.; Spatz, J. P., Activation of integrin function by nanopatterned adhesive interfaces. *Chemphyschem* **2004,** 5, (3), 383-388.
39. Discher, D. E.; Janmey, P.; Wang, Y. L., Tissue cells feel and respond to the stiffness of their substrate. *Science* **2005,** 310, (5751), 1139-1143.
40. Flanagan, L. A.; Ju, Y. E.; Marg, B.; Osterfield, M.; Janmey, P. A., Neurite branching on deformable substrates. *Neuroreport* **2002,** 13, (18), 2411-5.
41. Pelham, R. J.; Wang, Y. L., Cell locomotion and focal adhesions are regulated by substrate flexibility. *Proceedings of the National Academy of Sciences of the United States of America* **1997,** 94, (25), 13661-13665.
42. Paszek, M. J.; Zahir, N.; Johnson, K. R.; Lakins, J. N.; Rozenberg, G. I.; Gefen, A.; Reinhart-King, C. A.; Margulies, S. S.; Dembo, M.; Boettiger, D.; Hammer, D. A.; Weaver, V. M., Tensional homeostasis and the malignant phenotype. *Cancer Cell* **2005,** 8, (3), 241-254.
43. McDaniel, D. P.; Shaw, G. A.; Elliott, J. T.; Bhadriraju, K.; Meuse, C.; Chung, K. H.; Plant, A. L., The stiffness of collagen fibrils influences vascular smooth muscle cell phenotype. *Biophysical Journal* **2007,** 92, (5), 1759-1769.
44. Thompson, M. T.; Berg, M. C.; Tobias, I. S.; Rubner, M. F.; Van Vliet, K. J., Tuning compliance of nanoscale polyelectrolyte multilayers to modulate cell adhesion. *Biomaterials* **2005,** 26, (34), 6836-6845.
45. Boontheekul, T.; Hill, E. E.; Kong, H. J.; Mooney, D. J., Regulating myoblast phenotype through controlled gel stiffness and degradation. *Tissue Engineering* **2007,** 13, (7), 1431-1442.
46. Engler, A.; Bacakova, L.; Newman, C.; Hategan, A.; Griffin, M.; Discher, D., Substrate compliance versus ligand density in cell on gel responses. *Biophysical Journal* **2004,** 86, (1), 388A-388A.
47. Peyton, S. R.; Raub, C. B.; Keschrumrus, V. P.; Putnam, A. J., The use of poly(ethylene glycol) hydrogels to investigate the impact of ECM chemistry and mechanics on smooth muscle cells. *Biomaterials* **2006,** 27, (28), 4881-4893.

Chapter 3

1. Anderson, D. G.; Levenberg, S.; Langer, R., Nanoliter-scale synthesis of arrayed biomaterials and application to human embryonic stem cells. *Nat Biotechnol* **2004,** 22, (7), 863-6.
2. Derda, R.; Li, L.; Orner, B. P.; Lewis, R. L.; Thomson, J. A.; Kiessling, L. L., Defined substrates for human embryonic stem cell growth identified from surface arrays. *ACS Chem Biol* **2007,** 2, (5), 347-55.

3. Li, Y. J.; Chung, E. H.; Rodriguez, R. T.; Firpo, M. T.; Healy, K. E., Hydrogels as artificial matrices for human embryonic stem cell self-renewal. *J Biomed Mater Res A* **2006,** 79, (1), 1-5.
4. Melkoumian, Z.; Weber, J. L.; Weber, D. M.; Fadeev, A. G.; Zhou, Y.; Dolley-Sonneville, P.; Yang, J.; Qiu, L.; Priest, C. A.; Shogbon, C.; Martin, A. W.; Nelson, J.; West, P.; Beltzer, J. P.; Pal, S.; Brandenberger, R., Synthetic peptide-acrylate surfaces for long-term self-renewal and cardiomyocyte differentiation of human embryonic stem cells. *Nat Biotechnol* 28, (6), 606-10.
5. Rodin, S.; Domogatskaya, A.; Strom, S.; Hansson, E. M.; Chien, K. R.; Inzunza, J.; Hovatta, O.; Tryggvason, K., Long-term self-renewal of human pluripotent stem cells on human recombinant laminin-511. *Nat Biotechnol* 28, (6), 611-5.
6. Villa-Diaz, L. G.; Nandivada, H.; Ding, J.; Nogueira-de-Souza, N. C.; Krebsbach, P. H.; O'Shea, K. S.; Lahann, J.; Smith, G. D., Synthetic polymer coatings for long-term growth of human embryonic stem cells. *Nat Biotechnol* 28, (6), 581-3.
7. Chowdhury, F.; Li, Y.; Poh, Y. C.; Yokohama-Tamaki, T.; Wang, N.; Tanaka, T. S., Soft substrates promote homogeneous self-renewal of embryonic stem cells via downregulating cell-matrix tractions. *PLoS One* **2010,** 5, (12), e15655.
8. Keung, A. J.; Kumar, S.; Schaffer, D. V., Presentation Counts: Microenvironmental Regulation of Stem Cells by Biophysical and Material Cues. *Annual Review of Cell and Developmental Biology, Vol 26* **2010,** 26, 533-556.
9. Nemir, S.; West, J. L., Synthetic Materials in the Study of Cell Response to Substrate Rigidity. *Annals of Biomedical Engineering* **2010,** 38, (1), 2-20.
10. Discher, D. E.; Janmey, P.; Wang, Y. L., Tissue cells feel and respond to the stiffness of their substrate. *Science* **2005,** 310, (5751), 1139-1143.
11. Flanagan, L. A.; Ju, Y. E.; Marg, B.; Osterfield, M.; Janmey, P. A., Neurite branching on deformable substrates. *Neuroreport* **2002,** 13, (18), 2411-5.
12. Pelham, R. J.; Wang, Y. L., Cell locomotion and focal adhesions are regulated by substrate flexibility. *Proceedings of the National Academy of Sciences of the United States of America* **1997,** 94, (25), 13661-13665.
13. Paszek, M. J.; Zahir, N.; Johnson, K. R.; Lakins, J. N.; Rozenberg, G. I.; Gefen, A.; Reinhart-King, C. A.; Margulies, S. S.; Dembo, M.; Boettiger, D.; Hammer, D. A.; Weaver, V. M., Tensional homeostasis and the malignant phenotype. *Cancer Cell* **2005,** 8, (3), 241-254.
14. McDaniel, D. P.; Shaw, G. A.; Elliott, J. T.; Bhadriraju, K.; Meuse, C.; Chung, K. H.; Plant, A. L., The stiffness of collagen fibrils influences vascular smooth muscle cell phenotype. *Biophysical Journal* **2007,** 92, (5), 1759-1769.
15. Thompson, M. T.; Berg, M. C.; Tobias, I. S.; Rubner, M. F.; Van Vliet, K. J., Tuning compliance of nanoscale polyelectrolyte multilayers to modulate cell adhesion. *Biomaterials* **2005,** 26, (34), 6836-6845.
16. Boontheekul, T.; Hill, E. E.; Kong, H. J.; Mooney, D. J., Regulating myoblast phenotype through controlled gel stiffness and degradation. *Tissue Engineering* **2007,** 13, (7), 1431-1442.
17. Engler, A.; Bacakova, L.; Newman, C.; Hategan, A.; Griffin, M.; Discher, D., Substrate compliance versus ligand density in cell on gel responses. *Biophysical Journal* **2004,** 86, (1), 388A-388A.

18. Peyton, S. R.; Raub, C. B.; Keschrumrus, V. P.; Putnam, A. J., The use of poly(ethylene glycol) hydrogels to investigate the impact of ECM chemistry and mechanics on smooth muscle cells. *Biomaterials* **2006,** 27, (28), 4881-4893.
19. Saha, K.; Keung, A. J.; Irwin, E. F.; Li, Y.; Little, L.; Schaffer, D. V.; Healy, K. E., Substrate Modulus Directs Neural Stem Cell Behavior. *Biophysical Journal* **2008,** 95, (9), 4426-4438.
20. Engler, A. J.; Sen, S.; Sweeney, H. L.; Discher, D. E., Matrix elasticity directs stem cell lineage specification. *Cell* **2006,** 126, (4), 677-89.
21. Boiani, M.; Scholer, H. R., Regulatory networks in embryo-derived pluripotent stem cells. *Nat Rev Mol Cell Biol* **2005,** 6, (11), 872-84.
22. Mathur, D.; Danford, T. W.; Boyer, L. A.; Young, R. A.; Gifford, D. K.; Jaenisch, R., Analysis of the mouse embryonic stem cell regulatory networks obtained by ChIP-chip and ChIP-PET. *Genome Biol* **2008,** 9, (8), R126.
23. von Dassow, M.; Davidson, L. A., Natural variation in embryo mechanics: gastrulation in Xenopus laevis is highly robust to variation in tissue stiffness. *Dev Dyn* **2009,** 238, (1), 2-18.
24. Zhou, J.; Kim, H. Y.; Davidson, L. A., Actomyosin stiffens the vertebrate embryo during crucial stages of elongation and neural tube closure. *Development* **2009,** 136, (4), 677-688.
25. Zhou, J. A.; Kim, H. Y.; Wang, J. H. C.; Davidson, L. A., Macroscopic stiffening of embryonic tissues via microtubules, RhoGEF and the assembly of contractile bundles of actomyosin. *Development* **2010,** 137, (16), 2785-2794.
26. Zaman, M. H.; Trapani, L. M.; Siemeski, A.; MacKellar, D.; Gong, H. Y.; Kamm, R. D.; Wells, A.; Lauffenburger, D. A.; Matsudaira, P., Migration of tumor cells in 3D matrices is governed by matrix stiffness along with cell-matrix adhesion and proteolysis. *Proceedings of the National Academy of Sciences of the United States of America* **2006,** 103, (29), 10889-10894.
27. Semler, E. J.; Ranucci, C. S.; Moghe, P. V., Mechanochemical manipulation of hepatocyte aggregation can selectively induce or repress liver-specific function. *Biotechnology and Bioengineering* **2000,** 69, (4), 359-369.
28. Alcaraz, J.; Xu, R.; Mori, H.; Nelson, C. M.; Mroue, R.; Spencer, V. A.; Brownfield, D.; Radisky, D. C.; Bustamante, C.; Bissell, M. J., Laminin and biomimetic extracellular elasticity enhance functional differentiation in mammary epithelia. *Embo Journal* **2008,** 27, (21), 2829-2838.
29. Reed, J.; Walczak, W. J.; Petzold, O. N.; Gimzewski, J. K., In Situ Mechanical Interferometry of Matrigel Films. *Langmuir* **2009,** 25, (1), 36-39.
30. Soofi, S. S.; Last, J. A.; Liliensiek, S. J.; Nealey, P. F.; Murphy, C. J., The elastic modulus of Matrigel (TM) as determined by atomic force microscopy. *Journal of Structural Biology* **2009,** 167, (3), 216-219.
31. Peerani, R.; Rao, B. M.; Bauwens, C.; Yin, T.; Wood, G. A.; Nagy, A.; Kumacheva, E.; Zandstra, P. W., Niche-mediated control of human embryonic stem cell self-renewal and differentiation. *Embo Journal* **2007,** 26, (22), 4744-4755.
32. Lee, L. H.; Peerani, R.; Ungrin, M.; Joshi, C.; Kumacheva, E.; Zandstra, P. W., Micropatterning of human embryonic stem cells dissects the mesoderm and endoderm lineages. *Stem Cell Research* **2009,** 2, (2), 155-162.

33. Bauwens, C. L.; Peerani, R.; Niebruegge, S.; Woodhouse, K. A.; Kumacheva, E.; Husain, M.; Zandstra, P. W., Control of human embryonic stem cell colony and aggregate size heterogeneity influences differentiation trajectories. *Stem Cells* **2008,** 26, (9), 2300-2310.
34. Saha, K.; Mei, Y.; Reisterer, C. M.; Pyzocha, N. K.; Yang, J.; Muffat, J.; Davies, M. C.; Alexander, M. R.; Langer, R.; Anderson, D. G.; Jaenisch, R., Surface-engineered substrates for improved human pluripotent stem cell culture under fully defined conditions. *Proceedings of the National Academy of Sciences of the United States of America* **2011,** 108, (46), 18714-18719.
35. Ruiz, S. A.; Chen, C. S., Emergence of Patterned Stem Cell Differentiation Within Multicellular Structures. *Stem Cells* **2008,** 26, (11), 2921-2927.
36. Wang, N.; Ostuni, E.; Whitesides, G. M.; Ingber, D. E., Micropatterning tractional forces in living cells. *Cell Motility and the Cytoskeleton* **2002,** 52, (2), 97-106.
37. Irwin, E. E.; Gupta, R.; Dashti, D. C.; Healy, K. E., Engineered polymer-media interfaces for the long-term self-renewal of human embryonic stem cells. *Biomaterials* **2011,** 32, (29), 6912-6919.
38. Engler, A. J.; Griffin, M. A.; Sen, S.; Bonnetnann, C. G.; Sweeney, H. L.; Discher, D. E., Myotubes differentiate optimally on substrates with tissue-like stiffness: pathological implications for soft or stiff microenvironments. *Journal of Cell Biology* **2004,** 166, (6), 877-887.
39. Hahn, M. S.; Taite, L. J.; Moon, J. J.; Rowland, M. C.; Ruffino, K. A.; West, J. L., Photolithographic patterning of polyethylene glycol hydrogels. *Biomaterials* **2006,** 27, (12), 2519-2524.
40. Lutolf, M. P.; Doyonnas, R.; Havenstrite, K.; Koleckar, K.; Blau, H. M., Perturbation of single hematopoietic stem cell fates in artificial niches. *Integrative Biology* **2009,** 1, (1), 59-69.
41. Harris, A. K.; Wild, P.; Stopak, D., Silicone rubber substrata: a new wrinkle in the study of cell locomotion. *Science* **1980,** 208, (4440), 177-9.
42. Lee, J. N.; Jiang, X.; Ryan, D.; Whitesides, G. M., Compatibility of mammalian cells on surfaces of poly(dimethylsiloxane). *Langmuir* **2004,** 20, (26), 11684-11691.
43. Bordenave, L.; Bareille, R.; Lefebvre, F.; Caix, J.; Baquey, C., Cytocompatibility study of NHLBI primary reference materials using human endothelial cells. *J Biomater Sci Polym Ed* **1992,** 3, (6), 509-16.
44. Sherman, M. A.; Kennedy, J. P.; Ely, D. L.; Smith, D., Novel polyisobutylene/polydimethylsiloxane bicomponent networks: III. Tissue compatibility. *J Biomater Sci Polym Ed* **1999,** 10, (3), 259-69.
45. Park, J. H.; Park, K. D.; Bae, Y. H., PDMS-based polyurethanes with MPEG grafts: synthesis, characterization and platelet adhesion study. *Biomaterials* **1999,** 20, (10), 943-53.
46. Ertel, S. I.; Ratner, B. D.; Kaul, A.; Schway, M. B.; Horbett, T. A., In-Vitro Study of the Intrinsic Toxicity of Synthetic Surfaces to Cells. *Journal of Biomedical Materials Research* **1994,** 28, (6), 667-675.
47. van Kooten, T. G.; Whitesides, J. F.; von Recum, A., Influence of silicone (PDMS) surface texture on human skin fibroblast proliferation as determined by cell cycle analysis. *J Biomed Mater Res* **1998,** 43, (1), 1-14.

48. Interrante, L. V.; Shen, Q. H.; Li, J., Poly(dimethylsilylenemethylene-co-dimethylsiloxane): A regularly alternating copolymer of poly(dimethylsiloxane) and poly(dimethylsilylenemethylene). *Macromolecules* **2001,** 34, (6), 1545-1547.
49. Dahrouch, M.; Schmidt, A.; Leemans, L.; Linssen, H.; Gotz, H., Synthesis and properties of poly(butylene terephthalate)-poly(ethylene oxide)-poly(dimethylsiloxane) block copolymers. *Macromolecular Symposia* **2003,** 199, 147-162.
50. Sia, S. K.; Whitesides, G. M., Microfluidic devices fabricated in poly(dimethylsiloxane) for biological studies. *Electrophoresis* **2003,** 24, (21), 3563-3576.
51. Ostuni, E.; Kane, R.; Chen, C. S.; Ingber, D. E.; Whitesides, G. M., Patterning mammalian cells using elastomeric membranes. *Langmuir* **2000,** 16, (20), 7811-7819.
52. Ostuni, E.; Chen, C. S.; Ingber, D. E.; Whitesides, G. M., Selective deposition of proteins and cells in arrays of microwells. *Langmuir* **2001,** 17, (9), 2828-2834.
53. Folch, A.; Jo, B. H.; Hurtado, O.; Beebe, D. J.; Toner, M., Microfabricated elastomeric stencils for micropatterning cell cultures. *Journal of Biomedical Materials Research* **2000,** 52, (2), 346-353.
54. Folch, A.; Toner, M., Microengineering of cellular interactions. *Annual Review of Biomedical Engineering* **2000,** 2, 227-+.
55. Ng, J. M.; Gitlin, I.; Stroock, A. D.; Whitesides, G. M., Components for integrated poly(dimethylsiloxane) microfluidic systems. *Electrophoresis* **2002,** 23, (20), 3461-73.
56. McDonald, J. C.; Whitesides, G. M., Poly(dimethylsiloxane) as a material for fabricating microfluidic devices. *Accounts of Chemical Research* **2002,** 35, (7), 491-499.
57. Frimat, J. P.; Menne, H.; Michels, A.; Kittel, S.; Kettler, R.; Borgmann, S.; Franzke, J.; West, J., Plasma stencilling methods for cell patterning. *Analytical and Bioanalytical Chemistry* **2009,** 395, (3), 601-609.
58. Paik, I.; Scurr, D. J.; Morris, B.; Hall, G.; Denning, C.; Alexander, M. R.; Shakesheff, K. M.; Dixon, J. E., Rapid micropatterning of cell lines and human pluripotent stem cells on elastomeric membranes. *Biotechnol Bioeng* **2012**.
59. Evans, N. D.; Minelli, C.; Gentleman, E.; LaPointe, V.; Patankar, S. N.; Kallivretaki, M.; Chen, X. Y.; Roberts, C. J.; Stevens, M. M., Substrate Stiffness Affects Early Differentiation Events in Embryonic Stem Cells. *European Cells & Materials* **2009,** 18, 1-14.
60. Domke, J.; Radmacher, M., Measuring the elastic properties of thin polymer films with the atomic force microscope. *Langmuir* **1998,** 14, (12), 3320-3325.
61. Engler, A. J.; Richert, L.; Wong, J. Y.; Picart, C.; Discher, D. E., Surface probe measurements of the elasticity of sectioned tissue, thin gels and polyelectrolyte multilayer films: Correlations between substrate stiffness and cell adhesion. *Surface Science* **2004,** 570, (1-2), 142-154.
62. Irwin, E. F.; Saha, K.; Rosenbluth, M.; Gamble, L. J.; Castner, D. G.; Healy, K. E., Modulus-dependent macrophage adhesion and behavior. *Journal of Biomaterials Science-Polymer Edition* **2008,** 19, (10), 1363-1382.

63. Saha, K.; Kim, J.; Irwin, E.; Yoon, J.; Momin, F.; Trujillo, V.; Schaffer, D. V.; Healy, K. E.; Hayward, R. C., Surface Creasing Instability of Soft Polyacrylamide Cell Culture Substrates. *Biophysical Journal* **2010,** 99, (12), L94-L96.
64. Feng, X. D.; Guo, X. Q.; Qiu, K. Y., Study of the Initiation Mechanism of the Vinyl Polymerization with the System Persulfate N,N,N',N'-Tetramethylethylenediamine. *Makromolekulare Chemie-Macromolecular Chemistry and Physics* **1988,** 189, (1), 77-83.
65. http://www.siumed.edu/~bbartholomew/images/chapter6/F06-19.jpg (December 2012),
66. Maloney, J. M.; Walton, E. B.; Bruce, C. M.; Van Vliet, K. J., Influence of finite thickness and stiffness on cellular adhesion-induced deformation of compliant substrata. *Physical Review E* **2008,** 78, (4), -.
67. Boudou, T.; Ohayon, J.; Picart, C.; Tracqui, P., An extended relationship for the characterization of Young's modulus and Poisson's ratio of tunable polyacrylamide gels. *Biorheology* **2006,** 43, (6), 721-728.
68. Fujimoto, K.; Tadokoro, H.; Ueda, Y.; Ikada, Y., Polyurethane Surface Modification by Graft-Polymerization of Acrylamide for Reduced Protein Adsorption and Platelet-Adhesion. *Biomaterials* **1993,** 14, (6), 442-448.
69. Xiao, D. Q.; Zhang, H.; Wirth, M., Chemical modification of the surface of poly(dimethylsiloxane) by atom-transfer radical polymerization of acrylamide. *Langmuir* **2002,** 18, (25), 9971-9976.
70. Cringus-Fundeanu, I.; Luijten, J.; van der Mei, H. C.; Busscher, H. J.; Schouten, A. J., Synthesis and characterization of surface-grafted polyacrylamide brushes and their inhibition of microbial adhesion. *Langmuir* **2007,** 23, (9), 5120-5126.
71. Liu, Q. S.; Singh, A.; Lalani, R.; Liu, L. Y., Ultralow Fouling Polyacrylamide on Gold Surfaces via Surface-Initiated Atom Transfer Radical Polymerization. *Biomacromolecules* **2012,** 13, (4), 1086-1092.
72. Ghosh, K.; Pan, Z.; Guan, E.; Ge, S. R.; Liu, Y. J.; Nakamura, T.; Ren, X. D.; Rafailovich, M.; Clark, R. A. F., Cell adaptation to a physiologically relevant ECM mimic with different viscoelastic properties. *Biomaterials* **2007,** 28, (4), 671-679.
73. Gunn, J. W.; Turner, S. D.; Mann, B. K., Adhesive and mechanical properties of hydrogels influence neurite extension. *Journal of Biomedical Materials Research Part A* **2005,** 72A, (1), 91-97.
74. Schwendel, D.; Dahint, R.; Herrwerth, S.; Schloerholz, M.; Eck, W.; Grunze, M., Temperature dependence of the protein resistance of poly- and oligo(ethylene glycol)-terminated alkanethiolate monolayers. *Langmuir* **2001,** 17, (19), 5717-5720.
75. Li, L. Y.; Chen, S. F.; Zheng, J.; Ratner, B. D.; Jiang, S. Y., Protein adsorption on oligo(ethylene glycol)-terminated alkanethiolate self-assembled monolayers: The molecular basis for nonfouling behavior. *Journal of Physical Chemistry B* **2005,** 109, (7), 2934-2941.
76. Cao, L.; Sukavaneshvar, S.; Ratner, B. D.; Horbett, T. A., Glow discharge plasma treatment of polyethylene tubing with tetraglyme results in ultralow fibrinogen adsorption and greatly reduced platelet adhesion. *Journal of Biomedical Materials Research Part A* **2006,** 79A, (4), 788-803.
77. Zhang, M. Q.; Desai, T.; Ferrari, M., Proteins and cells on PEG immobilized silicon surfaces. *Biomaterials* **1998,** 19, (10), 953-960.

78. Branch, D. W.; Wheeler, B. C.; Brewer, G. J.; Leckband, D. E., Long-term stability of grafted polyethylene glycol surfaces for use with microstamped substrates in neuronal cell culture. *Biomaterials* **2001,** 22, (10), 1035-1047.
79. Herrwerth, S.; Eck, W.; Reinhardt, S.; Grunze, M., Factors that determine the protein resistance of oligoether self-assembled monolayers - Internal hydrophilicity, terminal hydrophilicity, and lateral packing density. *Journal of the American Chemical Society* **2003,** 125, (31), 9359-9366.
80. Harder, P.; Grunze, M.; Dahint, R.; Whitesides, G. M.; Laibinis, P. E., Molecular conformation in oligo(ethylene glycol)-terminated self-assembled monolayers on gold and silver surfaces determines their ability to resist protein adsorption. *Journal of Physical Chemistry B* **1998,** 102, (2), 426-436.
81. Sofia, S. J.; Premnath, V.; Merrill, E. W., Poly(ethylene oxide) grafted to silicon surfaces: Grafting density and protein adsorption. *Macromolecules* **1998,** 31, (15), 5059-5070.
82. Herold, D. A.; Keil, K.; Bruns, D. E., Oxidation of Polyethylene Glycols by Alcohol-Dehydrogenase. *Biochemical Pharmacology* **1989,** 38, (1), 73-76.
83. Sharma, S.; Johnson, R. W.; Desai, T. A., Evaluation of the stability of nonfouling ultrathin poly(ethylene glycol) films for silicon-based microdevices. *Langmuir* **2004,** 20, (2), 348-356.
84. ThermoScientific Light sources and conditions for photoactivation of aryl azide crosslinking and labeling reagents. http://www.piercenet.com/files/TR0011-Photoactivate-aryl-azides.pdf (December 2012),
85. Rowlands, A. S.; George, P. A.; Cooper-White, J. J., Directing osteogenic and myogenic differentiation of MSCs: interplay of stiffness and adhesive ligand presentation. *American Journal of Physiology-Cell Physiology* **2008,** 295, (4), C1037-C1044.
86. J.R., T.; A.J., E., Preperation of Hydrogel Substrates with Tunable Mechanical Properties. In *Current Protocols in Cell Biology*, Wiley: 2010; pp 1-16.
87. Gelse, K.; Poschl, E.; Aigner, T., Collagens - structure, function, and biosynthesis. *Advanced Drug Delivery Reviews* **2003,** 55, (12), 1531-1546.
88. Richard-Blum, S.; Ruggiero, F.; van der Rest, M., The Collagen Superfamily. In *Topics in Current Chemistry*, 2005; Vol. 247, pp 35-84.
89. Humphries, J. D.; Byron, A.; Humphries, M. J., Integrin ligands at a glance. *Journal of Cell Science* **2006,** 119, (19), 3901-3903.
90. Hynes, R. O., Integrins: Bidirectional, allosteric signaling machines. *Cell* **2002,** 110, (6), 673-687.
91. Ruoslahti, E.; Pierschbacher, M. D., New Perspectives in Cell-Adhesion - Rgd and Integrins. *Science* **1987,** 238, (4826), 491-497.
92. Hayman, E. G.; Pierschbacher, M. D.; Ruoslahti, E., Detachment of Cells from Culture Substrate by Soluble Fibronectin Peptides. *Journal of Cell Biology* **1985,** 100, (6), 1948-1954.
93. Trappmann, B.; Gautrot, J. E.; Connelly, J. T.; Strange, D. G. T.; Li, Y.; Oyen, M. L.; Stuart, M. A. C.; Boehm, H.; Li, B. J.; Vogel, V.; Spatz, J. P.; Watt, F. M.; Huck, W. T. S., Extracellular-matrix tethering regulates stem-cell fate. *Nature Materials* **2012,** 11, (7), 642-649.

94. Braam, S. R.; Zeinstra, L.; Litjens, S.; Ward-van Oostwaard, D.; van den Brink, S.; van Laake, L.; Lebrin, F.; Kats, P.; Hochstenbach, R.; Passier, R.; Sonnenberg, A.; Mummery, C. L., Recombinant vitronectin is a functionally defined substrate that supports human embryonic stem cell self-renewal via alphavbeta5 integrin. *Stem Cells* **2008,** 26, (9), 2257-65.
95. Hautanen, A.; Gailit, J.; Mann, D. M.; Ruoslahti, E., Effects of Modifications of the Rgd Sequence and Its Context on Recognition by the Fibronectin Receptor. *Journal of Biological Chemistry* **1989,** 264, (3), 1437-1442.
96. Sniadecki, N. J.; Chen, C. S., Microfabricated Silicone Elastomeric Post Arrays for Measuring Traction Forces of Adherent Cells. In *Methods in Cell Biology - Cell Mechanics*, DE, W. Y. a. D., Ed. Elsevier: New York, 2007; Vol. 83, pp 313-328.
97. http://www.microchem.com/pdf/SU8_50-100.pdf
98. Quist, A. P.; Pavlovic, E.; Oscarsson, S., Recent advances in microcontact printing. *Analytical and Bioanalytical Chemistry* **2005,** 381, (3), 591-600.
99. Hui, C. Y.; Jagota, A.; Lin, Y. Y.; Kramer, E. J., Constraints on microcontact printing imposed by stamp deformation. *Langmuir* **2002,** 18, (4), 1394-1407.
100. Beaulleu, I.; Geissler, M.; Mauzeroll, J., Oxygen Plasma Treatment of Polystyrene and Zeonor: Substrates for Adhesion of Patterned Cells. *Langmuir* **2009,** 25, (12), 7169-7176.
101. Vesel, A.; Mozetic, M.; Jaganjac, M.; Milkovic, L.; Cipak, A.; Zarkovic, N., Biocompatibility of oxygen-plasma-treated polystyrene substrates. *European Physical Journal-Applied Physics* **2011,** 56, (2).
102. Geisthardt, D.; Kruppa, J., Polyacrylamide-Gel Electrophoresis - Reaction of Acrylamide at Alkaline Ph with Buffer Components and Proteins. *Analytical Biochemistry* **1987,** 160, (1), 184-191.
103. Caglio, S.; Righetti, P. G., On the Ph-Dependence of Polymerization Efficiency, as Investigated by Capillary Zone Electrophoresis. *Electrophoresis* **1993,** 14, (5-6), 554-558.
104. Lin, H. R., Solution polymerization of acrylamide using potassium persulfate as an initiator: kinetic studies, temperature and pH dependence. *European Polymer Journal* **2001,** 37, (7), 1507-1510.
105. Beningo, K. A.; Wang, Y. L., Double-hydrogel substrates as model system for 3D cell culture. In *Adhesion Protein Protocols*, 2 ed.; Coutts, A., Ed. Humana Press: Totowa, NJ, 2007.
106. Li, B.; Lin, M.; Tang, Y.; Wang, B.; Wang, J. H. C., A novel functional assessment of the differentiation of micropatterned muscle cells. *Journal of Biomechanics* **2008,** 41, (16), 3349-3353.
107. Ulrich, T. A.; Pardo, E. M. D.; Kumar, S., The Mechanical Rigidity of the Extracellular Matrix Regulates the Structure, Motility, and Proliferation of Glioma Cells. *Cancer Research* **2009,** 69, (10), 4167-4174.
108. Semler, E. J.; Lancin, P. A.; Dasgupta, A.; Moghe, P. V., Engineering hepatocellular morphogenesis and function via ligand-presenting hydrogels with graded mechanical compliance. *Biotechnology and Bioengineering* **2005,** 89, (3), 296-307.

109. Gray, D. S.; Tien, J.; Chen, C. S., Repositioning of cells by mechanotaxis on surfaces with micropatterned Young's modulus. *Journal of Biomedical Materials Research Part A* **2003,** 66A, (3), 605-614.
110. Beningo, K. A.; Lo, C. M.; Wang, Y. L., Flexible polyacrylamide substrata for the analysis of mechanical interactions at cell-substratum adhesions. *Methods in Cell-Matrix Adhesion* **2002,** 69, 325-339.
111. Malinin, T. I.; Perry, V. P., Toxicity of Dimethyl Sulfoxide on Hela Cells. *Cryobiology* **1967,** 4, (2), 90-&.
112. Dinsmore, J.; Ratliff, J.; Deacon, T.; Pakzaban, P.; Jacoby, D.; Galpern, W.; Isacson, O., Embryonic stem cells differentiated in vitro as a novel source of cells for transplantation. *Cell Transplantation* **1996,** 5, (2), 131-143.
113. Adler, S.; Pellizzer, C.; Paparella, M.; Hartung, T.; Bremer, S., The effects of solvents on embryonic stem cell differentiation. *Toxicology in Vitro* **2006,** 20, (3), 265-271.
114. Biebuyck, H. A.; Larsen, N. B.; Delamarche, E.; Michel, B., Lithography beyond light: Microcontact printing with monolayer resists. *Ibm Journal of Research and Development* **1997,** 41, (1-2), 159-170.
115. Delamarche, E.; Schmid, H.; Michel, B.; Biebuyck, H., Stability of molded polydimethylsiloxane microstructures. *Advanced Materials* **1997,** 9, (9), 741-746.
116. Schmid, H.; Michel, B., Siloxane polymers for high-resolution, high-accuracy soft lithography. *Macromolecules* **2000,** 33, (8), 3042-3049.
117. Tan, J. L.; Tien, J.; Chen, C. S., Microcontact printing of proteins on mixed self-assembled monolayers. *Langmuir* **2002,** 18, (2), 519-523.
118. Kim, H.; Doh, J.; Irvine, D. J.; Cohen, R. E.; Hammond, P. T., Large area two-dimensional B cell arrays for sensing and cell-sorting applications. *Biomacromolecules* **2004,** 5, (3), 822-827.
119. Berg, M. C.; Yang, S. Y.; Hammond, P. T.; Rubner, M. F., Controlling mammalian cell interactions on patterned polyelectrolyte multilayer surfaces. *Langmuir* **2004,** 20, (4), 1362-1368.
120. Yang, Z. P.; Belu, A. M.; Liebmann-Vinson, A.; Sugg, H.; Chilkoti, A., Molecular imaging of a micropatterned biological ligand on an activated polymer surface. *Langmuir* **2000,** 16, (19), 7482-7492.
121. Ma, H. W.; Hyun, J.; Zhang, Z. P.; Beebe, T. P.; Chilkoti, A., Fabrication of biofunctionalized quasi-three-dimensional microstructures of a nonfouling comb polymer using soft lithography. *Advanced Functional Materials* **2005,** 15, (4), 529-540.
122. Park, J. S.; Chu, J. S.; Tsou, A. D.; Diop, R.; Tang, Z.; Wang, A.; Li, S., The effect of matrix stiffness on the differentiation of mesenchymal stem cells in response to TGF-beta. *Biomaterials* **2011,** 32, (16), 3921-30.
123. Huebsch, N.; Gilbert, M.; Healy, K. E., Analysis of sterilization protocols for peptide-modified hydrogels. *J Biomed Mater Res B Appl Biomater* **2005,** 74, (1), 440-7.
124. Cohen, S.; Samadikuchaksaraei, A.; Polak, J. M.; Bishop, A. E., Antibiotics reduce the growth rate and differentiation of embryonic stem cell cultures. *Tissue Eng* **2006,** 12, (7), 2025-30.

125. Caulfield, M. J.; Qiao, G. G.; Solomon, D. H., Some aspects of the properties and degradation of polyacrylamides. *Chem Rev* **2002,** 102, (9), 3067-84.
126. Wu, S.; Shanks, R. A., Solubility Study of Polyacrylamide in Polar Solvents. *Journal of Applied Polymer Science* **2004,** 93, 1493-1499.
127. Andrade, J. D.; Hlady, V.; Jeon, S. I., Poly(ethylene oxide) and protein resistance - Principles, problems, and possibilities. In *Hydrophilic Polymers: Performance with Environmental Acceptance*, Amer Chemical Soc: Washington, 1996; Vol. 248, pp 51-59.
128. Jeon, S. I.; Lee, J. H.; Andrade, J. D.; Degennes, P. G., PROTEIN SURFACE INTERACTIONS IN THE PRESENCE OF POLYETHYLENE OXIDE .1. SIMPLIFIED THEORY. *Journal of Colloid and Interface Science* **1991,** 142, (1), 149-158.
129. Jeon, S. I.; Andrade, J. D., PROTEIN SURFACE INTERACTIONS IN THE PRESENCE OF POLYETHYLENE OXIDE .2. EFFECT OF PROTEIN SIZE. *Journal of Colloid and Interface Science* **1991,** 142, (1), 159-166.
130. Osterberg, E.; Bergstrom, K.; Holmberg, K.; Riggs, J. A.; Vanalstine, J. M.; Schuman, T. P.; Burns, N. L.; Harris, J. M., Comparison of Polysaccharide and Poly(Ethylene Glycol) Coatings for Reduction of Protein Adsorption on Polystyrene Surfaces. *Colloids and Surfaces a-Physicochemical and Engineering Aspects* **1993,** 77, (2), 159-169.
131. Prime, K. L.; Whitesides, G. M., Adsorption of Proteins onto Surfaces Containing End-Attached Oligo(Ethylene Oxide) - a Model System Using Self-Assembled Monolayers. *Journal of the American Chemical Society* **1993,** 115, (23), 10714-10721.
132. Prime, K. L.; Whitesides, G. M., Self-Assembled Organic Monolayers - Model Systems for Studying Adsorption of Proteins at Surfaces. *Science* **1991,** 252, (5009), 1164-1167.
133. Merrill, E. W.; Salzman, E. W.; Sadacosta, V.; Brierrussell, D.; Dincer, A.; Pape, P.; Lindon, J. N., Platelet Retention on Polymer Surfaces - Some Invitro Experiments. *Advances in Chemistry Series* **1982**, (199), 35-42.
134. Harbers, G. M.; Gamble, L. J.; Irwin, E. F.; Castner, D. G.; Healy, K. E., Development and characterization of a high-throughput system for assessing cell-surface receptor-ligand engagement. *Langmuir* **2005,** 21, (18), 8374-8384.
135. Hommel, H.; Halli, A.; Touhami, A.; Legrand, A. P., From isolated coils to brushes of poly(ethylene oxide) grafted on silica: A spin-labelling study. *Colloids and Surfaces a-Physicochemical and Engineering Aspects* **1996,** 111, (1-2), 67-74.
136. Degennes, P. G., Conformations of Polymers Attached to an Interface. *Macromolecules* **1980,** 13, (5), 1069-1075.
137. Szleifer, I., Protein adsorption on surfaces with grafted polymers: A theoretical approach. *Biophysical Journal* **1997,** 72, (2), 595-612.
138. Milner, S. T., Polymer Brushes. *Science* **1991,** 251, (4996), 905-914.
139. Devanand, K.; Selser, J. C., Asymptotic-Behavior and Long-Range Interactions in Aqueous-Solutions of Poly(Ethylene Oxide). *Macromolecules* **1991,** 24, (22), 5943-5947.
140. Pierschbacher, M. D.; Ruoslahti, E., Cell Attachment Activity of Fibronectin Can Be Duplicated by Small Synthetic Fragments of the Molecule. *Nature* **1984,** 309, (5963), 30-33.

141. Sato, M.; Garsky, V.; Majeska, R. J.; Einhorn, T. A.; Murray, J.; Tashjian, A. H.; Gould, R. J., Structure-Activity Studies of the S-Echistatin Inhibition of Bone-Resorption. *Journal of Bone and Mineral Research* **1994,** 9, (9), 1441-1449.
142. Maeda, T.; Hashino, K.; Oyama, R.; Titani, K.; Sekiguchi, K., Artificial Cell Adhesive Proteins Engineered by Grafting the Arg-Gly-Asp Cell Recognition Signal - Factors Modulating the Cell Adhesive Activity of the Grafted Signal. *Journal of Biochemistry* **1991,** 110, (3), 381-387.
143. Horton, M. A.; Dorey, E. L.; Nesbitt, S. A.; Samanen, J.; Ali, F. E.; Stadel, J. M.; Nichols, A.; Greig, R.; Helfrich, M. H., Modulation of Vitronectin Receptor-Mediated Osteoclast Adhesion by Arg-Gly-Asp Peptide Analogs - a Structure-Function Analysis. *Journal of Bone and Mineral Research* **1993,** 8, (2), 239-247.
144. Rezania, A.; Healy, K. E., Biomimetic peptide surfaces that regulate adhesion, spreading, cytoskeletal organization, and mineralization of the matrix deposited by osteoblast-like cells. *Biotechnology Progress* **1999,** 15, (1), 19-32.
145. Rezania, A.; Healy, K. E., Integrin subunits responsible for adhesion of human osteoblast-like cells to biomimetic peptide surfaces. *Journal of Orthopaedic Research* **1999,** 17, (4), 615-623.
146. Rezania, A.; Johnson, R.; Lefkow, A. R.; Healy, K. E., Bioactivation of metal oxide surfaces. 1. Surface characterization and cell response. *Langmuir* **1999,** 15, (20), 6931-6939.
147. Little, L. E.; Dane, K. Y.; Daugherty, P. S.; Healy, K. E.; Schaffer, D. V., Exploiting bacterial peptide display technology to engineer biomaterials for neural stem cell culture. *Biomaterials* **2011,** 32, (6), 1484-1494.
148. Massia, S. P.; Hubbell, J. A., An Rgd Spacing of 440nm Is Sufficient for Integrin Alpha-V-Beta-3-Mediated Fibroblast Spreading and 140nm for Focal Contact and Stress Fiber Formation. *Journal of Cell Biology* **1991,** 114, (5), 1089-1100.
149. Drumheller, P. D.; Elbert, D. L.; Hubbell, J. A., Multifunctional Poly(Ethylene Glycol) Semiinterpenetrating Polymer Networks as Highly Selective Adhesive Substrates for Bioadhesive Peptide Grafting. *Biotechnology and Bioengineering* **1994,** 43, (8), 772-780.
150. Bearinger, J. P.; Castner, D. G.; Healy, K. E., Biomolecular modification of p(AAm-co-EG/AA) IPNs supports osteoblast adhesion and phenotypic expression. *Journal of Biomaterials Science-Polymer Edition* **1998,** 9, (7), 629-652.
151. Hubbell, J. A.; Massia, S. P.; Desai, N. P.; Drumheller, P. D., Endothelial Cell-Selective Materials for Tissue Engineering in the Vascular Graft Via a New Receptor. *Bio-Technology* **1991,** 9, (6), 568-572.
152. Brandley, B. K.; Schnaar, R. L., Covalent Attachment of an Arg-Gly-Asp Sequence Peptide to Derivatizable Polyacrylamide Surfaces - Support of Fibroblast Adhesion and Long-Term Growth. *Analytical Biochemistry* **1988,** 172, (1), 270-278.
153. Pollock, J. F.; Ashton, R. S.; Rode, N. A.; Schaffer, D. V.; Healy, K. E., Molecular Characterization of Multivalent Bioconjugates by Size-Exclusion Chromatography with Multiangle Laser Light Scattering. *Bioconjugate Chemistry* 23, (9), 1794-1801.
154. Barber, T. A.; Harbers, G. M.; Park, S.; Gilbert, M.; Healy, K. E., Ligand density characterization of peptide-modified biomaterials. *Biomaterials* **2005,** 26, (34), 6897-6905.

155. Tan, J. L.; Liu, W.; Nelson, C. M.; Raghavan, S.; Chen, C. S., Simple approach to micropattern cells on common culture substrates by tuning substrate wettability. *Tissue Engineering* **2004,** 10, (5-6), 865-872.
156. Deegan, R. D.; Bakajin, O.; Dupont, T. F.; Huber, G.; Nagel, S. R.; Witten, T. A., Capillary flow as the cause of ring stains from dried liquid drops. *Nature* **1997,** 389, (6653), 827-829.
157. Hu, H.; Larson, R. G., Marangoni effect reverses coffee-ring depositions. *Journal of Physical Chemistry B* **2006,** 110, (14), 7090-7094.
158. Desai, R. A.; Khan, M. K.; Gopal, S. B.; Chen, C. S., Subcellular spatial segregation of integrin subtypes by patterned multicomponent surfaces. *Integr Biol (Camb)* 3, (5), 560-7.
159. Larson, R. G. G. L., M.A.; Lim, D.W.; Lahann J. In *Complex Protein Patterns in Drying Droplets*, MRS Proceedings, San Francisco, 2010; San Francisco, 2010.

Chapter 4

1. Chowdhury, F.; Na, S.; Li, D.; Poh, Y. C.; Tanaka, T. S.; Wang, F.; Wang, N., Material properties of the cell dictate stress-induced spreading and differentiation in embryonic stem cells. *Nature Materials* **2010,** 9, (1), 82-88.
2. Poh, Y. C.; Chowdhury, F.; Tanaka, T. S.; Wang, N., Embryonic Stem Cells Do Not Stiffen on Rigid Substrates. *Biophysical Journal* **2010,** 99, (2), L19-L21.
3. Chowdhury, F.; Li, Y. Z.; Poh, Y. C.; Yokohama-Tamaki, T.; Wang, N.; Tanaka, T. S., Soft Substrates Promote Homogeneous Self-Renewal of Embryonic Stem Cells via Downregulating Cell-Matrix Tractions. *Plos One* **2010,** 5, (12).
4. Ginis, I.; Luo, Y. Q.; Miura, T.; Thies, S.; Brandenberger, R.; Gerecht-Nir, S.; Amit, M.; Hoke, A.; Carpenter, M. K.; Itskovitz-Eldor, J.; Rao, M. S., Differences between human and mouse embryonic stem cells. *Developmental Biology* **2004,** 269, (2), 360-380.
5. Rao, M., Conserved and divergent paths that regulate self-renewal in mouse and human embryonic stem cells. *Developmental Biology* **2004,** 275, (2), 269-286.
6. Mathur, D.; Danford, T. W.; Boyer, L. A.; Young, R. A.; Gifford, D. K.; Jaenisch, R., Analysis of the mouse embryonic stem cell regulatory networks obtained by ChIP-chip and ChIP-PET. *Genome Biol* **2008,** 9, (8), R126.
7. Boyer, L. A.; Mathur, D.; Jaenisch, R., Molecular control of pluripotency. *Curr Opin Genet Dev* **2006,** 16, (5), 455-62.
8. Loh, Y. H.; Wu, Q.; Chew, J. L.; Vega, V. B.; Zhang, W. W.; Chen, X.; Bourque, G.; George, J.; Leong, B.; Liu, J.; Wong, K. Y.; Sung, K. W.; Lee, C. W. H.; Zhao, X. D.; Chiu, K. P.; Lipovich, L.; Kuznetsov, V. A.; Robson, P.; Stanton, L. W.; Wei, C. L.; Ruan, Y. J.; Lim, B.; Ng, H. H., The Oct4 and Nanog transcription network regulates pluripotency in mouse embryonic stem cells. *Nature Genetics* **2006,** 38, (4), 431-440.
9. Bibikova, M.; Chudin, E.; Wu, B.; Zhou, L. X.; Garcia, E. W.; Liu, Y.; Shin, S.; Plaia, T. W.; Auerbach, J. M.; Arking, D. E.; Gonzalez, R.; Crook, J.; Davidson, B.; Schulz, T. C.; Robins, A.; Khanna, A.; Sartipy, P.; Hyllner, J.; Vanguri, P.; Savant-Bhonsale, S.; Smith, A. K.; Chakravarti, A.; Maitra, A.; Rao, M.; Barker, D. L.; Loring, J. F.; Fan, J. B.,

Human embryonic stem cells have a unique epigenetic signature. *Genome Research* **2006,** 16, (9), 1075-1083.
10. Collas, P.; Noer, A.; Timoskainen, S., Programming the genome in embryonic and somatic stem cells. *Journal of Cellular and Molecular Medicine* **2007,** 11, (4), 602-620.
11. Zvetkova, I.; Apedaile, A.; Ramsahoye, B.; Mermoud, J. E.; Crompton, L. A.; John, R.; Feil, R.; Brockdorff, N., Global hypomethylation of the genome in XX embryonic stem cells. *Nature Genetics* **2005,** 37, (11), 1274-1279.
12. Daheron, L.; Opitz, S. L.; Zaehres, H.; Lensch, W. M.; Andrews, P. W.; Itskovitz-Eldor, J.; Daley, G. Q., LIF/STAT3 signaling fails to maintain self-renewal of human embryonic stem cells (vol 22, pg 770, 2004). *Stem Cells* **2007,** 25, (12), 3273-3273.
13. Livak, K. J.; Schmittgen, T. D., Analysis of relative gene expression data using real-time quantitative PCR and the 2(T)(-Delta Delta C) method. *Methods* **2001,** 25, (4), 402-408.
14. Schmittgen, T. D.; Livak, K. J., Analyzing real-time PCR data by the comparative C-T method. *Nature Protocols* **2008,** 3, (6), 1101-1108.
15. Bookout, A. L.; Mangelsdorf, D. J., Quantitative real-time PCR protocol for analysis of nuclear receptor signaling pathways. *Nucl Recept Signal* **2003,** 1, e012.
16. Thompson, M. T.; Berg, M. C.; Tobias, I. S.; Rubner, M. F.; Van Vliet, K. J., Tuning compliance of nanoscale polyelectrolyte multilayers to modulate cell adhesion. *Biomaterials* **2005,** 26, (34), 6836-6845.
17. McDaniel, D. P.; Shaw, G. A.; Elliott, J. T.; Bhadriraju, K.; Meuse, C.; Chung, K. H.; Plant, A. L., The stiffness of collagen fibrils influences vascular smooth muscle cell phenotype. *Biophysical Journal* **2007,** 92, (5), 1759-1769.
18. Discher, D. E.; Janmey, P.; Wang, Y. L., Tissue cells feel and respond to the stiffness of their substrate. *Science* **2005,** 310, (5751), 1139-1143.
19. Engler, A.; Bacakova, L.; Newman, C.; Hategan, A.; Griffin, M.; Discher, D., Substrate compliance versus ligand density in cell on gel responses. *Biophysical Journal* **2004,** 86, (1), 388A-388A.
20. Chowdhury, F.; Li, Y.; Poh, Y. C.; Yokohama-Tamaki, T.; Wang, N.; Tanaka, T. S., Soft substrates promote homogeneous self-renewal of embryonic stem cells via downregulating cell-matrix tractions. *PLoS One* **2010,** 5, (12), e15655.
21. Watanabe, K.; Ueno, M.; Kamiya, D.; Nishiyama, A.; Matsumura, M.; Wataya, T.; Takahashi, J. B.; Nishikawa, S.; Nishikawa, S.-i.; Muguruma, K.; Sasai, Y., A ROCK inhibitor permits survival of dissociated human embryonic stem cells. *Nature Biotechnology* **2007,** 25, (6), 681-686.
22. Hayashi, K.; Lopes, S. M. C. d. S.; Tang, F.; Surani, M. A., Dynamic Equilibrium and Heterogeneity of Mouse Pluripotent Stem Cells with Distinct Functional and Epigenetic States. *Cell Stem Cell* **2008,** 3, (4), 391-401.
23. Singh, A. M.; Hamazaki, T.; Hankowski, K. E.; Terada, N., A heterogeneous expression pattern for nanog in embryonic stem cells. *Stem Cells* **2007,** 25, (10), 2534-2542.
24. Toyooka, Y.; Shimosato, D.; Murakami, K.; Takahashi, K.; Niwa, H., Identification and characterization of subpopulations in undifferentiated ES cell culture. *Development* **2008,** 135, (5), 909-918.

25. Carter, M. G.; Stagg, C. A.; Falco, G.; Yoshikawa, T.; Bassey, U. C.; Aiba, K.; Sharova, L. V.; Shaik, N.; Ko, M. S. H., An in situ hybridzation-based screen for heterogeneously expressed genes in mouse ES cells. *Gene Expression Patterns* **2008,** 8, (3), 181-198.
26. Tanaka, T. S., Transcriptional heterogeneity in mouse embryonic stem cells. *Reproduction Fertility and Development* **2009,** 21, (1), 67-75.
27. Enver, T.; Soneji, S.; Joshi, C.; Brown, J.; Iborra, F.; Orntoft, T.; Thykjaer, T.; Maltby, E.; Smith, K.; Abu Dawud, R.; Jones, M.; Matin, M.; Gokhale, P.; Draper, J.; Andrews, P. W., Cellular differentiation hierarchies in normal and culture-adapted human embryonic stem cells. *Human Molecular Genetics* **2005,** 14, (21), 3129-3140.
28. Carpenter, M. K.; Rosler, E. S.; Fisk, G. J.; Brandenberger, R.; Ares, X.; Miura, T.; Lucero, M.; Rao, M. S., Properties of four human embryonic stem cell lines maintained in a feeder-free culture system. *Developmental Dynamics* **2004,** 229, (2), 243-258.
29. Stewart, M. H.; Bosse, M.; Chadwick, K.; Menendez, P.; Bendall, S. C.; Bhatia, M., Clonal isolation of hESCs reveals heterogeneity within the pluripotent stem cell compartment. *Nature Methods* **2006,** 3, (10), 807-815.
30. Moogk, D.; Stewart, M.; Gamble, D.; Bhatia, M.; Jervis, E., Human ESC Colony Formation Is Dependent on Interplay Between Self-Renewing hESCs and Unique Precursors Responsible for Niche Generation. *Cytometry Part A* 77A, (4), 321-327.
31. de Souza, N., Taming stem cell heterogeneity. *Nature Methods* 9, (7), 645-645.
32. Willems, E.; Leyns, L.; Vandesompele, J., Standardization of real-time PCR gene expression data from independent biological replicates. *Analytical Biochemistry* **2008,** 379, (1), 127-129.
33. McBeath, R.; Pirone, D. M.; Nelson, C. M.; Bhadriraju, K.; Chen, C. S., Cell shape, cytoskeletal tension, and RhoA regulate stem cell lineage commitment. *Developmental Cell* **2004,** 6, (4), 483-495.
34. Chen, C. S.; Mrksich, M.; Huang, S.; Whitesides, G. M.; Ingber, D. E., Geometric control of cell life and death. *Science* **1997,** 276, (5317), 1425-8.
35. Singhvi, R.; Kumar, A.; Lopez, G. P.; Stephanopoulos, G. N.; Wang, D. I.; Whitesides, G. M.; Ingber, D. E., Engineering cell shape and function. *Science* **1994,** 264, (5159), 696-8.
36. Lee, J. Y.; Jones, C.; Zern, M. A.; Revzin, A., Analysis of local tissue-specific gene expression in cellular micropatterns. *Anal Chem* **2006,** 78, (24), 8305-12.
37. Itano, N.; Okamoto, S.; Zhang, D. X.; Lipton, S. A.; Ruoslahti, E., Cell spreading controls endoplasmic and nuclear calcium: A physical gene regulation pathway from the cell surface to the nucleus. *Proceedings of the National Academy of Sciences of the United States of America* **2003,** 100, (9), 5181-5186.
38. Braam, S. R.; Zeinstra, L.; Litjens, S.; Ward-van Oostwaard, D.; van den Brink, S.; van Laake, L.; Lebrin, F.; Kats, P.; Hochstenbach, R.; Passier, R.; Sonnenberg, A.; Mummery, C. L., Recombinant vitronectin is a functionally defined substrate that supports human embryonic stem cell self-renewal via alpha V beta 5 integrin. *Stem Cells* **2008,** 26, (9), 2257-2265.
39. Humphries, J. D.; Byron, A.; Humphries, M. J., Integrin ligands at a glance. *Journal of Cell Science* **2006,** 119, (19), 3901-3903.

Chapter 5

1. Takahashi, K.; Yamanaka, S., Induction of pluripotent stem cells from mouse embryonic and adult fibroblast cultures by defined factors. *Cell* **2006,** 126, (4), 663-676.
2. Takahashi, K.; Tanabe, K.; Ohnuki, M.; Narita, M.; Ichisaka, T.; Tomoda, K.; Yamanaka, S., Induction of pluripotent stem cells from adult human fibroblasts by defined factors. *Cell* **2007,** 131, (5), 861-872.
3. Yu, J.; Vodyanik, M. A.; Smuga-Otto, K.; Antosiewicz-Bourget, J.; Frane, J. L.; Tian, S.; Nie, J.; Jonsdottir, G. A.; Ruotti, V.; Stewart, R.; Slukvin, I. I.; Thomson, J. A., Induced pluripotent stem cell lines derived from human somatic cells. *Science* **2007,** 318, (5858), 1917-1920.
4. Robinton, D. A.; Daley, G. Q., The promise of induced pluripotent stem cells in research and therapy. *Nature* 481, (7381), 295-305.
5. Stadtfeld, M.; Hochedlinger, K., Induced pluripotency: history, mechanisms, and applications. *Genes & Development* 24, (20), 2239-2263.
6. Gonzalez, F.; Boue, S.; Izpisua Belmonte, J. C., Methods for making induced pluripotent stem cells: reprogramming a la carte. *Nature Reviews Genetics* 12, (4), 231-242.
7. Warren, L.; Manos, P. D.; Ahfeldt, T.; Loh, Y.-H.; Li, H.; Lau, F.; Ebina, W.; Mandal, P. K.; Smith, Z. D.; Meissner, A.; Daley, G. Q.; Brack, A. S.; Collins, J. J.; Cowan, C.; Schlaeger, T. M.; Rossi, D. J., Highly Efficient Reprogramming to Pluripotency and Directed Differentiation of Human Cells with Synthetic Modified mRNA. *Cell Stem Cell* 7, (5), 618-630.
8. Miyoshi, N.; Ishii, H.; Nagano, H.; Haraguchi, N.; Dewi, D. L.; Kano, Y.; Nishikawa, S.; Tanemura, M.; Mimori, K.; Tanaka, F.; Saito, T.; Nishimura, J.; Takemasa, I.; Mizushima, T.; Ikeda, M.; Yamamoto, H.; Sekimoto, M.; Doki, Y.; Mori, M., Reprogramming of Mouse and Human Cells to Pluripotency Using Mature MicroRNAs. *Cell Stem Cell* 8, (6), 633-638.
9. Yu, J.; Hu, K.; Smuga-Otto, K.; Tian, S.; Stewart, R.; Slukvin, I. I.; Thomson, J. A., Human Induced Pluripotent Stem Cells Free of Vector and Transgene Sequences. *Science* **2009,** 324, (5928), 797-801.
10. Kim, D.; Kim, C.-H.; Moon, J.-I.; Chung, Y.-G.; Chang, M.-Y.; Han, B.-S.; Ko, S.; Yang, E.; Cha, K. Y.; Lanza, R.; Kim, K.-S., Generation of Human Induced Pluripotent Stem Cells by Direct Delivery of Reprogramming Proteins. *Cell Stem Cell* **2009,** 4, (6), 472-476.
11. Zhou, H.; Wu, S.; Joo, J. Y.; Zhu, S.; Han, D. W.; Lin, T.; Trauger, S.; Bien, G.; Yao, S.; Zhu, Y.; Siuzdak, G.; Schoeler, H. R.; Duan, L.; Ding, S., Generation of Induced Pluripotent Stem Cells Using Recombinant Proteins. *Cell Stem Cell* **2009,** 4, (5), 381-384.
12. Park, I. H.; Arora, N.; Huo, H.; Maherali, N.; Ahfeldt, T.; Shimamura, A.; Lensch, M. W.; Cowan, C.; Hochedlinger, K.; Daley, G. Q., Disease-specific induced pluripotent stem cells. *Cell* **2008,** 134, (5), 877-886.

13. Ebert, A. D.; Yu, J. Y.; Rose, F. F.; Mattis, V. B.; Lorson, C. L.; Thomson, J. A.; Svendsen, C. N., Induced pluripotent stem cells from a spinal muscular atrophy patient. *Nature* **2009,** 457, (7227), 277-U1.
14. Kulczycki, L. L.; Kostuch, M.; Bellanti, J. A., A clinical perspective of cystic fibrosis and new genetic findings: Relationship of CFTR mutations to genotype-phenotype manifestations. *American Journal of Medical Genetics Part A* **2003,** 116A, (3), 262-267.
15. Mall, M.; Grubb, B. R.; Harkema, J. R.; O'Neal, W. K.; Boucher, R. C., Increased airway epithelial Na+ absorption produces cystic fibrosis-like lung disease in mice. *Nat Med* **2004,** 10, (5), 487-493.
16. Krenz, M.; Robbins, J., Impact of beta-myosin heavy chain expression on cardiac function during stress. *Journal of the American College of Cardiology* **2004,** 44, (12), 2390-2397.
17. Bellin, M.; Marchetto, M. C.; Gage, F. H.; Mummery, C. L., Induced pluripotent stem cells: the new patient? *Nat Rev Mol Cell Biol* **2012,** 13, (11), 713-26.
18. Hedley, P. L.; Jorgensen, P.; Schlamowitz, S.; Wangari, R.; Moolman-Smook, J.; Brink, P. A.; Kanters, J. K.; Corfield, V. A.; Christiansen, M., The Genetic Basis of Long QT and Short QT Syndromes: A Mutation Update. *Human Mutation* **2009,** 30, (11), 1486-1511.
19. Moretti, A.; Bellin, M.; Welling, A.; Jung, C. B.; Lam, J. T.; Bott-Fluegel, L.; Dorn, T.; Goedel, A.; Hoehnke, C.; Hofmann, F.; Seyfarth, M.; Sinnecker, D.; Schoemig, A.; Laugwitz, K.-L., Patient-Specific Induced Pluripotent Stem-Cell Models for Long-QT Syndrome. *New England Journal of Medicine* **2010,** 363, (15), 1397-1409.
20. Itzhaki, I.; Maizels, L.; Huber, I.; Zwi-Dantsis, L.; Caspi, O.; Winterstern, A.; Feldman, O.; Gepstein, A.; Arbel, G.; Hammerman, H.; Boulos, M.; Gepstein, L., Modelling the long QT syndrome with induced pluripotent stem cells. *Nature* 471, (7337), 225-U113.
21. Yazawa, M.; Hsueh, B.; Jia, X.; Pasca, A. M.; Bernstein, J. A.; Hallmayer, J.; Dolmetsch, R. E., Using induced pluripotent stem cells to investigate cardiac phenotypes in Timothy syndrome. *Nature* **2011,** 471, (7337), 230-U120.
22. Lahti, A. L.; Kujala, V. J.; Chapman, H.; Koivisto, A.-P.; Pekkanen-Mattila, M.; Kerkela, E.; Hyttinen, J.; Kontula, K.; Swan, H.; Conklin, B. R.; Yamanaka, S.; Silvennoinen, O.; Aalto-Setala, K., Model for long QT syndrome type 2 using human iPS cells demonstrates arrhythmogenic characteristics in cell culture. *Disease Models & Mechanisms* 5, (2), 220-230.
23. Itzhaki, I.; Maizels, L.; Huber, I.; Zwi-Dantsis, L.; Caspi, O.; Winterstern, A.; Feldman, O.; Gepstein, A.; Arbel, G.; Hammerman, H.; Boulos, M.; Gepstein, L., Modelling the long QT syndrome with induced pluripotent stem cells. *Nature* **2011,** 471, (7337), 225-9.
24. Matsa, E.; Rajamohan, D.; Dick, E.; Young, L.; Mellor, I.; Staniforth, A.; Denning, C., Drug evaluation in cardiomyocytes derived from human induced pluripotent stem cells carrying a long QT syndrome type 2 mutation. *Eur Heart J* **2011,** 32, (8), 952-62.
25. Braam, S. R.; Tertoolen, L.; Casini, S.; Matsa, E.; Lu, H. R.; Teisman, A.; Passier, R.; Denning, C.; Gallacher, D. J.; Towart, R.; Mummery, C. L., Repolarization reserve

determines drug responses in human pluripotent stem cell derived cardiomyocytes. *Stem Cell Res* **2012,** 10, (1), 48-56.
26. Kehat, I.; Kenyagin-Karsenti, D.; Snir, M.; Segev, H.; Amit, M.; Gepstein, A.; Livne, E.; Binah, O.; Itskovitz-Eldor, J.; Gepstein, L., Human embryonic stem cells can differentiate into myocytes with structural and functional properties of cardiomyocytes. *Journal of Clinical Investigation* **2001,** 108, (3), 407-414.
27. He, J. Q.; Ma, Y.; Lee, Y.; Thomson, J. A.; Kamp, T. J., Human embryonic stem cells develop into multiple types of cardiac myocytes - Action potential characterization. *Circulation Research* **2003,** 93, (1), 32-39.
28. Xu, C. H.; Police, S.; Rao, N.; Carpenter, M. K., Characterization and enrichment of cardiomyocytes derived from human embryonic stem cells. *Circulation Research* **2002,** 91, (6), 501-508.
29. Zhang, J.; Wilson, G. F.; Soerens, A. G.; Koonce, C. H.; Yu, J.; Palecek, S. P.; Thomson, J. A.; Kamp, T. J., Functional Cardiomyocytes Derived From Human Induced Pluripotent Stem Cells. *Circulation Research* **2009,** 104, (4), E30-E41.
30. Osafune, K.; Caron, L.; Borowiak, M.; Martinez, R. J.; Fitz-Gerald, C. S.; Sato, Y.; Cowan, C. A.; Chien, K. R.; Melton, D. A., Marked differences in differentiation propensity among human embryonic stem cell lines. *Nature Biotechnology* **2008,** 26, (3), 313-315.
31. Ng, E. S.; Davis, R. P.; Azzola, L.; Stanley, E. G.; Elefanty, A. G., Forced aggregation of defined numbers of human embryonic stem cells into embryoid bodies fosters robust, reproducible hematopoietic differentiation. *Blood* **2005,** 106, (5), 1601-1603.
32. Burridge, P. W.; Anderson, D.; Priddle, H.; Munoz, M. D. B.; Chamberlain, S.; Allegrucci, C.; Young, L. E.; Denning, C., Improved human embryonic stem cell embryoid body homogeneity and cardiomyocyte differentiation from a novel V-96 plate aggregation system highlights interline variability. *Stem Cells* **2007,** 25, (4), 929-938.
33. Ungrin, M. D.; Joshi, C.; Nica, A.; Bauwens, C.; Zandstra, P. W., Reproducible, Ultra High-Throughput Formation of Multicellular Organization from Single Cell Suspension-Derived Human Embryonic Stem Cell Aggregates. *PLoS One* **2008,** 3, (2).
34. Mohr, J. C.; Zhang, J.; Azarin, S. M.; Soerens, A. G.; de Pablo, J. J.; Thomson, J. A.; Lyons, G. E.; Palecek, S. P.; Kamp, T. J., The microwell control of embryoid body size in order to regulate cardiac differentiation of human embryonic stem cells. *Biomaterials* 31, (7), 1885-1893.
35. Bauwens, C. L.; Peerani, R.; Niebruegge, S.; Woodhouse, K. A.; Kumacheva, E.; Husain, M.; Zandstra, P. W., Control of human embryonic stem cell colony and aggregate size heterogeneity influences differentiation trajectories. *Stem Cells* **2008,** 26, (9), 2300-2310.
36. Yang, L.; Soonpaa, M. H.; Adler, E. D.; Roepke, T. K.; Kattman, S. J.; Kennedy, M.; Henckaerts, E.; Bonham, K.; Abbott, G. W.; Linden, R. M.; Field, L. J.; Keller, G. M., Human cardiovascular progenitor cells develop from a KDR plus embryonic-stem-cell-derived population. *Nature* **2008,** 453, (7194), 524-U6.
37. Filipczyk, A. A.; Passier, R.; Rochat, A.; Mummery, C. L., Regulation of cardiomyocyte differentiation of embryonic stem cells by extracellular signalling. *Cellular and Molecular Life Sciences* **2007,** 64, (6), 704-718.

38. Gaur, M.; Ritner, C.; Sievers, R.; Pedersen, A.; Prasad, M.; Bernstein, H. S.; Yeghiazarians, Y., Timed inhibition of p38MAPK directs accelerated differentiation of human embryonic stem cells into cardiomyocytes. *Cytotherapy* 12, (6), 807-817.
39. Graichen, R.; Xu, X.; Braam, S. R.; Balakrishnan, T.; Norfiza, S.; Sieh, S.; Soo, S. Y.; Tham, S. C.; Mummery, C.; Colman, A.; Zweigerdt, R.; Davidson, B. P., Enhanced cardiomyogenesis of human embryonic stem cells by a small molecular inhibitor of p38 MAPK. *Differentiation* **2008,** 76, (4), 357-370.
40. Sadek, H.; Hannack, B.; Choe, E.; Wang, J.; Latif, S.; Garry, M. G.; Garry, D. J.; Longgood, J.; Frantz, D. E.; Olson, E. N.; Hsieh, J.; Schneider, J. W., Cardiogenic small molecules that enhance myocardial repair by stem cells. *Proceedings of the National Academy of Sciences of the United States of America* **2008,** 105, (16), 6063-6068.
41. Qyang, Y.; Martin-Puig, S.; Chiravuri, M.; Chen, S.; Xu, H.; Bu, L.; Jiang, X.; Lin, L.; Granger, A.; Moretti, A.; Caron, L.; Wu, X.; Clarke, J.; Taketo, M. M.; Laugwitz, K.-L.; Moon, R. T.; Gruber, P.; Evans, S. M.; Ding, S.; Chien, K. R., The renewal and differentiation of Isl1(+) cardiovascular progenitors are controlled by a Wnt/beta-catenin pathway. *Cell Stem Cell* **2007,** 1, (2), 165-179.
42. Hao, J.; Daleo, M. A.; Murphy, C. K.; Yu, P. B.; Ho, J. N.; Hu, J.; Peterson, R. T.; Hatzopoulos, A. K.; Hong, C. C., Dorsomorphin, a Selective Small Molecule Inhibitor of BMP Signaling, Promotes Cardiomyogenesis in Embryonic Stem Cells. *PLoS One* **2008,** 3, (8).
43. Kattman, S. J.; Witty, A. D.; Gagliardi, M.; Dubois, N. C.; Niapour, M.; Hotta, A.; Ellis, J.; Keller, G., Stage-Specific Optimization of Activin/Nodal and BMP Signaling Promotes Cardiac Differentiation of Mouse and Human Pluripotent Stem Cell Lines. *Cell Stem Cell* 8, (2), 228-240.
44. Dubois, N. C.; Craft, A. M.; Sharma, P.; Elliott, D. A.; Stanley, E. G.; Elefanty, A. G.; Gramolini, A.; Keller, G., SIRPA is a specific cell-surface marker for isolating cardiomyocytes derived from human pluripotent stem cells. *Nature Biotechnology* 29, (11), 1011-U82.
45. Laflamme, M. A.; Chen, K. Y.; Naumova, A. V.; Muskheli, V.; Fugate, J. A.; Dupras, S. K.; Reinecke, H.; Xu, C.; Hassanipour, M.; Police, S.; O'Sullivan, C.; Collins, L.; Chen, Y.; Minami, E.; Gill, E. A.; Ueno, S.; Yuan, C.; Gold, J.; Murry, C. E., Cardiomyocytes derived from human embryonic stem cells in pro-survival factors enhance function of infarcted rat hearts. *Nature Biotechnology* **2007,** 25, (9), 1015-1024.
46. Mummery, C. L.; Zhang, J.; Ng, E. S.; Elliott, D. A.; Elefanty, A. G.; Kamp, T. J., Differentiation of Human Embryonic Stem Cells and Induced Pluripotent Stem Cells to Cardiomyocytes A Methods Overview. *Circulation Research* 111, (3), 344-358.
47. Paige, S. L.; Osugi, T.; Afanasiev, O. K.; Pabon, L.; Reinecke, H.; Murry, C. E., Endogenous Wnt/beta-Catenin Signaling Is Required for Cardiac Differentiation in Human Embryonic Stem Cells. *PLoS One* 5, (6).
48. Lian, X.; Hsiao, C.; Wilson, G.; Zhu, K.; Hazeltine, L. B.; Azarin, S. M.; Raval, K. K.; Zhang, J.; Kamp, T. J.; Palecek, S. P., Robust cardiomyocyte differentiation from human pluripotent stem cells via temporal modulation of canonical Wnt signaling. *Proceedings of the National Academy of Sciences of the United States of America* 109, (27), E1848-E1857.

49. Zhang, J.; Raval, K. K.; Lian, X.; Herman, A. M.; Wilson, G. F.; Barron, M. R.; Yu, J.; Palecek, S. P.; Thomson, J. A.; Kamp, T. J., Matrix-Promoted Efficient Cardiac Differentiation of Human iPS and ES Cells. *Circulation* 122, (21).
50. Engler, A. J.; Carag-Krieger, C.; Johnson, C. P.; Raab, M.; Tang, H.-Y.; Speicher, D. W.; Sanger, J. W.; Sanger, J. M.; Discher, D. E., Embryonic cardiomyocytes beat best on a matrix with heart-like elasticity: scar-like rigidity inhibits beating. *Journal of Cell Science* **2008,** 121, (22), 3794-3802.
51. McDevitt, T. C.; Angello, J. C.; Whitney, M. L.; Reinecke, H.; Hauschka, S. D.; Murry, C. E.; Stayton, P. S., In vitro generation of differentiated cardiac myofibers on micropatterned laminin surfaces. *Journal of Biomedical Materials Research* **2002,** 60, (3), 472-479.
52. Siedner, S.; Kruger, M.; Schroeter, M.; Metzler, D.; Roell, W.; Fleischmann, B. K.; Hescheler, J.; Pfitzer, G.; Stehle, R., Developmental changes in contractility and sarcomeric proteins from the early embryonic to the adult stage in the mouse heart. *Journal of Physiology-London* **2003,** 548, (2), 493-505.

Appendix A.1 Polyacrylamide Gels

Adapted from: Kris Saha (Healy lab)[1], Elizabeth Irwin (Healy lab)[2], and Adam Engler[3]

Materials

Quartz discs (1.375" diameter x 1/16" thick) (Quartz Scientific; # 21006031)
Glass cover slips (45 mm * 50 mm) (Fischer Scientific; # 12-545-H)
Glass Petri dishes (150 mm * 20 mm)
100 ml beaker (to make MTMS solution), should never be used for anything besides MTMS preparation
graduated cylinder (to measure methanol in glove box). Should never leave glove box
1L beakers
10 cm plastic culture plates
1.5 mL Eppendorf tube

Hydrogen Peroxide 30%
Sulfuric Acid
** Methacryloxypropyltrimethoxysilane (MTMS) (Gelest; #SIM6487.4)
*** Dichlorodimethylsilane (Sigma Aldrich; #440272)
* 40% Acrylamide solution (Amersco; Acryl 40 Solution Ultra Pure Grade #0132-500ML)
* 2% Bisacrylamide solution (Amersco; Bis-2 solution Ultra Pure Grade #0832-500ML)
* Tetramethylethylenediamine (TEMED)
*** Ammonium Persulfate
deionized water

* keep refrigerated
**store in a nitrogen glove box
*** keep refrigerated in a container with desiccant

Equipment

Oxygen Plasma
Nitrogen glove box
Laminar fume hood that vents outside of the lab
Oven
Vacuum Desiccator

Steps:

Perform all steps in a laminar fume hood to prevent dust from settling on the surfaces, and cause defects. Perform the silane step in a chemical fume hood that vents outside of the lab.

1. **Prepare polyacrylamide monomer solutions:** Dilute 40% acrylamide and 2% bisacrylamide stock solutions with deionized water. A number of references provide expected moduli based on monomer solution.[1-4] The following table (Table S1) from Saha et al.[1] is particularly useful due to the swelling information that is also presented. For printed hydrogels it is crucial to minimize the swelling ratio in order to avoid unwanted topography at the interface between the gel and the cells.

TABLE S1. Complete modulus and swelling data for samples in Figure 3B.

AAm content w_m (wt %)	Bis content w_x (wt %)	G' (Pa)*	λ_f*	Surface-attached gel
3.0 %	0.025 %	12	1.79	Creased
	0.051 %	80	1.46	Flat
	0.075 %	130	1.39	Flat
	0.10 %	130	1.33	Flat
	0.20 %	160	1.18	Flat
5.0 %	0.025 %	140	1.66	Creased
	0.051 %	57	1.41	Flat
	0.075 %	440	1.34	Flat
	0.10 %	670	1.27	Flat
	0.20 %	1140	1.16	Flat
10.0 %	0.020 %	400	1.51	Creased
	0.040 %	820	1.44	Flat
	0.10 %	2250	1.28	Flat
	0.15 %	5460	1.18	Flat
	0.30 %	9580	1.11	Flat

*Typical estimated uncertainties are ± 10 Pa for G' and ± 0.04 for λ_f.

Prepare 5 mL for every 4-5 gels you plan on making. Distribute 5 mL monomer solution per 15 mL falcon tube. Each tube will be initiated separately. Degas monomer solutions in a vacuum desiccator until there are no bubbles left, which may take a few hours depending on the strength of the vacuum used.

2. **Prepare Quartz Substrates:** If using new quartz discs, expose the discs to oxygen plasma for 5 min at 80 W 1 Torr, in order to prime the surface for better adhesion to the fluorinated silane. Approximately 20 quartz discs can be treated with oxygen plasma at once in the Plasma Preen oxygen plasma machine. If reusing a disc, use a piranha etch solution✪ to clean the discs prior to oxygen plasma treatment.
Note: For best results, allow the vacuum of the oxygen plasma to be on for at least 5 minutes before opening the oxygen line, then allow at least 5 minutes of oxygen flow before turning on the plasma. Plasma should be blue indicating oxygen content. If plasma is pink then it is mostly nitrogen.
✪ **Piranha Etching** Combine 3:1 sulfuric acid: 30% hydrogen peroxide to a to a total volume of ~600 mL in a 1L beaker inside a chemical fume hood dedicated to piranha etching. Make sure there are no organic solvent around which can react the Piranha solution!! Wear full protective gear as solution

has a pH lower than 1. Place quartz discs into a Teflon caddy and place caddy into the solution, and leave for 1 hour. Move caddy into another 1L beaker full of water. Flow that beaker under water in a sink until pH is neutral. Dispose of the piranha solution following EH&S guidelines. Never store waste piranha solution in an unvented bottle, as the solution outgases and this can lead to explosion.

3. **Deposit Silane Solution:** While quartz discs are being treated with oxygen plasma, make a solution of 1% (v/v) MTMS and 94% (v/v) methanol, in the nitrogen glove box. Remove from glove box and add acetic acid (6 uL/100 mL solution) and 5% (v/v) deionized water. Wait 5 min for silane to deposit onto the glass. Rinse 3x for 1 min in methanol. Bake for 30 min in 110°C.

4. **Prepare hydrophobic top cover slip:**
    - **4.1 Oxygen Plasma:** expose the glass cover slips to oxygen plasma for 1 min at 80 W, 1 Torr. Place the cover slips into a chemical fume hood, on top of paper towels.
    - **4.2 Apply hydrophobic silane:** Remove dichlorodimethylsilane from refrigerator and use a syringe with needle to remove about 1-2 ml solution. This should be sufficient to coat about 20 coverslips. Apply a drop to each coverglass and use a kimwipe to spread that drop onto the entire surface. Let sit at least 30 min, and usually, until monomer solutions have fully degassed, and you are ready to make APS and TEMED solutions.
    - **4.3 Rinse Silane:** using the water source in the hood rinse the cover slips, to remove excess dichlorodimethyl silane and use a kimwipe to dry the cover slips.

5. **Prepare APS and TEMED:** Weigh <0.1g APS in Eppendorf tube. Make sure APS has warmed to room temperature before you weight it. Add water to make 10 wt% APS in deionized solution. Prepare only right before you are ready to make gels. Prepare TEMED, by removing it from refrigerator.

6. **Make gels:**
    - **6.1** Remove Quartz discs from oven, and place 5 at a time into the laminar fume hood where the hydrophobic coverslips are.
    - **6.2** Make no more than 5 gels at a time, using one 15 mL falcon monomer solution. Only make one tube at a time. Into the degassed 15 mL monomer falcon tube, pipette APS and TEMED and vortex at a medium setting for good mixing, but not at the highest setting which can introduce bubbles.
    - **6.3** Immediately pipette 65 μL of monomer solution onto the quartz discs, and place the coverslip onto of the monomer solution.
    - **6.4** Let **polymerize** for 15 min. Check left over solution in 15 mL tube to see when gelation is complete. Reaction is exothermic and tube

should heat up. Do not allow the gel to dry out. (In many cases, white lines form at the edges of the gel at the onset of overdrying.)

6.5 Remove top coverslip by taking the sandwich of a quartz-acrylamide-coverslip and immersing into in a 1L beaker full of water and gently sliding the hydrophobic coverslip off.

6.6 Inspect the polyacrylamide gel for any defects and place into a 10 cm dish with deionized water to rinse away unreacted reagents Rinse overnight on a rocker. Four discs can fit into one 10 cm dish.

1. Saha, K.; Keung, A. J.; Irwin, E. F.; Li, Y.; Little, L.; Schaffer, D. V.; Healy, K. E., Substrate Modulus Directs Neural Stem Cell Behavior. *Biophysical Journal* **2008,** 95, (9), 4426-4438.

2. Irwin, E. F.; Saha, K.; Rosenbluth, M.; Gamble, L. J.; Castner, D. G.; Healy, K. E., Modulus-dependent macrophage adhesion and behavior. *Journal of Biomaterials Science-Polymer Edition* **2008,** 19, (10), 1363-1382.

3. J.R., T.; A.J., E., Preperation of Hydrogel Substrates with Tunable Mechanical Properties. In *Current Protocols in Cell Biology*, Wiley: **2010**; pp 1-16.

4. Saha, K.; Kim, J.; Irwin, E.; Yoon, J.; Momin, F.; Trujillo, V.; Schaffer, D. V.; Healy, K. E.; Hayward, R. C., Surface Creasing Instability of Soft Polyacrylamide Cell Culture Substrates. *Biophysical Journal* **2010,** 99, (12), L94-L96.

Appendix A.2 Photolithography – SU-8 Masters

A dollop (~ 3ml) of SU-8 50 was poured onto 3" Silicon wafers (3" N/PH <1-0-0> 10-20 OHM-CM, 381±25μm Test grade wafer from Silicon Quest International Inc, San Jose, CA). The SU-8 was then spun cast on the silicon wafer using a Headway Research Spincaster (model PWM32) at 500 rpm, ramping up from 0 rpm to 500 rpm at 100 rpm/second and held at 500 rpm for 10 seconds. The spin speed was then raised to 1,000 rpm using a 300 rpm/second ramp rate, and left at 1,000 rpm for 1 minute. The SU-8 was then soft-baked to evaporate the solvent (which is part of the SU-8 system, which sufficiently decreases the viscosity of the SU-8 to allow for easy pouring and spin casting). Soft-baking was accomplished by placing the wafer on a hot plate, inside of a laminar flow fume hood for 10 minutes at 65°C followed by 30 minutes at 95°C.

After allowing the SU-8 to cool to room temperature gradually, the wafer was exposed to 365 nm UV light through a photomask to cure the SU-8. The photomask was printed at 10,000 dpi (Outputcity, Oregon), and was placed ink side down on the SU-8. A ¼" square of UV transparent glass was placed on top of the photomask to ensure conformal contact with the SU-8, there by minimizing diffraction, which leads to negative sidewall profiles. Additionally a 365 nm wavelength bandpass filter was used on the broad spectrum light source (EXFO Omnicure 1500W), as the manufacturer stipulates that while SU-8 is transparent and insensitive to light longer than 400 nm, it has high actinic absorption below 350 nm, which can lead to over-exposure of the top part of the film, again leading to negative sidewall profiles. UV exposure leads to the creation of an acid in the SU-8 film. After the exposure step, the film was baked (at 65°C for 1 minute and then at 95°C for 10 minutes), which allows the acid to catalyze the crosslinking of the SU-8. After the crosslinking step, the SU-8 wafer was gradually cooled down to room temperature and then incubated with the developer 1-methoxy-2-propyl acetate (Microchem, Newton, MA) for at least 20 minutes in a sonicator, to remove all uncrosslinked SU-8. After development, the wafer was rinsed with isopropyl alcohol (IPA), and then dried with Nitrogen. It can be stored in a nitrogen environment until ready for use.

Appendix A.3 UV-Activated Microcontact Printing Protocol

Materials:
10 cm plastic tissue culture dishes
50 mL falcon tubes
0.22 µm Steriflip filters (Millipore; #SCGP00525)
Aluminum foil
Aluminum weigh boats with 3" bottom diameters
Disposable hexagonal weigh boats
Razor blade
Glass microscope slides 1mm thick (either 25 mm * 75 mm or 45 mm * 50 mm)
Jack
6 well tissue culture plate (BD falcon; #353046)

> **NOTE:** Do not use Costar 6 well plates – the quartz discs will not fit inside of their wells, as they are slightly smaller than the wells of the BD falcon plates

Ethanol
Deionized water
Phosphate Buffered Saline (PBS) pH 7.4 (ie Life Technologies; 10010-023)

3" Silicon wafers (3" N/PH <1-0-0> 10-20 OHM-CM, 381±25µm Test grade wafer) (Silicon Quest International Inc)
✣ SU-8 50 (Microchem)
Polydimethylsiloxane (PDMS) (Dow Corning, Sylgard 184)
** Tridecafluoro-1,1,2,2-tetrahydrooctyl)-1-trichlorosilane (Gelest; SIT8174.0)
✣ *** Sulfo-SANPAH (Thermo Scientific; 22589)
Adhesive ligands :

- * Fibronectin, human (Life Technologies; #33016-015)
- *** Vitronectin, human, recombinant (Sigma Aldrich; # SRP3186)
- *** HESC-qualified Matrigel (BD Bioscience; #354277)
- * KO-DMEM (for Matrigel dilution)

✣ cover in aluminum foil to avoid light exposure
* refrigerate
** store in a nitrogen glove box
*** store at -20°C in a container with desiccant

Equipment:
Oxygen Plasma
Laminar flow and sterile hoods
Spin Caster (for making SU-8 masters)
Vacuum Desiccator
Oven (and hot plate or making SU-8 masters)
Hot water bath
Vortexer
UV light source capable of producing at least 1.25 W/cm^2

Prepare polyacrylamide gels:

1. **Make polyacrylamide gels** as described in **Appendix A.1,** and allow them to rinse overnight with deionized water on a rocker overnight. Four quartz backed gel can fit into one 10 cm dish cell culture dish (BD falcon), for easy overnight rinsing.

2. **Sterilize gels:** In a sterile hood, or at least a laminar flow hood, aspirate the water from the 10cm dishes. Take new sterile 10cm dishes and add 70% ethanol to each 10cm dish. Place quartz backed polyacrylamide gels into the 70% ethanol dishes. Return dishes to the rocker and allow to incubate for at least 20 minutes. Perform all subsequent steps in sterile hood. Make sure to spray down the outsides of the 10 cm dishes with 70% ethanol before returning them to the sterile hood.
   NOTE: gels will become opaque upon exposure to 70% ethanol. Ensure that opacity is uniform throughout the gel and that no holes are present in gel. Opacity will also be a function of gel modulus, with stiffer gels being more opaque. Prepare with deionized water, and prepare freshly, as the ethanol evaporates over time in the spray bottle, leading to a lower concentration of ethanol.

3. **Wash gels:** Aspirate 70% ethanol from 10 cm dishes, and rinse 3 times with deionized water.

4. **Dry gels:** Aspirate water and allow gels to dry for at least one hour in the sterile hood.

Prepare PDMS stamps:

1. **Make a photomask:** Use Adobe Illustrator to prepare photomasks. SU-8 is a negative photoresist, so all black areas in the photomask correspond to features in the PDMS. For example, an array of black dots will yield a PDMS stamp with an array of columns. Have the photomask printed at appropriate DPI for feature sizes. For features that are the sizes of colonies (>200 μm) and spaced at least one colony apart, 10,000 DPI should be sufficient, but you can always consult with the printer. Outputcity.com was used to print photomasks, and is highly recommended.

2. Follow instructions in **Appendix A.2** to **prepare SU-8 master**

3. **Silanize SU-8 master to ease PDMS release from master:**
    3.1 **Oxygen Plasma:** Expose SU-8 master to oxygen plasma for 30 seconds at 80 W 1 Torr, in order to prime the surface for better adhesion to the fluorinated silane.
    3.2 **Prepare Silane:** Place 200 µL of tridecafluoro-1,1,2,2-tetrahydrooctyl)-1-trichlorosilane, which should be stored in a nitrogen glove box, into a 1.5 ml cryotube.
    3.3 **Vapor Deposition of Silane onto SU-8 master:** Immediately after the oxygen plasma treatment of the wafer is over, place the wafer into an aluminum weigh boat* with the same dimension as the wafer, and place the aluminum weigh boat with wafer into a vacuum desiccator (avoid getting dust on the wafer during the transfer). Open the cryotube of tridecafluoro-1,1,2,2-tetrahyrooctyl)-1-trichlorosilane and place it in the vacuum desiccator on a support so it will not fall over. Apply vacuum for at least 3 hours, overnight is preferred.
    * the aluminum weigh boat is used to ease the removal of PDMS and the master, after PDMS curing.
    NOTE: Make sure that the vacuum is exhausting into a hood that vents outside of the lab, as fumes from the silane, can be hazardous to health. Make sure the vacuum has filters both at the inlet and outlet and that the filter are replaced often.

4. **Prepare PDMS** (Sygard 184, Dow Corning) by mixing base:curing agent at 10:1 by weight. Using 20 g base and 2 g curing agent will provide an appropriate thickness for the PDMS stamp (higher volumes will be hard to remove without cracking the SU-8 master, and smaller volumes may not cover the entire master. It is easiest to do the weighing into hexagonal plastic weigh boats, which allow for easy pouring.

5. **Degas PDMS:** After weighing out the base and curing agent, mix vigorously with a wooden stick for 5 minutes. Place weigh boat with PDMS mixture into a vacuum dessicator until all bubbles are gone (at least 30 minutes). Inside a laminar flow hood, pour the degassed PDMS onto the SU-8 master, and using the back of a 2ml aspirator, gently press down on the SU-8 master, to remove any trapped PDMS or gas from beneath the master. Place the Aluminum weigh boat with the SU-8 master and the PDMS into a vacuum dessicator and apply vacuum until no bubbles remain. Depending on the strength of the vacuum
    Note: Do not skip the first degassing step. The reaction between the base and curing agent outgasses, and if the first degassing step is skipped, the gas generated can get trapped in the holes/features of the SU-8 master.

6. **Cure PDMS:** After degassing, cure the PDMS with master at 110°C in an oven for at least 2 hours. If not using an aluminum weigh boat

7. **Release PDMS from master:** Remove PDMS from the oven, and place in a laminar flow hood to cool, avoid taking the PDMS out of the hood to avoid dust. Remove aluminum weigh boat carefully. Use a razor blade to help remove PDMS from SU-8 master, and cut PDMS into appropriate size. Place master into a 10 cm cell culture dish, and places that dish into a nitrogen box for storage until the next use. To reuse master, repeat from step 5.

Stamping:

1. **Attach PDMS to glass backing:** Expose PDMS stamp, and a glass microscope slide (25mm * 75mm * 1mm or 45mm * 50mm*1mm) to oxygen plasma for 30 seconds at 80W, 1 Torr. Immediately after oxygen plasma, bring the back of the PDMS stamp and the glass slide into conformal contact inside laminar flow hood, and press out any air bubbles.

2. **Sterilize Stamp:** After a tight bond is ensured between the PDMS and the glass microscope slide, spray the stamp and glass fixture with 70% ethanol and allow to evaporate. Meanwhile, prepare sulfo-SANPAH solution.

   *****Make sure all steps are performed sterilely from this point onwards****

3. **Prepare sulfo-SANPAH:** Weigh sulfo-SANPAH, and add water to make 0.2 mg/mL solution in a 50 mL falcon tube. Never weigh less than 1 mg as scale is not accurate for such small mass. Wrap the tube in aluminum foil so as to protect the sulfo-SANPAH from light and place the tube into a hot water bath (37°C) for about 2 minutes to help solubilize the sulfo-SANPAH. Then vortex the solution, and make sure that not precipitates are seen in the tube. Use a 0.22 μm Steriflip filter (Millipore), cover the newly filtered solution with aluminum foil.

4. **Prepare adhesive ligand**
   - 4.1 **Fibronectin:** Fibronectin comes in a 5 mg bottle that should be store at 4°C. Allow fibronectin to warm up to room temperature. Add 5 mL sterile PBS to fibronectin bottle, and leave to dissolve (may take ~ 30 minutes). DO NOT VORTEX or pipette vigorously. Aliquots of 1 mg/mL fibronectin should be stored at -20°C. For printing onto gels fibronectin aliquots should be thawed and diluted into sterile PBS, and then sterile filtered with a 0.22 μm Steriflip filters. Keep diluted fibronectin refrigerated until **step 11**.
   - 4.2 **Vitronectin**: Same general protocol as fibronectin, however it is stored at -20°C, and only has 250μg per vial, so aliquoting is not usually necessary.
   - 4.3 **Matrigel**: Every lot of HESC-qualified Matrigel comes with a specification sheet that indicates what size aliquot to freeze for each lot (as concentration varies). Typical values are ~300μL, and the aliquots are prepared in 50 mL falcon tubes. Matrigel, the tips

used for aliquoting, and the 50 mL falcon tubes that will store the aliquots must be on ice at the time of aliquoting, to prevent the Matrigel from gelling. Aliquots are stores at -20°C. To use an aliquot, 25 mL of 4°C KO-DMEM is added to the aliquot and pipetted repeatedly, without introducing bubbles to ensure homogenous solution. Keep the diluted Matrigel in a refrigerator or on ice until **step 11**. Diluted Matrigel should only be kept for two weeks.

5. **Ink Stamp:** Add enough sulfo-SANPAH solution to completely cover the PDMS stamp (1-3 mL), and leave stamps with sulfo-SANPAH in the dark for 30 minutes.

6. **Dry Stamp:** Use a nitrogen gun to dry the stamps.

7. **Set up UV source:** Turn on UV bulb (usually requires a few minutes to warm up, if using the EXFO Omnicure UV source, the display will stop blinking once the bulb is ready to use. Make sure the UV filter is in if using a broad spectrum source. Make sure the light is collimated. Use a light sensor to find the height at which the UV power is 1.25 W/cm^2, and raise the jack that will hold the samples to that height.
   NOTE: make sure you are shielded from the UV. Hoods used for cell culture have UV opaque sashes, but other hoods may not, so please check first, and wear eye protection.

8. **Printing:** Place the quartz backed acrylamide gel on the jack below the UV illuminator, under the light path. Apply the PDMS stamp to the gel gently, and immediately turn on the UV for 10 seconds, at a minimum of 1.25 W/cm^2. Gently remove stamp. There should be some resistance if the stamp adequately contacted the gel due to capillary forces. If there is no resistance at all, the stamp did not properly contact the gel.

9. **Wash Acrylamide Gels:** Immediately after stamping place acrylamide gels in a 10 cm dish full of fresh PBS. Exchange the PBS three times.

10. **Place Gels into Culture Plates:** Take a 6 well tissue culture plate and place ~ 5ml of PBS into each well. Then gently put the quartz backed acrylamide gels into each well. The disc should drop on its own, thus avoiding trapped air bubbles, however an air bubble occasionally may get trapped between the quartz and the cell culture dish, and it can be eliminated by quickly pushing the quartz down with a tweezer, but with care so as not to rip the gel.

11. **Add adhesive ligand:** Aspirate the PBS from each well, and 1 mL of desired adhesive ligand to each well. Incubate for 1 hour at room temperature or overnight at 4°C. Aspirate, and wash once with PBS. It is best to seed

patterned gels with cells on the same day that they are made, though the gels could probably be stored at 4°C until they are ready for use.

Appendix A.5 Limitations of Alternate Cell Counting Methods for hES cells

Two alternate cell counting methodologies were considered but ultimately not chosen for determining proliferation, as they are inappropriate to use for hES cells cultured on thick swollen hydrogels. One of the most common assays used for cell proliferation is the Cyquant kit (Molecular Probes), which like propidium iodide, contains a molecule that fluoresces when bound to nucleic acids.[1] In order to count cells with Cyquant, cell plates are frozen (to lyse the cells) and they are subsequently incubated with a proprietary cell lysis buffer, while still in the culture plate. Cell number is then quantified with a fluorescent plate reader, using the original cell culture plate, or by pipetting 200μL of the cell lysate into a 96 well plate compatible with a fluorescent reader. Since the polyacrylamide gels are fabricated on glass inserts that are then placed into tissue culture plates, the proliferation assay cannot be carried out in the 96 well or 48 well plate, as those wells are too small for use with quartz inserts. Even if glass inserts of appropriate size were suitable for those smaller plates, there is significant fluorescent background from both the quartz and the polyacrylamide gel. Therefore, after hES cells would be lysed in their 6 well culture plates, 200μL of cell lysate would need to be transferred, into a 96 well in order to quantify fluorescence. However, lysing the cells on a porous material such as thick polyacrylamide, allows for cell lysate to get trapped in the hydrogel, so that when lysate is removed and transferred into a 96 well plate for fluorescent measurement, it is not an accurate sampling of the total cell lysate. Additionally, the linear range of the Cyquant dye has a maximum of 25,000-50,000 cells, which is too low for hES cells grown in 6 well plate format, which have a cell concentration of approximately 1 million cells per well of a 6 well plate right after passaging.[2] Using the Cyquant dye at a higher concentration can increase the linear range to a few hundred thousand cells, but not one million cells (at higher concentrations, the background fluorescence of the dye becomes problematic).[1]

In the past, in order to avoid using Cyquant when performing proliferation assays on cells grown on swollen hydrogels, cell counting software scripts have been used to count cells on swollen hydrogels, however this technique is only useful for cells that grow as single cells, or that are seeded at low enough density that they remain as single cells through out the proliferation assay, with easily discernable cell borders or nuclei (if counting via nuclear fluorescent stain). [3, 4] hES cells grow as colonies, precluding this method, but opening the option of measuring colony area, as a measure of cell number. However, colony area measurement does not work for cells passaged with Accutase and ROCK inhibitor. When passaging with Accutase and ROCK inhibitor, many of the cells are single cells immediately after passaging, however they grow into colonies. Furthermore, the size of the cell changes during culture. When rock inhibitor is removed at day 1, cells contract, and adopt the high nucleus to cytoplasm ratio evident when hES are passaged as colonies. As the colony begins to proliferate the cells continue to contract in size, as the colony grows larger precluding colony area measurements from being an accurate assessment of cell number (**Appendix Figure AF.4**).

1. Jones, L. J.; Gray, M.; Yue, S. T.; Haugland, R. P.; Singer, V. L., Sensitive determination of cell number using the CyQUANT (R) cell proliferation assay. *Journal of Immunological Methods* **2001,** 254, (1-2), 85-98.
2. Melkoumian, Z.; Weber, J. L.; Weber, D. M.; Fadeev, A. G.; Zhou, Y.; Dolley-Sonneville, P.; Yang, J.; Qiu, L.; Priest, C. A.; Shogbon, C.; Martin, A. W.; Nelson, J.; West, P.; Beltzer, J. P.; Pal, S.; Brandenberger, R., Synthetic peptide-acrylate surfaces for long-term self-renewal and cardiomyocyte differentiation of human embryonic stem cells. *Nat Biotechnol* 28, (6), 606-10.
3. Irwin, E. F.; Saha, K.; Rosenbluth, M.; Gamble, L. J.; Castner, D. G.; Healy, K. E., Modulus-dependent macrophage adhesion and behavior. *Journal of Biomaterials Science-Polymer Edition* **2008,** 19, (10), 1363-1382.
4. Saha, K.; Keung, A. J.; Irwin, E. F.; Li, Y.; Little, L.; Schaffer, D. V.; Healy, K. E., Substrate Modulus Directs Neural Stem Cell Behavior. *Biophysical Journal* **2008,** 95, (9), 4426-4438.

Appendix Figures

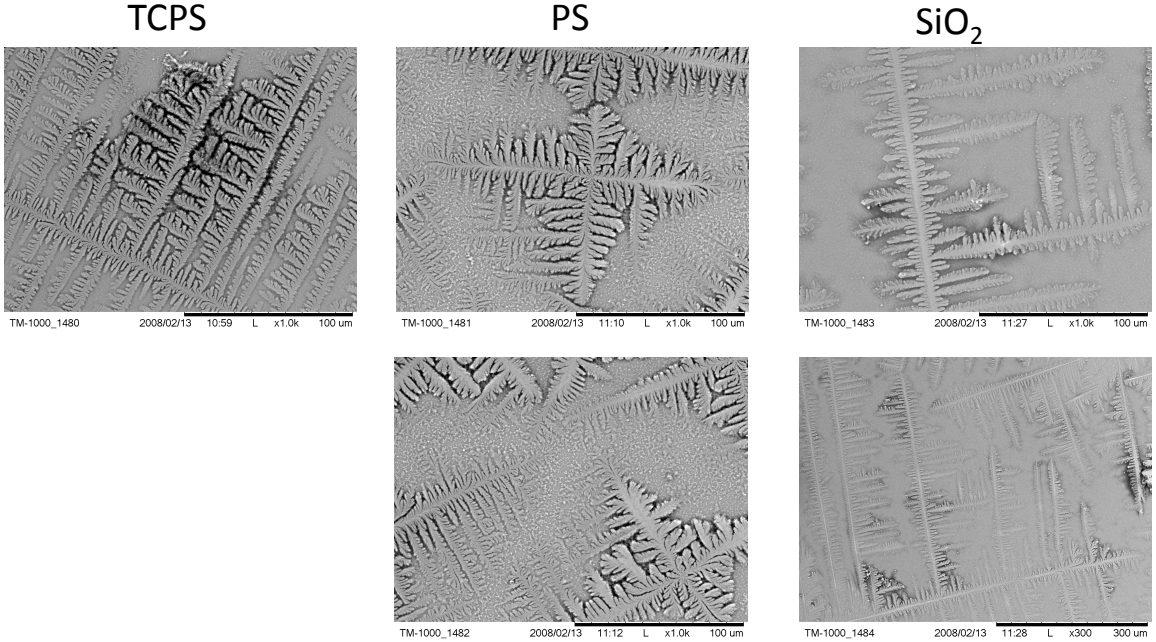

AF.1 Environmental Scanning Electron Microscopy (ESEM) images of air-dried Matrigel on Tissue Culture Polystyrene (TCPS), Polystyrene (PS), and SiO_2 (glass). Scale bar = 100 μm except for the bottom panel of SiO_2 where scale bar = 300 μm. On all three surfaces, salt dendrites from air-drying are visible.

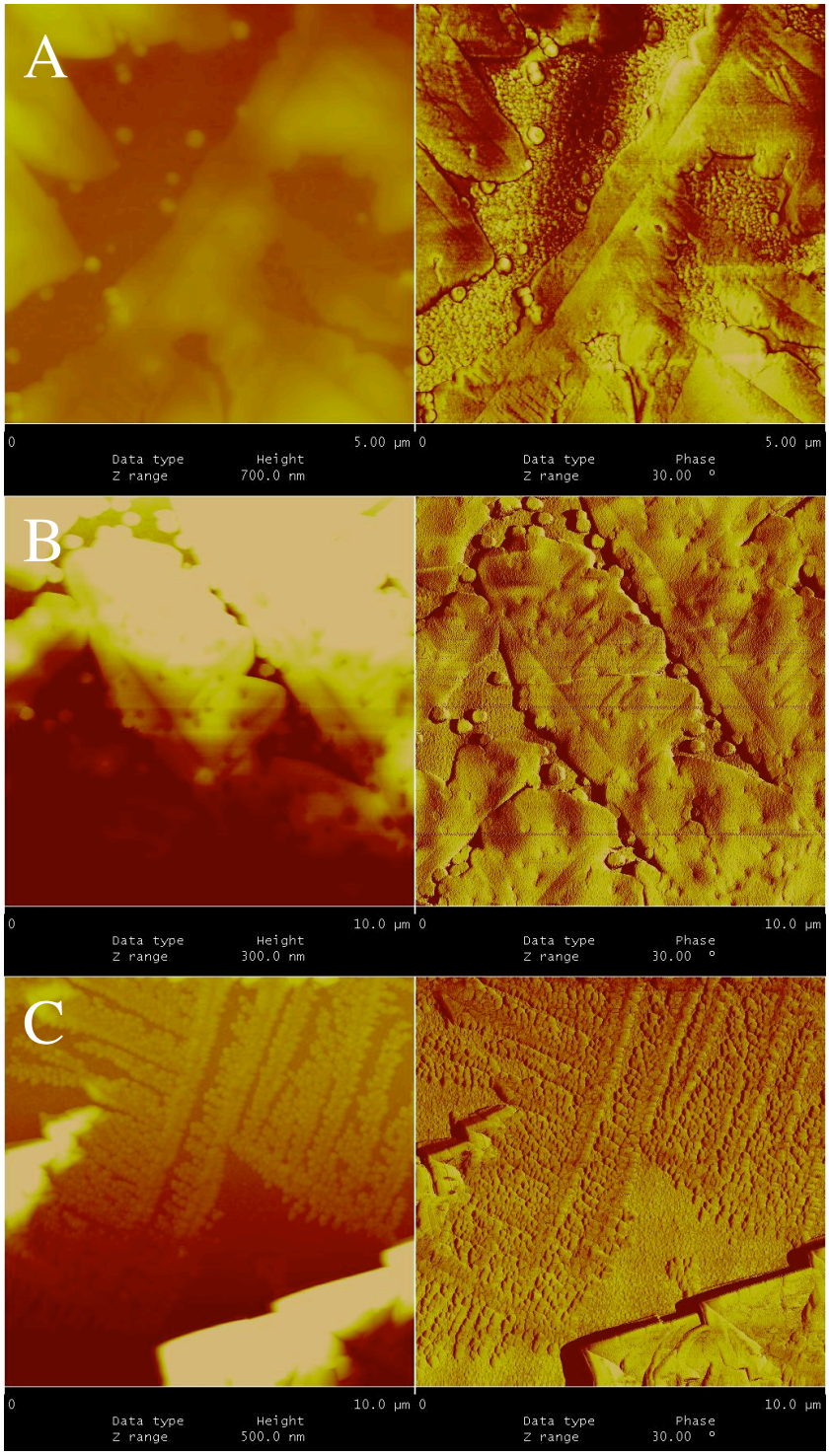

AF.2 Atomic Force Microscopy of Matrigel on (A) polystyrene. (B) SiO_2 (C) TCPS. Height images are on the left and phase images are on the right. All surfaces show characteristic salt dendrites from air-drying.

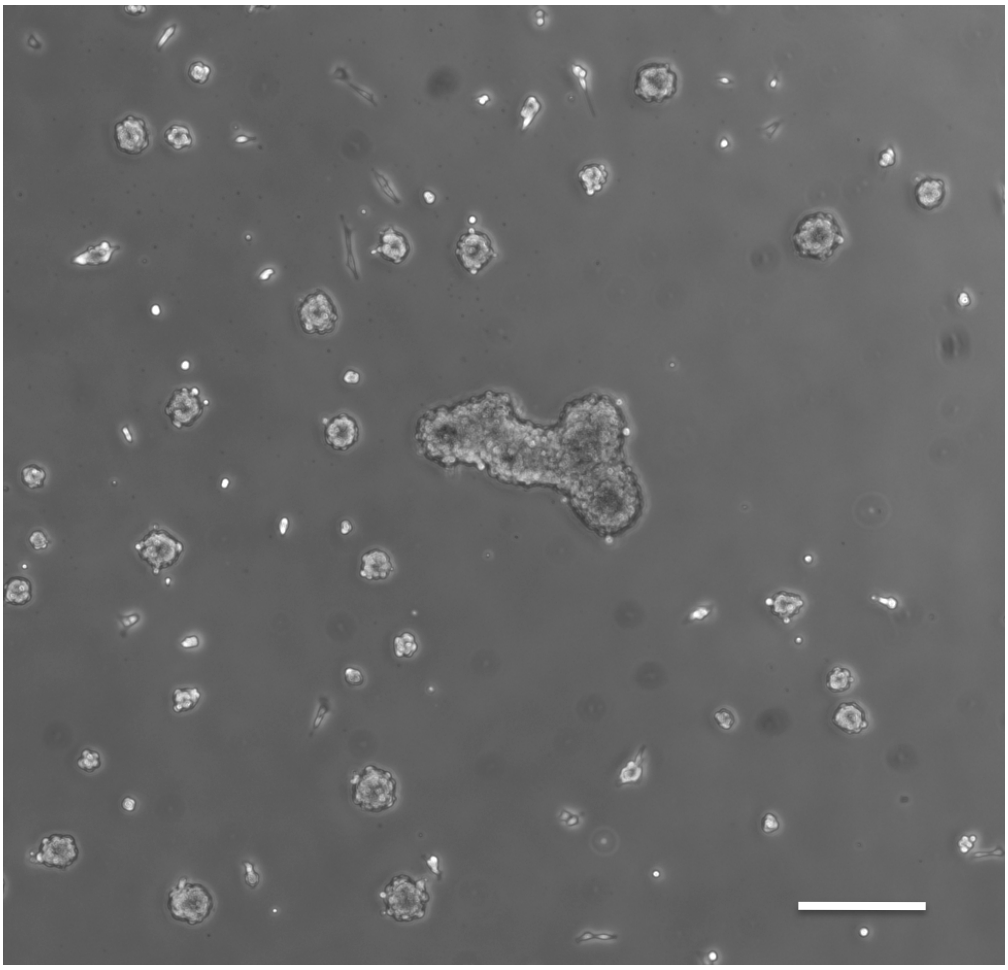

AF.3 On non-fouling or poorly adhesive surfaces, hES cells form aggregates that float in solution, similar to embryoid bodies. HES cells floating as aggregates on a polyacrylamide gel.
Scale bar = 500 μm

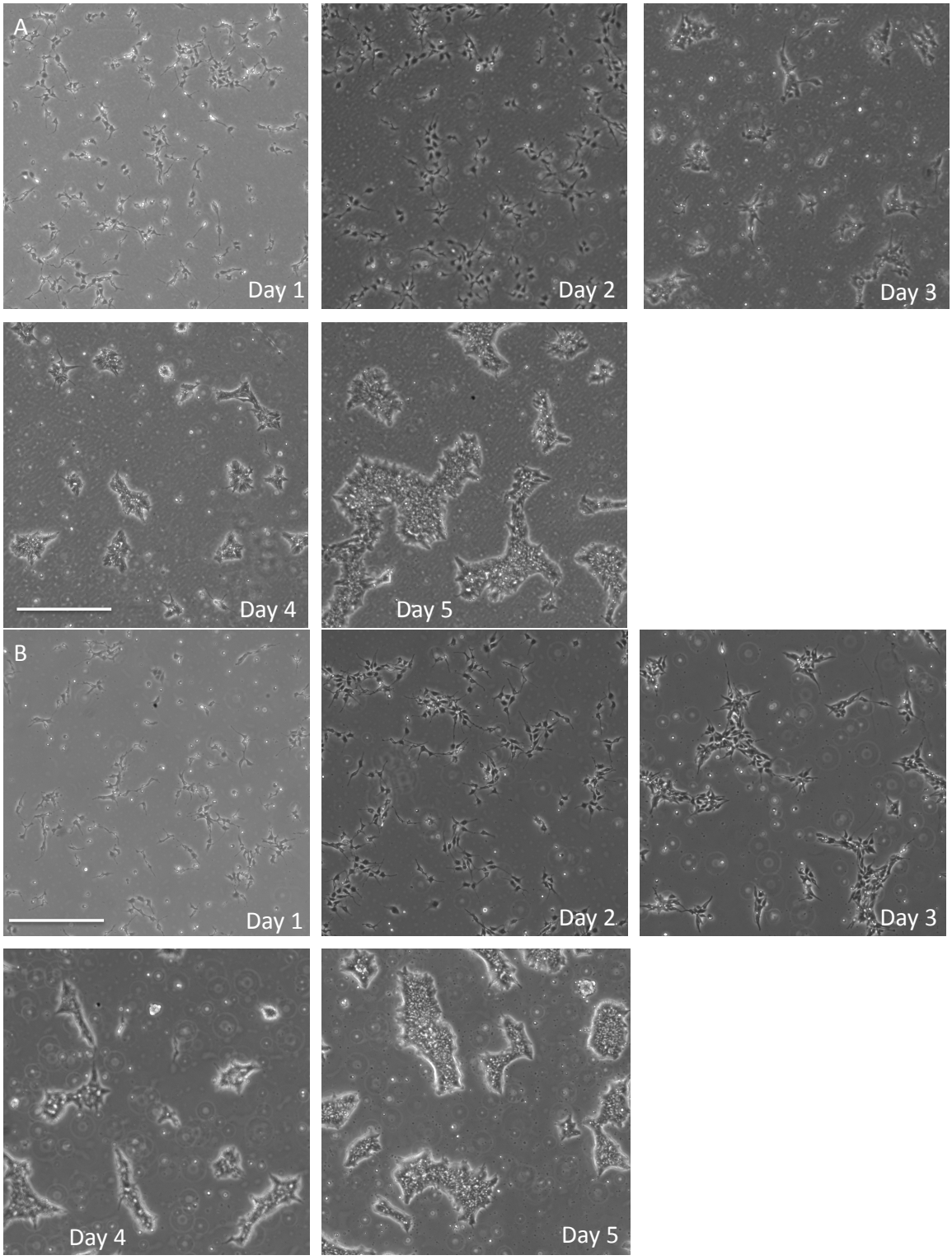

AF.4 H1 hES cell and colony shape and density change as a function of time when they are passaged with Accutase and ROCK inhibitor (ROCK inhibitor is removed at day 1 by media exchange). (A) cells on Matrigel on TCPS and (B) cells on Matrigel conjugated to 10 kPa polyacrylamide.